REMOBILISATION OF URANIUM AND THORIUM BY ORE-FORMING FLUIDS: A MINERALOGICAL STUDY

VOL. II

CHRISTOPHER MICHAEL POINTER

Doctor of Philosophy

THE UNIVERSITY OF ASTON IN BIRMINGHAM

May 1987

List of Tables

List of Figures

List of Plates

Key to abbreviations

LREE	Light rare earth elements
HREE	Heavy rare earth elements

Energy dispersive (ED) spectra for Ririwai samples:

BG	Biotite granite
AG	Albitised granite
M	Microclinite
GW	Greisenised wallrock
G	Greisen

ED spectra for Helmsdale samples:

BH.2, 9.5 m	Borehole 2, 9.5 metres depth.
Anom. 5	Surface Anomaly 5 in the Ousdale arkose.

Photomicrographs:

TPPL	Transmitted, plane polarised light.
TXPL	Transmitted, crossed polarised light.
RPPL	Reflected, plane polarised light.
ROIL	Reflected light, oil immersion.
SEM	Scanning electron micrograph.
BSEI	Back scattered electron image.
EPMA	Electron probe microanalysis.
XRD	X-ray diffraction.
F.O.V.	Field of view.

Fission track radiography:

FFT	Fine fission tracks
MFT	Medium " "
DFT	Dense " "
BFT	"Burned out" " (ie. U content exceeds recording capacity of Lexan detector)

Rocks and water	U Range (ppm)	U Mean (ppm)	Th Mean (ppm)
Continental crust		2.8	9.6
Igneous rocks			
Ultramafic	0.001-0.03	0.01	
Mafic, basaltic	0.1-1	0.75	2.2
Intermediate, andesitic	1-6	2	
Granite, silicic	2-15	4	17
Syenite	0.1-20	4	
Sedimentary rocks			
Red and green shale	1-5	3	11
Black shale	5-80	10	
Sandstone	0.5-4	1	
Carbonate	0.1-9	2	
Evaporite	0.1-0.2	0.1	
Metamorphic rocks			
Greenschist grade	0.1-4		
Amphibolite grade	0.1-4		
Granulite	0.05-0.5		
Seawater	0.0003-0.004	0.003	0.00005
Groundwater	0.0001-0.04	0.002	

Table 1 Uranium and thorium contents of common rocks and water. (U compiled by Nash et al., 1981 and Th by Krauskopf, 1967)

Element	Oxidation state	Ionic radius, Å (six-fold coordination)
U	+4	0.97
U	+6	0.80
Th	+4	1.02
Ca	+2	0.99
Zr	+4	0.79
Hf	+4	0.78
Y	+3	0.92
La	+3	1.14
Ce	+3	1.07
Ce	+4	0.91
Ho	+3	0.91
Er	+3	0.89
Lu	+3	0.85
Ta	+5	0.68
Nb	+5	0.77
Ti	+4	0.69

Table 2 Ionic charges and radii for U, Th and elements for which they commonly substitute (from Krauskopf, 1967)

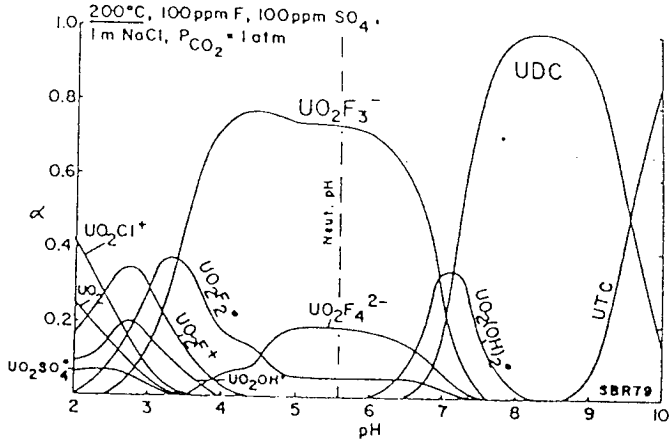

Fig. 1 Distribution diagram showing distribution of uranyl complexes at 200°C in solutions containing 100 ppm F, 100 ppm SO_4 and 1 m NaCl at P_{CO_2} of 1 atm (after Romberger, 1984)

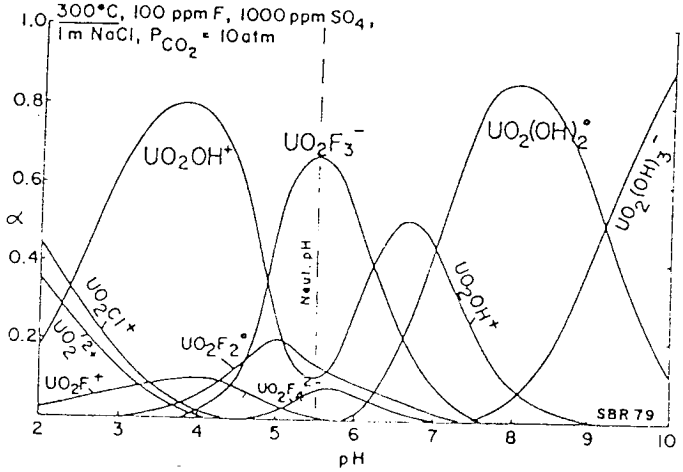

Fig. 2 Distribution diagram showing distribution of uranyl complexes at 300°C in solutions containing 100 ppm F, 1000 ppm SO_4 and 1 m NaCl at P_{CO_2} of 10 atm (after Romberger, 1984)

Table 3 List of uranyl and uranous complexes known to form with various anions (after Romberger, 1984)

H_2O:	U^{4+}, UOH^{3+}, $U(OH)_2^{2+}$, $U(OH)_3^{+}$, $U(OH)_4^{\circ}$, $U(OH)_5^{-}$, UO_2^{2+}, UO_2OH^{+}, $UO_2(OH)_2^{\circ}$, $UO_2(OH)_3^{-}$, $U_2(OH)_5^{3+}$, $(UO_2)_2(OH)_2^{2+}$, $(UO_2)_3(OH)_5^{+}$, U^{3+}, UO_2^{+},
SULFATE:	USO_4^{2+}, $U(SO_4)_2^{\circ}$, $UO_2SO_4^{\circ}$, $UO_2(SO_4)_2^{2-}$,
CARBONATE:	$UO_2CO_3^{\circ}$, $UO_2(CO_3)_2^{2-}$, $UO_2(CO_3)_3^{4-}$,
PHOSPHATE:	$UHPO_4^{2+}$, $U(HPO_4)_2^{\circ}$, $U(HPO_4)_3^{2-}$, $U(HPO_4)_4^{4-}$, $UO_2HPO_4^{\circ}$, $UO_2(HPO_4)_2^{2-}$, $UO_2H_2PO_4^{+}$, $UO_2(H_2PO_4)_2^{\circ}$, $UO_2(H_2PO_4)_3^{+}$,
CHLORIDE:	UCl^{3+}, UO_2Cl^{+}.
FLUORIDE:	UF^{3+}, UF_2^{2+}, UF_3^{+}, UF_4°, UF_5^{-}, UF_6^{2-}, UO_2F^{+}, $UO_2F_2^{\circ}$, $UO_2F_3^{-}$, $UO_2F_4^{2-}$.

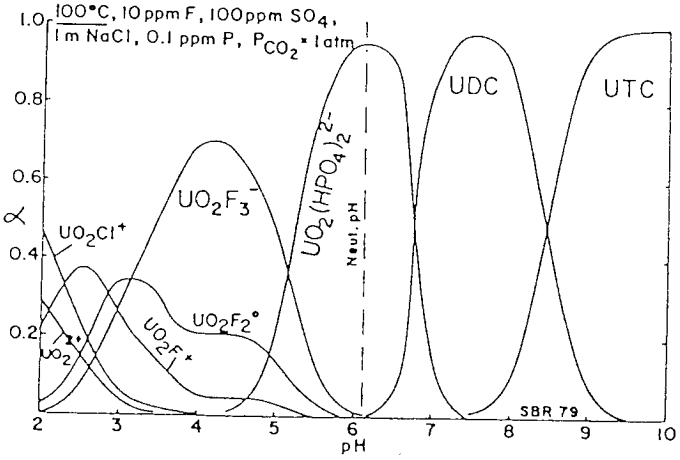

Fig. 3 Distribution diagram showing distribution of uranyl complexes at 100°C in solutions containing 10 ppm F, 100 ppm SO_4, 0.1 ppm P and 1 m NaCl at P_{CO_2} of 1 atm (after Romberger, 1984)

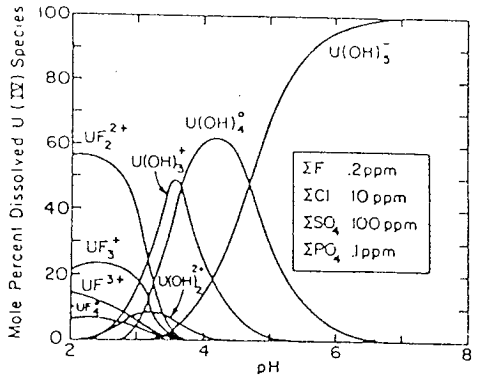

Fig. 4 Distribution of uranous complexes vs pH for some typical ligand concentrations in ground water at 25 C. (after Langmuir, 1978)

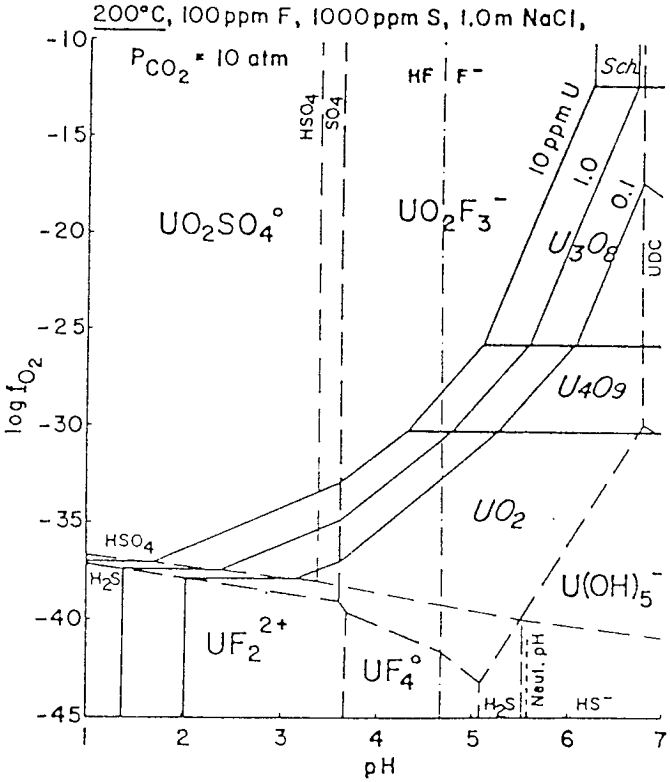

Fig. 5 Log f_{O_2}-pH diagram showing distribution of uranyl and uranous complexes and solubility of uranium oxides at 200°C in solutions containing 100 ppm F, 1000 ppm S and 1 m NaCl at P_{CO_2} of 10 atm (see text for explanation) (after Romberger, 1984)

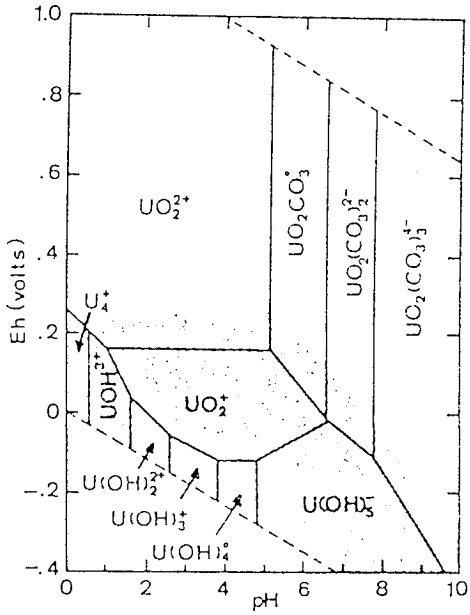

Fig 6 Eh-pH diagram of U-O_2-H_2O-CO_2 system at 25°C and 1 atm for $U = 10^{-6}$ M and $P_{CO_2} = 10^{-2}$ atm. Modified from Langmuir.[10] Upper and lower boundaries within diagram (dotted lines) are limits within which water itself is chemically stable. Above upper limit water is oxidized to give oxygen and below lower limit reduced to yield hydrogen. Stability field for crystalline uraninite shaded; predominant U species in solution indicated in various unshaded areas; unbroken lines represent equilibrium conditions

(modified by Dongarra, 1984 after Langmuir, 1978)

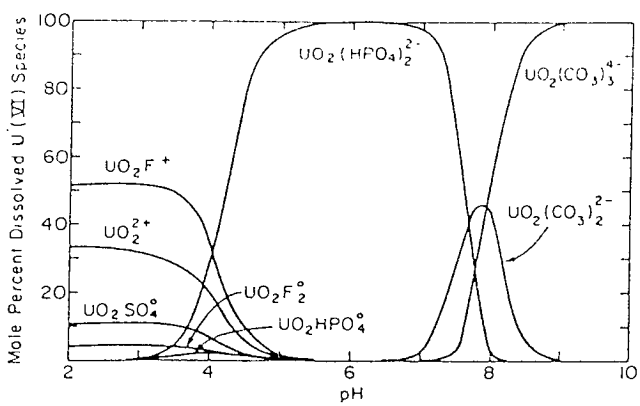

Fig. 7 Distribution of uranyl complexes vs pH for some typical ligand concentrations in ground waters of the Wind River Formation at 25 C. $P_{CO_2} = 10^{-2.5}$ atm, $\Sigma F = 0.3$ ppm, $\Sigma Cl = 10$ ppm, $\Sigma SO_4 = 100$ ppm, $\Sigma PO_4 = 0.1$ ppm, $\Sigma SiO_2 = 30$ ppm.

(after Langmuir, 1978)

Material	Enrichment Factor
Amorphous $Ti(OH)_4$	$8 \times 10^4 - 10^6$
Amorphous Fe(III) oxyhydroxides	$1.1 \times 10^6 - 2.7 \times 10^6$
Peat	$10^4 - 10^6$
Fine-grained natural goethite	4×10^3
Phosphorites	15
Montmorillonite	6
Kaolinite	2

Table 4 Typical enrichment factor (E.F.) values for natural materials (quoted by Langmuir, 1978), where:

$$E.F. = \frac{\text{Wt. of sorbed U per weight of sorbent plus U}}{\text{Wt. of dissolved U per weight of solution}}$$

Ref. No.	Reference	Analytical Details
1	Arribas (1966)	U originally as U_3O_8
2	Harrison (1975)	
3	Harrison et al. (1983)	Recalculated free from impurities and normalised 7 semi-quantitative analyses.
4	Ludwig and Grauch (1980)	
5	Rimsaite (1977)	
6	Silver et al. (1980)	REE include La, Ce, Nd, Ho, Lu
7	Webb and Brown (1984a)	"U-Nb-Ti silicate" U originally as UO_2 and Pb as PbO_2 Also includes 3% Nb_2O_5 and 1.1% Ta_2
8	Kim (1978)	Wt. % H_2O by difference
9	Rimsaite (1983a)	"Coffinite-like" phase S originally as SO_3
10	Rimsaite (1984)	Unidentified Y-Si-U-Th phase
11	Marlow (1981)	Unidentified U-Si phase U originally as U_3O_8 and Pb as Pb
12		8 analyses.
13	Tiangang and Zhizhang (1986)	H
14	Premoli (1982)	

Literature analyses of coffinite and "coffinite-like"

Ref. No.	Reference	Analytical Details
1	Arribas (1966)	U originally as U_3O_8
2	Harrison (1975)	
3	Harrison et al. (1983)	Recalculated free from impurities and normalised 7 semi-quantitative analyses.
4	Ludwig and Grauch (1980)	REE include La, Ce, Nd, Ho, Lu
5	Rimsaite (1977)	"U-Nb-Ti silicate"
6	Silver et al. (1980)	U originally as UO_3 and Pb as PbO_2
7	Webb and Brown (1984a)	Also includes 3% Nb_2O_5 and 1.1% Ta_2O_5
8	Kim (1978)	Wt. % H_2O by difference
9	Rimsaite (1983a)	"Coffinite-like" phase
10	Rimsaite (1984)	S originally as SO_3
11	Marlow (1981)	Unidentified Y-Si-U-Th phase
12		Unidentified U-Si phase
13	Tiangang and Zhizhang (1986)	U originally as U_3O_8 and Fe as Fe_2O_3
14	Premoli (1982)	8 analyses. H_2O by difference Originally as element wt. % 14 analyses.

Literature analyses of coffinite and "coffinite-like" phases

Ref. No.	1	2	3	4	5	6	6	7
ThO_2						3.6	17.3	4.2
UO_2	43.77	79.6	64.32	70.8 - 75.8	75.8	63.3	36.4	30.3
Y_2O_3			8.96			tr	1.1	1.6
CaO	3.72			2.0 - 4.2	1.2	5.4	3.9	0.7
FeO	7.46				0	2.1	16.0	7.56
Al_2O_3	1.61	0.8			1.7		0.7	4.7
MgO	0.95				0.2		0.1	
V_2O_5		2.4						
PbO					0.3	0.3	0.3	2.6
TiO_2					0		0.2	4.5
REE_2O_3						1.8	3.5	0.3
SiO_2	24.09	10.6	22.13	14.3 - 16.8	16.7	13.7	15.5	11.8
P_2O_5	2.1	5.2	4.59				0.4	0.2
S	5.82							
F	2.2					0.5	1.0	
H_2O	6.52							
Total	100.8	98.6	100	88.9 - 94.6	95.9	90.7	96.4	73.4

Ref. No.	8	9	10	11	12	13	14
ThO_2		5.0	14.6	0.5 - 29.6			
UO_2	67.49	64.0	26.0	33.1 - 66.8	67.49	66.30	40.6 - 71.8
Y_2O_3		1.3	20.3				0 - 12.9
CaO	2.34	0.7	0.8	1.49 - 8.3	2.34	0.98	0.8 - 5.9
ZrO_2				0.65 - 2.1			
FeO	0.30	1.9	2.3	0 - 1.22	0.3	0.91	0 - 2.4
Al_2O_3	0.79	2.0	1.1	0 - 0.5		0.79	0 - 3.4
MgO							0 - 0.1
V_2O_5	0.64				0.64		0 - 0.1
PbO	0.38	3.2	0.4	0 - 5.0	0.38	0.92	0 - 3.2
K_2O				0 - 1.85			
TiO_2		0.9		0 - 0.1			0 - 8.5
REE_2O_3			7.8				
SiO_2	15.24	14.9	13.3	10.8 - 15.09	15.24	18.55	5.8 - 16.5
P_2O_5	2.18		1.4		2.18		0 - 6.7
S		0.56					
H_2O	10.65				10.65		
Total	100	95.26	88.0	80.0 - 98.0	100	87.66	73.8 - 88.8

Table 5 Literature analyses of coffinite and "coffinite-like" phases (Wt. % ranges)

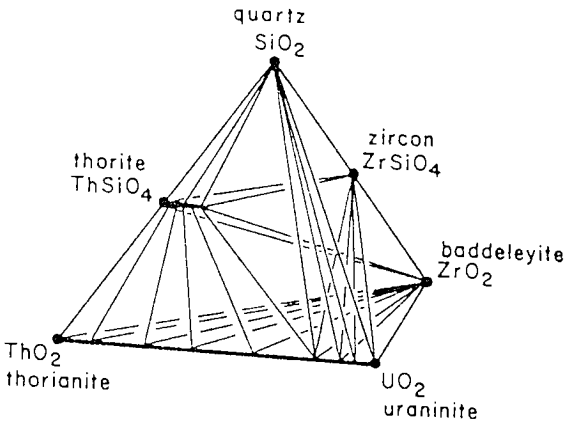

Fig. 8 Subsolidus phase assemblages in the system SiO_2-ThO_2-UO_2-ZrO_2 based on the work of Mumpton and Roy (1961) (after Speer, 1982)

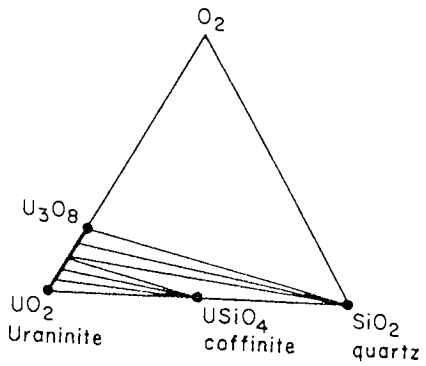

Fig. 9 Possible phase relations in coffinite-bearing assemblages. (after Speer, 1982)

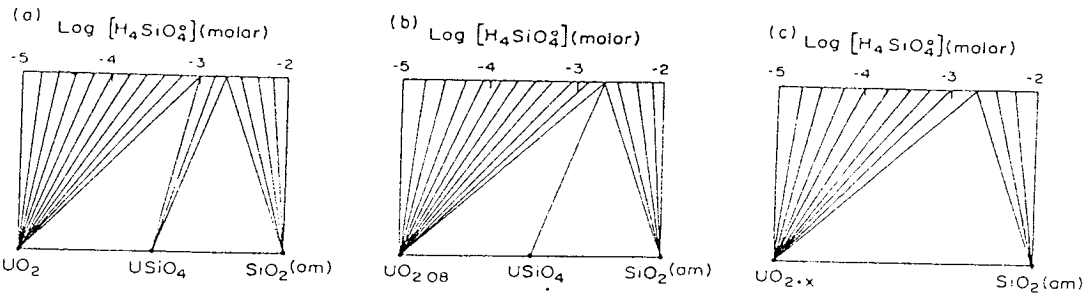

Fig. 10 Possible equilibrium conditions involving dissolved silica (as $[H_4SiO_4^o]$), amorphous silica, coffinite and uraninite of increasing degrees of oxidation. Fig. 10c, $0.08 < x < 0.25$ (after Langmuir, 1978)

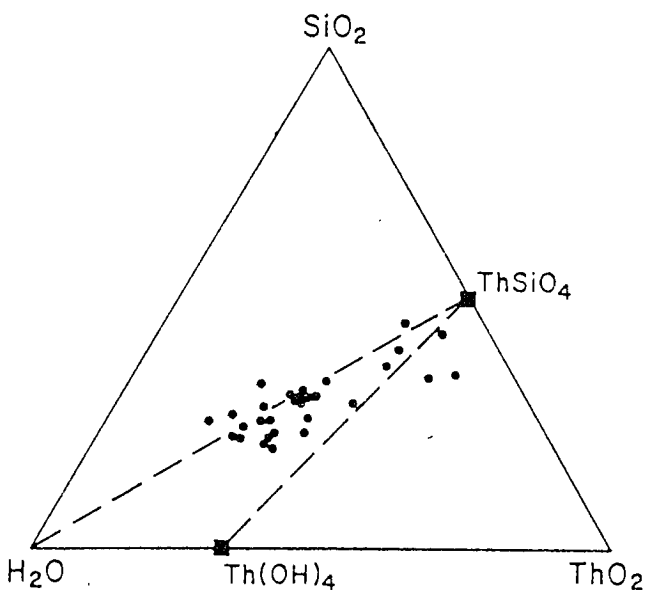

Figure II Compositions of natural thorites plotted on a molecular basis. Substituents for Th are not specified. It is evident that natural thorites are not of the type $Th(SiO_4)_{1-x}(OH)_{4x}$ which would have compositions along $ThSiO_4$-$Th(OH)_4$, but lie along the $ThSiO_4$-H_2O join, indicating that the water is present as molecular water. After Mumpton and Roy (1961).

Ref. No.	Reference	Analytical Details
1	Barritt (1983)	U originally as UO_3 and V as element 11 analyses
2	Webb and Brown (1984)	5 analyses
3	Cameron-Schimann (1978)	U originally as UO_3 and Fe as Fe_2O_3 HREE includes Y_2O_3. Plus < 0.58 % WO_3 5 analyses
4	Foord et al. (1985)	Average of 4 analyses
5	George (1951)	Wet chemical analysis of bluish-green thorite concentrate
6	Heinrich (1963)	U originally as U_3O_8 and Fe as Fe_2O_3 Plus 3.6% SnO_2. Partial analysis by XRF
7	Hutton (1950)	Fe originally as Fe_2O_3
8	Rimsaite (1983a)	S originally as SO_3. 6 analyses.
9	Rimsaite (1984)	
10	Yang and Li (1980)	
11	Semenov and Kazakova (1961)	Fe originally as Fe_2O_3 and Mn as MnO, Plus 1.13 - 0.83 wt% BeO
12	Robinson and Abbey (1957)	11 partial, wet chemical analyses.
13	Silver et al. (1984)	Fe originally as Fe_2O_3 and U as U_3O_8 6 analyses
14	Silver et al. (1980)	
15	Marlow (1981)	
16	Staatz et al. (1976)	Fe originally as Fe_2O_3 and U as U_3O_8 4 analyses by XRF. U originally as UO_3
17	Perez (1985)	and Fe as Fe_2O_3 The high FeO value is probably due to inclusions of Fe-oxide. From 9 analyses.
18	Ballantyne and Littlejohn (1982)	4 of the 7 analyses originally given as mean element wt. % of several analyses. H_2O by difference.
19	Staatz and Brownfield (1986)	Fe originally as Fe_2O_3. 8 analyses.
20	Cathelineau (1987)	
21	Kinnaird (1985)	Plus 1.2 % SnO_2 and 5.95 % L.O.I.
22	Frondel (1958)	12 analyses from a variety of sources. Fe originally as Fe_2O_3 and U as UO_3

Table 6 Literature analyses of thorite/thorogummite

Ref. No.	1	2	3	4	5	6	7	8	9
ThO_2	57.62 - 77.15	50.9 - 66.5	21.2 - 43.1	56.8	69.36	40.4	62.6	32.7 - 50.4	42.6
UO_2	0.19 - 6.07	0.2 - 6.3	4.44 - 35.24	25.4	8.1	3.9	11.5	0 - 21.9	12.5
Y_2O_3	0 - 3.82	0.6 - 3.5	0 - 7.0			2.4		0 - 5.1	3.6
CaO	0 - 2.58	0.5 - 1.9	0 - 10.0				0.3	0 - 5.2	0.3
ZrO_2	0 - 4.55				0.07	1.5		0 - 4.3	
FeO	0.33 - 2.53	1.6 - 4.6	0 - 2.56		0.57	6.0	2.1	0 - 11.1	1.0
Al_2O_3	0 - 2.23	1.0 - 3.0	0 - 8.84		1.25			1.0 - 3.9	1.1
MgO	0 - 0.89	0 - 0.6	0 - 0.16		0.01		0.3	0 - 0.5	
PbO	0 - 0.64	0 - 1.2	0 - 7.78		0.09	0.1	0.47	0 - 4.3	
TiO_2	0 - 0.98	0 - 1.7			0.1			0 - 9.4	0.7
Nb_2O_5	0 - 1.28		0 - 7.81						
MnO	0 - 0.34	0 - 0.1						0 - 0.5	
K_2O	0 - 1.31	0 - 0.5							
V_2O_5	0 - 0.55	0 - 0.6							
LREE	0 - 4.36	0.17 - 2.6	0.08 - 2.63		0.52	3.8	1.1	0 - 10.3	5.5
HREE	0 - 2.07	0 - 0.3	0 - 9.47			0.8		0 - 1.2	
SiO_2	8.50 - 19.98	10.1 - 16.5	13.08 - 24.4	17.3	15.96		19.5	14.3 - 21.4	12.4
P_2O_5	0 - 2.94	1.4 - 7.4	0 - 2.65			2.1		0 - 2.3	2.7
S	0 -1.09							0 - 4.0	0.4
H_2O			9.11 - 13.43		0.82		1.93		
Total	89.10 - 97.65	86.4 - 88.3	85.86 - 101.54	99.5	96.85	61.1	99.8	80.5 - 94.9	83.5

Table 6 Literature analyses of thorite/thorogummite (Wt. % ranges)

Ref. No.	10	11	12	13	14	15
ThO_2	50 - 50.24	41.5 - 51.66	39.46 - 58.98	32.9 - 61.3	47.7	32.5 - 58.9
UO_2	25 - 30	0 - 0.77	1.62 - 19.94	0.9 - 9.9	2.2	5.77 - 29.0
Y_2O_3				tr - 8.0	5.1	
CaO		1.54 - 4.33	2.16 - 5.75	0.4 - 2.4	1.5	0.7 - 2.5
ZrO_2				0 - 4.4	5.6	0 - 9.2
FeO	0 - 3.23	2.83 - 4.71	0.18 - 3.56	2.0 - 11.2	0.6	0 - 1.0
Al_2O_3		2.04		0 - 2.1	0.7	0 - 1.4
MgO		0.07		0 - 0.2		
PbO		1.27 - 0.88	0.50 - 3.62	0 - 1.1		0 - 3.2
TiO_2		5.19 - 1.6		0 - 0.8	0.6	0 - 0.8
Nb_2O_5		1.75		0 - 7.0	0.6	
Ta_2O_5				0 - 0.2	0.3	
MnO		9.01 - 1.39				
K_2O						
V_2O_5						
HfO_2						
LREE		1.27 - 2.5	<0.2 - 4.00	0 - 0.3	0.2	
HREE				0.3 - 4.8	1.00	
SiO_2	19.37 - 20	13.92 - 16.83	17.62 - 21.06	tr - 4.6	3.6	
P_2O_5				11.6 - 25.9	17.7	9.2 - 17.4
F				0.2 - 1.9	1.1	
C				0.5 - 1.1	0.7	
CO_2			0 - 0.59			
H_2O		14.8 - 26.4	0 - 0.54 8.92 - 11.1			
Total			86.27 - 101.29	91.8 - 100.2	89.2	65.9 - 96.2

Table 6 Literature analyses of thorite/thorogummite (Wt. % ranges)

Ref. No.	16	17	18	19	20	21	22
ThO_2	49.2 - 57.4	33.39 - 63.93	48.0 - 56.6	57.05 - 74.75	38.27	63.00	21.20 - 72.93
UO_2	3.25 - 14.12	0.33 - 11.33	3.0 - 23.4	0.39 - 0.78	13.84	1.33	0.41 - 35.60
Y_2O_3	5.1 - 6.24	2.35 - 11.4	0.8 - 12.6	0.40 - 5.10	11.79		
CaO		0.32 - 2.2	0 - 2.6	0.53 - 1.19	4.73		0.35 - 4.38
ZrO_2		0 - 9.55			0	0.84	0.05 - 4.78
FeO	0.26 - 4.5	0.02 - 25.76	0 - 5.4	7.16 - 24.22	0.16	3.10	0.58 - 14.37
Al_2O_3	0.34 - 0.6				0		0.13 - 8.84
MgO							0.01 - 0.60
PbO	0 - 0.7		0 - 1.2	0.10 - 2.15	0	0.13	tr - 7.90
TiO_2					0		0.04 - 0.13
LREE	1.1 - 2.33	0.12 - 6.4				1.92	tr - 0.57
HREE	10.55 - 13.33					1.4	0.25 - 12.19
SiO_2	7.00 - 13.2	9.32 - 21.51	9.2 - 22.9	8.17 - 12.30	8.47	12.80	7.64 - 22.03
P_2O_5	0.25 - 0.80	0 - 1.32	0 - 6.0	0 - 0.29	13.60		tr - 7.46
F		0 - 1.02					
H_2O	6.1 - 9.7		0 - 24.5				0.22 - 15.18
Total	99.23 - 99.48	84.60 - 91.09	80.1 - 100	91.35 - 96.40	90.97	91.68	96.5 - 100.49

Table 6 Literature analyses of thorite/thorogummite (Wt. % ranges)

	A	B	X
Major:	Th, U^{4+}, U^{6+}	Si	O
Minor:	Fe^{3+}, Ca	H, P	
Trace:	Mn, Ti, Nb, Ta, Fe^{2+}, Al, Pb, Be, Mg, Ge, Sn, Zr, Hf, Zn, K, Na, Cu, Ce, La, Pr, Nd, Sm, Eu, Gd, Tb, Dy, Ho, Er, Tm, Yb, Lu, Y	S, As, B	F, Cl (?) CO_2 (?)

Table 7 Elements which have been reported as occurring in thorite, huttonite and coffinite with the general formula ABX_4 (after Speer, 1982)

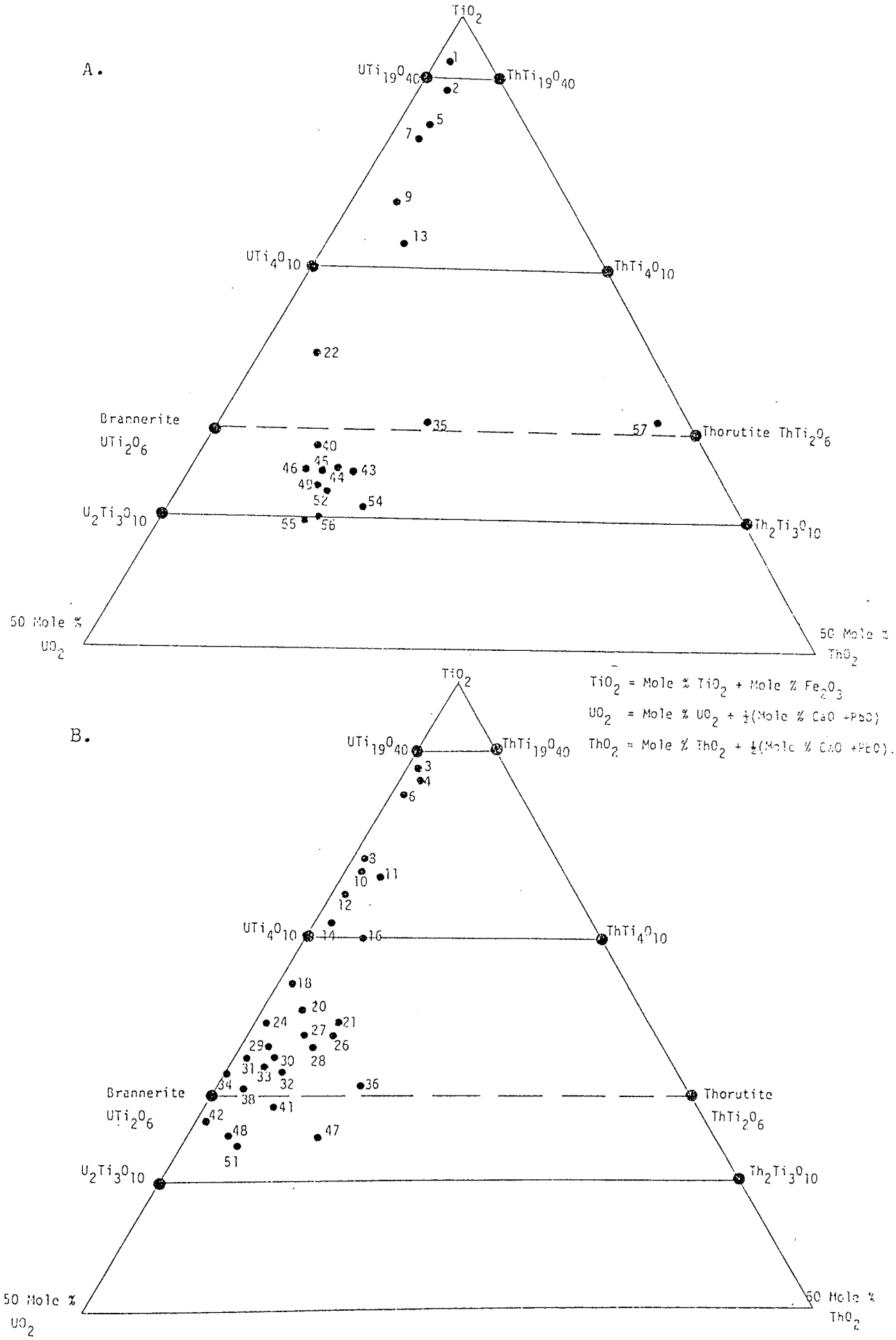

Fig. 12 EPMA data of brannerite expressed as molecular %
A. Annealed (35, 40, 45-54) and natural (1-22, 43, 44, 55, 56) brannerite from Crockers Well, South Australia
B. Analyses of Ferris and Ruud (1971)
(after Jenkins, 1974)

Grain No.	4			8			18	
An. Spot	1	2	3	1	2	3	1	2
UO_2	27.21	10.83	4.93	41.59	17.19	27.22	49.67	55.46
ThO_2	2.04	0.81	0.31	2.68	0.67	1.93	1.64	1.91
CaO	0.41	0.26	0.19	nd	0.64	0.40	-	0.27
TiO_2	20.52	10.16	4.47	26.93	13.80	16.40	11.95	7.13
FeO	4.72	9.95	1.76	3.54	14.54	12.77	11.12	7.0
PbO	0.52	1.00	0.15	4.75	9.13	5.52	4.68	5.04
Al_2O_3	-	-	2.24	1.58	12.59	5.48	-	-
SiO_2	26.9	55.78	87.8	12.89	16.7	14.53	15.77	10.73
S	0.80	5.00	0.73	0.76	1.18	6.94	7.55	3.01
Total	83.12	93.79	102.58	94.72	86.44	91.19	102.38	90.55

- not determined nd not detected

Table 8 EPMA of uraniferous inclusions in phyllosilicates (Plate 3) and porous pyrite clasts (Plates 1 and 5) from conglomerate (Sample 1022), Wiwatersrand basin, South Africa

Table 9. The pyrochlore group

SUBGROUPS defined by B atoms viz: Nb, Ta, Ti			PYROCHLORE Nb+Ta>2Ti Nb>Ti	MICROLITE Nb+Ta>2Ti Ta≥Nb	BETAFITE 2Ti≥Nb+Ta
SPECIES defined by A-atoms: K, Sn, Ba, REE, Pb, Bi, U	Na+Ca, but no other A-atoms >20% total A-atoms		pyrochlore	microlite	
	One or more A-atoms, other than Na or Ca, >20% total A-atoms. Species named by most abundant A-atom, other than Na or Ca	K	kalipyrochlore		
		Sn		stannomicrolite	
		Ba	bariopyrochlore	bariomicrolite	
		REE*	yttropyrochlore(ΣY>ΣCe)** ceriopyrochlore(ΣCe>ΣY)		yttrobetafite(ΣY>ΣCe)
		Pb	plumbopyrochlore	plumbomicrolite	plumbobetafite
		Bi		bismutomicrolite	
		U	uranpyrochlore	uranmicrolite	betafite

*REE = Y + (La + Lu), and for purposes of species definition, REE counts as one A-atom.
**ΣY = Y + (Gd + Lu); ΣCe = La + Eu.

(after Hogarth, 1977)

Plate No.	Sample No.	Grain No.	Description
			Conglomerate from the Orange Free State, Witwatersrand basin, South Africa
1	1022	8	Porous pyrite concretion with position of a U-Ti phase inclusion marked (EPMA spot 1). (RPPL)
2	"	"	Lexan of same concretionary pyrite, showing point sources of U in phyllosilicates (EPMA spot 1). (TPPL)
3	"	4	Granule of phyllosilicates, with positions of U-Ti phase inclusions marked (analyses in Table 8). (TPPL)
4	"	"	Lexan of the same granule, showing point sources of U. (TPPL)
5	"	8	U-Ti phase inclusion (A) in porous pyrite (B) concretion (EPMA spot 1 in Plate 1). (SEM)
6	"	"	X-ray map for U of the inclusion in Plate 5. (SEM)
7	"	"	X-ray map for Ti of the inclusion in Plate 5. (SEM)
8	"	"	X-ray map for Pb of the inclusion in Plate 5. (SEM)


1
1
300µm

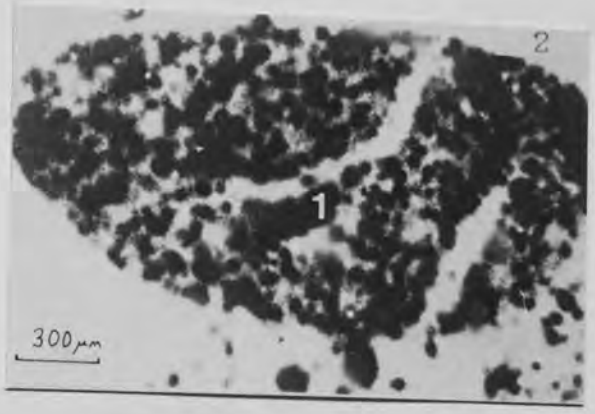
2
1
300µm

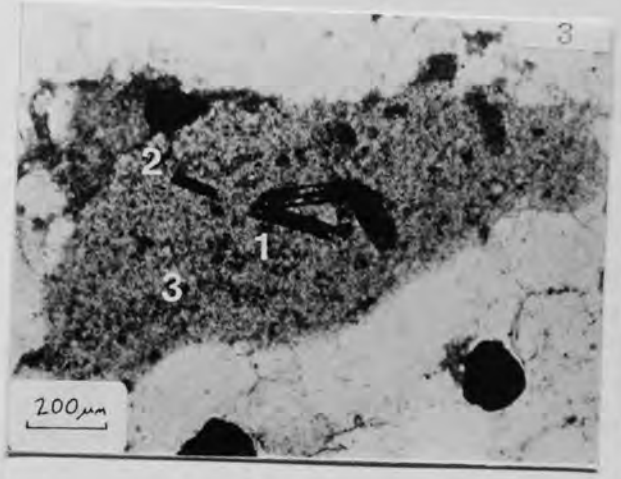
3
2
1
3
200µm

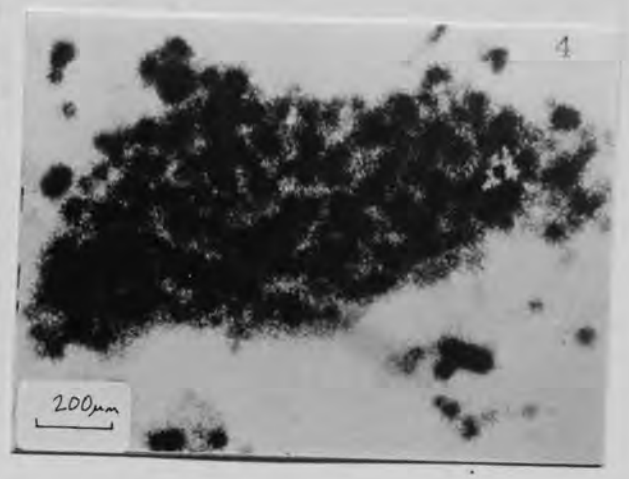
4
200µm

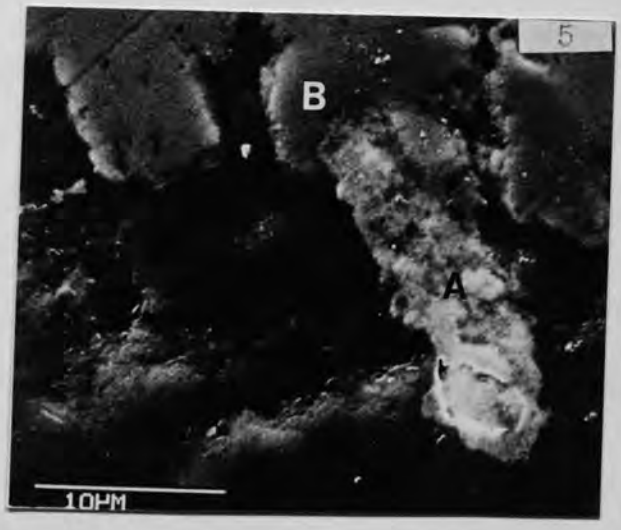
5
B
A
10µM

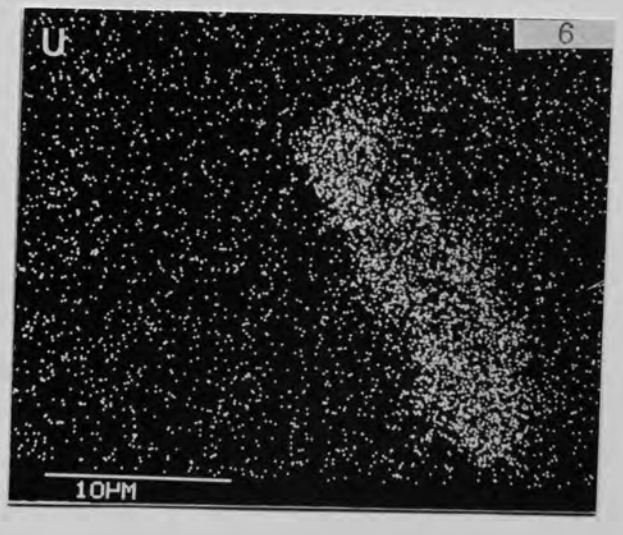
U
6
10µM

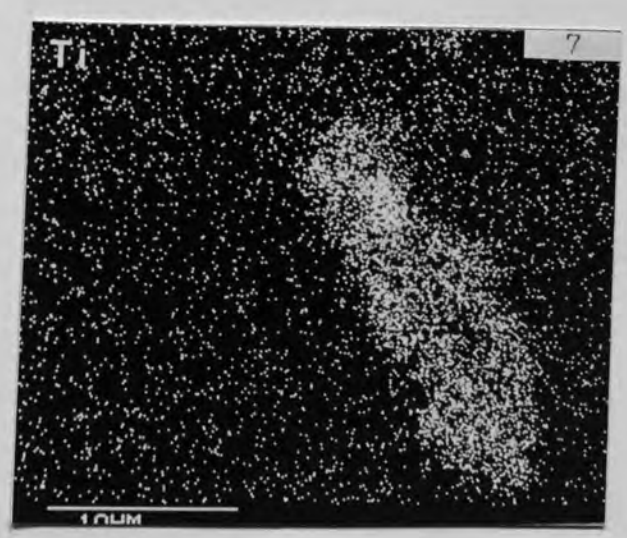
Ti
7
10µM

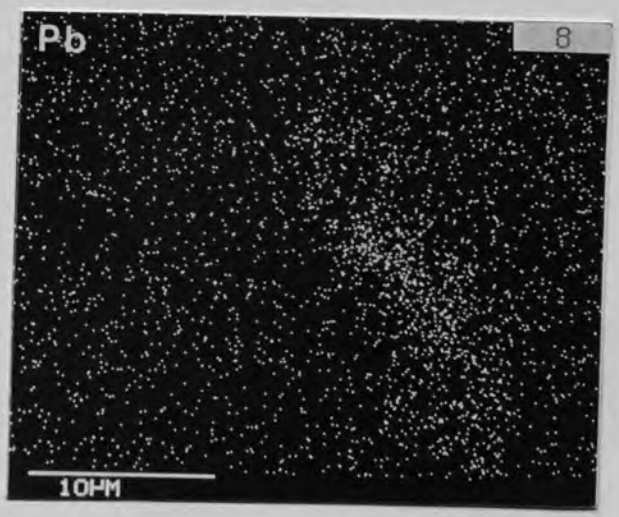
Pb
8
10µM

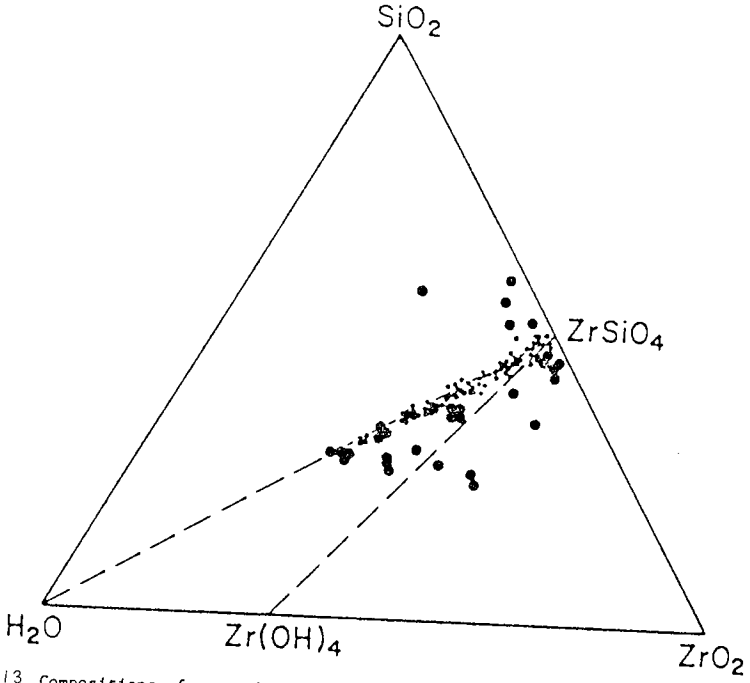

Figure 13 Compositions of natural zircons plotted on a molecular basis. Substituents for Zr are not specified. Zircons of the type $Zr(SiO_4)_{1-x}(OH)_{4x}$ would lie along the $ZrSiO_4$-$Zr(OH)_4$ join, whereas zircons with molecular water lie along the $ZrSiO_4$-H_2O join. Large circles are literature values compiled by Mumpton and Roy (1961). Small circles are based on microprobe analyses where (OH) is calculated from $((Si,P,Al)O_4)_{1-x}$ + $(OH)_{4x}$ and molecular H_2O obtained by difference from the oxide sum (Sommerauer, 1976).

(after Speer, 1982)

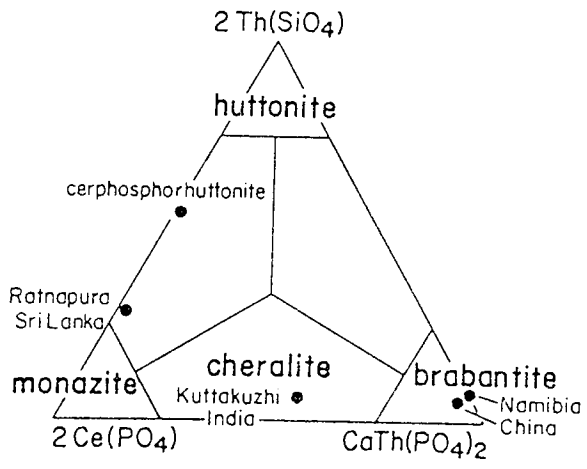

Figure 14 Nomenclature for the monazite-structure silicate and phosphate minerals. Plotted analyses are the recently described brabantites as well as the intermediate composition minerals from Kuttakuzhi and Ratnapura (Bowie and Horne, 1953) and the Russian "cerphosphorhuttonite" (Pavlenko *et al.*, 1965).

(after Speer, 1982)

1. Absorption of H_2O; presence of Pb, Tl, He.
2. Decrease in refractive index and birefringence.
3. Broadening of X-ray peaks.
4. Increasingly larger cell parameters.
5. Decreasing density.
6. Decreasing hardness and loss of hardness anisotropy.
7. Increasing thermoluminescence.
8. Darker colour.
9. Increasing susceptibility to chemical attack.
10. Increasing chemical diffusion.
11. Broadening and decreased intensity of the optical and infra red absorption spectra with loss of polarised spectra.
12. Decreased thermal conductivity.
13. Decreased elastic constants.

Table 10 Radiation effects detected in zircon with increasing metamictisation (after Speer, 1982)

A	Radius	A	Radius	B	Radius
Zr^{+4}	0.84	Pb^{+2}	1.29	Si^{+4}	0.26
Hf^{+4}	0.83	Pb^{+4}	0.94	Al^{+3}	0.39
Y^{+3}	1.02	Ca^{+2}	1.12	P^{+5}	0.17
U^{+4}	1.00	Fe^{+3}	0.78	S^{+6}	0.12
Th^{+4}	1.05	Fe^{+2}	0.92		
La^{+3}	1.16	Na^{+1}	1.18		
↓		K^{+1}	1.51		
REE		Ti^{+4}	0.74		
↓		Nb^{+5}	0.74		
Lu^{+3}	0.98	Ta^{+5}	0.74		

Table 11 Ionic radii (in Ångstroms, from Shannon, 1976) of elements substituting for 8-coordinated Zr(A) and 4-coordinated Si(B) in zircon (ABO_4)

HfO_2 wt % range	No. of Analyses	Reference
1.7-3.4	3	Silver et al. (1980)
1.6-4.8	16	Silver et al. (1984)
1.0-1.4*	3	Webb and Brown (1984a)
0.9-1.7*	7	Webb and Brown (1984b)
1.2-3.1	5	Rimsaite (1981a)
1.02-3.89*	47	Barritt (1983)
0.59-2.02	7	Cameron-Schimann (1978)
1.30	1	Romans et al. (1975)
5.13	1	Tole (1985)

* originally as Hf_2O_3

Table 12 HfO_2 contents of zircon

Key to references in Figs. 15A and 15B

1 Silver et al. (1980)
2 Silver et al. (1984)
3 Webb and Brown (1984 a and b)
4 Deer et al. (1966)
5 Barritt (1983)
6 Vlasov (1966b)
7 Perez (1985)
8 Romans et al. (1975)
9 Tole (1985)
10 Jefford (1962)
11 Heinrich (1963)
12 Harrison et al. (1983)
13 Premoli (1982)
14 Cameron-Schimann (1978)
15 Rimsaite (1983)
16 Rimsaite (1984)
17 Marlow (1981)
18 Staatz et al. (1976)
19 Ballantyne and Littlejohn (1982)
20 Staatz and Brownfield (1986)
21 Cathelineau (1987)
22 Frondel (1958)
23 Kinnaird (1985)

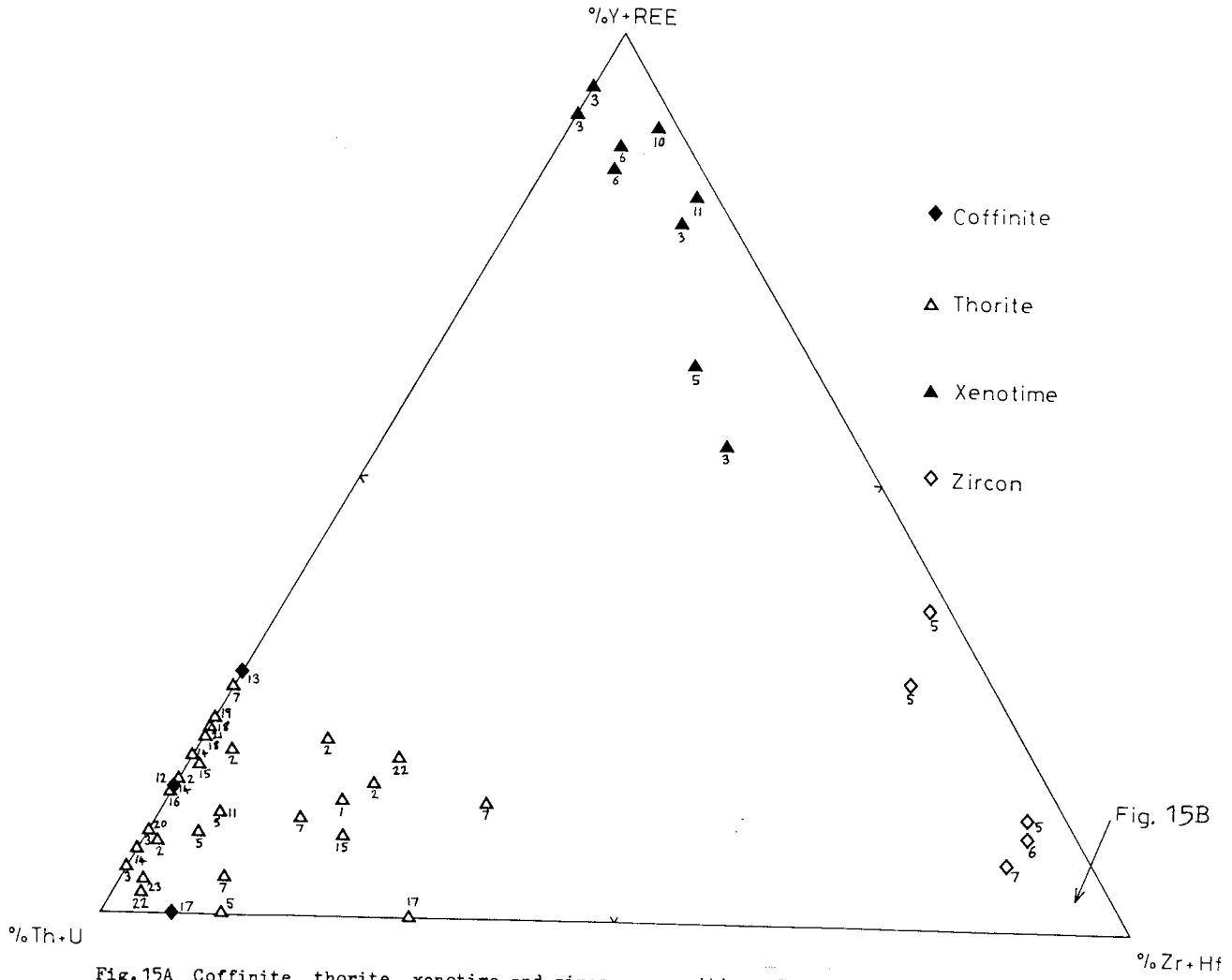

Fig. 15A Coffinite, thorite, xenotime and zircon compositions from the literature plotted as mole %

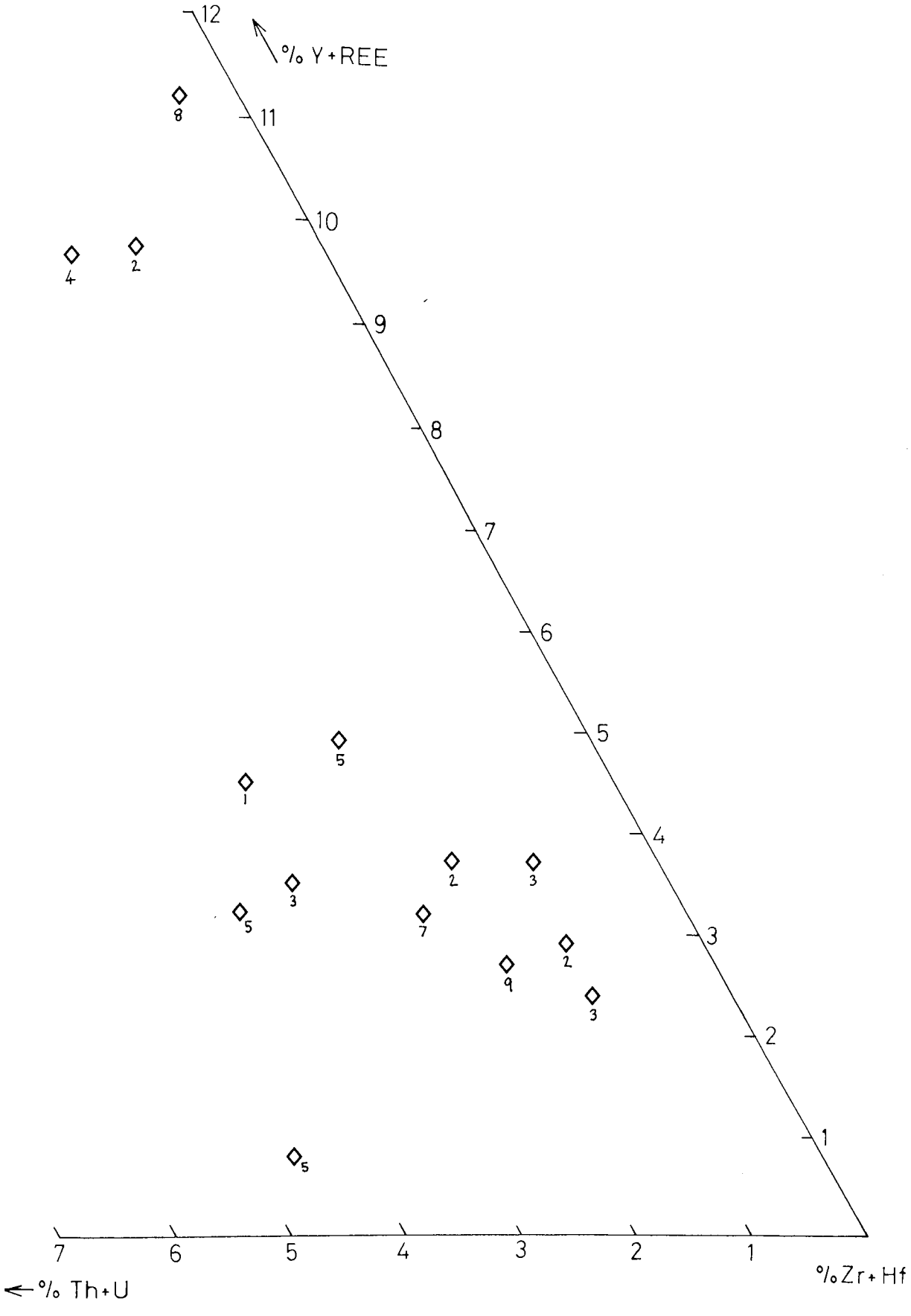

Fig. 15B Zircon compositions from the literature plotted as mole %

Table 13 U and Th contents of zircon
(Partly compiled from a review by Speer, 1982)

U*	Th*	Details	Reference
5		In kimberlite	Kresten et al. (1975); Davis (1976)
7 wt%		In pegmatite	Muench (1931)
		In metasomatic rocks,	Pavlenko et al. (1957)
	10 wt%	co-existing with thorite and thorianite,	"
0.5 wt%		co-existing with uraninite.	"
	2	Kimberlite	
4.46 wt%	3.23 wt%	Max. values by EPMA.	Ahrens et al. (1967)
5-4000	2-2000		Medenbach (1976)
	<300	Co-existing with thorite	Gorz (1974); Ahrens et al. (1967)
			Steiger and Wasserburg (1966);
700	700	Co-existing with uraninite and thorite	Silver and Deutsch (1963)
>300	>100	In granitoids	Effimoff (1972)
47	5	Average) In kimberlites and mantle	Ahrens et al. (1967)
4.8-440		Range) xenoliths	Ahrens et al. (1967); Kresten (1974)
1330	560		Davis (1976; 1977)
100-6000	100-10000		Rogers and Adams (1969)
1330	630	Average of 72 zircons from granitoids	"
300		Homogeneously distributed in zircon	Ahrens (1965)
500		Margins of zircon) Veporides	Chovan and Kral (1979)
150		Centres of zircon) Czechoslovakia	"
8000		In pegmatite	"
<5	<1	Moles % $USiO_4$ and $ThSiO_4$ respectively,	Grauert and Seitz (1973)
		compiled from 90 published analyses	Mumpton and Roy (1961)
600-800		Helmsdale granite, Scotland	
100-1000	1-2 wt%	Bois Noirs Granite	Pidgeon and Aftalion (1978)
636		Geometric mean of 963 zircon separates	Cuney (1978)
		from igneous rocks of the U.S.A.	Stuckless and VanTrump (1982)

* values in ppm unless otherwise specified

Table 13 (continued)

U*	Th*	Details	Reference
<2.4 wt%	<0.4 wt%	East Highlands granites	Webb and Brown (1984a)
<0.5 wt%	<1.1 wt%	Shap granite, Lake District	"
<1.1		Skiddaw granite	"
155-320		In metaquartzite	Grauert et al.(1974)
540-850		In metaquartzite inclusions in pegmatite	"
1900		Rim)	"
100		Core)	"
0.5-1.3wt%	0.78 wt%	Cyrtolite	Yeliseyeva (1977)
500-2600		Zircon	"
710-1620		Zircon	Berzina et al.(1974)
5000-13000		Cyrtolite	"
300-4400		Core)	Pagel (1982)
3.1 wt%		Rim)	"
	1.8-2.6wt%	Maximum values in metamict zircon	Vlasov (1966b)
.85-2.54wt%			"
	7.8 wt%	Maximum values	Rimsaite (1981a)
6.8 wt%			"
Th/U ratios			
0.47		Mean average (72 zircons from	Ahrens (1965)
0.35		Modal average granitic rocks)	"

* values in ppm unless otherwise specified

Table 14 U and Th contents of monazite

U %	Th %	Details	No. of Analyses	Reference
0.3	12.5	Variety of sources		Rogers and Adams (1969)
0.05-0.3	4.97	"		"
	2-20	"		"
0.21-2.01	5.64-11.08	Carnmenellis granite, Cornwall	21	Jefferies (1985a)
0.1-0.9	2.6-16	East Highlands granites, Scotland	3	Webb and Brown (1984a)
	6.2-6.8	Skiddaw granite	2	Webb and Brown (1984b)
<0.99	<3.57	Taghouaji ring complex, Niger	11	Perez (1985)
<0.88	2.33-12.2	Cairngorm and Starav granites, Scotl.	12	Barritt (1983)
<1.5	2.4-13.6	Lawler Peak granite, S.W. U.S.A.	9	Silver et al. (1984)
0.14-0.52	5.53-13.14	N. Saskatchewan and Quebec, Canada	6	Cameron-Schimann (1978)
0.1-0.4		São Pedro do Sul granite, Portugal		Basham et al. (1982d)
	1.4-14.7	Total range	222	Price et al. (1982)
	4.8	Total Mean	222	"
0.26-1.18	1.87-8.66	Range of mean values by site	222	"
0.78-2.29	5.1-8.12	Variation within one grain	20	"
1.24	5.94	Mean values of this grain	20	"
	3.5-11.1	Variation within another grain	3	"
	1.85-24.78	Various localities	7	Vlasov (1966b)
0.16-0.26		Veporides, Czechoslovakia	13	Chovan and Kral (1979)
	3.51-8.67	Variation within a grain	1	Cameron-Schimann (1978)
	2.3-7.12	Centre to edge respectively	2	Silver et al. (1980)
0.18-1.04	2.65-12.76	Compilation of various sources	7	Deer et al. (1962)

Table 15 U and Th contents of xenotime

U %	Th %	Location	Details	Reference
0.8-2.8	0.7-4.6	East Highlands granites, Scotland.		Webb and Brown (1984a)
1.4	1.1	Skiddaw granite, Lake District.		Webb and Brown (1984b)
0.7-2.26	0.31-2.29	Cairngorm granite, Scotland.		Barritt (1983)
0.79-1.25	0.54-5.6	" "	Xenotime/zircon.	"
3.79	3.73	Baie Johan Beetz area, Quebec, Canada.		Cameron-Schimann (1978)
0.48	0.2	" "	Churchite alteration rim to above grain.	"
0.19	0.83	Alkali granite, Rayfield, Nigeria.		Jefford (1962)
	0.88	Granite in the Urals.		Various sources in Vlasov (1966b)
2.79	2.17	Isaka, Japan		"
3.64		Brindletown, North Carolina		"
1.47	0	Pegmatite in North Carolina		"
3.64	0	" "		"
1.15-2.38	0.7-0.97	Lawler Peak Granite, S.W. U.S.A.	Within one grain	Silver et al. (1980)
1.2	0.8	" "	Grain centre	Silver et al. (1984)
1.9	0.9	" "	Grain edge	"
0.3-1.7	0.2-1.2	" "	5 analyses	"
0.31	0.97	Alkali granite, Jos-Bukuru complex Nigeria		Heinrich (1963)
0-0.42	0.02-0.37	Graphite schist, Azad Kashmir, Pakistan	Detrital grains	Rahman (1979)
	6.1	Th-rich veins, Bokan Mountain, S.E. Alaska		Staatz (1978)
0.03-4				Rogers and Adams (1969)

Table 16 U and Th contents of allanite (and epidote where specified)

U*	Th*	Details	Reference
30-650	0.31-1.96 %	Variety of sources	Deer et al. (1966)
200	0.91 %	" "	Rogers and Adams (1969)
30-1000	0.1-2 %	" "	"
0.3 %	0.35-0.6 %	Hercynian granites, Vosges, France	Pagel (1982)
	1.2 %	Lawler Peak granite, S.W. U.S.A.	Silver et al. (1984)
	1.8 %	Liberty Hill pluton, S. Carolina.	Speer et al. (1981)
0	1.56 %	N.E. Cairngorm granite, Scotland.	Barritt (1983)
0	1.4-1.5 %	Rim and centre respectively. Baie Johan Beetz area, Quebec.	Cameron-Schimann (1978)
40-177		Biotite granodiorite, Veporides, Czechoslovakia	Chovan and Kral (1979)
175-882		Biotite granite " "	"
0.1 %		Granite, Baffin Island, N.W.T., Canada	Maurice (1982)
0.1-1.1 %	1.0-1.3 %	Bancroft area, Ontario (rim and core respectively)	Rimsaite (1981b)
2.2-3.2 %	1.1-3.6 %	Altered allanite, Mont Laurier area, Quebec	Rimsaite (1982b)
50- >300		Metamorphic, secondary in Precambrian granite Olden Window, Sweden.	Smellie (1982b)
< 0.1 %	0.7-3.5 %	E. Highlands granites, Scotland.	Webb and Brown (1984a)
	2.2 %	Shap granite, Lake District.	Webb and Brown (1984b)
50-500		Low and high Fe areas respectively of allanite from Mount Osceola and Conway granites, New Hampshire, U.S.A.	Caruso and Simmons (1985)
43	200	Epidote	Rogers and Adams (1969)
20-200	50-500	"	"
20-150		Epidote, remobilised along fractures and grain boundaries in Precambrian granites, Olden Window Sweden.	Smellie (1982b)
< 7000		Epidote, deuteric in leucogranite, Namaqualand metamorphic complex, South Africa.	Robb and Schoch (1985)
36-656	0.35-2.23 %		Smith et al. (1957)
150-400	0.23-1.79 %	Range in a compilation of 10 analyses.	Deer et al. (1962)

* values in ppm unless otherwise specified

Table 17 U and Th contents of apatite

U ppm	Th ppm	Details	Reference
	1900	Bancroft area, Ontario.	Rimsaite (1980)
<1000	<1000	E. Highlands granites, Scotland.	Webb and Brown (1984a)
6000		Francolite (CO_2-, F-bearing apatite) from Egypt.	El Shazly et al. (1974)
800	0	Outer Starav granite, Etive complex, Scotland.	Barritt (1983)
15-67		Range of 7 analyses.	"
65	70	Granite from Veporides, Czechoslovakia	Chovan and Kral (1979)
10-100	50-250	Various sources.	Rogers and Adams (1969)
10-100		"	"
		Igneous rocks	Clarke and Altschuler (1958)
50-300			"
30-280		Sedimentary rocks	Thiel et al. (1972)
		Lunar basalt.	

Table 18 U and Th contents of sphene

U*	Th*	Details	Reference
40-250		Secondary, metamorphic. Precambrian granite, Olden Window, Sweden.	Smellie (1982b)
0.2 %	0.4 %	Shap granite, Lake District.	Webb and Brown (1984b)
<0.1 %	<0.1 %	E. Highlands granite, Scotland.	Webb and Brown (1984a)
50-130		Granitoids, U.S.S.R.	Yeliseyeva (1977)
100-150		Granite, Baffin Island, N.W.T., Canada.	Maurice (1982)
0-0.33	0.04-0.3 %	Etive complex and Cairngorm granite, Scotland	Barritt (1983)
	0.25 %	Sphene beach sand, Wainu inlet, N. W. Nelson New Zealand.	Hutton (1950)
<1.2 %	<0.03 %	Maximum contents in dendritic sphene over-growths from Sierra Nevada batholith, California	Sawka and Chappell (1985)
0.2 %		Average contents of the same overgrowths.	"
280	510	Variety of sources	Rogers and Adams (1969)
10-700	100-1000	" "	"
50-160		Granites from Nikazakhstan, U.S.S.R.	Berzina et al. (1974)
600		As fracture fillings in hydrothermally altered granite, Eye-Dashwa Lakes pluton, N.W. Ontario.	Kamineni (1986)

* values in ppm unless otherwise specified

Autunite group	$A(UO_2)_2(XO_4)_2.8\text{-}12\ H_2O$ where: A = Ca, Mg, Fe^{+2}, Cu, Ba, Na_2, Mn X = P, As, V
*Autunite	$Ca(UO_2)_2(PO_4)_2.10\text{-}12\ H_2O$
*Torbernite	$Cu(UO_2)_2(PO_4)_2.8\text{-}12\ H_2O$
Meta-autunite group	$A(UO_2)_2(XO_4)_2.4\text{-}8\ H_2O$ where: A = K_2, $(NH_4)_2$, Ca, Ba, Mg, Fe^{+2}, Co, Cu, Zn X = P, As
*Meta-autunite	$Ca(UO_2)_2(PO_4)_2.2\text{-}6\ H_2O$
*Meta-torbernite	$Cu(UO_2)_2(PO_4)_2.8\ H_2O$
*Kasolite	$Pb(UO_2)SiO_4.H_2O$
Carnotite	$K_2(UO_2)_2(VO_4)_2.3\ H_2O$
Tyuyamunite	$Ca(UO_2)_2(VO_4)_2.5\text{-}8\ H_2O$
Uranophane	$Ca(UO_2)_2Si_2O_7.6\ H_2O$

* Identified in the Helmsdale area (Chapters 6-8)

Table 19 Some of the more important uranyl minerals

Mineral	Range U ppm
Quartz	0.1 - 10
Feldspar	0.1 - 10
Muscovite	2 - 8
Biotite	1 - 60
Hornblende	0.2 - 60
Pyroxene	0.01 - 50
Olivine	0.05
Garnet	6 - 30
Ilmenite	1 - 50

Table 20 U content (ppm) of igneous rock-forming minerals (data from compilations by Clark et al., 1966 and Rogers and Adams, 1967)

Table 21 U and Th contents of TiO_2

U ppm	Th ppm	Details	References
3200		Leucoxene aggregates in weathered conglomerates; Pongola Supergroup, South Africa.	Saager et al. (1981)
7000	3000	Alteration rim to brannerite; Lawler Peak granite, S.W. U.S.A.	Silver et al. (1984)
170-340		Leucoxene replacement of sphene.	Berzina et al. (1974)
0.7-2.4		Rutile and anatase.	"
190		Rutile; Granites from N. Kazakhstan, U.S.S.R.	"
22-31		Rutile; São Pedro do Sul granite, Portugal.	Basham et al. (1982d)
1600	1300-2500	Anatase/ilmeno-rutile; amphibolite and biotite granite, Taghouaji Complex, Niger.	Perez (1985)
6000		Yellowish alteration of sphene.	Goni (1957)
108-557		Leucoxene; Uitkyk Formation, Pietersburg greenstone belt, South Africa.	Thiel et al. (1979)
256-27800		Basal Reef, Witwatersrand Basin, South Africa.	"

Table 22 U and Th contents of Fe-oxide

U ppm	Th ppm	Details	References
18.21	34.23	Mean contents.	Kamineni (1986)
15.9-21.2	29-38	Ranges.	"
		Goethite fractures in hydrothermally altered granite from Eye-Dashwa pluton, N.W. Ontario.	
200-600		Fe-hydroxide coatings around clasts in weathered conglomerates, Pongola Supergroup, South Africa.	Saager et al. (1981)
50-190			"
10-40		Dispersed hydroxy Fe-oxides in Precambrian granites from the Olden Window, Sweden.	Smellie (1982b)
1-30	0.3-20	Magnetite	Rogers and Adams (1969)
2.7-11.6		Haematite grains.	Yeliseyeva (1977)

Table 23 U and Th contents of phyllosilicates

U*	Th*	Details	Reference
100´s		Biotite intersected by microfractures.	Maurice (1982)
5-150		Sericitised plagioclase; Baffin Island, N.W. Territory.	"
100-300		Relatively fresh biotite; Leucogranite, Namaqualand complex, South Africa.	Robb and Schoch (1985)
1-60	0.5-50	Biotite.	Rogers and Adams (1969)
2-8		Muscovite.	"
10	11	Kaolinite.	Kamineni (1986)
<1 %		Zeolite	Katayama et al. (1974)
6.5-9,000		Clay minerals; Uitkyk Formation, Pietersburg greenstone belt, South Africa.	Thiel et al. (1979)
0.55-0.69 %		Basal Reef, Wiwatersrand Basin, South Africa.	"

Table 24 U and Th contents of organic matter

U*	Th*	Details	References
<200		Kupferschiefer.	Barthel (1974)
<400		Rotliegende coal and shale.	"
<23 %	<2 %	Hydrocarbon mantles around uraninite; São Pedro do Sul granite, Portugal.	Basham et al. (1982d)
2400		"Thucolite"	Robinson (1950)
<20 %		"	Bowie (1955)
	4500	Hydrocarbon in fossil fish.	Bowie and Atkin (1956)
<16.5 %		Coalified logs, Triassic and Jurassic sediments of Colorado Plateau.	Breger (1974)
1.22-1.9 %		"Fly-speck" carbonaceous matter; Uitkyk Formation of Pietersburg greenstone belt;	Thiel et al. (1979)
1.56-4.9 %		Basal Reef of Witwatersrand Basin, South Africa.	"

* values in ppm unless otherwise specified

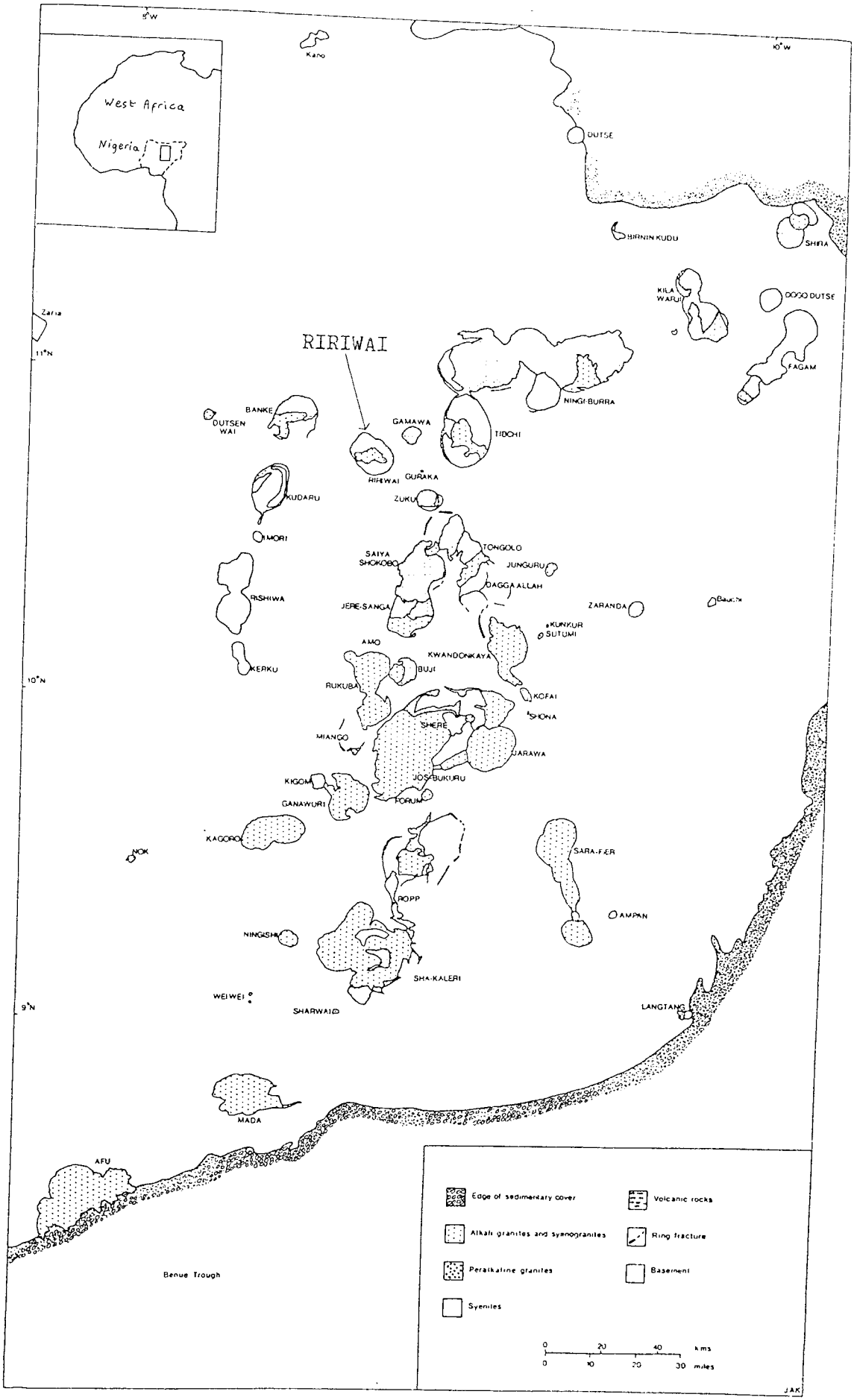

Fig. 16 The Mesozoic ring complexes of Nigeria

(after Kinnaird, 1985)

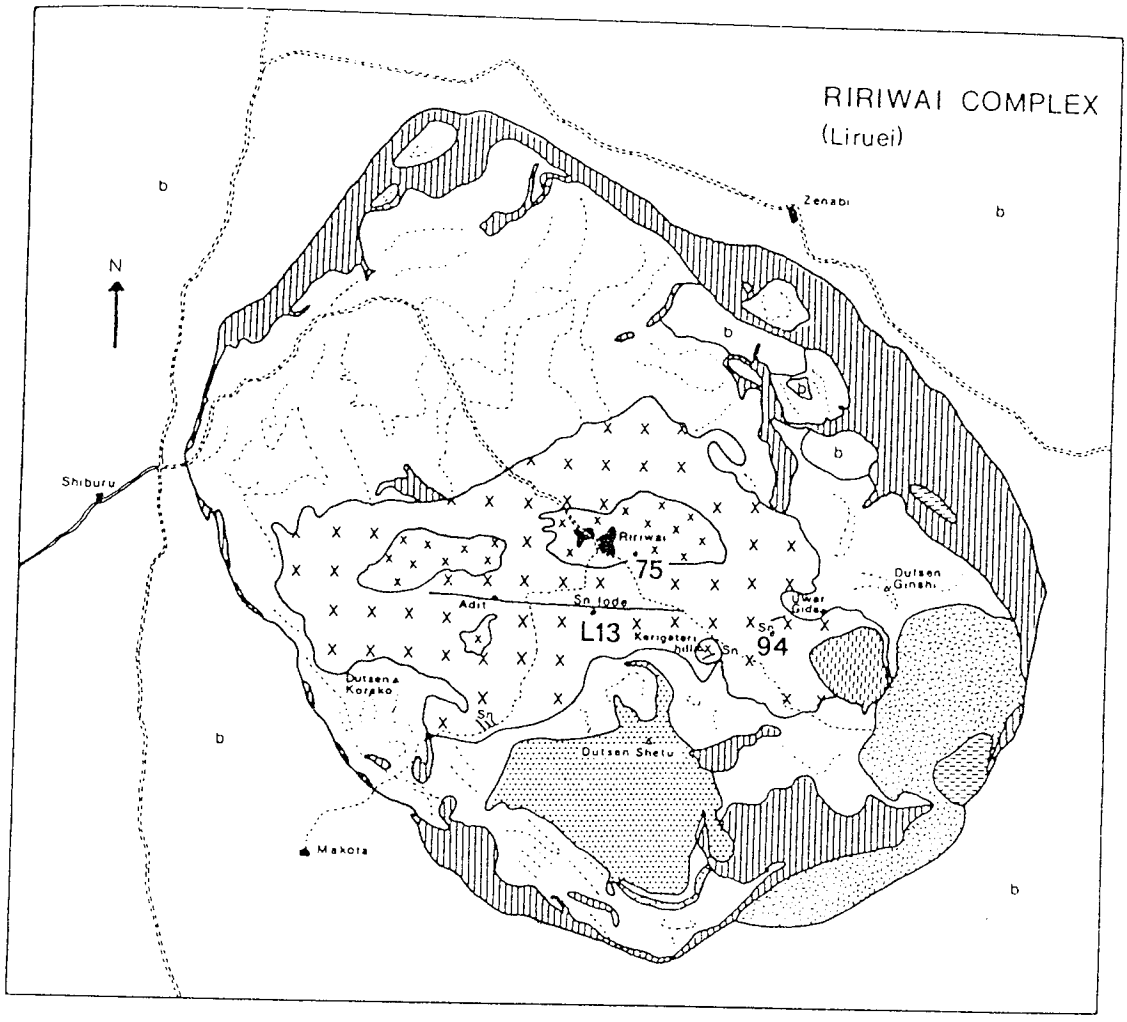

Fig.17 Simplified geological sketch map of the Ririwai complex, showing location of surface samples N75 and N94, Borehole L13 and the Ririwai tin lode

(after Kinnaird et al., 1985b)

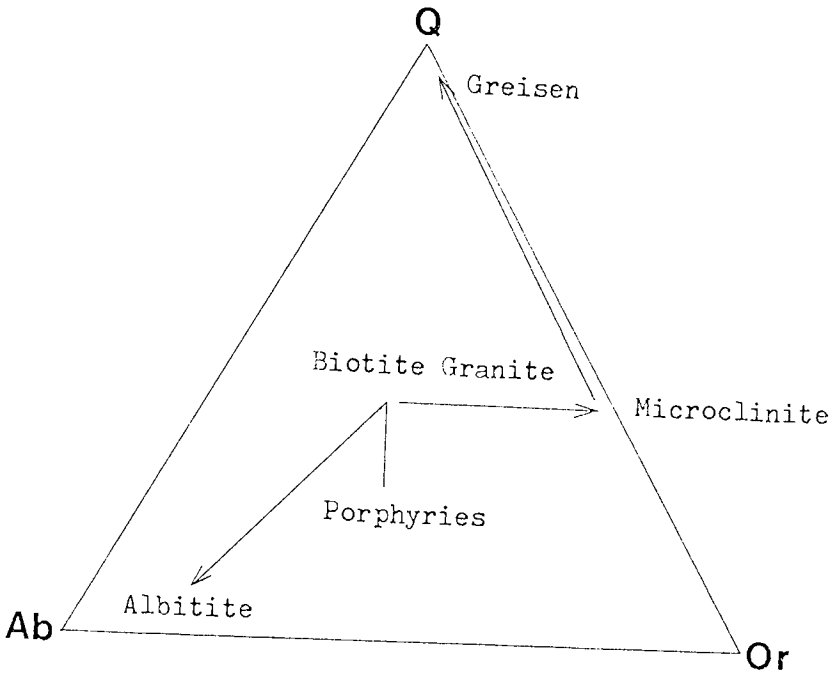

Fig. 18 Summary of main post-magmatic transformations in the Ririwai granite
(modified after Martin and Bowden, 1981)

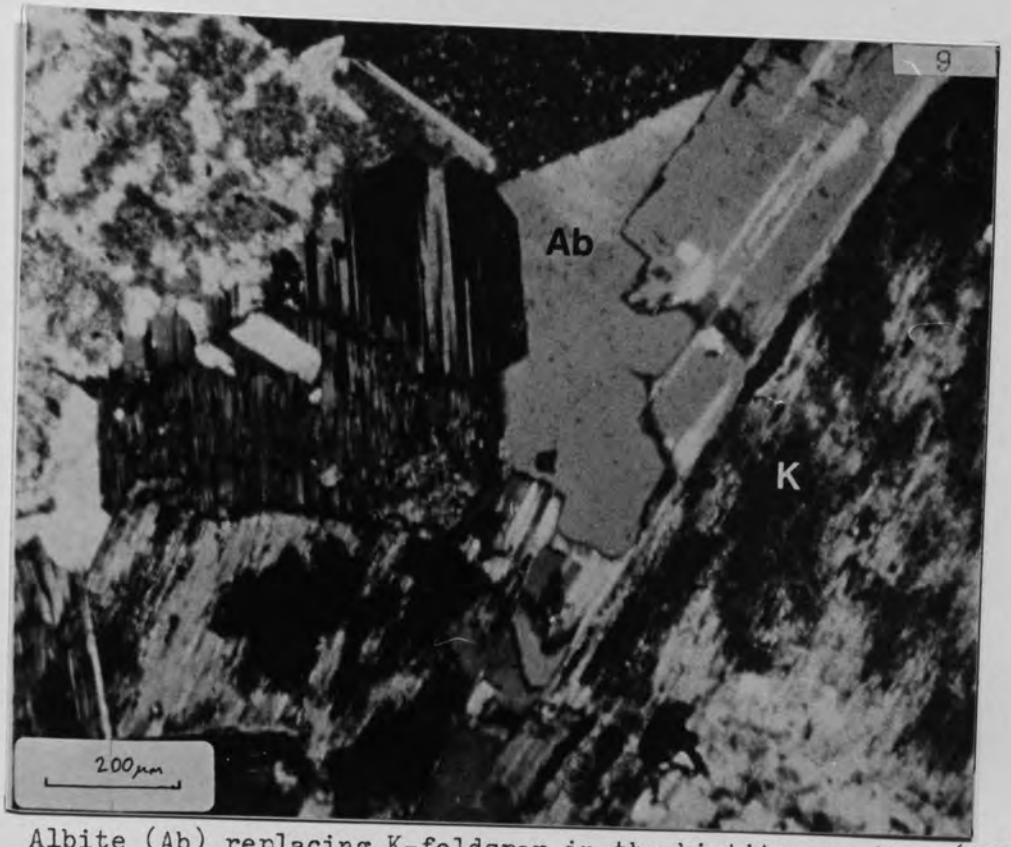

Plate 9 Albite (Ab) replacing K-feldspar in the biotite granite (205 m) (TXPL)

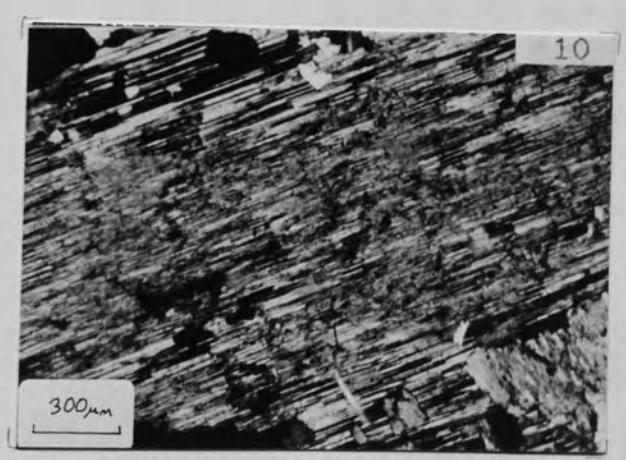

Plate 10 Poorly defined albite twinning grading outwards into well-defined twinning in the albitised granite (390 m) (TXPL)

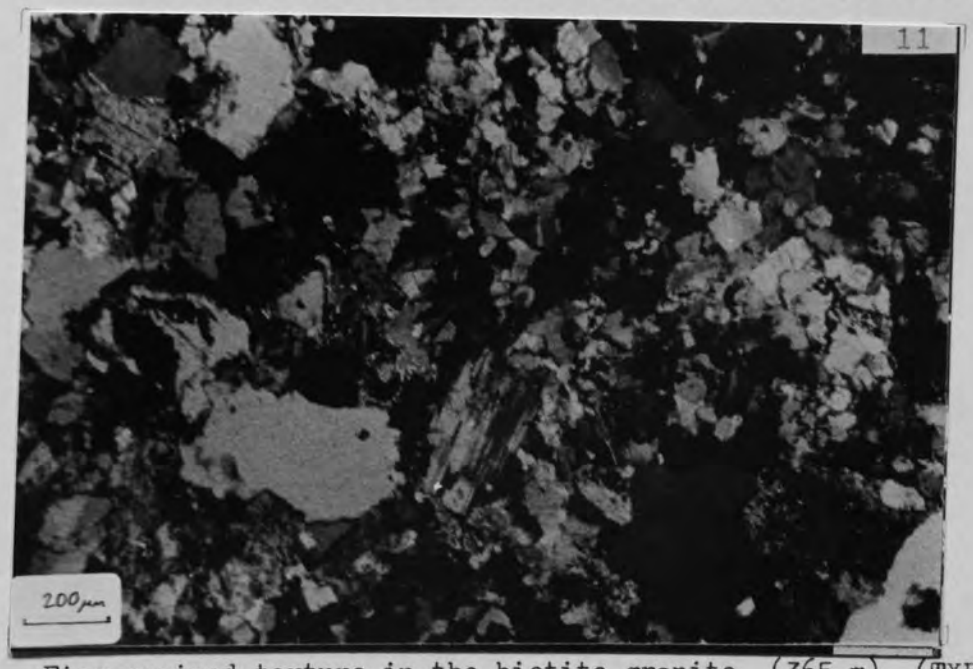

Plate 11 Fine-grained texture in the biotite granite (365 m) (TXPL)

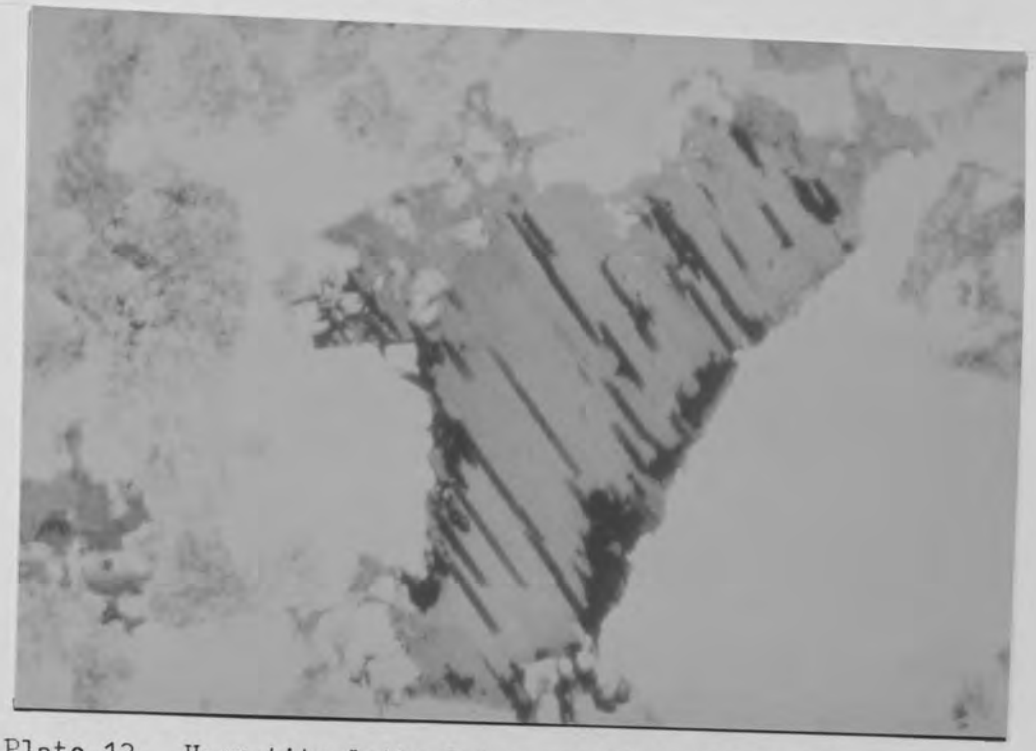

Plate 12 Haematite laths lying parallel to the cleavage in biotite. (365 m) (TPPL)

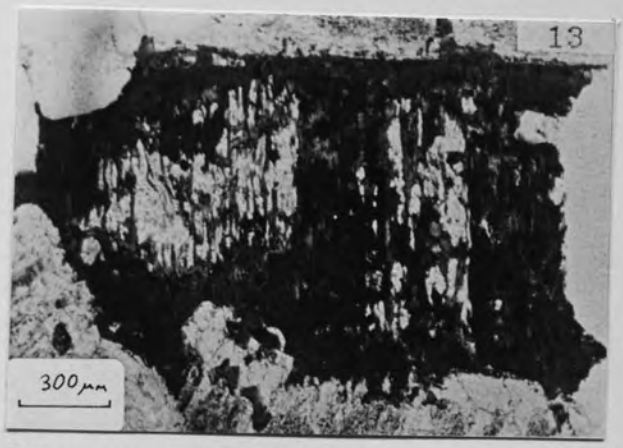

Plate 13 Replacement of biotite along cleavage by fine mosaic of feldspar. (205 m) (TPPL)

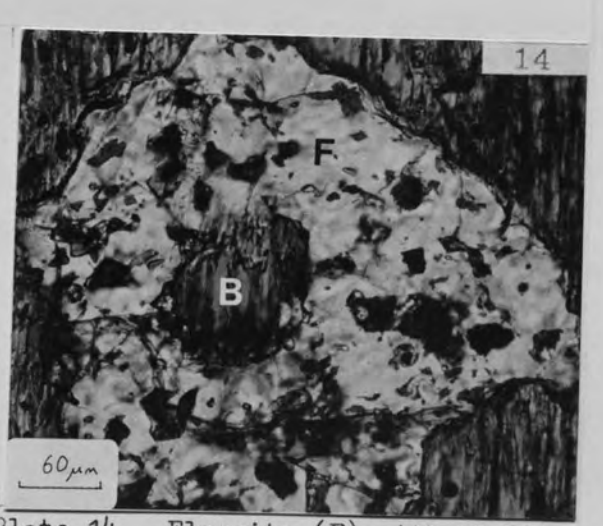

Plate 14 Fluorite (F) with biotite inclusion (B) in a larger biotite. (350 m) (TPPL)

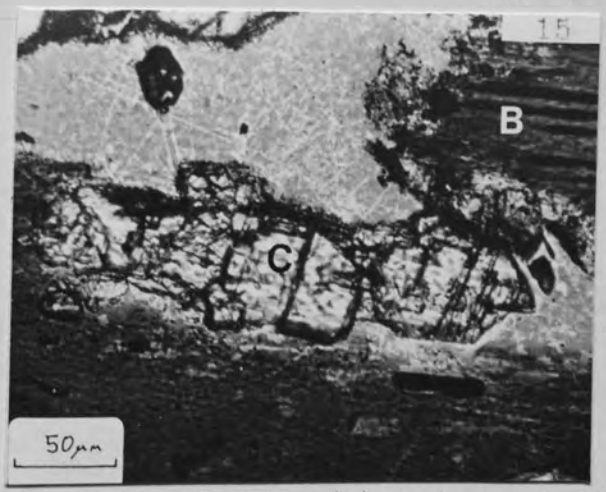

Plate 15 Calcite (C) included in biotite (B) (256 m) (TPPL)

Plate No.	Sample No.	Description
16	445	Polished block of albitite.
	450	Core sample of albitite (left).
	390	Core sample of albitised granite (middle).
	365	Core sample of altered biotite granite (right). (actual size)
17	423	Interstitial calcite (c) with haematite (h) inclusions, in the albitite. (TXPL)
18	423	High magnification of haematite inclusions in calcite. (TPPL)
19	R1/23	Polished slab of microclinite (M) - greisen (G) - quartz vein (Q) contact in Ririwai lode.

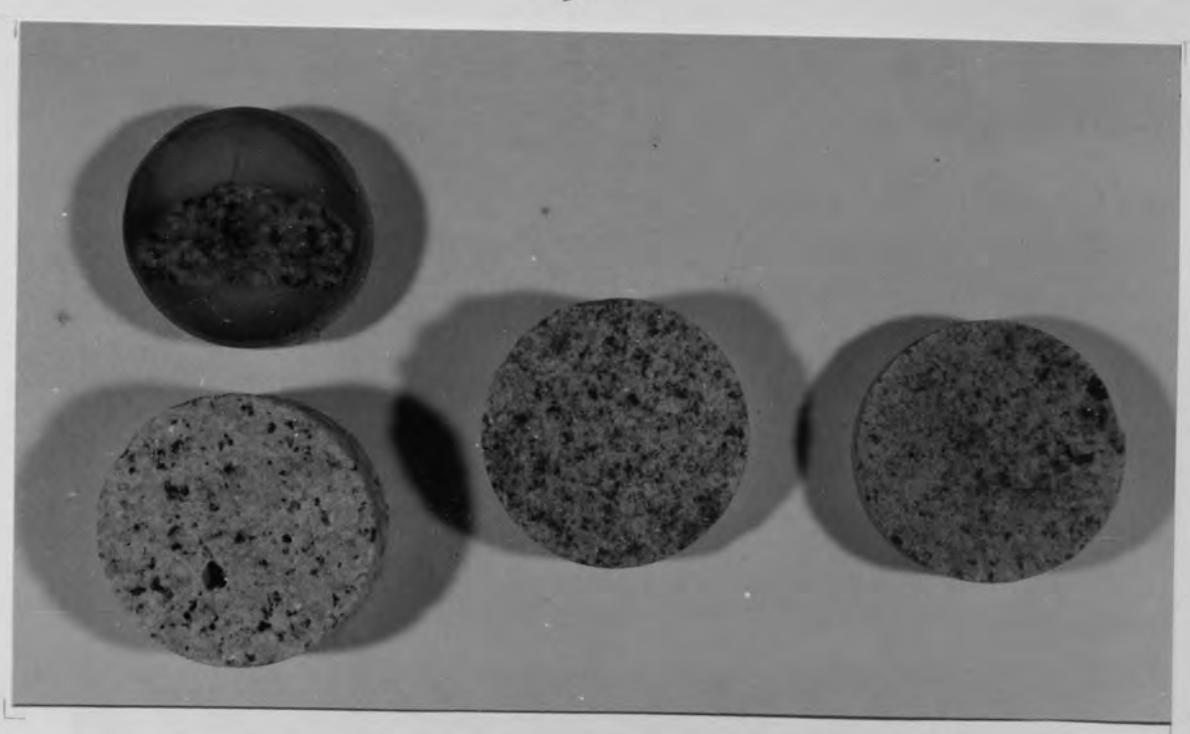

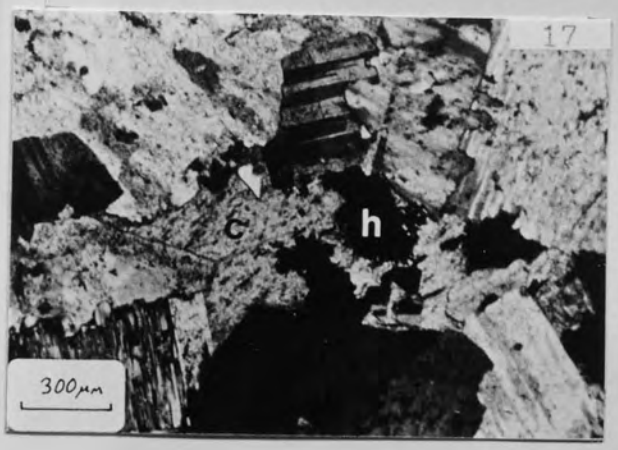
17
C
h
300μm

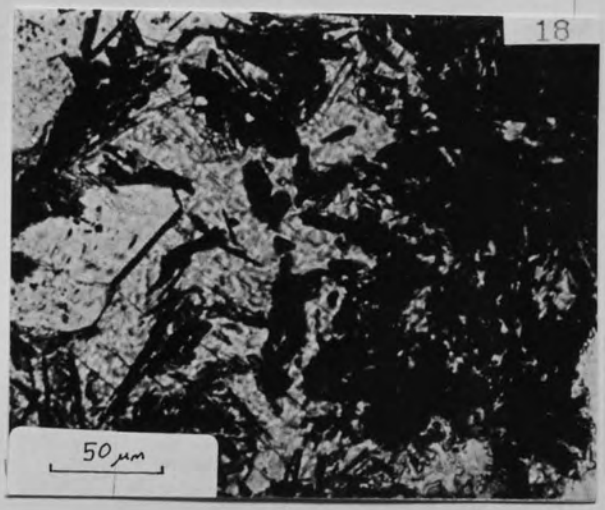
18
50μm


Q
G
M
0
1
2
3
4
5
6
7
8
9
10
11
12
13
MADE IN ENGLAND

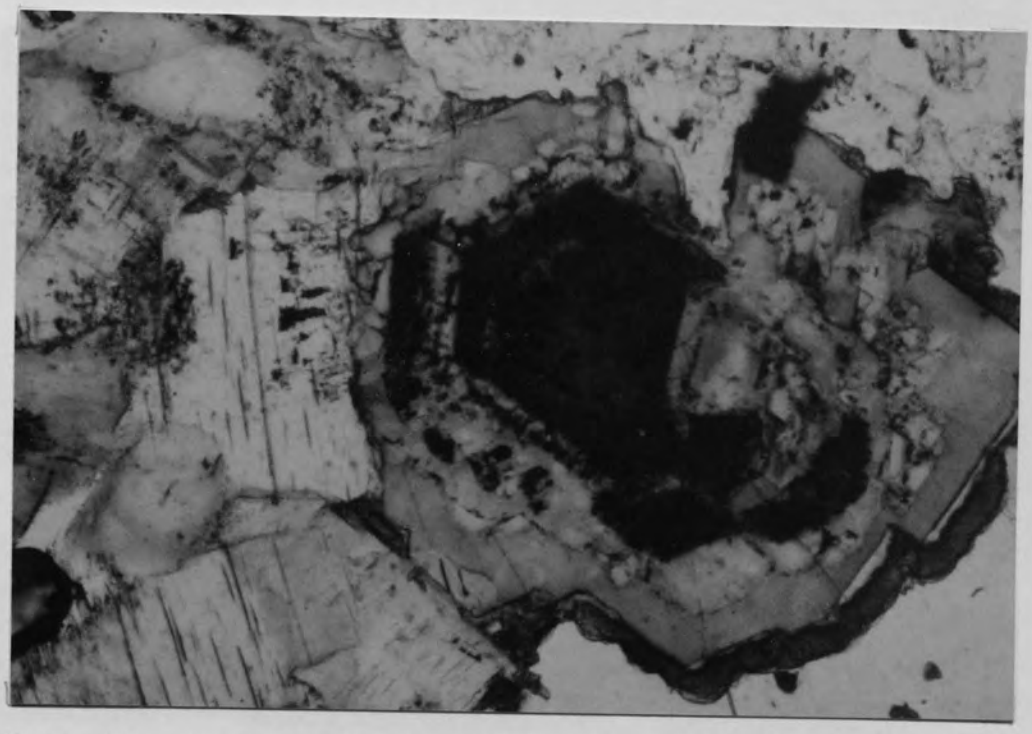

Plate 20 Zoned Li-mica crystal in greisenised granite. (125 m)
(TPPL)

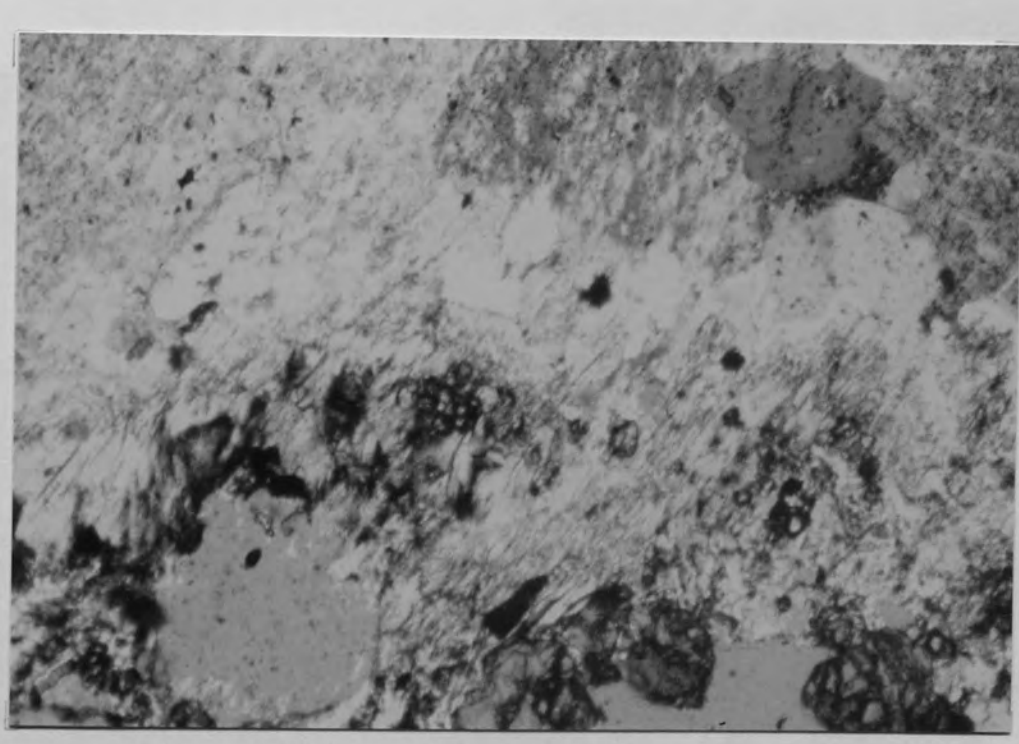

Plate 21 White mica replacing chloritised biotite in the greisenised wallrock (R1/13-1)
(TXPL)

Plate 22 White mica replacing microcline in the greisenised granite (125 m).

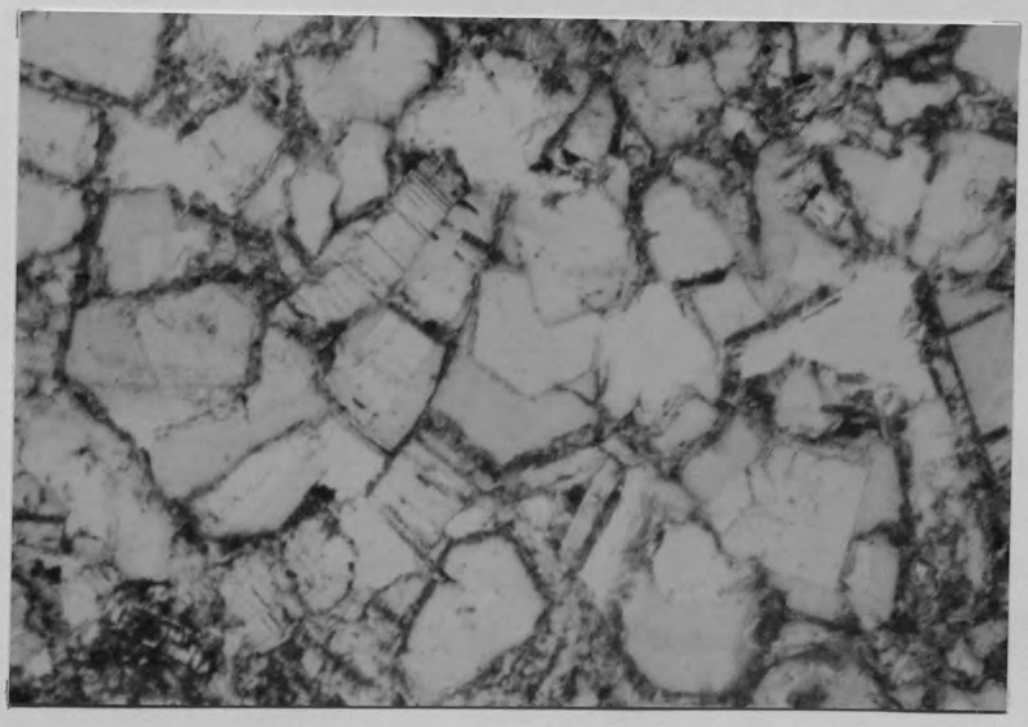

Plate 23 Li-mica in the greisen, Ririwai lode (R1/14-1). (TPPL)

Ignimbrite from the Goundaï volcanic centre, Aïr, Niger.
(Sample GN13)

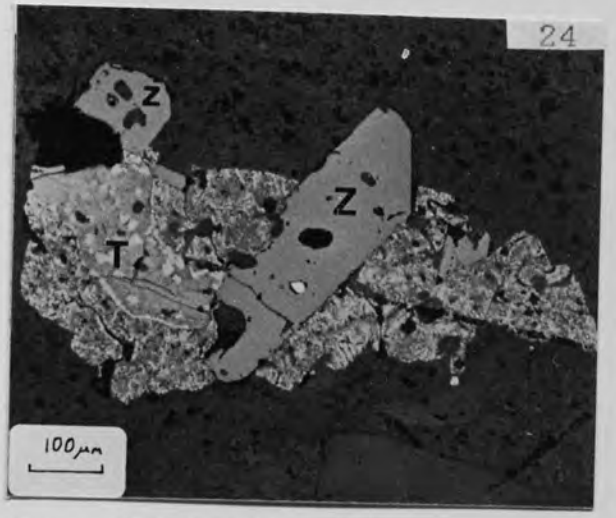

Zircon (Z) in TiO_2 (T).
(RPPL)

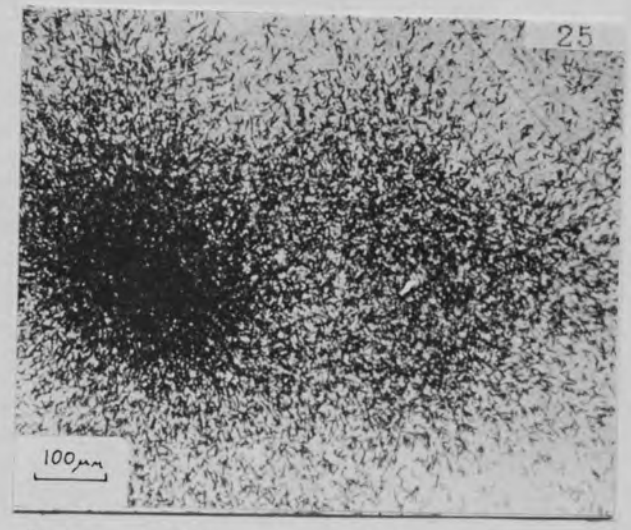

Lexan of the area in Plate 24, showing densest fission tracks with the TiO_2 and lower density tracks with the zircon.
(TPPL)

Uraniferous zircons associated with very dense fission tracks. The low reflectance patches may be analagous to similar patches observed in zircons from Ririwai (see Section 2.c.i., Chapter 4).
The white inclusions are pyrite.
(RPPL)

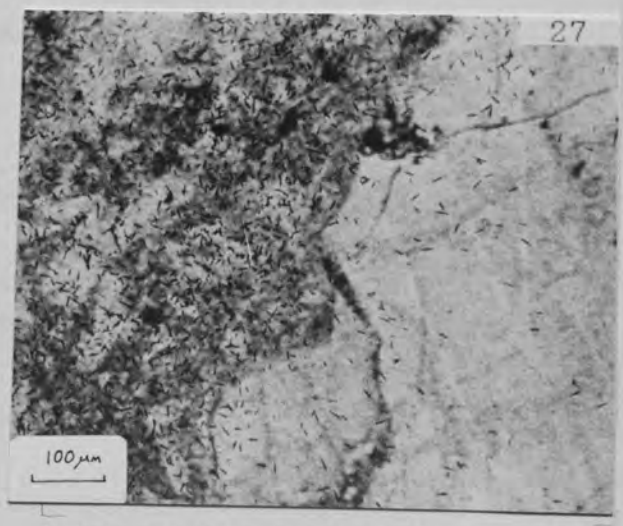

Lexan superimposed on the ignimbrite showing low concentrations of U associated with the matrix (left). On the right is part of a quartz clast.
(TPPL)

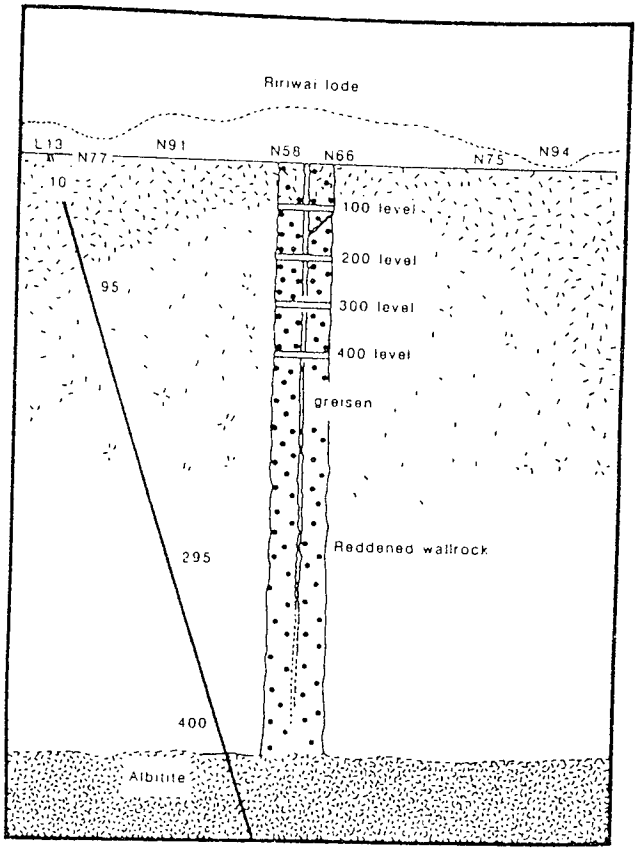

Fig. 19 Schematic diagram of relationships in a cross-section of biotite granite, Ririwai, showing location of mining levels, relative sampling position of drill-core L13, and surface sample locations.

(after Kinnaird et al., 1985b)

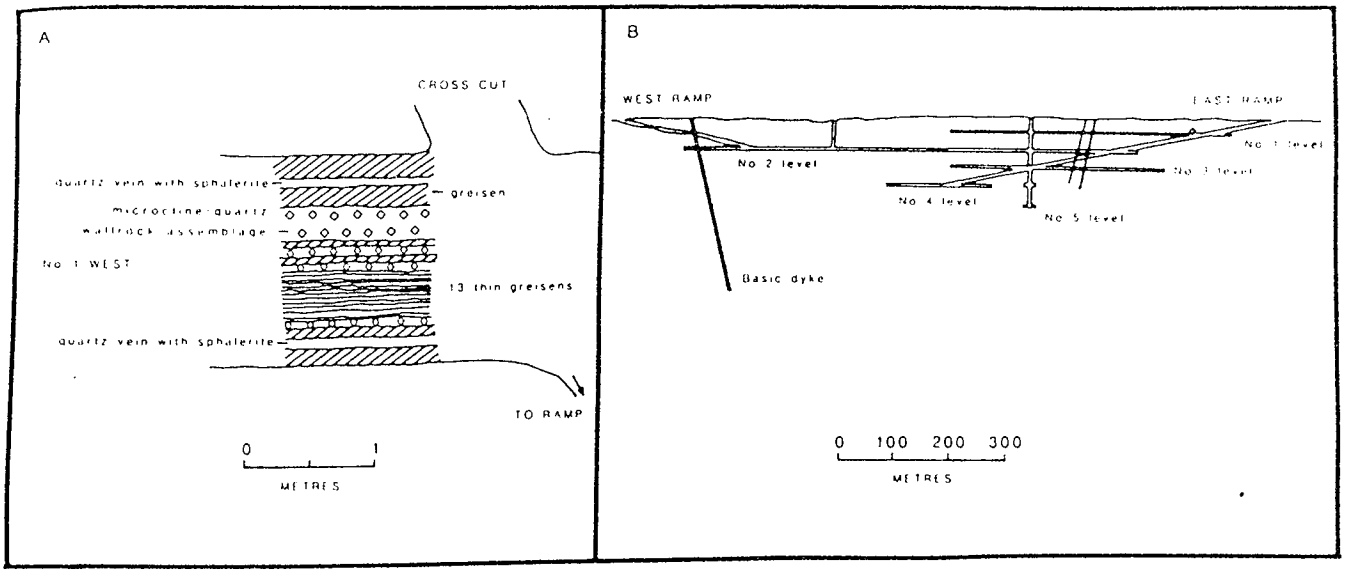

Fig. 20 Sections showing (A) mineralogical variations across the lode at the No. 1 level intersection with the east ramp (taken from a field report compiled by J. N. Bennett 1975); (B) the extent of underground mining operations in the Ririwai lode (cross-section (B) adapted from the Ririwai project report RIR80-4 (Nigerian Mining Corporation)). Small asterisk below east ramp is location of cross-section (A). No. 1 level is equivalent to the 100 level of Fig. 13, No. 2 to the 200 level, etc.

(after Kinnaird et al., 1985b)

Plate No.	Sample No.	Grain No.	Description
			Surface samples of biotite granite
28	N75	19	Zircon with a core containing abundant, tiny haematite inclusions, surrounded by a clear rim. A thorite overgrowth on the left (1) is surrounded by haematite (opaque). EPMA spots are shown. (TPPL)
29	N94	17	Two thorites with cores containing abundant inclusions of haematite and clearer rims enclosed by haematite (opaque). A zircon (D) is partly enclosed by the thorite. EPMA spots are shown. (TPPL)
	Depth(m)		Borehole samples of biotite granite
30	305		Fluorite (F), zircon (Z) and columbite/TiO_2 (C) included in biotite. (RPPL)
31	125	P.1a	Corroded zircon (EPMA spots 2, 4, 5) with thorite overgrowths (EPMA spots 1, 3), containing tiny pyrite inclusions. (Greisenised biotite granite). (RPPL)
32	315	8	Zircon (left) with low reflectance patches along outer zones and internal cracks. The associated thorite (right) contains inclusions of haematite (white) and cassiterite (grey). (RPPL)
33	315	10	Euhedral zircon (Z) with an anhedral zircon overgrowth (3) containing a thorite inclusion (1). EPMA spots shown. (TPPL)
34	315	10	The same zircon with the thorite inclusion more evident (1). (scale bar is 20 μm).
35	350	2	Zircon containing large inclusions of thorite (EPMA spots 1, 2, and 3) and haematite (light grey). (RPPL)


28
1
2
4
5
40 µm


29
1
2
3
4
D
5
60 µm

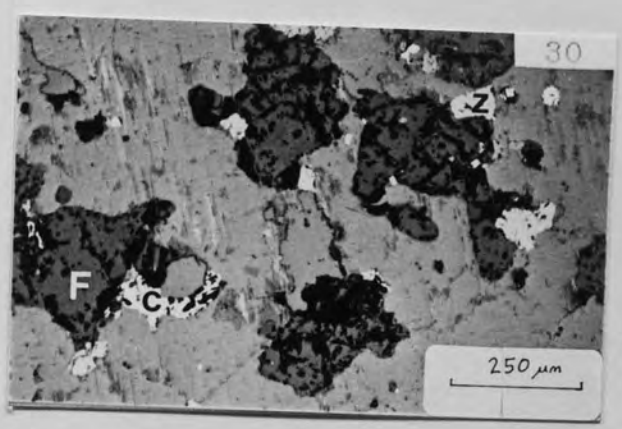
30
Z
F
C
250 µm

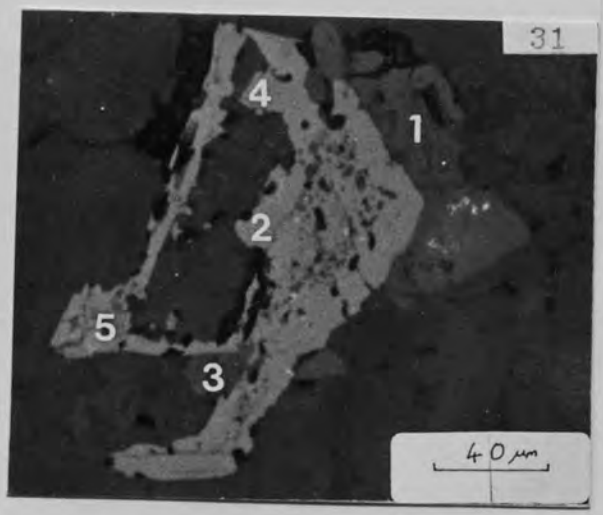
31
4
1
2
5
3
40 µm

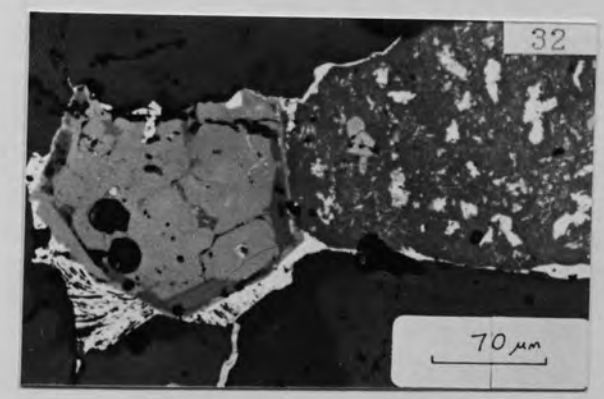
32
70 µm

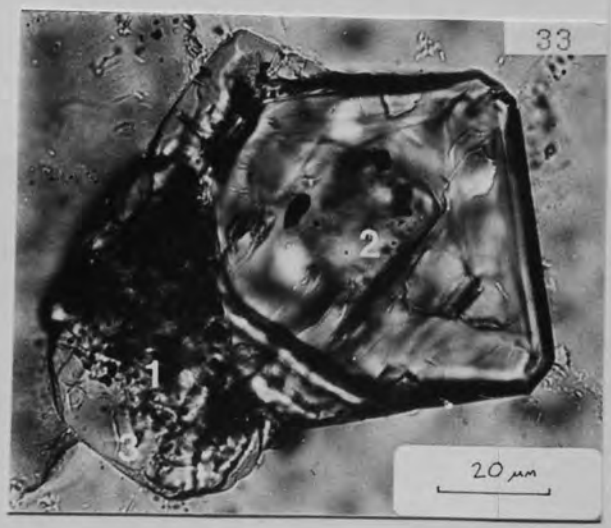
33
2
1
20 µm

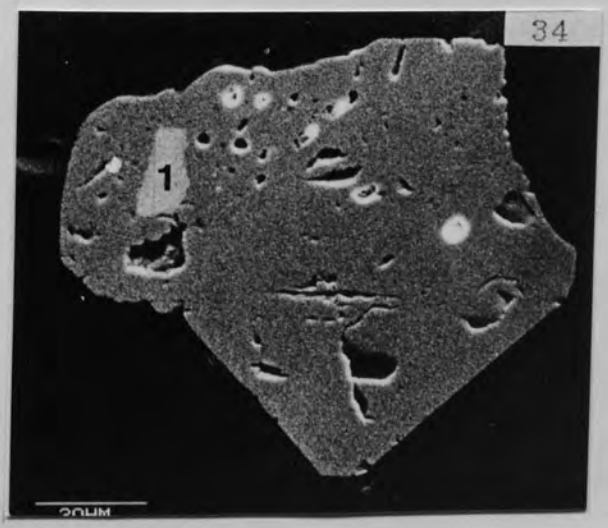
34
1

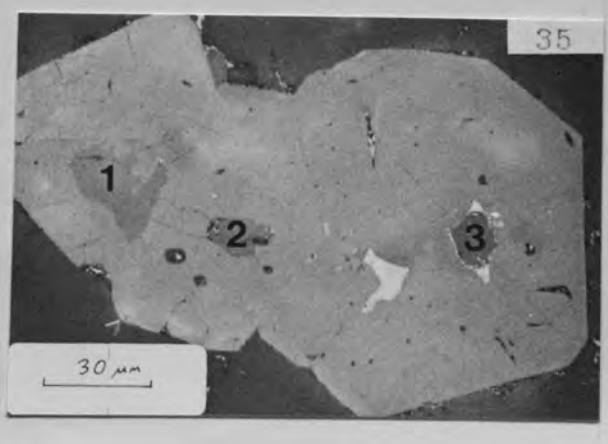
35
1
2
3
30 µm

Table 25 Size (maximum dimensions in μm) and abundance of radioactive accessories and fluorite in borehole and surface samples of granite

Rock Type	No. Sections	Sample No.	Zircon						Thorite				Fluorite			LREE Phase		Monazite			Other Accessories	Size
			Mean Size (μm)	Size Range	No. ⩾ 300 μm	No. with low R % patches	No. with thorite inclusions	Total No.	No. replacing zircon	No. discrete grains	Size range of discrete grains	No. overgrowths on zircon	Total No.	No. included in biotite	Size Range	No. fluorites with inclusions	No. intergrown with monazite	Total No.	Size Range	Total No. of Xenotimes		
Biotite Granite	1	N75	240	70-500	2	0	3	7	0	0		1	1	0	80	0	0	0		0		
	1	N94	87	5-250	0	0	0	>16	0	4	120-180	0	6	3	30-250	0	0	0		0		
	1	100	98	30-350	1	>7	0	>100	0	0		0		>30	60-120	1	0	0		0	Coffinite	250
	1	125	164	70-250	0	>1	5	>>5	1	4	60-120	5				0	0	0		0		
	1	145	257	120-400	1	0	0	>>3	0	0		0		>2	60-140	0	0	1	800	0		
	1	155	163	40-400	2	0	2	30	0	0		0	6	3	60-300	0	0	0		0		
	1	185	126	60-250	0	>4	2	>>5	0	0		0				0	0	3	100	0		
	1	205	74	15-250	0	16	0	47	0	1	60	0	61	58	20-250	>7	0	1	250	0		
	1	256	119	60-180	0	1	3	>>8	0	1	60	0	21	21	20-400	>3	0	0		0		
	1	305	58	10-150	0	16	0	88	0	2	170-260	0	50	47	30-1000	3	0	1	120	0	Pb-pyrochlore	40
	1	315	92	50-160	0	>6	1	>>12	0	4	100-250	0	1	0	120	0	1	1	250	0		
	1	350	100	40-180	0	0	2	107	0	1	120	0	42	38	40-600	4	0	1	300	0	U-pyrochlore	25
	2	365	206	40-500	3	0	>12	28	1	1	120	0	2	0	60-80	0	0	4	15-500	0		
Alb.Granite	1	385	140	70-300	1	0	0	10	0	1	20	0	2	2	20-40	0	1	2	5-20	0		
	2	390	203	100-500	2	0	1	9	0	1	500	0	7	1	60-400	1	0	2	80-1000	0		
	2	395	260	60-750	3	0	1	8	0	1	25-500	0	1	0	300-400	1	1	2	60-400	0		
	2	400	300	60-750	5	0	5	12	0	0		0	12	11	30-500	4	0	0		0		
	2	408	230	70-460	2	0	6	8	0	1	50-250	0	6	5	90-300	6	0	0		0		
	2	411	240	60-560	2	0	3	5	1	0		1	>3	0	60-280	2	0	0		1		
Albitite	2	416	200	20-500	4	0	>8	20	0	0		1	7	1	150-1000	1	0	1	190	0		
	2	423	320	120-500	2	0	3	4	0	1	40	0	4	1	120-500	2	0	0		0		
	2	436	190	60-500	2	0	2	11	0	0		0	8	0	80-500	2	0	0		0		
	2	440	112	40-300	1	0	>1	>5	0	0		0	>1	0	80-140	>1	0	0		2		
	4	445	290	20-750	3	0	>4	10	0	0		0	>2	1	80-120	2	2	2	80-800	4	?U-Pb-microlite	60
	2	450	265	40-1000	2	0	2	10	0	0		0	3	1	60-4000	2	0	0		>4		

Table 25 Size (maximum dimensions in μm) and abundance of radioactive accessories and fluorite in borehole and surface samples of granite

Rock Type	No. Sections	Sample No.	Zircon						Thorite				Fluorite			LREE Phase		Monazite			Other Accessories	
			Mean Size (μm)	Size Range	No. ⩾ 300 μm	No. with low R % patches	No. with thorite inclusions	Total No.	No. replacing zircon	No. discrete grains	Size range of discrete grains	No. overgrowths on zircon	Total No.	No. included in biotite	Size Range	No. fluorites with inclusions	No. intergrown with monazite	Total No.	Size Range	Total No. of Xenotimes		Size
Biotite Granite	1	N75	240	70-500	2	0	3	7	0	0		1	1	0	80	0	0	0		0		
	1	N94	87	5-250	0	0	0	>16	0	4	120-180	0	6	3	30-250	0	0	0		0		
	1	100	98	30-350	1	>7	0	>100	0	0		0		>30	60-120	1	0	0		0	Coffinite	250
	1	125	164	70-250	0	>1	5	>>5	1	4	60-120	5				0	0	0		0		
	1	145	257	120-400	1	0	0	>>3	0	0		0		>2	60-140	0	0	1	800	0		
	1	155	163	40-400	2	0	2	30	0	0		0	6	3	60-300	0	0	0		0		
	1	185	126	60-250	0	>4	2	>>5	0	0		0				0	0	3	100	0		
	1	205	74	15-250	0	16	0	47	0	1	60	0	61	58	20-250	>7	0	1	250	0		
	1	256	119	60-180	0	1	3	>>8	0	1	60	0	21	21	20-400	>3	0	0		0		
	1	305	58	10-150	0	16	0	88	0	2	170-260	0	50	47	30-1000	3	0	1	120	0	Pb-pyrochlore	40
	1	315	92	50-160	0	>6	1	>>12	0	4	100-250	0	1	0	120	0	1	1	250	0		
	1	350	100	40-180	0	0	2	107	0	1	120	0	42	38	40-600	4	0	1	300	0	U-pyrochlore	25
	2	365	206	40-500	3	0	>12	28	1	1	120	0	2	0	60-80	0	0	4	15-500	0		
Alb.Granite	1	385	140	70-300	1	0	0	10	0	1	20	0	2	2	20-40	0	1	2	5-20	0		
	2	390	203	100-500	2	0	1	9	0	1	500	0	7	1	60-400	1	0	2	80-1000	0		
	2	395	260	60-750	3	0	1	8	0	1	25-500	0	1	0	300-400	1	1	2	60-400	0		
	2	400	300	60-750	5	0	5	12	0	0		0	12	11	30-500	4	0	0		0		
	2	408	230	70-460	2	0	6	8	0	1	50-250	0	6	5	90-300	6	0	0		0		
	2	411	240	60-560	2	0	3	5	1	0		1	⩾3	0	60-280	2	0	0		1		
Albitite	2	416	200	20-500	4	0	>8	20	0	0		1	7	1	150-1000	1	0	1	190	0		
	2	423	320	120-500	2	0	3	4	0	1	40	0	4	1	120-500	2	0	0		0		
	2	436	190	60-500	2	0	2	11	0	0		0	8	0	80-500	2	0	0		0		
	2	440	112	40-300	1	0	>1	>5	0	0		0	>1	0	80-140	>1	0	0		2		
	4	445	290	20-750	3	0	>4	10	0	0		0	>2	1	80-120	2	2	2	80-800	4	?U-Pb-microlite	60
	2	450	265	40-1000	2	0	2	10	0	0		0	3	1	60-4000	2	0	0		>4		

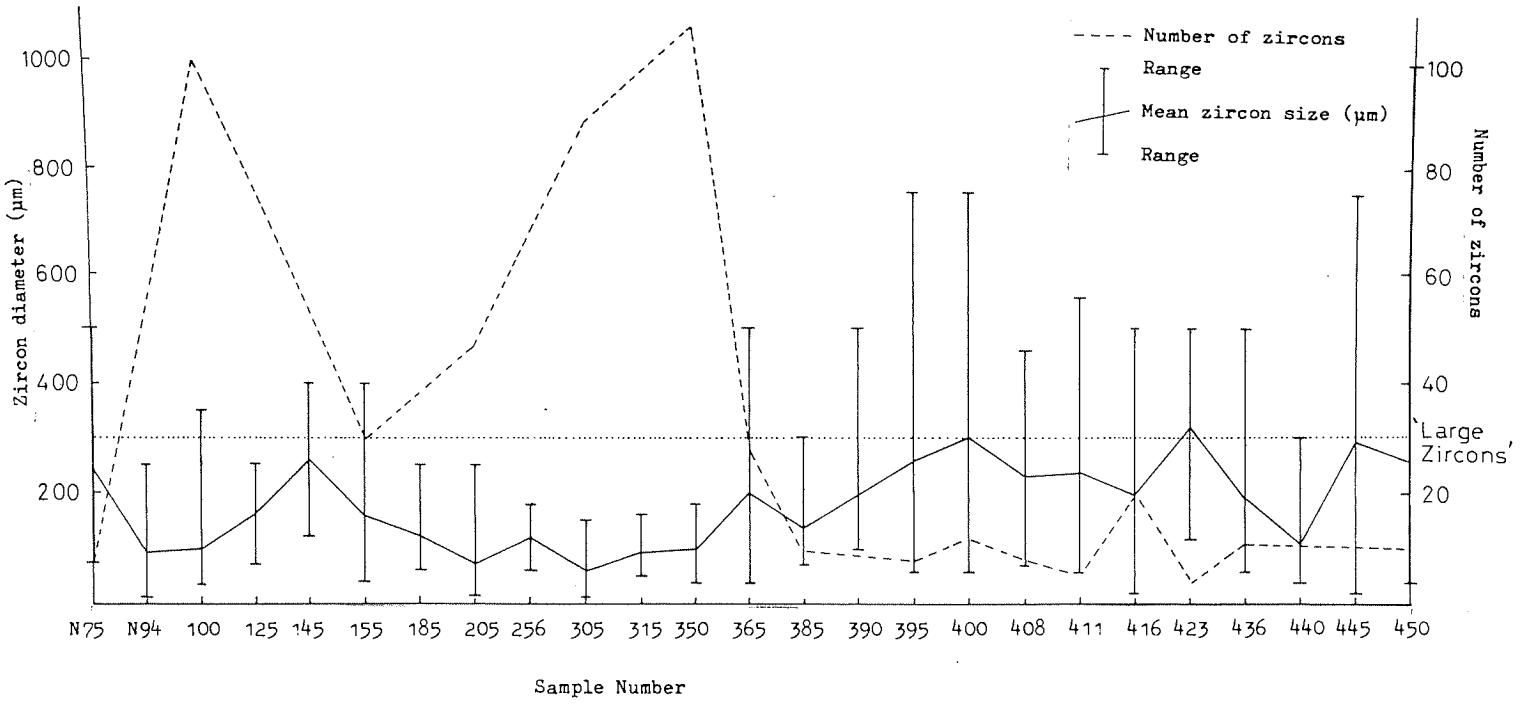

Fig. 21 Size (mean and range) and abundance of zircons from the borehole samples of granite

Fig. 22 Concentration profiles of thorite grains from sample N94

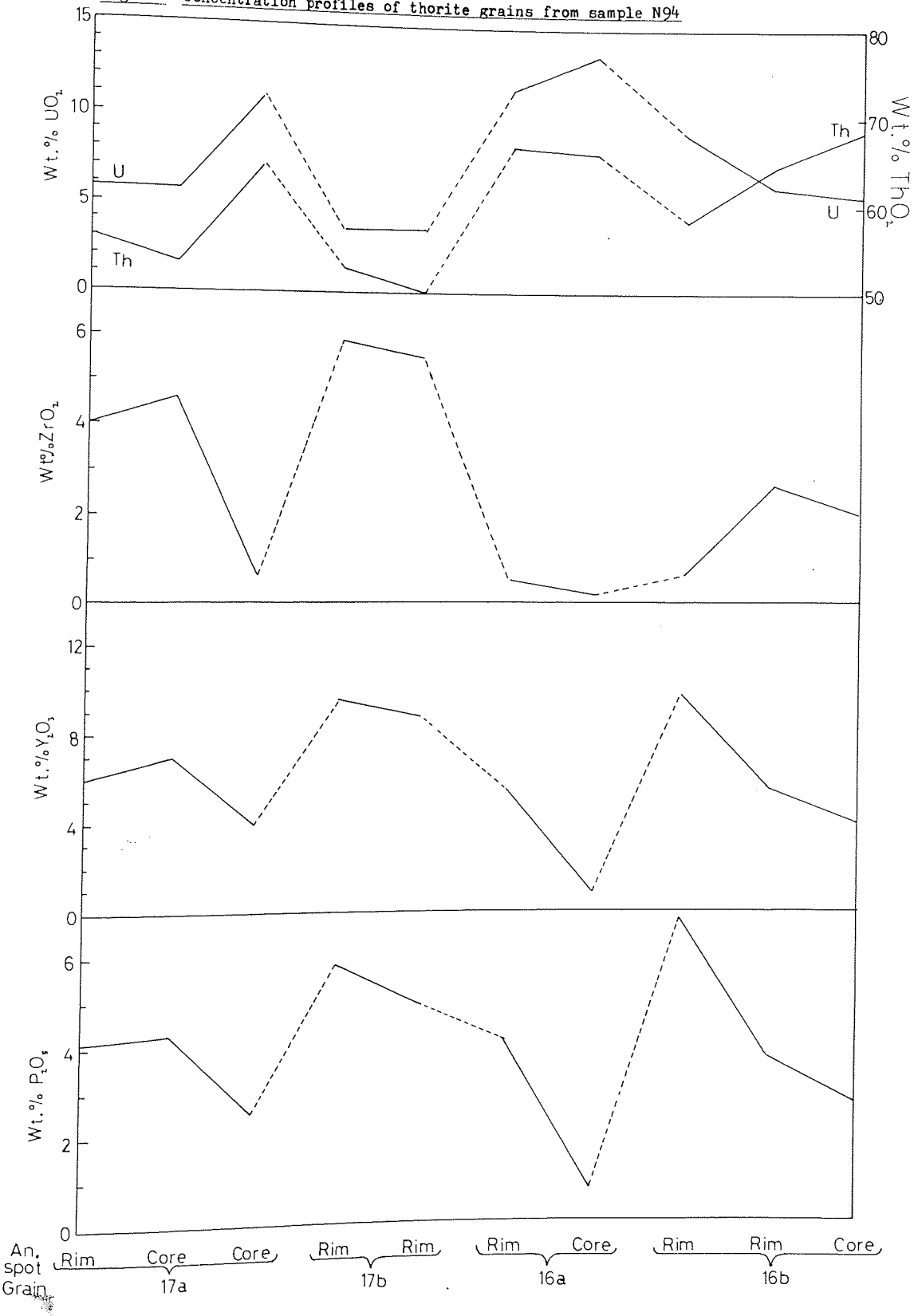

Plate No.	Sample No.	Grain No.	Description
			Borehole samples of biotite granite
36	365A	27	Zircon containing abundant inclusions of thorite (slightly darker than the zircon) and haematite (lightest grey). Very dark features are pits. (RPPL)
37	365A	9	Zircon (EPMA spots 1, 2, 4) embayed by white mica (M). There are abundant, small thorite inclusions (e.g. EPMA spot 3) (RPPL)
38	125	P.1b	Residual rim of corroded zircon. Greisenised granite. (RPPL)
39	315	7	Zircon with haematite-rich core surrounded by a clear, finely-banded outer zone. (TPPL)
40	365A	12	Haematite- and thorite-rich zircon with clear rims. (TPPL)

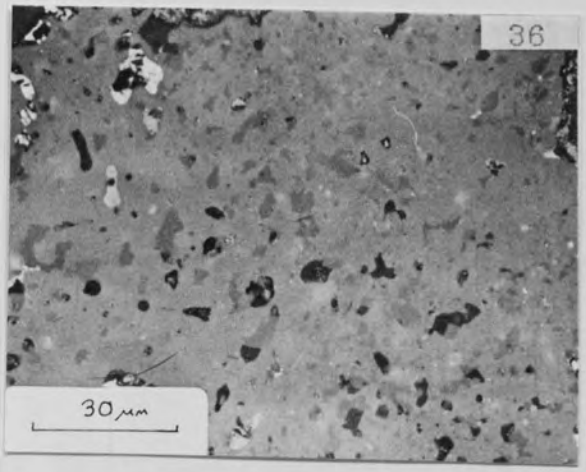
36
30 µm

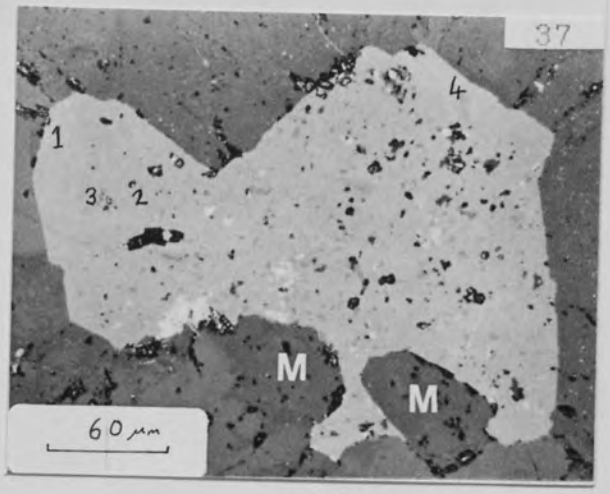
37
1
2
3
4
M
M
60 µm

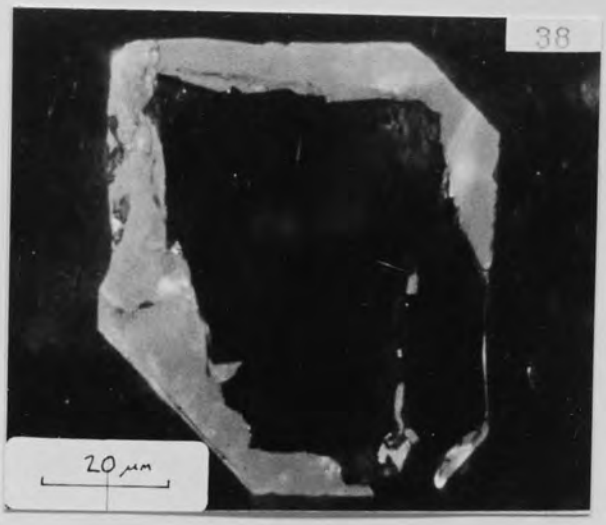
38
20 µm

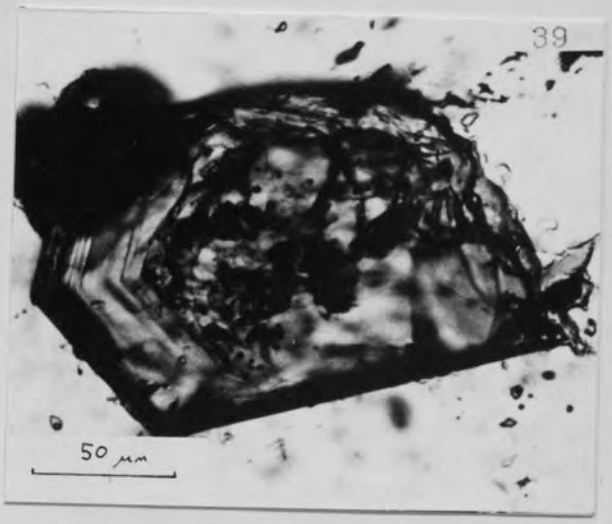
39
50 µm


40
140 µm

Plate No.	Sample No.	Grain No.	Description
			Borehole samples of biotite granite
41	100	1	Zircon showing embayment by fluorite (F). Low reflectance, trace-element enriched patches pick out the primary growth-zoning. EPMA spots are shown. (RPPL)
42	100	1	BSEI of part of the same zircon, showing the trace-element enriched patches as darker areas. (EPMA spots).
43	100	1	Part of the same zircon, just left of spot 7. Some of the dark patches follow late cracks. (BSEI)
44	100	1	Part of the same zircon just below spot 1, showing incipient development of the dark patch along a pre-existing growth-zone. (BSEI)
45	315	4	Zircon included in quartz. Low reflectance, trace-element enriched patches pick out the concentric growth-zoning. (RPPL)

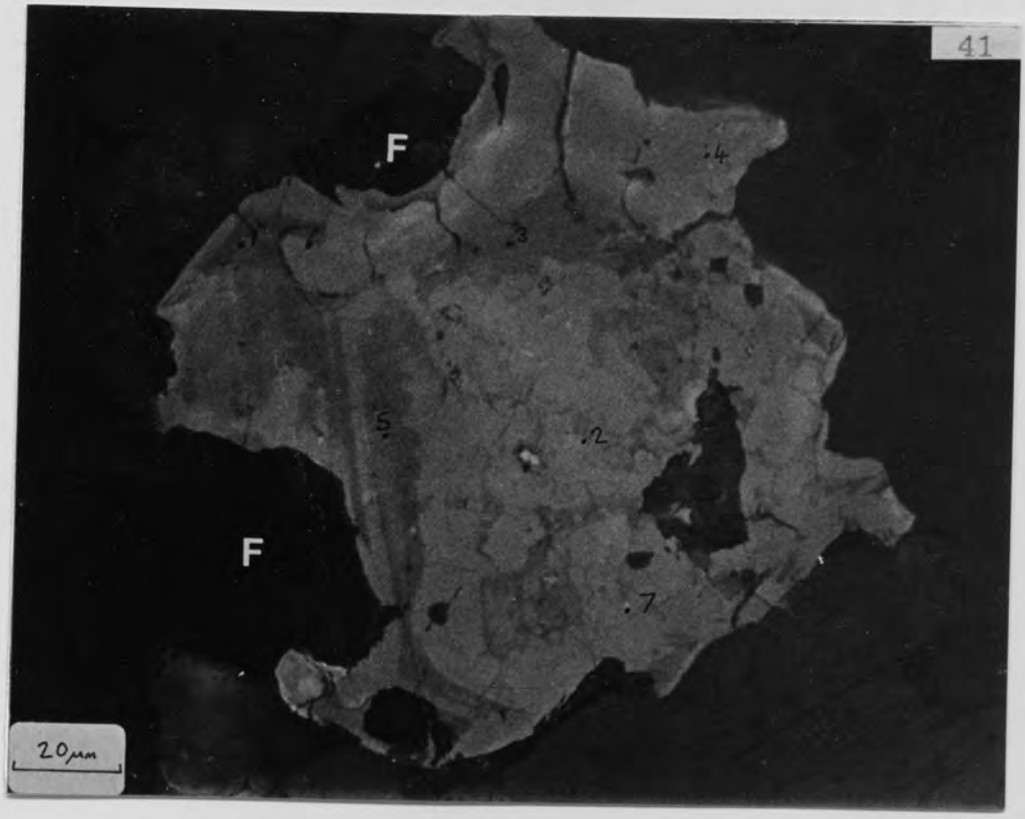
41
F
F
20 µm

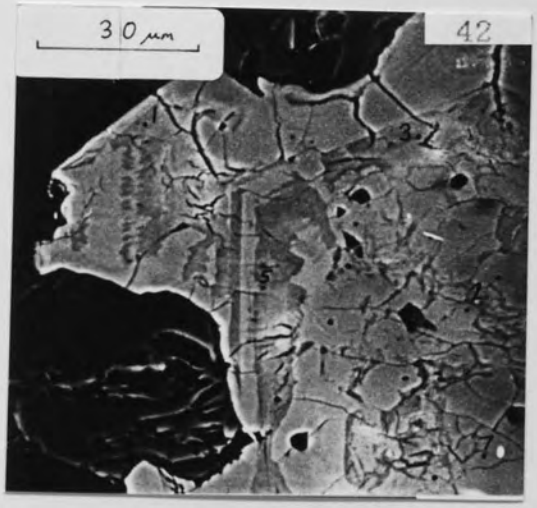
30 µm
42

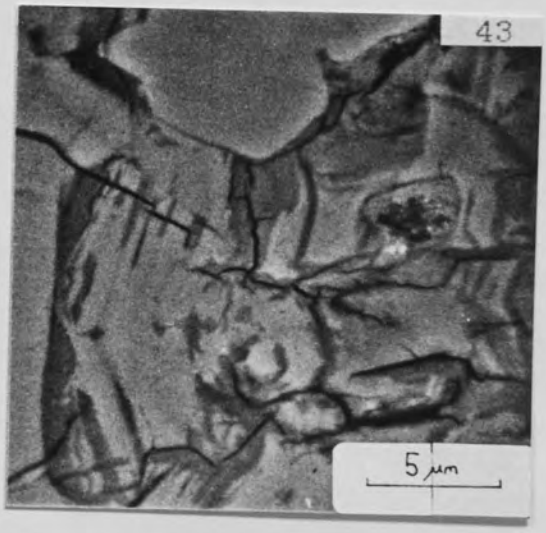
43
5 µm

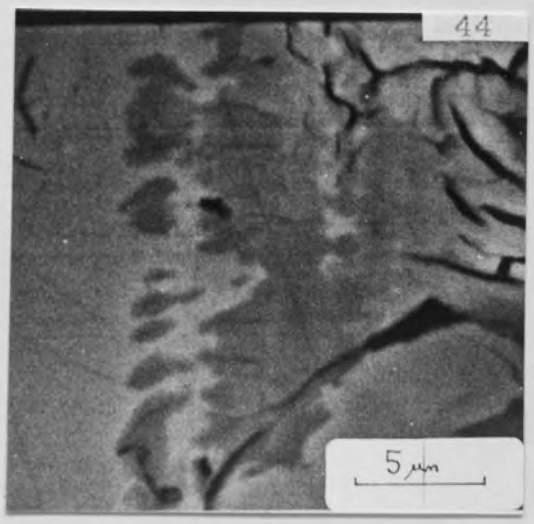
44
5 µm

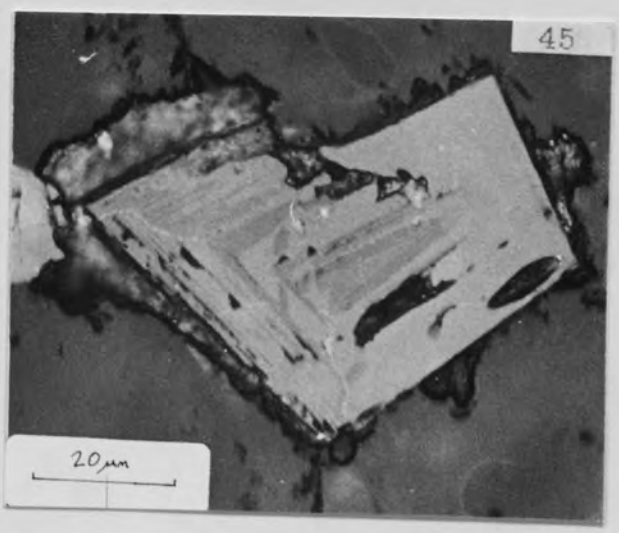
45
20 µm

Plate No.	Sample No.	Grain No.	Description
			Borehole samples of biotite granite
46	305	5(i)	Zircon included in biotite and adjacent to fluorite (F). Low reflectance, trace-element enriched patches pick out part of the outer, primary zone. EPMA spots are shown. (RPPL)
47	305	5(ii)	Zircon included in biotite, close to zircon 5(i) and with similar patches. EPMA spots are shown. (RPPL)
48	185	P.2a	Zircon, with low reflectance patches, included in altered biotite. EPMA spots are shown. (RPPL)
49	185	P.3	Zircon with outer, haematite-rich zone and low-reflectance patches (EPMA spot 6). (RPPL)
50	155	11	Zircon included in quartz, with positions of semi-quantitative, partial analyses and quantitative full analyses marked (see Table 27). Spot 2 is thorite. (RPPL)
51	305	4	Two thorite grains in altered biotite. The white inclusions are of haematite. EPMA spots are shown. (RPPL)
52	256	P.6	Two thorite grains, with haematite rims, in K-feldspar EPMA spots are shown. (RPPL)
53	350	21	Thorite (EPMA spots 1 and 2) with fluorite (F) in biotite. (TPPL)

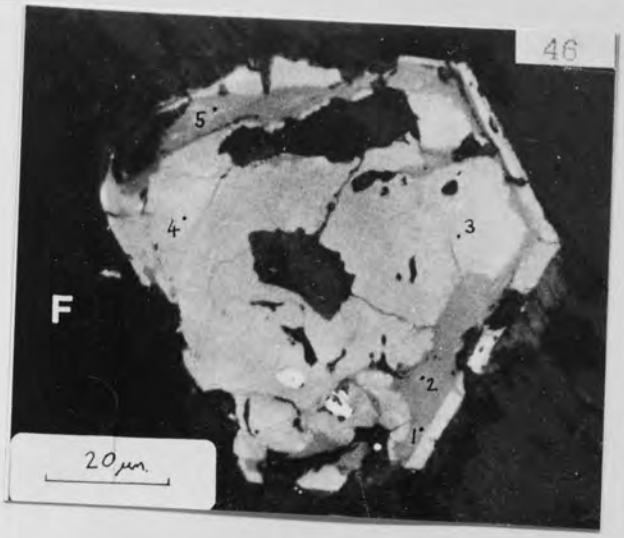
46
5
4
3
F
2
1
20 µm

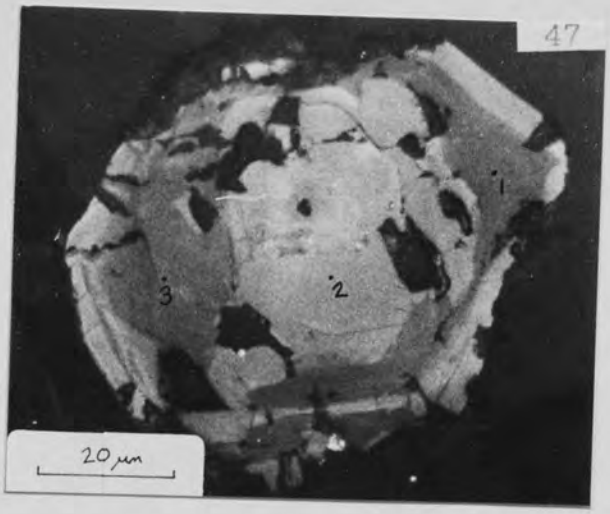
47
1
3
2
20 µm

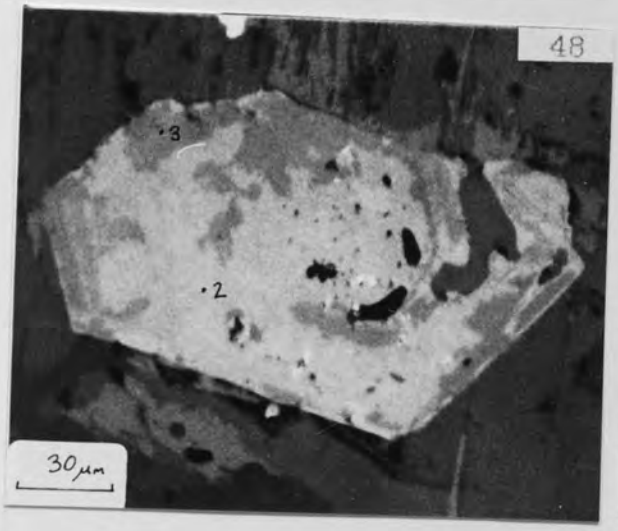
48
3
2
30 µm


49
6
2
20 µm
5

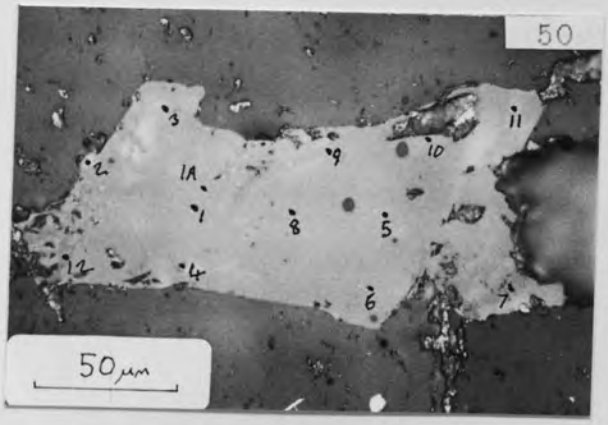
50
3
11
2
9
10
1A
1
8
5
12
4
6
7
50 µm

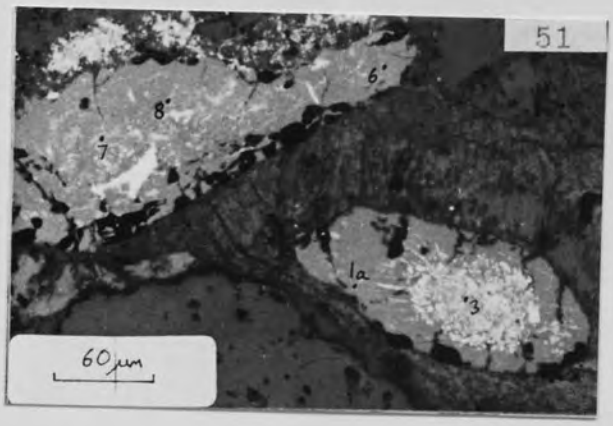
51
6
8
7
1a
3
60 µm

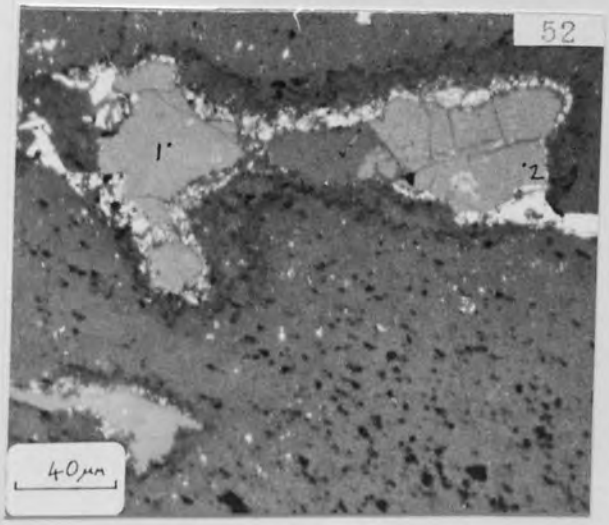
52
1
2
40 µm


53
1
F
2
40 µm

Table 26 Zircon from surface and borehole samples of biotite granite

Sample No.	Grain No.	An. Spot	Description	Plate No.
N75	19	2	Haematite inclusion-rich core	28
		4	Clear outer zone	
		5	Clear outer zone	
N94	16b	4	Analysis close to the edge of a 60 µm diameter enclosed by thorite (Grain 16b).	
100	1	1	Low reflectance patch	41
		3	" " "	
		5	" " "	
		2	High " "	
		4	" " "	
		7	" " "	
125	P.1c	6	Partly enclosed by Li-mica. Haematite-inclusion rich. Analysis quite close to grain edge.	
	P.2	5	Partially corroded, where enclosed by Li-mica. Analysis of high reflectance, inclusion-free spot near core.	
155	11		150 µm long zircon included in quartz.	50
		1	Analysis close to grain centre.	
		1A	10 µm away from An. 1.	
		3	Close to grain edge.	

Table 26 Probe Analyses of Zircon from Surface and Borehole Samples of Biotite Granite
(recalculations based on four oxygens)

Sample	75			94	100						125		155		
Grain	19			16b	1						P.1c	P.2	11		
An.Spot	2	4	5	4	1	2	3	4	5	7	6	5	1	1a	3
ZrO_2	52.73	61.88	58.44	52.11	53.67	62.46	50.93	62.79	52.20	60.97	59.33	59.32	62.19	60.84	62.49
HfO_2	2.51	6.65	7.01	11.78	2.72	2.54	2.34	4.41	2.34	2.73	4.99	3.34	2.49	2.44	2.77
ThO_2	4.50	0.66	1.64	0.69	4.22	0.96	3.48	0.40	4.88	0.69	2.58	2.32	0.66	1.17	0.25
UO_2	1.63	0.43	0.53	0.46	0.75	0.35	0.86	0.21	0.91	0.27	0.51	0.63	1.12	1.57	0.65
Y_2O_3	0.68	0.13	0.26	0.26	1.34	0.31	1.22	0.12	1.39	0.31	0.34	1.28	0.44	0.71	0.23
CaO	0.19	0.03	0.06	0.05	0.69	0.23	0.47	0.07	1.52	0.95	0.10	0.17	nd	–	–
FeO	1.57	0.26	0.24	1.48	1.73	0.42	1.61	0.37	1.76	0.52	2.21	0.67	nd	–	–
MnO	–	–	–	–	0.63	0.11	0.60	nd	0.53	0.09	–	–	–	–	–
SiO_2	26.33	31.34	30.30	31.19	26.61	32.43	25.55	32.37	26.36	31.00	30.26	30.31	30.66	31.01	31.43
P_2O_5	0.47	0.14	0.14	0.18	0.25	0.10	0.17	0.09	0.22	0.08	0.21	0.33	0.17	0.27	0.10
Total	90.61	101.52	98.62	98.20	92.61	99.91	87.23	100.83	92.11	97.61	100.53	98.37	97.73	98.01	97.92
Zr	0.924	0.943	0.924	0.831	0.921	0.945	0.922	0.946	0.903	0.948	0.924	0.932	0.971	0.949	0.966
Hf	0.026	0.059	0.065	0.110	0.027	0.022	0.025	0.039	0.024	0.025	0.045	0.031	0.023	0.022	0.025
Th	0.037	0.005	0.012	0.005	0.034	0.007	0.029	0.003	0.039	0.005	0.019	0.017	0.005	0.009	0.002
U	0.013	0.003	0.004	0.003	0.006	0.002	0.007	0.001	0.007	0.002	0.004	0.005	0.008	0.011	0.005
Y	0.013	0.002	0.004	0.005	0.025	0.005	0.024	0.002	0.026	0.005	0.006	0.022	0.007	0.012	0.004
Ca	0.007	0.001	0.002	0.002	0.026	0.008	0.019	0.002	0.058	0.032	0.003	0.006	0.000	0.000	0.000
Fe	0.047	0.007	0.007	0.040	0.051	0.011	0.050	0.010	0.052	0.014	0.059	0.018	0.000	0.000	0.000
Mn	0.000	0.000	0.000	0.000	0.019	0.003	0.019	0.000	0.016	0.002	0.000	0.000	0.000	0.000	0.000
Total	1.067	1.020	1.018	0.996	1.109	1.003	1.095	1.003	1.125	1.033	1.060	1.031	1.014	1.003	1.002
Si	0.946	0.980	0.983	1.020	0.936	1.006	0.948	1.000	0.935	0.989	0.966	0.976	0.982	0.991	0.996
P	0.014	0.004	0.004	0.005	0.007	0.003	0.005	0.002	0.007	0.002	0.006	0.009	0.005	0.007	0.003
Total	0.960	0.984	0.987	1.025	0.943	1.009	0.953	1.002	0.942	0.991	0.972	0.985	0.987	0.998	0.999

– Not determined nd Not detected

Table 27 Partial analyses of zircon 11 (Plate 50) from 155 m depth in the biotite granite
Analyses 1, 1a and 3 are quantitative (see Table 26) and the others are semi-quantitative (wt %)

Analysis Spot	UO_2	ThO_2	Y_2O_3	P_2O_5
1	1.12	0.66	0.44	0.17
1a	1.57	1.17	0.71	0.27
3	0.65	0.25	0.23	0.10
4	0.72	0.48	0.27	0.10
5	0.57	0.14	0.14	0.19
6	0.62	0.20	0.11	0.18
7	0.63	0.73	1.20	0.22
8	0.84	0.49	1.40	0.35
9	0.78	0.96	1.39	0.37
10	0.70	0.15	0.26	0.24
11	0.56	0.72	0.52	0.30
12	0.60	0.35	0.33	0.12

Table 28 Correlation coefficients for elements in Table 27

	UO_2	ThO_2	Y_2O_3
ThO_2	0.668		
Y_2O_3	0.211	0.627	
P_2O_5	0.219	0.523	0.755

Table 29 Zircon from borehole samples of biotite granite

Sample No.	Grain No.	An. Spot	Description	Plate No.
185	P.3	2	Higher reflectance area, close to grain edge	49
		5	" " " very close " "	
		6	Lower " "	
	P.2a	2	Higher reflectance area.	48
		3	Lower reflectance area, close to grain edge.	
305	5(i)	1	Low reflectance area	46
		2	" " "	
		5	" " "	
		3	High " "	
		4	" " "	
	5(ii)	1	Low " "	47
		3	" " "	
		2	High " "	
315	10	2	Zircon core	33
		3	Zircon overgrowth	

Table 29 Probe analyses of zircon from the borehole samples of biotite granite (recalculations based on four oxygens)

Sample	185					305								315	
Grain	P.3			P.2a		5(i)					5(ii)			10	
An.Spot	2	5	6	2	3	1	2	3	4	5	1	2	3	2	3
ZrO_2	63.70	59.50	48.40	61.81	54.50	49.70	48.70	63.00	63.70	52.00	51.70	63.90	50.30	63.00	60.30
HfO_2	4.09	5.79	4.19	3.07	3.10	2.47	2.42	2.72	2.65	2.73	2.54	2.41	2.63	2.80	4.54
ThO_2	0.33	0.76	3.61	0.30	3.08	7.33	5.90	0.02	0.05	4.87	4.85	0.10	5.43	nd	0.20
UO_2	0.28	1.21	0.32	0.57	0.58	4.00	1.88	0.43	0.25	2.32	1.19	0.32	1.14	0.14	0.58
Y_2O_3	0.16	0.37	1.85	0.25	2.99	1.92	2.12	0.02	0.01	1.27	2.07	0.72	1.97	0.05	0.17
CaO	0.05	0.02	0.60	nd	0.20	0.39	0.51	0.03	0.14	0.76	0.51	0.04	0.51	0.01	0.01
FeO	nd	nd	3.31	0.18	1.42	1.70	1.84	0.51	0.20	1.20	1.60	0.35	1.40	nd	0.11
MnO	0.03	nd	0.27	nd	0.18	0.45	0.52	nd	nd	0.40	0.59	nd	0.49	nd	nd
SiO_2	32.95	32.65	27.18	31.77	28.19	24.55	24.10	31.34	32.36	24.73	25.33	32.13	25.01	31.26	30.84
P_2O_5	0.20	0.21	0.24	0.19	0.31	0.36	0.40	0.14	0.05	0.24	0.32	0.19	0.34	0.07	0.25
Total	101.79	100.51	89.97	98.14	94.55	92.87	88.39	98.21	99.41	90.52	90.70	100.16	89.22	97.33	97.00
Zr	0.947	0.905	0.848	0.951	0.904	0.893	0.899	0.970	0.964	0.933	0.917	0.963	0.909	0.977	0.947
Hf	0.036	0.052	0.043	0.028	0.030	0.026	0.026	0.025	0.023	0.029	0.026	0.021	0.028	0.025	0.042
Th	0.002	0.005	0.030	0.002	0.024	0.061	0.051	0.000	0.000	0.041	0.040	0.001	0.046	0.000	0.001
U	0.002	0.008	0.003	0.004	0.004	0.033	0.016	0.003	0.002	0.019	0.010	0.002	0.009	0.001	0.004
Y	0.003	0.006	0.035	0.004	0.054	0.038	0.043	0.000	0.000	0.025	0.040	0.012	0.039	0.001	0.003
Ca	0.002	0.001	0.023	0.000	0.007	0.015	0.021	0.001	0.005	0.030	0.020	0.001	0.020	0.000	0.000
Fe	0.000	0.000	0.099	0.005	0.040	0.052	0.058	0.013	0.005	0.037	0.049	0.009	0.043	0.000	0.003
Mn	0.001	0.000	0.008	0.000	0.005	0.014	0.017	0.000	0.000	0.012	0.018	0.000	0.015	0.000	0.000
Total	0.993	0.977	1.089	0.994	1.068	1.132	1.131	1.012	0.999	1.126	1.120	1.009	1.109	1.004	1.000
Si	1.004	1.018	0.976	1.003	0.959	0.904	0.912	0.990	1.004	0.910	0.921	0.993	0.926	0.994	0.993
P	0.005	0.006	0.007	0.005	0.009	0.011	0.013	0.004	0.001	0.007	0.010	0.005	0.011	0.002	0.007
Total	1.009	1.024	0.983	1.008	0.968	0.915	0.925	0.994	1.005	0.917	0.931	0.998	0.937	0.996	1.000

- Not determined nd Not detected

Table 30 Comparative analyses of low and high reflectance areas in zircon from various samples (wt.% range and average of several analyses)

Rock type		Biotite granite						Greisen	
Sample No.		100		185		305		R1/13-4	
	(No. Ans.)	Range (3)	Ave.	Range	Ave.	Range (3)	Ave.	Range (6)	Ave.
HIGH REFLEC	ZrO_2	60.97-62.79	62.07	61.81		63.00-63.90	63.53	50.99-62.47	56.84
	SiO_2	31.00-32.43	31.93	31.77		31.34-32.36	31.94	27.13-31.32	30.19
	HfO_2	2.54 - 4.41	3.23	3.07		2.41 - 2.72	2.59	3.55 - 17.3	8.85
	ThO_2	0.40 - 0.96	0.68	0.30		0.02 - 0.10	0.06	0.06 - 0.63	0.20
	UO_2	0.21 - 0.35	0.28	0.57		0.25 - 0.43	0.33	0.56 - 1.74	0.95
	Y_2O_3	0.12 - 0.31	0.25	0.25		0.01 - 0.72	0.25	0.08 - 4.11	0.77
	P_2O_5	0.08 - 0.10	0.09	0.19		0.05 - 0.19	0.13	0.06 - 3.35	0.64
	CaO	0.07 - 0.95	0.42	0		0.03 - 0.14	0.17	0 - 0.03	0.01
	FeO	0.37 - 0.52	0.44	0.18		0.20 - 0.51	0.35	0.06 - 0.45	0.17
	MnO	0 - 0.11	0.07	0		0	0	0 - 0.01	0
Ave.Total			99.45	98.14			98.94		98.62
	(No. Ans.)	(3)		(2)		(6)		(2)	
LOW REFLEC	ZrO_2	50.93-53.67	52.27	41.61-54.50	48.05	47.10-52.00	49.92	40.54-49.48	45.01
	SiO_2	25.55-26.61	26.17	24.96-28.19	26.58	22.87-25.33	24.43	24.48-26.67	25.58
	HfO_2	2.34 - 2.72	2.47	2.49 - 3.10	2.80	2.42 - 2.73	2.56	3.79 - 7.46	5.63
	ThO_2	3.48 - 4.88	4.19	3.08 - 8.04	5.56	4.85 - 7.33	5.91	4.42 - 7.85	6.14
	UO_2	0.75 - 0.91	0.84	0.58 - 0.96	0.77	1.14 - 4.00	2.15	2.52 - 3.80	3.16
	Y_2O_3	1.22 - 1.39	1.32	2.99 - 5.42	4.21	1.27 - 2.12	1.90	3.49 - 4.78	4.14
	P_2O_5	0.17 - 0.25	0.21	0.31 - 0.32	0.32	0.24 - 0.40	0.34	0.41 - 0.95	0.68
	CaO	0.47 - 1.52	0.89	0.20 - 0.25	0.23	0.39 - 0.76	0.55	0.31 - 0.32	0.32
	FeO	1.61 - 1.76	1.70	1.42 - 2.96	2.19	1.20 - 1.84	1.57	0.73 - 1.02	0.88
	MnO	0.53 - 0.63	0.59	0.18	0.18	0.40 - 0.59	0.51	0.58	0.58
Ave.Total			90.65		90.90		89.88		92.09

Table 31 Thorite from surface samples of biotite granite

Sample No.	Grain No.	An. Spot	Description	Plate No.
75	1	2	Small inclusion in zircon	
	19	1	Overgrowth on zircon	28
94			Ovoid thorites included in biotite	
	16a	1	Haematite-rich core	
		2	Clear outer zone	
	16b	1	Haematite-rich core	
		2	Clear outer zone	
		3	"	
	17a	1	Haematite-rich outer zone	29
		2	" " core	
		3	" " "	
	17b	4	" " outer zone	
		5	" " " "	

Table 31 Probe analyses of thorite from surface samples of the biotite granite (recalculations based on four oxygens)

Sample	75		94									
Grain	1	19	16a		16b			17a			17b	
An.Spot	2	1	1	2	1	2	3	1	2	3	4	5
ThO_2	44.07	42.19	66.12	66.56	68.45	64.37	58.20	56.23	52.60	64.56	52.62	49.74
UO_2	6.85	3.57	13.43	11.59	5.39	6.13	9.09	5.69	5.63	11.04	3.43	3.63
Y_2O_3	2.95	3.24	0.93	5.60	4.02	5.44	9.78	6.14	7.14	3.85	9.60	8.80
CaO	0.67	0.78	0.97	0.98	0.58	0.68	1.16	0.64	0.67	0.87	0.57	0.58
ZrO_2	17.13	21.26	0.15	0.52	1.98	2.59	0.57	4.03	4.58	0.62	5.92	5.54
HfO_2	1.61	2.35	0.22	0.18	0.23	0.07	nd	0.30	0.21	nd	0.27	nd
FeO	3.06	1.73	5.91	0.65	2.97	1.82	1.81	3.23	6.90	2.59	2.23	3.09
SiO_2	15.13	15.83	10.84	9.28	10.99	11.37	8.22	10.65	10.75	10.37	10.74	10.93
P_2O_5	1.19	1.29	0.70	4.09	2.71	3.72	6.84	4.10	4.34	2.52	5.83	4.86
Total	92.66	92.24	99.27	99.45	97.32	96.19	95.67	91.01	92.82	96.42	91.21	87.17
Th	0.507	0.468	0.909	0.874	0.895	0.816	0.730	0.726	0.648	0.875	0.636	0.629
U	0.077	0.039	0.180	0.149	0.069	0.076	0.111	0.072	0.068	0.146	0.041	0.045
Y	0.079	0.084	0.030	0.172	0.123	0.161	0.287	0.185	0.206	0.122	0.271	0.260
Ca	0.036	0.041	0.063	0.061	0.036	0.041	0.069	0.039	0.039	0.056	0.032	0.035
Zr	0.422	0.505	0.004	0.015	0.055	0.070	0.015	0.112	0.121	0.018	0.153	0.150
Hf	0.023	0.033	0.004	0.003	0.004	0.001	0.000	0.005	0.003	0.000	0.004	0.000
Fe	0.129	0.071	0.299	0.031	0.143	0.085	0.083	0.153	0.312	0.130	0.099	0.144
Total	1.273	1.241	1.489	1.305	1.325	1.250	1.295	1.292	1.397	1.347	1.236	1.263
Si	0.765	0.771	0.655	0.535	0.631	0.633	0.453	0.604	0.582	0.618	0.570	0.607
P	0.051	0.053	0.036	0.200	0.132	0.175	0.319	0.197	0.199	0.127	0.262	0.228
Total	0.816	0.824	0.691	0.735	0.763	0.808	0.772	0.801	0.781	0.745	0.832	0.835

nd Not detected

Table 32 Thorite from borehole sample of greisenised biotite granite

Sample No.	Grain No.	An. Spot	Description	Plate No.
125	P.1a	1 3	20 µm and 120 µm long, anhedral, pyrite-bearing overgrowths on zircon.	31
	P.1c	1 4	Small thorite inclusions close to zircon edge.	
	P.3	2	30 µm diameter overgrowth on corroded zircon	
	P.4	1	120 µm long, ovoid grain included in Li-mica. Minute pyrite inclusions.	
	B.1a	2	70 µm long, included in Li-mica.	
	B.1c.	1 2	Ovoid, 170 µm long grain containing abundant pyrite inclusions and veinlets in core. Both analyses at grain margin.	
	B.2	2	Enclosed by 150 µm diameter zircon which, itself, is partly enclosed in cassiterite.	56

Table 32 Probe analyses of thorite from borehole sample of greisenised biotite granite (recalculations based on four oxygens)

Sample	125										
Grain	P.1a		P.1c		P.3	P.4		B.1a	B.1c		B.2
An.Spot	1	3	1	4	2	1	2	2	1	2	2
ThO_2	40.68	40.08	39.49	38.77	41.54	41.99	43.01	42.65	43.19	46.40	43.08
UO_2	1.29	3.09	3.01	1.41	3.15	1.27	1.10	1.23	1.17	2.06	2.95
Y_2O_3	7.51	7.09	7.44	6.13	7.08	6.75	7.10	7.06	6.93	7.19	7.11
CaO	0.76	0.77	0.64	0.69	0.84	0.83	0.88	0.66	0.54	1.59	0.71
ZrO_2	23.27	24.74	25.12	28.99	22.60	22.80	22.01	21.01	22.32	20.70	23.47
HfO_2	1.36	1.77	1.73	2.08	1.39	1.35	1.33	1.42	1.26	1.36	1.38
FeO	0.69	0.62	0.67	0.55	0.80	1.33	1.75	0.58	1.10	0.71	1.53
SiO_2	17.63	19.10	19.04	20.86	17.73	17.81	17.61	17.44	17.44	17.53	17.45
P_2O_5	1.26	1.07	1.22	1.00	1.17	1.17	1.20	1.27	1.24	1.27	1.23
Total	94.45	98.33	98.36	100.48	96.30	95.30	95.99	93.32	95.19	98.81	98.91
Th	0.421	0.396	0.388	0.361	0.428	0.434	0.444	0.453	0.451	0.476	0.437
U	0.013	0.030	0.029	0.013	0.032	0.013	0.011	0.013	0.012	0.021	0.029
Y	0.182	0.164	0.171	0.134	0.171	0.163	0.171	0.175	0.169	0.172	0.168
Ca	0.037	0.036	0.030	0.030	0.041	0.040	0.043	0.033	0.027	0.077	0.034
Zr	0.517	0.523	0.529	0.579	0.499	0.504	0.487	0.478	0.499	0.455	0.510
Hf	0.018	0.022	0.021	0.024	0.018	0.017	0.017	0.019	0.016	0.017	0.018
Fe	0.026	0.022	0.024	0.019	0.030	0.050	0.066	0.023	0.042	0.027	0.057
Total	1.214	1.193	1.192	1.160	1.219	1.221	1.239	1.194	1.216	1.245	1.253
Si	0.803	0.828	0.822	0.854	0.803	0.808	0.799	0.814	0.800	0.790	0.777
P	0.049	0.039	0.045	0.035	0.045	0.045	0.046	0.050	0.048	0.048	0.046
Total	0.852	0.867	0.867	0.889	0.848	0.853	0.845	0.864	0.848	0.838	0.823

Table 33 Thorite from borehole samples of biotite granite

Sample No.	Grain No.	An. Spot	Description	Plate No.
155	11	2	10 μm diameter overgrowth on zircon.	50
185	B.3	4	10 μm diameter inclusion in zircon.	
256	P.6		60 μm diameter grain, with marginal haematite interstitial to K-feldspar.	52
		1	Analysis in core	
		2	Analysis close to edge.	
305	4		Ovoid grains in Fe-stained biotite.	51
		1a	Clear, outer zone.	
		6	" "	
		7	Haematite-inclusion rich core	
		8	" " " "	
315	8	16a	Close to margin of a 250 μm long thorite which is interstitial to quartz. Contains abundant haematite inclusions.	32
	10	1	20 μm long thorite inclusion in a zircon overgrowth.	34
350	21		Associated with fluorite and included in biotite.	53
		1	Haematite-rich core.	
		2	Clear outer zone.	
	2	1,2	15-30 μm diameter inclusions in zircon, which	35
		3	is included in quartz.	

Table 33 Probe analyses of thorite from the borehole samples of biotite granite (recalculations based on four oxygens)

Sample	155	185	256		305				315		350				
Grain	11	B.3	P.6		4				8	10	21		2		
An.Spot	2	4	1	2	1a	6	7	8	16a	1	1	2	1	2	3
ThO_2	69.52	53.32	40.03	39.68	53.80	60.15	59.12	60.62	70.85	76.90	67.52	48.70	64.48	63.93	63.66
UO_2	4.82	14.07	0.76	0.74	1.50	3.18	1.86	2.28	4.80	5.32	4.55	3.14	20.57	19.03	17.07
Y_2O_3	2.54	2.34	2.86	2.65	2.77	2.83	2.23	2.32	0.19	0.66	4.74	6.26	0.43	0.55	0.63
CaO	-	0.47	1.00	1.27	0.72	0.74	0.59	0.61	0.92	0.67	0.95	1.73	1.12	1.31	1.54
ZrO_2	4.97	7.30	27.11	25.50	17.30	11.65	8.60	7.90	4.35	2.30	1.73	12.89	0.47	1.13	-
HfO_2	0.72	0.60	1.83	1.69	1.03	0.74	0.47	0.05	-	-	-	-	-	-	-
FeO	-	0.13	0.65	1.38	1.29	0.93	7.64	5.51	3.79	1.47	2.51	2.20	0.05	0.02	0.52
SiO_2	13.93	12.50	16.89	16.27	17.02	14.74	13.09	13.30	11.52	11.27	13.79	17.00	13.19	13.54	12.98
P_2O_5	0.74	0.43	0.75	0.71	0.96	1.15	1.01	1.09	0.58	0.44	0.67	0.79	0.49	0.54	0.48
Total	97.24	91.16	91.88	89.89	96.39	96.11	94.61	93.68	97.00	99.03	96.46	92.71	100.80	100.05	96.87
Th	0.898	0.731	0.427	0.436	0.592	0.717	0.732	0.763	0.960	1.068	0.874	0.551	0.864	0.847	0.876
U	0.061	0.189	0.008	0.008	0.016	0.037	0.023	0.028	0.064	0.072	0.058	0.035	0.269	0.246	0.230
Y	0.077	0.075	0.071	0.068	0.071	0.079	0.065	0.068	0.006	0.021	0.143	0.166	0.014	0.017	0.020
Ca	0.000	0.030	0.050	0.066	0.037	0.042	0.034	0.036	0.059	0.044	0.058	0.092	0.071	0.082	0.100
Zr	0.138	0.215	0.620	0.600	0.408	0.298	0.228	0.213	0.126	0.068	0.048	0.312	0.014	0.032	0.000
Hf	0.012	0.010	0.024	0.023	0.014	0.011	0.007	0.001	0.000	0.000	0.000	0.000	0.000	0.000	0.000
Fe	0.000	0.007	0.025	0.056	0.052	0.041	0.348	0.255	0.189	0.075	0.119	0.091	0.003	0.001	0.026
Total	1.186	1.258	1.227	1.257	1.190	1.225	1.437	1.364	1.404	1.348	1.300	1.247	1.235	1.225	1.252
Si	0.790	0.753	0.792	0.785	0.823	0.773	0.712	0.735	0.686	0.688	0.784	0.845	0.776	0.788	0.785
P	0.036	0.022	0.030	0.029	0.039	0.051	0.047	0.051	0.029	0.023	0.032	0.033	0.024	0.027	0.025
Total	0.826	0.775	0.822	0.814	0.862	0.824	0.759	0.786	0.715	0.711	0.816	0.878	0.800	0.815	0.810

- Not determined

Fig. 23 Variation of analytical oxide total for thorite from the Ririwai samples

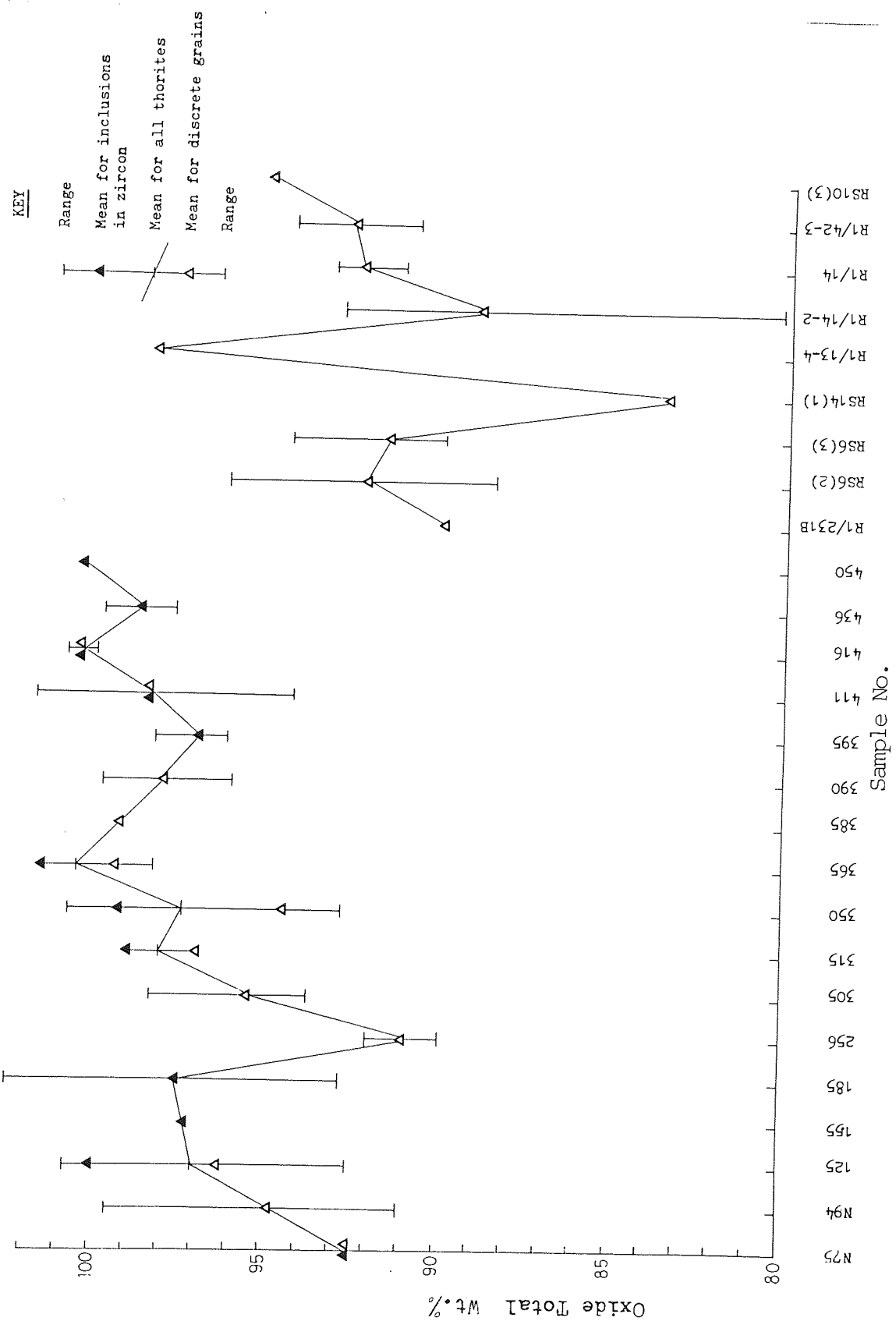

Fig. 24 Variation of wt. % UO_2 in thorite from the Ririwai samples

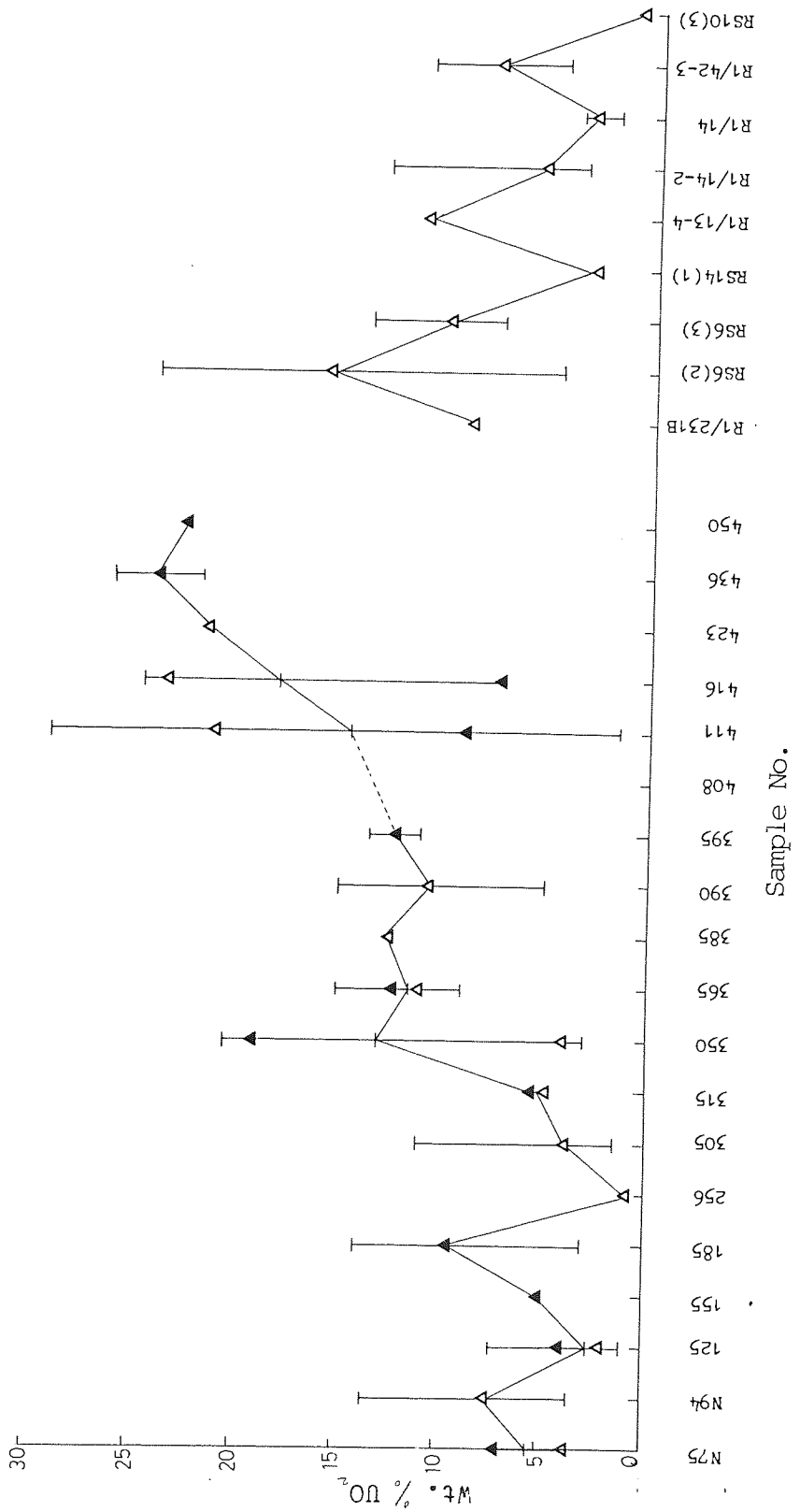

Fig. 25 Variation of wt. % Y_2O_3 in thorite from the Ririwai samples

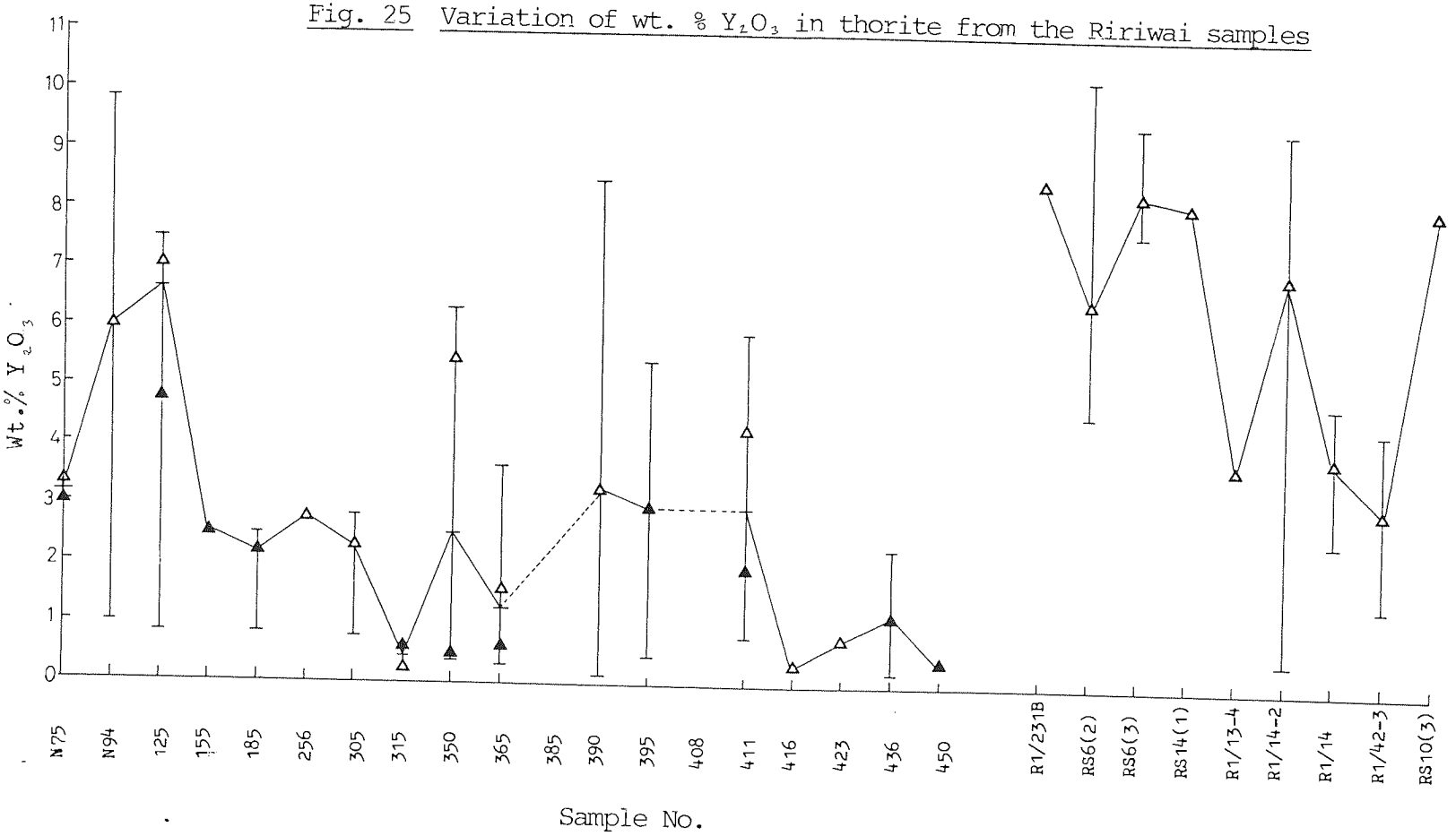

Fig. 26 Variation of wt. % ZrO_2 in thorite from the Ririwai samples

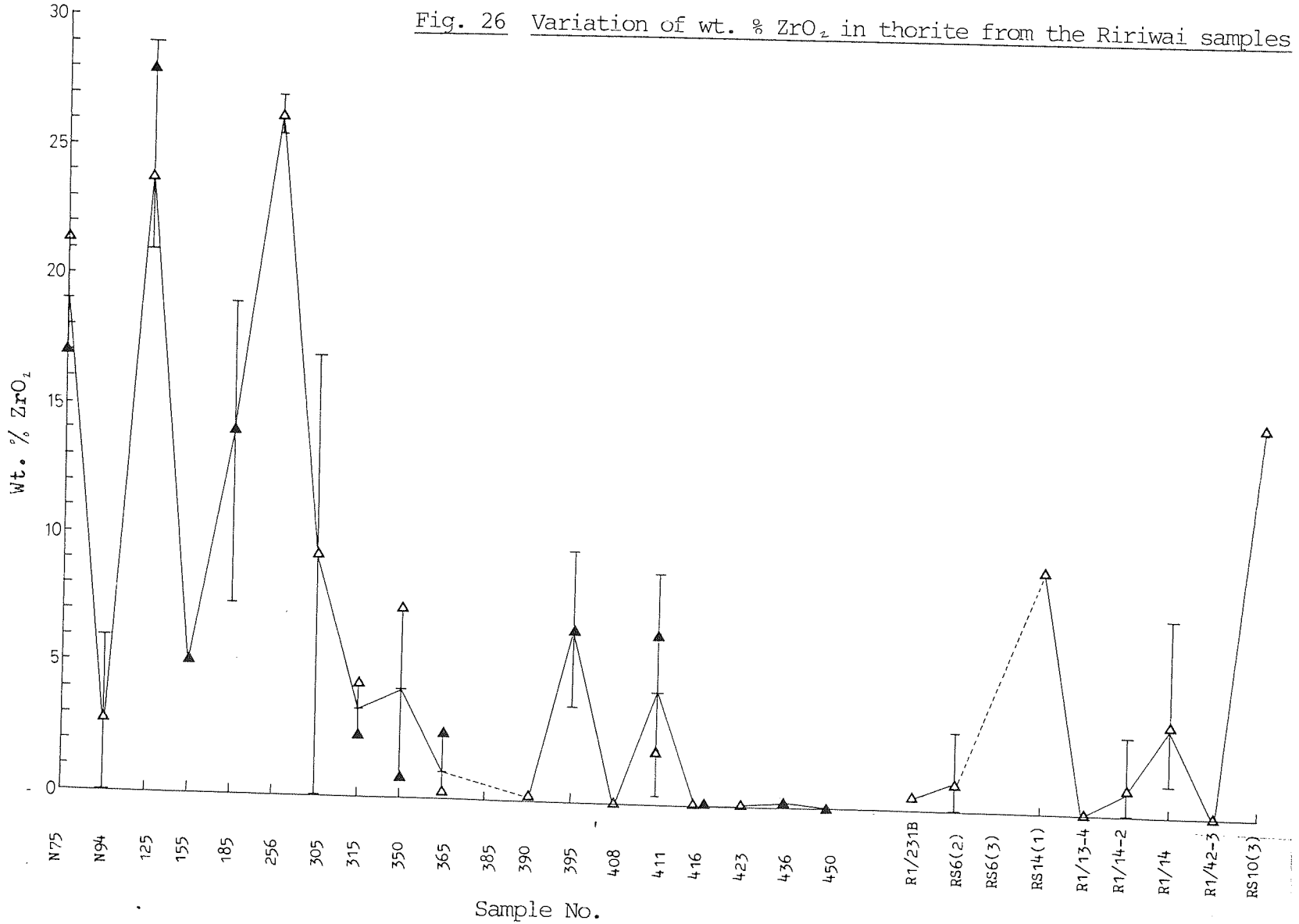

Plate No.	Sample No.	Grain No.	Description
			Borehole samples of biotite granite
54	365A	21	Interstitial thorite showing zoning of fine haematite inclusions and surrounded by a thick rim of haematite. (TPPL)
55	365B	5	Thorite (EPMA spots 1-3) replacing and overgrowing zircon (Z). Haematite (H) forms overgrowth and veinlets. (RPPL)
56	125	B.2	Zircon (EPMA spots 1 and 3) partially enclosed in cassiterite (C) and itself enclosing/replaced by thorite (EPMA spot 2). (RPPL)
57	145	1	Monazite interstitial to quartz and feldspar (EPMA spots). (TPPL)
58	365B	18	Irregular monazite (M), interstitial to quartz and feldspar. (TXPL)

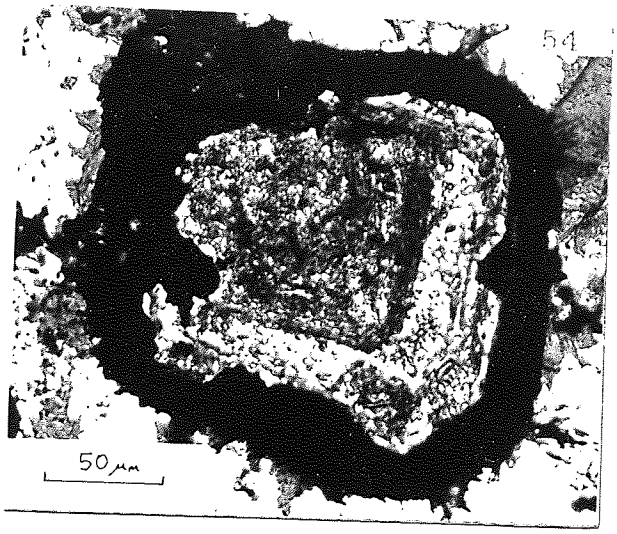
54
50 µm

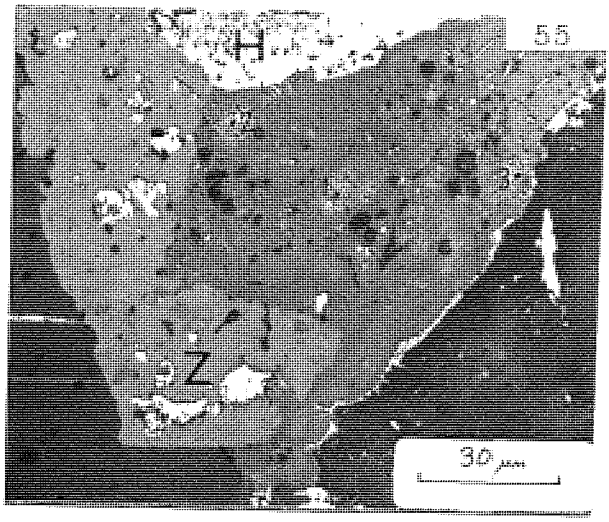
55
H
Z
30 µm

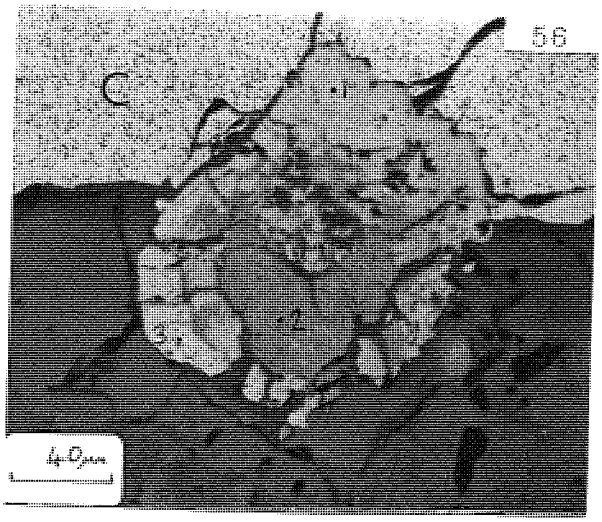
56
C
1
2
3
40 µm

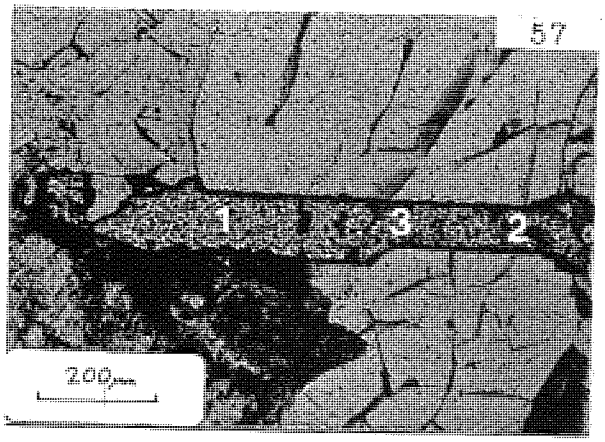
57
1
3
2
200 µm

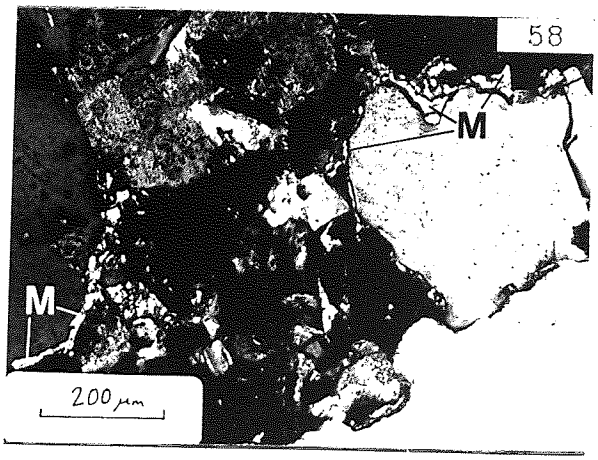
58
M
M
200 µm

Table 34 Monazite from the biotite granite (borehole) and greisenised wallrock (Ririwai lode)

Sample No.	Grain No.	An. Spot	Description	Plate No.
145	1	1	1 mm long, euhedral crystal, interstitial to quartz.	57
185	P.2	1	100 µm long, euhedral crystal included in K-feldspar.	
315	6	1	250 µm diameter, subhedral crystal partly enclosed by biotite and altering to a LREE-phase.	59
350	4		300 µm long, anhedral crystal interstitial to K-feldspar.	
		1	Close to grain edge.	
		2	"	
		3	Close to grain core.	
RS6(2)	10	1	300-500 µm long euhedral crystals included	
	10a	1	partly in quartz and in chlorite-sericite intergrowth.	

Table 34 Probe analyses of monazite from the biotite granite and greisenised wallrock (recalculations based on four oxygens)

Sample	145			185	315	350			RS6(2)	
Grain	1			P.2	6	4			10	10a
An.Spot	1	2	3	1	1	1	2	3	1	1
Ce_2O_3	35.86	37.01	35.06	37.49	32.07	38.16	36.82	37.90	33.78	33.14
La_2O_3	19.13	19.92	19.23	17.65	26.27	15.41	13.75	15.55	18.54	18.28
Nd_2O_3	7.58	7.29	7.04	9.66	4.90	10.77	13.17	10.83	9.60	9.66
Pr_2O_3	-	-	-	-	-	3.01	3.38	3.09	-	2.41
Sm_2O_3	-	-	-	-	-	0.71	1.06	0.65	-	-
Y_2O_3	-	-	-	0.07	0.07	-	-	-	-	0.24
CaO	0.73	0.59	0.87	0.43	0.29	0.17	0.20	0.18	0.67	0.63
ThO_2	8.86	7.30	10.38	7.26	12.16	2.68	2.97	2.77	7.92	6.82
UO_2	nd	nd	nd	0.04	0.32	0.23	0.24	0.27	0.31	0.34
P_2O_5	28.76	29.42	28.97	28.24	26.30	28.85	29.04	28.96	30.25	28.85
SiO_2	1.03	0.84	1.17	1.45	2.41	0.37	0.41	0.38	0.72	0.89
Total	101.95	102.37	102.72	102.29	104.79	100.36	101.04	100.58	101.79	101.26
Ce	0.514	0.525	0.499	0.538	0.464	0.556	0.533	0.550	0.476	0.477
La	0.276	0.285	0.275	0.255	0.383	0.226	0.200	0.227	0.263	0.265
Nd	0.106	0.101	0.098	0.135	0.069	0.153	0.186	0.153	0.132	0.136
Pr	0.000	0.000	0.000	0.000	0.000	0.044	0.049	0.045	0.000	0.035
Sm	0.000	0.000	0.000	0.000	0.000	0.010	0.014	0.009	0.000	0.000
Y	0.000	0.000	0.000	0.001	0.001	0.000	0.000	0.000	0.000	0.005
Ca	0.031	0.025	0.036	0.018	0.012	0.007	0.008	0.008	0.028	0.027
Th	0.079	0.064	0.092	0.065	0.109	0.024	0.027	0.025	0.069	0.061
U	0.000	0.000	0.000	0.000	0.003	0.002	0.002	0.002	0.003	0.003
Total	1.006	1.000	1.000	1.012	1.041	1.022	1.019	1.019	0.971	1.009
P	0.954	0.966	0.953	0.937	0.879	0.971	0.971	0.972	0.986	0.960
Si	0.040	0.033	0.045	0.057	0.095	0.015	0.016	0.015	0.028	0.035
Total	0.994	0.999	0.998	0.994	0.974	0.986	0.987	0.987	1.014	0.995

- Not determined nd Not detected

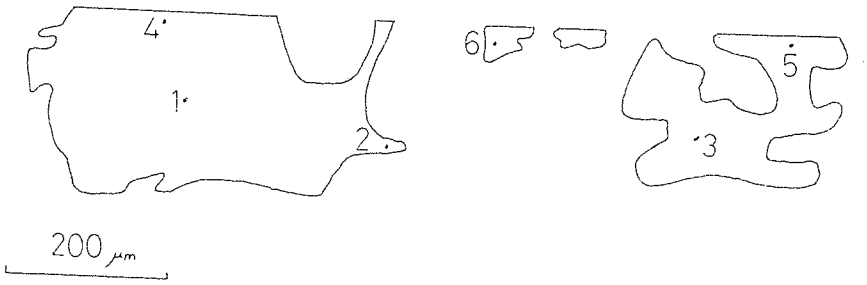

Fig. 27 Cluster of anhedral monazite grains (Plate 78). These may represent the residual fragments of a 1 mm long, euhedral crystal that has since been corroded. Numbers refer to semi-quantitative partial analyses (Table 35).

Analysis Spot	ThO_2	UO_2	SiO_2
1	6.24	0.35	0.77
2	7.02	0.36	0.84
3	0.33	0.15	0.10
4	6.77	0.27	0.80
5	4.15	0.24	0.56
6	0.85	0.15	0.19

Table 35 Semi-quantitative, partial analyses of the monazite grains in Fig. 27 and Plate 78, (wt. %).

Plate No.	Sample No.	Grain No.	Description
			Borehole samples of biotite granite
59	315	6	Monazite (EPMA spot 1) showing alteration to a LREE-phase (EPMA spot 13) of lower reflectance, in biotite (B). (RPPL)
60	350	21	LREE-phase (EPMA spot 1) included in fluorite (F) in biotite. (RPPL)
61	100	3	Interstitial coffinite (C) infilling biotite cleavages and grain boundaries. (SEM)
62	100	4	Coffinite (c) enclosing molybdenite (m) and admixed with sphalerite (s). EPMA spots are shown. (RPPL)
63	305	2a	Pyrochlore (p) intergrown with columbite (c). (ROIL)

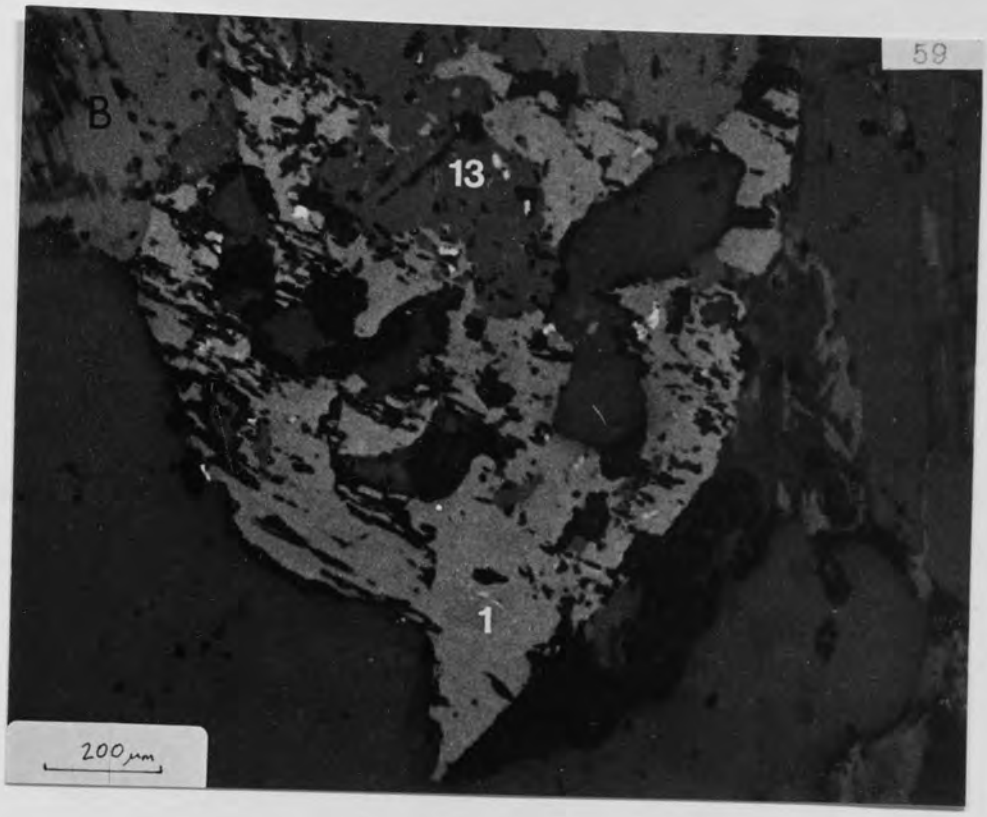
59
B
13
1
200µm

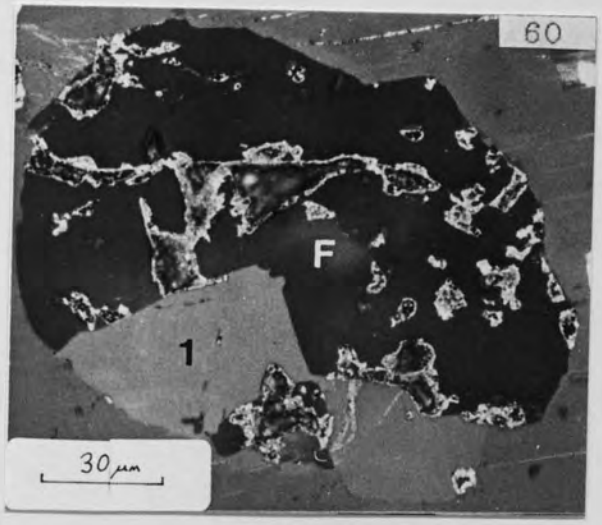
60
F
1
30µm


61
C
C
20µM

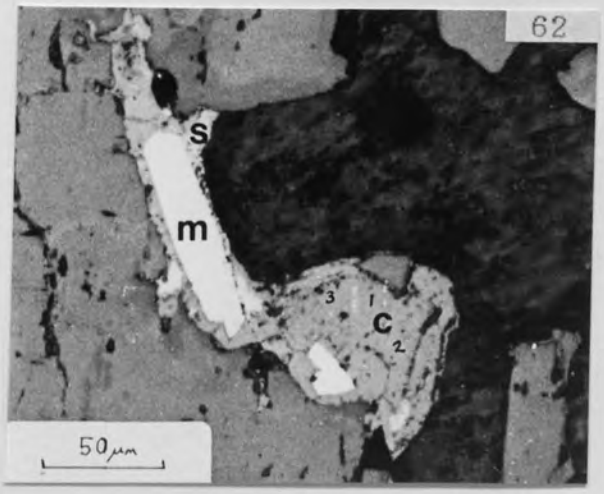
62
s
m
3
1
C
2
50µm

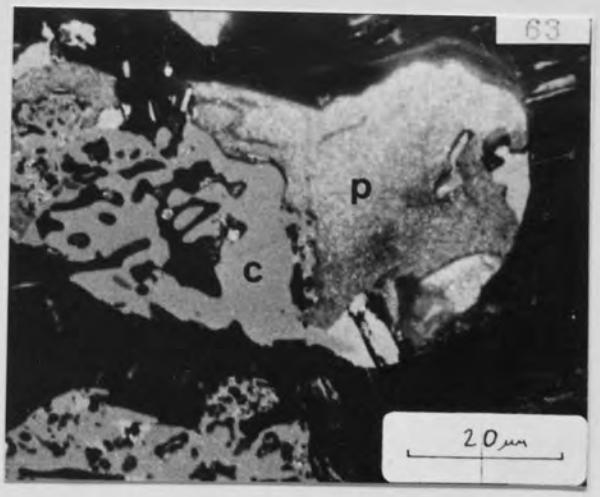
63
p
c
20µm

Table 36 LREE-phase(s) from the biotite and albitised granites and Ririwai lode

Sample No.	Grain No.	An. Spot	Description	Plate No.
315	6	13	Intergrown with monazite in the biotite granite	59
350	21	1	50 μm diameter inclusion in fluorite and biotite from the granite.	60
411	4	L	20 μm diameter inclusion in fluorite which embays zircon from the albitised granite.	81
	3	1,2	10 μm diameter inclusions in zircon.	
450A	2	1	50 μm diameter inclusion in fluorite which is intergrown with (replacing?) zircon in the albitised granite.	83
RS6(2)	3a	4	20 μm diameter grain included in fluorite and overgrowing a zircon-thorite-xenotime intergrowth, in the greisenised wall-rock of the Ririwai lode.	101
R1/14-2	1a	1	Complex Th-LREE phase overgrowing zircon in the greisen of the Ririwai lode. (LREE were not measured but see Fig. 55)	119

Table 36 Probe analyses of LREE-phase(s) from the biotite and albitised granites and Ririwai lode

(recalculations based on three oxygens)

Sample	315	350	411			450A	RS6(2)	R1/14-2
Grain	6	21	4	3		2	3a	1a
An.Spot	13	1	L	1	2	1	4	1 *
Ce_2O_3	40.27	37.57	33.90	37.70	38.02	40.19	37.31	-
La_2O_3	44.52	20.87	17.21	19.95	20.31	21.04	20.38	-
Nd_2O_3	5.49	11.90	12.63	12.16	12.10	14.43	13.25	-
Pr_2O_3	-	3.17	-	-	-	3.32	-	-
Sm_2O_3	-	1.08	-	-	-	1.65	-	-
Y_2O_3	0.10	-	3.94	1.16	1.07	1.14	2.68	3.31
CaO	0.54	0.34	7.32	0.11	0.11	0.36	1.30	3.10
ThO_2	2.41	0.33	2.37	1.51	1.65	1.38	1.28	23.05
UO_2	0.17	0.12	0.21	0.20	0.19	nd	0.25	0.60
FeO	nd	nd	0.75	0.51	0.61	nd	nd	1.16
ZrO_2	nd	nd	nd	0.80	0.57	nd	-	2.48
P_2O_5	0.04	0.02	0.03	nd	nd	nd	nd	7.31
SiO_2	0.13	0.02	0.34	0.63	0.48	0.07	1.05	2.70
Total	93.67	75.42	78.70	74.73	75.11	83.58	77.50	43.71
Ce	0.853	0.994	0.769	0.973	0.984	0.956	0.907	-
La	0.950	0.557	0.393	0.519	0.530	0.504	0.499	-
Nd	0.113	0.307	0.279	0.306	0.306	0.335	0.314	-
Pr	0.000	0.084	0.000	0.000	0.000	0.079	0.000	-
Sm	0.000	0.027	0.000	0.000	0.000	0.037	0.000	-
Y	0.003	0.000	0.130	0.044	0.040	0.039	0.095	0.129
Ca	0.033	0.026	0.486	0.008	0.008	0.025	0.092	0.243
Th	0.032	0.005	0.033	0.024	0.027	0.020	0.019	0.384
U	0.002	0.002	0.003	0.003	0.003	0.000	0.004	0.010
Fe	0.000	0.000	0.039	0.030	0.036	0.000	0.000	0.071
Zr	0.000	0.000	0.000	0.028	0.020	0.000	0.000	0.089
Total	1.986	2.002	2.132	1.935	1.954	1.995	1.930	0.926
P	0.002	0.001	0.002	0.000	0.000	0.000	0.000	0.453
Si	0.008	0.001	0.021	0.044	0.034	0.005	0.070	0.198
Total	0.010	0.002	0.023	0.044	0.034	0.005	0.070	0.651

\- Not determined
nd Not detected
* Partial analysis

Table 37 Coffinite and U-Th-Y-Si phases from the biotite granite and Ririwai lode

Sample No.	Grain No.	An. Spot	Description	Plate No.
100	3	1,2	Interstitial coffinite along grain boundaries	61
		3	and cleavage of biotite in the granite.	
	4	1	Coffinite intergrown with molybdenite and	62
		2	sphalerite.	
RS6(4)	1		Poorly crystallised, interstitial coffinite in the microclinite, Ririwai lode.	95
R1/13-3	7	5	Unidentified U-Th-Y-Si phase, intergrown with pyrite and ?REE-microlite which overgrow columbite, in the microclinite.	94
RS6(2)	6	1	Cluster of U-Th-Y-Si phase grains in chlorite-	111
		2	sericite intergrowth from the greisenised wall-rock, Ririwai lode.	

Table 37 Probe analyses of coffinite and U-Th-Y-Si-phases from the biotite granite and Ririwai lode (recalculations based on four oxygens)

Sample	100					RS6(4)					Rl/13-3	RS6(2)	
Grain	3			4		1					7	6	
An.Spot	1	2	3	1*	2*	1a	2	4	6a	7	5	1	2
ThO_2	3.29	3.68	1.35	1.94	4.94	3.18	2.68	3.45	2.91	3.19	8.19	16.74	17.87
UO_2	57.75	57.39	75.73	69.20	64.78	46.18	59.54	48.42	60.59	55.86	22.17	34.12	33.24
Y_2O_3	0.54	0.69	0.26	0.30	0.33	15.91	11.61	16.03	8.61	11.53	9.65	12.28	12.14
CaO	0.97	0.98	1.07	0.81	0.91	0.82	1.33	1.06	1.46	1.14	0.25	0.75	0.77
ZrO_2	11.69	10.49	2.86	4.01	4.97	0.29	–	–	0.04	0.07	1.59	0.54	0.57
HfO_2	0.43	0.32	0.43	0.37	0.44	nd	–	–	nd	nd	–	–	–
FeO	1.68	1.98	0.45	0.01	0.03	2.03	–	–	0.33	1.28	3.89	nd	nd
SiO_2	16.89	17.82	14.92	14.23	14.06	10.96	13.05	12.13	12.36	12.78	14.33	16.28	14.24
P_2O_5	0.19	0.21	0.22	0.12	0.11	4.71	1.94	3.21	1.05	2.76	2.09	2.76	2.67
Ce_2O_3	0.73	0.75	0.55	0.24x	nd x	nd	–	–	nd	nd	nd	–	–
Total	94.16	94.31	97.84	91.23	90.57	84.08	90.15	84.30	87.35	88.61	62.16	83.47	81.50
Th	0.039	0.044	0.018	0.027	0.068	0.042	0.036	0.046	0.041	0.042	0.125	0.211	0.239
U	0.677	0.664	0.971	0.938	0.876	0.592	0.772	0.633	0.843	0.718	0.332	0.420	0.434
Y	0.015	0.019	0.008	0.010	0.011	0.488	0.360	0.501	0.286	0.354	0.346	0.361	0.379
Ca	0.055	0.055	0.066	0.053	0.059	0.051	0.083	0.067	0.098	0.071	0.018	0.044	0.048
Zr	0.300	0.266	0.080	0.119	0.147	0.008	0.000	0.000	0.001	0.002	0.052	0.015	0.016
Hf	0.006	0.005	0.007	0.006	0.008	0.000	0.000	0.000	0.000	0.000	0.000	0.000	0.000
Fe	0.074	0.086	0.022	0.001	0.002	0.098	0.000	0.000	0.017	0.062	0.219	0.000	0.000
Total	1.166	1.139	1.172	1.154	1.171	1.279	1.251	1.247	1.286	1.249	1.092	1.051	1.116
Si	0.890	0.926	0.860	0.867	0.855	0.631	0.761	0.712	0.773	0.738	0.964	0.900	0.836
P	0.008	0.009	0.011	0.006	0.006	0.230	0.096	0.160	0.056	0.135	0.119	0.129	0.133
Total	0.898	0.935	0.871	0.873	0.861	0.861	0.857	0.872	0.829	0.873	1.083	1.029	0.969

* Analyses by J.R.Ashworth (Ixer et al., in press) x As_2O_3 – Not determined nd Not detected

Table 38 Pyrochlore and related phases from the arfvedsonite and biotite granites, albitite and Ririwai lode

Sample No.	Grain No.	An. Spot	Description	Plate No.
81	1		Pyrochlore from the arfvedsonite granite.	
		1	Core of main part of grain.	
		2	Rim and crack which appear brighter in a BSEI.	
305	2a	1-5	Plumbopyrochlore intergrown with columbite in biotite granite.	63
350	6	1	25 μm diameter inclusion in zircon from the biotite granite.	
R1/13-3	7	2	?Microlite intergrown with pyrite, U-Th-Y-Si phase and overgrowing columbite from microclinite. (Approximately 7 wt.% $LREE_2O_3$ estimated from semi-quantitative analyses).	94
445	4	3	?Pb-microlite in the albitite. Enclosed by pyrite.	91

Table 38 Probe analyses of pyrochlore and related phases from the arfvedsonite and biotite granites, albitite and Ririwai lode
(recalculations based on 7 oxygens)

Sample	81		305				350	445	R1/13-3
Grain	1		2a				6	4	7
An.Spot	1	2	1*	3*	4*	5*	1	3*	2
Nb_2O_5	32.04	34.05	19.77	19.34	19.49	19.18	55.10	13.69	9.08
Ta_2O_5	2.73	1.64	21.85	20.57	22.7	22.55	5.77	38.38	45.26
TiO_2	6.22	7.08	2.21	2.42	2.00	2.32	1.39	1.58	0.70
FeO	1.63	1.49	3.15	3.44	3.62	3.32	3.05	2.56	0.44
MnO	–	–	0.19	0.15	0.15	0.14	0.47	–	–
CaO	0.54	0.33	0.89	0.43	0.49	0.45	4.15	1.30	2.71
Na_2O	–	–	1.18	1.44	1.36	1.32	–	–	–
PbO	30.32	35.13	26.13	23.14	18.67	28.57	6.60	15.08	–
ThO_2	0.45	0.71	0.38	0.41	0.32	0.47	1.33	0.80	1.75
UO_2	7.19	3.60	15.42	17.40	19.39	13.66	8.39	8.39	0.48
Ce_2O_3	5.05	5.41	–	–	–	–	4.50	1.64	–
La_2O_3	0.93	1.82	nd	nd	nd	nd	1.17	0.34	–
Y_2O_3	0.45	0.37	–	–	–	–	nd	–	–
SiO_2	8.23	4.03	nd	nd	nd	nd	3.70	12.17	nd
Total	95.78	95.66	91.17	88.44	88.19	92.12	95.62	95.92	60.42
Nb	1.251	1.426	1.052	1.050	1.041	1.022	1.889	0.534	0.620
Ta	0.064	0.041	0.699	0.662	0.729	0.722	0.119	0.901	1.858
Ti	0.404	0.493	0.196	0.219	0.178	0.206	0.079	0.103	0.079
Fe	0.118	0.115	0.310	0.345	0.358	0.327	0.193	0.185	0.056
Mn	–	–	0.019	0.015	0.015	0.014	0.030	–	–
Total	1.837	2.075	2.276	2.291	2.321	2.291	2.310	1.823	2.613
Ca	0.050	0.033	0.112	0.055	0.062	0.057	0.337	0.120	0.438
Na	–	–	0.269	0.335	0.311	0.302	–	–	–
Pb	0.705	0.876	0.828	0.748	0.594	0.906	0.135	0.350	–
Th	0.009	0.015	0.010	0.011	0.009	0.013	0.023	0.016	0.060
U	0.138	0.074	0.404	0.465	0.510	0.358	0.142	0.161	0.016
Ce	0.160	0.183	–	–	–	–	0.125	0.052	–
La	0.030	0.062	0.000	0.000	0.000	0.000	0.033	0.011	–
Y	0.021	0.018	–	–	–	–	0.000	–	–
Total	1.113	1.261	1.623	1.614	1.486	1.636	0.795	0.710	0.514
Si	0.711	0.373	0.000	0.000	0.000	0.000	0.281	1.051	0.000

* Analyses by J. R. Ashworth
– Not determined
nd Not detected

Plate No.	Sample No.	Grain No.	Description
			Albitised granite
64	395B	1	Large, concentrically zoned zircon, showing outer, rhythmically zoned Type 1 zircon (2), intermediate Type 2 zircon (6) which contains white thorite inclusions (5) and inner Type 3 zircon core (1 and 3). Irregular, thorite-bearing patches of Type 2 zircon also occur in the core (4). EPMA spots are shown. (BSEI)
65	395B	1	The same zircon, partly included in biotite (b) and over-grown by bladed haematite (h). (TPPL)
66	411	2	Hf-enriched, outer Type 1 zone of zircon in Plates 69 and 70. EPMA spots are shown. (BSEI)
67	390B	25	Zircon showing embayment by feldspar. (TPPL)
68	395	15	Banding in Type 3 zircon. EPMA spots are shown. (TXPL)

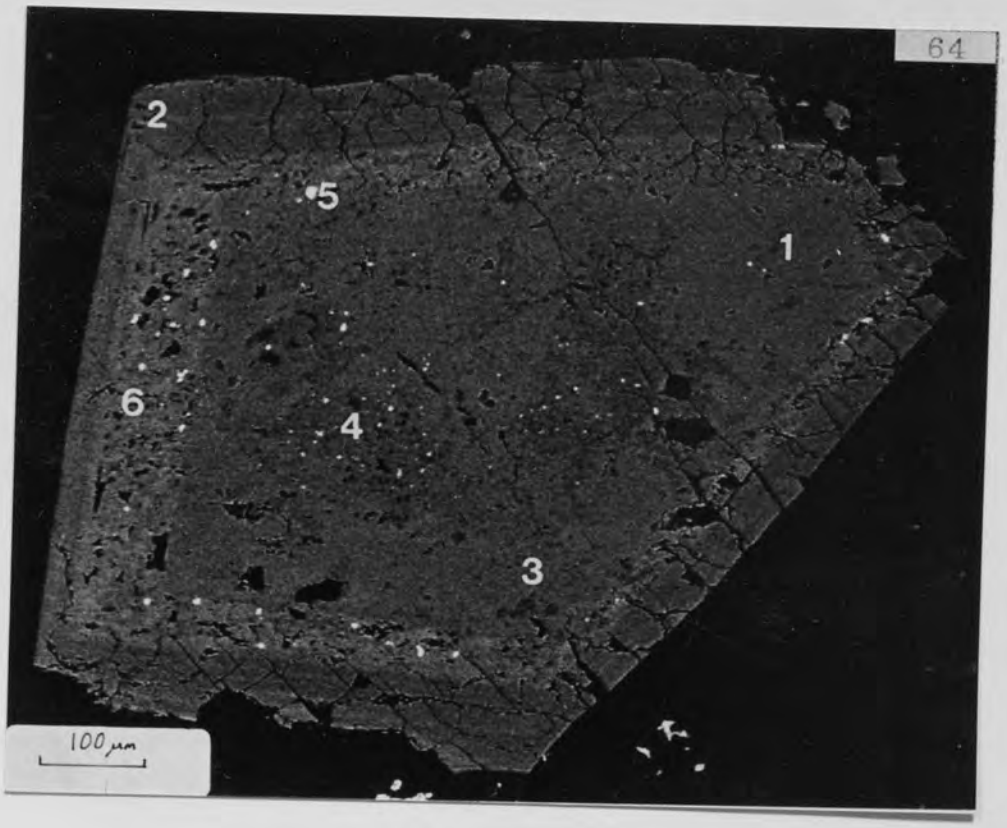
64
2
5
1
6
4
3
100 µm

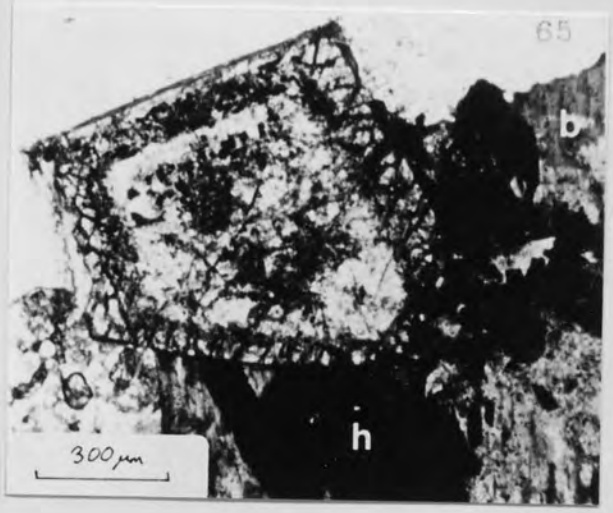
65
b
h
300 µm

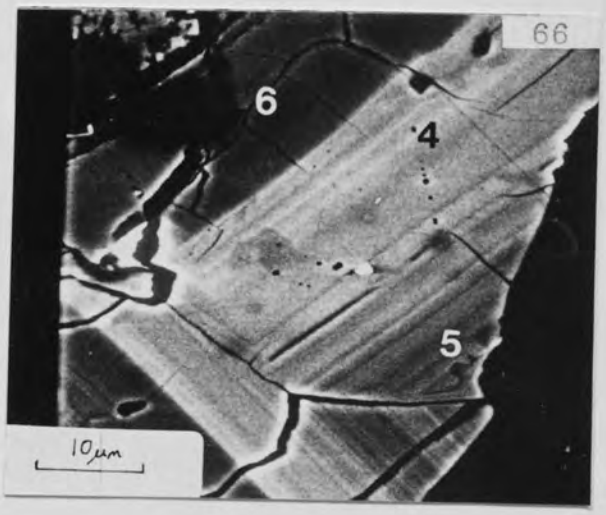
66
6
4
5
10 µm

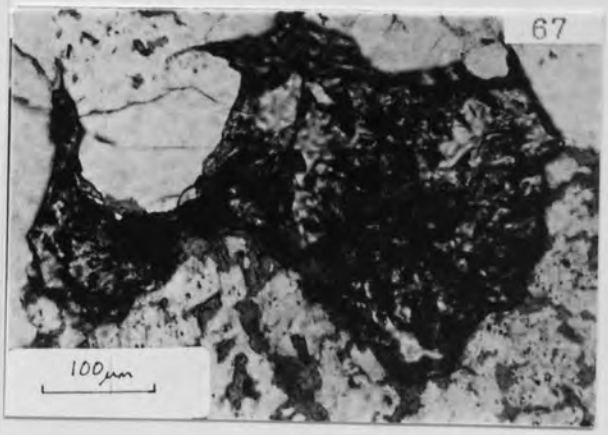
67
100 µm

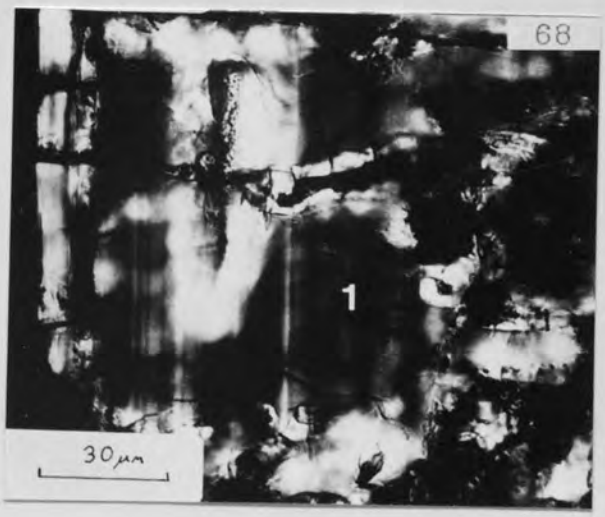
68
1
30 µm

Table 39 Zircon from the biotite and albitised granites

Sample No.	Grain No.	An. Spot	Description	Plate No.
365A	9	1	Clear rim of zircon from the biotite micro-granite	37
		2	Haematite and thorite rich core of zircon.	
		4	Clear rim.	
	29	1	Haematite and thorite rich part of zircon.	
390A	1	1	120 μm diameter, clear, interstitial zircon from the albitised granite.	
395B	1		700 μm diameter, concentrically zoned zircon, partly enclosed by biotite in the albitised granite.	64
		1	Type 3 (clear, isotropic) core.	
		2	Type 1 (clear, rhythmically zoned) rim.	
		3	Type 3	
		4	Type 2 (anisotropic with abundant haematite and thorite inclusions) core.	
		6	Type 2, intermediate zone.	
	4	1	370 μm long zircon with abundant haematite	
		2	inclusions, interstitial to quartz and feldspar.	
	15	1	Both analyses from peripheral, Type 3 domains	
		3	in a 250 μm diameter zircon, which is partly enclosed in biotite.	

Table 39 Probe analyses of zircon from the biotite and albitised granites (recalculations based on four oxygens)

Sample	365A				390A	395B								
Grain	9			29	1	1					4		15	
An.Spot	1	2	4	1	1	1	2	3	4	6	1	2	1	3
ZrO_2	61.80	62.10	62.11	59.77	58.60	59.96	61.00	59.38	60.63	54.98	59.04	60.35	59.33	61.20
HfO_2	5.48	4.81	4.94	4.61	10.53	6.38	8.09	6.55	5.52	10.90	8.08	6.30	5.10	2.90
ThO_2	0.01	0.04	0.16	0.76	0.06	0.45	nd	0.47	0.55	0.01	0.11	0.11	1.05	0.85
UO_2	0.36	0.56	0.57	1.33	0.22	1.10	0.42	1.10	0.93	0.78	0.50	0.67	1.21	1.05
Y_2O_3	0.06	0.08	0.12	0.27	0.09	0.37	0.02	0.35	0.12	0.19	0.09	0.32	0.59	0.55
CaO	nd	nd	nd	nd	-	nd	nd	nd	nd	nd	nd	nd	-	-
FeO	0.02	0.06	0.07	0.67	nd	0.07	0.04	0.04	0.70	0.56	0.11	0.08	0.44	0.07
MnO	-	-	-	-	-	-	-	-	-	-	-	-	-	-
SiO_2	31.42	32.88	30.89	30.16	30.30	30.19	30.58	29.80	30.65	28.83	30.18	30.17	30.63	31.02
P_2O_5	0.15	0.21	0.18	0.24	0.09	0.17	0.11	0.17	0.24	0.50	0.09	0.06	0.24	0.32
Total	99.30	100.74	99.04	97.81	99.89	98.69	100.26	97.86	99.34	96.75	98.20	98.06	98.59	97.96
Zr	0.951	0.933	0.961	0.944	0.921	0.944	0.946	0.945	0.943	0.897	0.935	0.952	0.930	0.952
Hf	0.049	0.042	0.045	0.043	0.097	0.059	0.073	0.061	0.050	0.104	0.075	0.058	0.047	0.026
Th	0.000	0.000	0.001	0.006	0.000	0.003	0.000	0.003	0.004	0.000	0.001	0.001	0.008	0.006
U	0.003	0.004	0.004	0.010	0.002	0.008	0.003	0.008	0.007	0.006	0.004	0.005	0.009	0.007
Y	0.001	0.001	0.002	0.005	0.002	0.006	0.000	0.006	0.002	0.003	0.002	0.006	0.010	0.009
Ca	0.000	0.000	0.000	0.000	0.000	0.000	0.000	0.000	0.000	0.000	0.000	0.000	0.000	0.000
Fe	0.001	0.002	0.002	0.018	0.000	0.002	0.001	0.001	0.019	0.016	0.003	0.002	0.012	0.002
Mn	0.000	0.000	0.000	0.000	0.000	0.000	0.000	0.000	0.000	0.000	0.000	0.000	0.000	0.000
Total	1.005	0.982	1.015	1.026	1.022	1.022	1.023	1.024	1.025	1.026	1.020	1.024	1.016	1.002
Si	0.991	1.012	0.980	0.977	0.976	0.975	0.973	0.972	0.977	0.965	0.980	0.976	0.985	0.989
P	0.004	0.005	0.005	0.007	0.002	0.005	0.003	0.005	0.006	0.014	0.002	0.002	0.007	0.009
Total	0.995	1.017	0.985	0.984	0.978	0.980	0.976	0.977	0.983	0.979	0.982	0.978	0.992	0.998

- Not determined nd Not detected

Table 40 Thorite from the biotite and albitised granites

Sample No.	Grain No.	An. Spot	Description	Plate No.
365A	9	3	13 μm diameter inclusion in haematite-rich core of zircon from the biotite granite.	37
	14	1	Inclusion in zircon.	
365B	5	1-3	100 μm diameter thorite replacing and over growing zircon.	55
385	6	1	Inclusion in columbite from the albitised granite.	73
390A	1	1-5	500 μm diameter interstitial thorite with haematite rim in the albitised granite.	77
395B	1	5	Inclusion from intermediate zone of Type 2 zircon in the albitised granite.	64
	15	4	12 μm diameter inclusion in zircon.	

Table 40 Probe analyses of thorite from the biotite and albitised granites (recalculations based on four oxygens)

Sample	365A		365B			385	390A					395B	
Grain	9	14	5			6	1					1	15
An.Spot	3	1	1	2	3	1	1	2	3	4	5	5	4
ThO_2	67.10	71.09	70.10	71.11	69.30	69.19	69.39	65.39	68.27	69.92	63.34	56.41	57.20
UO_2	15.14	9.58	11.19	13.00	8.92	12.50	10.91	5.15	14.92	13.26	8.31	10.87	13.46
Y_2O_3	0.28	1.05	0.70	0.60	3.66	-	0.61	6.95	0.14	0.11	8.51	5.40	0.51
CaO	0.39	0.17	0.21	0.77	0.41	1.15	0.79	0.20	0.63	1.06	0.44	0.84	0.09
ZrO_2	2.44	2.42	0.06	0.13	0.36	-	nd	nd	nd	nd	0.22	3.68	9.72
HfO_2	0.60	0.71	-	-	-	-	-	-	-	-	-	1.31	0.48
FeO	0.06	0.26	0.33	1.42	1.42	-	2.66	2.12	0.02	0.35	0.69	0.57	0.33
SiO_2	15.25	15.70	15.23	13.87	14.06	16.41	13.70	15.09	14.70	14.99	14.75	15.60	16.22
P_2O_5	0.33	0.55	0.47	0.44	0.39	-	0.22	0.97	0.09	0.11	1.07	1.19	0.29
Total	101.59	101.53	98.29	101.34	98.52	99.25	98.28	95.87	98.77	99.80	97.33	95.87	98.30
Th	0.850	0.884	0.919	0.932	0.910	0.886	0.931	0.829	0.912	0.916	0.797	0.692	0.689
U	0.187	0.116	0.143	0.167	0.114	0.156	0.143	0.064	0.195	0.170	0.102	0.130	0.158
Y	0.008	0.031	0.021	0.018	0.112	0.000	0.019	0.206	0.004	0.003	0.250	0.155	0.014
Ca	0.023	0.010	0.013	0.048	0.025	0.069	0.050	0.012	0.040	0.065	0.026	0.048	0.005
Zr	0.066	0.065	0.002	0.004	0.010	0.000	0.000	0.000	0.000	0.000	0.006	0.097	0.251
Hf	0.010	0.011	0.000	0.000	0.000	0.000	0.000	0.000	0.000	0.000	0.000	0.020	0.007
Fe	0.003	0.012	0.016	0.068	0.068	0.000	0.131	0.099	0.001	0.017	0.032	0.026	0.015
Total	1.147	1.129	1.114	1.237	1.239	1.111	1.274	1.210	1.152	1.171	1.213	1.168	1.139
Si	0.849	0.858	0.877	0.799	0.811	0.923	0.808	0.840	0.863	0.863	0.816	0.840	0.858
P	0.016	0.025	0.023	0.021	0.019	0.000	0.011	0.046	0.004	0.005	0.050	0.054	0.013
Total	0.865	0.883	0.900	0.820	0.830	0.923	0.819	0.886	0.867	0.868	0.866	0.894	0.871

- Not determined nd Not detected

Plate No.	Sample No.	Grain No.	Description
			Albitised granite
69	411	2	Large, concentrically zoned, subhedral zircon partly enclosed by chlorite. Inner core of Type 3 zircon (7), intermediate Type 2 zircon (2) and outer Type 1 zircon (5). White inclusions, veinlets and overgrowths are of sulphides and haematite. Thorite inclusions (e.g. 9) are darker than zircon. EPMA spots are shown. (RPPL)
70	411	2	The same zircon, emphasising the abundant, small inclusions of thorite (white, e.g. 9) in the intermediate zone. Xenotime (X) overgrows the right-hand edge of the zircon. A-E marks the line of concentration profiles illustrated in Fig. 28. EPMA spots are shown. (BSEI)


69
9
7
2
5
70 µm


70
9
E
X
7
5
2
A
70 µm

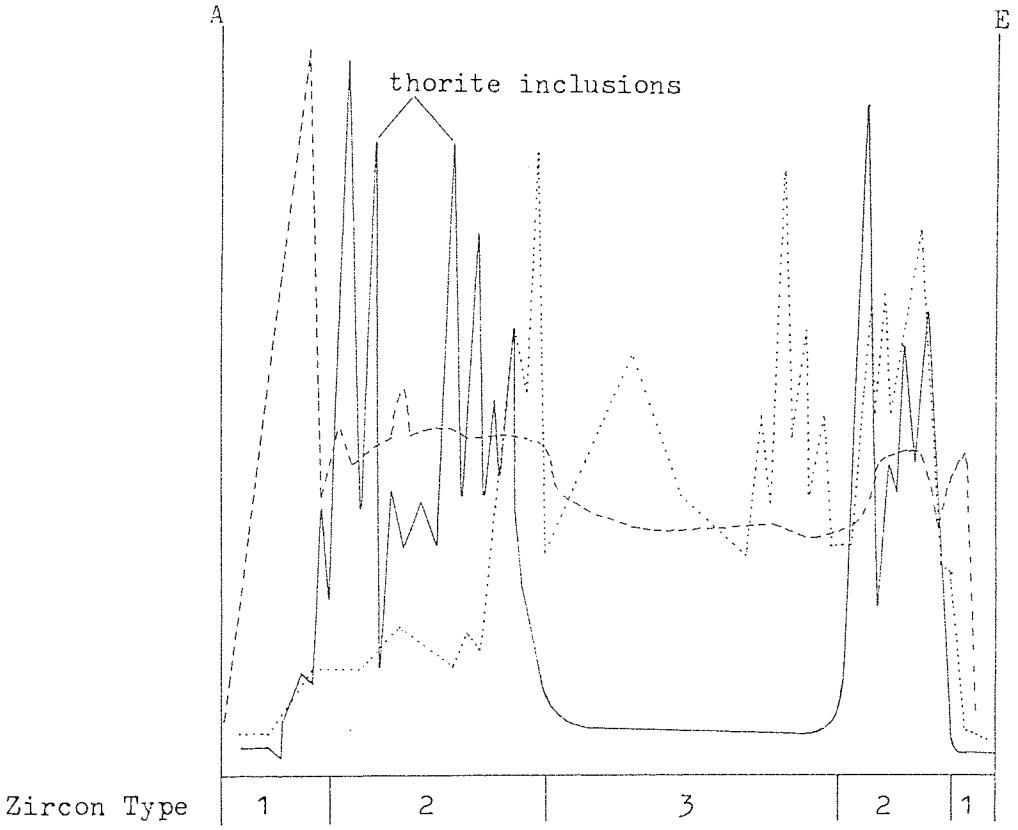

Fig. 28 Concentration profiles for Th (line), U (dots) and Hf (dashes) across a 300 µm diameter, concentrically zoned zircon from the albitised granite (Plate 70, A-E).

The profiles illustrate the chemical characteristics of the three zircon types.

Table 41 Zircon from the albitised granite and albitite

Sample No.	Grain No.	An. Spot	Description	Plate No.
411	1		Concentrically zoned, 250 μm diameter zircon from the albitised granite.	71
		4	Type 3 core of clear zircon.	
		9	" "	
		11	Type 1 outer zone.	
	2		Concentrically zoned, 300 μm diameter zircon.	70
		2	Intermediate zone of Type 2 zircon, containing abundant inclusions of thorite and haematite.	72
		4	Lightest band in BSEI of outer Type 1 zone.	66
		5	Mid-grey " " " "	
		6	Dark-grey " " " "	
		7	Type 3 core of clear zircon.	70
Block 411	1	11	Intermediate zone of Type 2 zircon in a 600 μm long grain.	
436B	1		500 μm diameter, polycrystalline zircon in the albitite.	
		1	Type 1 zircon rim.	
		2	Type 3, isotropic, clear domain away from edge.	
445	1		Subhedral, concentrically zoned zircon in albitite.	
		1	Area of Type 3 zircon.	
		4	Type 2 zircon, close to grain edge.	
		7	Type 2 zircon in grain core.	

Table 41 Probe analyses of zircon from the albitised granite and albitite (recalculations based on four oxygens)

Sample	411								Block411	436B		445		
Grain	1			2					1	1		1		
An.Spot	4	9	11	2	4	5	6	7	11	1	2	1	4	7
ZrO_2	62.38	59.38	63.21	61.23	54.80	57.47	62.42	60.56	53.94	61.77	61.35	61.52	59.06	61.91
HfO_2	2.85	3.07	5.22	6.02	12.94	11.31	5.33	3.29	14.00	5.33	2.63	2.29	8.21	5.09
ThO_2	1.02	0.51	0.09	0.35	0.47	0.13	0.07	0.77	0.42	0.02	0.41	0.32	0.09	0.08
UO_2	1.40	6.10	nd	0.46	0.27	0.17	0.18	1.35	0.06	0.32	1.48	1.29	0.60	0.59
Y_2O_3	–	–	–	0.14	0.41	0.09	0.12	0.37	0.24	0.04	0.31	0.33	0.10	0.04
CaO	–	–	–	nd	nd	–	–	–	nd	nd	nd	–	–	–
FeO	–	–	–	1.07	0.07	nd	0.24	0.04	nd	nd	nd	nd	0.21	0.30
MnO	–	–	–	–	–	–	–	–	–	–	–	–	–	–
SiO_2	29.95	28.11	31.65	30.25	29.29	30.19	30.70	29.86	32.13	30.80	29.88	33.42	33.89	34.05
P_2O_5	–	–	–	0.19	0.36	0.16	0.11	0.17	0.31	0.07	0.29	–	–	–
Total	97.60	97.17	100.17	99.71	98.61	99.52	99.17	96.41	101.10	98.35	96.35	99.17	102.16	102.06
Zr	0.986	0.975	0.964	0.952	0.884	0.908	0.967	0.966	0.836	0.962	0.974	0.929	0.882	0.915
Hf	0.026	0.029	0.047	0.055	0.122	0.105	0.048	0.031	0.127	0.049	0.024	0.020	0.072	0.044
Th	0.008	0.004	0.001	0.003	0.004	0.001	0.001	0.006	0.003	0.000	0.003	0.002	0.001	0.001
U	0.010	0.046	0.000	0.003	0.002	0.001	0.001	0.010	0.000	0.002	0.011	0.009	0.004	0.004
Y	0.000	0.000	0.000	0.002	0.007	0.002	0.002	0.006	0.004	0.001	0.005	0.005	0.002	0.001
Ca	0.000	0.000	0.000	0.000	0.000	0.000	0.000	0.000	0.000	0.000	0.000	0.000	0.000	0.000
Fe	0.000	0.000	0.000	0.029	0.002	0.000	0.006	0.001	0.000	0.000	0.000	0.000	0.005	0.008
Mn	0.000	0.000	0.000	0.000	0.000	0.000	0.000	0.000	0.000	0.000	0.000	0.000	0.000	0.000
Total	1.030	1.054	1.012	1.044	1.021	1.017	1.025	1.020	0.970	1.014	1.017	0.965	0.966	0.973
Si	0.970	0.946	0.989	0.965	0.969	0.978	0.975	0.977	1.021	0.984	0.973	1.035	1.038	1.032
P	0.000	0.000	0.000	0.005	0.010	0.004	0.003	0.005	0.008	0.002	0.008	0.000	0.000	0.000
Total	0.970	0.946	0.989	0.970	0.979	0.982	0.978	0.982	1.029	0.986	0.981	1.035	1.038	1.032

– Not determined nd Not detected

Plate No.	Sample No.	Grain No.	Description
			Albitised granite
71	411	1	Zircon close to the one in Plates 69 and 70, showing similar pattern of zoning, i.e. rim of Type 1 zircon (11), intermediate zone of Type 2 zircon (lower reflectance) and Type 3 zircon core (4 and 9). EPMA spots are shown. (RPPL)
72	411	2	High magnification of the analysis 2 area in Plate 70, showing the inclusions of thorite (white) and haematite (black). (BSEI)
73	385	6	Thorite inclusion (1) in columbite (c) which is associated with fluorite (f) and monazite (m) in biotite (b). EPMA spots are shown. (Scale bar is 40 μm). (SEM)
74	408A	1	Interstitial thorite with indistinct banding structure. (TXPL)
75	411	4	Thorite (EPMA spots 1-4) replacing the outer zone of zircon. (SEM)
76	411	5	Thorite (T) overgrowing/replacing zircon (Z) (SEM)
77	390A	1	Interstitial thorite surrounded by rim of Fe-oxide (opaque). EPMA spots shown. H is a hole in section. (TPPL)
78	390B	1	Monazite (EPMA spots 1-6) included in feldspar. The grain probably comprises the remains of a 1 mm long, euhedral crystal, since anhedral fragments in optical continuity occur locally (outlined in white and shown in more detail in Fig. 27). Semi-quantitative, partial analyses are given in Table 35. (TPPL)

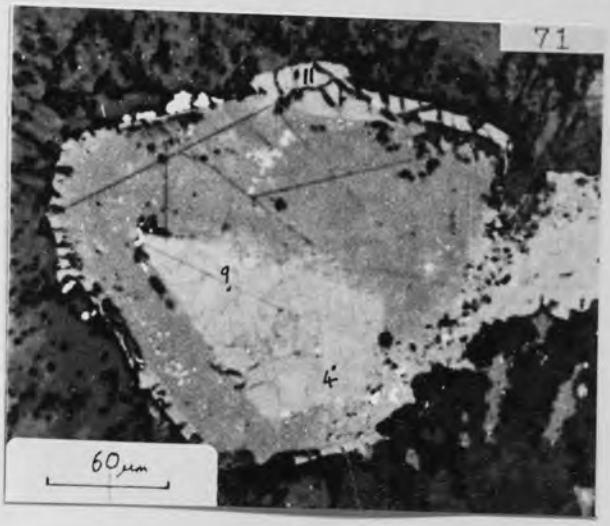
71
60µm

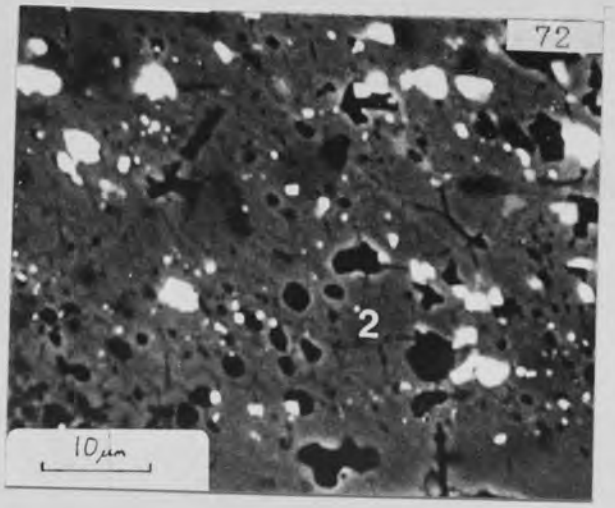
72
2
10µm

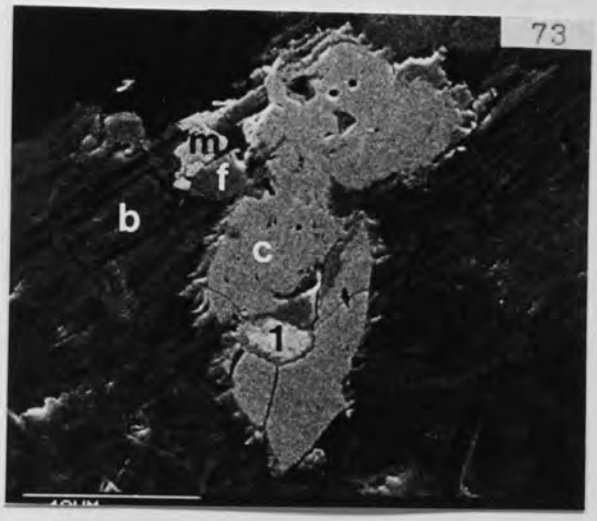
73
m
f
b
c
1


74
70µm

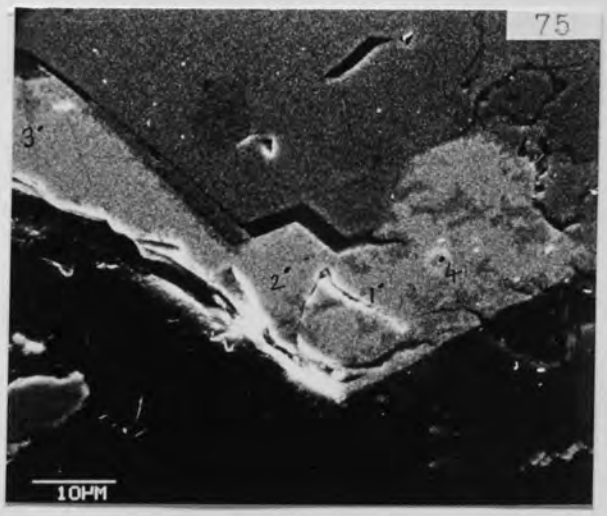
75
3
2
1
4
10µm


76
T
Z
10µm

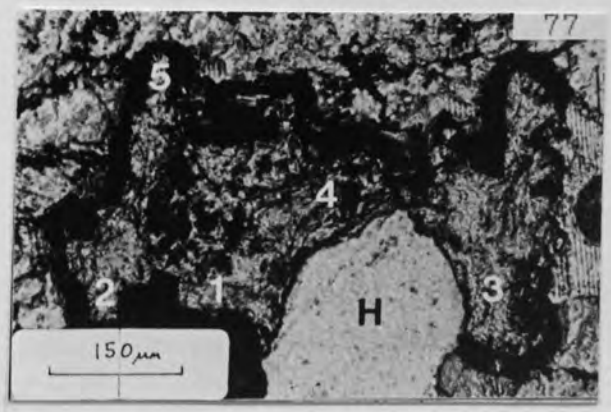
77
5
4
2
1
H
3
150µm

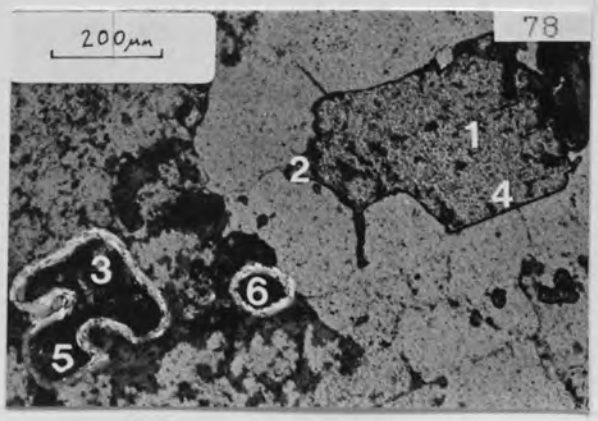
78
200µm
1
2
4
3
6
5

Table 42 Thorite from the albitised granite and albitite

Sample No.	Grain No.	An. Spot	Description	Plate No.
411	2		Concentrically zoned, 300 μm diameter zircon from the albitised granite.	70
		9	10 μm diameter thorite inclusion in intermediate zone of Type 2 zircon.	
	4	1-5	90 μm long, peripheral thorite replacement of zircon.	75
Block 411	1	5	10 μm diameter thorite inclusion from zone of Type 2 zircon.	
		8	Thorite veinlet in 600 μm long zircon.	
416A	4	1	80 μm long thorite overgrowing zircon in the albitite.	88
		3		
		2	40 μm long thorite included in same zircon, close to the thorite overgrowth.	
436B	8	1	15 μm diameter thorite inclusion in zircon from the albitite.	
		2	20 μm diameter thorite inclusion in zircon.	
450A	8	2	40 μm diameter, irregular thorite inclusion in zircon from the albitite.	85

Table 42 Probe analyses of thorite from the albitised granite and albitite (recalculations based on four oxygens)

Sample	411						Block 411		416A			436B		450A
Grain	2	4					1		4			8		8
An.Spot	9	1	2	3	4	5	5	8	1	2	3	1	2	2
ThO_2	53.30	48.92	52.16	58.82	53.00	80.08	72.07	59.34	59.66	76.82	61.41	57.81	58.67	61.27
UO_2	28.92	18.03	19.76	23.72	19.97	4.96	1.47	1.84	24.39	7.24	22.05	26.04	21.78	22.43
Y_2O_3	0.78	5.90	5.28	0.81	5.07	-	1.07	1.29	0.44	0.53	0.33	0.25	2.28	0.37
CaO	1.12	0.87	0.91	1.42	0.94	0.39	1.06	0.38	1.12	0.14	1.16	nd	0.97	1.22
ZrO_2	-	3.50	2.53	0.20	1.89	-	2.30	7.65	0.04	0.07	0.05	0.13	0.32	0.08
HfO_2	-	-	-	-	-	-	1.40	2.30	-	-	-	nd	nd	-
FeO	-	0.68	0.68	0.77	0.73	-	2.04	5.06	1.03	0.08	1.04	0.07	0.50	-
SiO_2	16.85	16.09	16.36	15.68	16.47	16.32	15.33	17.57	13.71	15.31	13.71	15.14	12.57	14.81
P_2O_5	-	1.23	1.06	0.38	1.15	-	0.59	0.63	0.41	0.34	0.40	0.33	0.62	0.31
Total	100.97	95.22	98.74	101.80	99.22	101.75	97.33	96.06	100.80	100.53	100.15	99.77	97.71	100.49
Th	0.668	0.596	0.627	0.739	0.636	1.016	0.910	0.686	0.790	0.996	0.817	0.760	0.804	0.799
U	0.354	0.215	0.232	0.291	0.234	0.062	0.018	0.021	0.316	0.092	0.287	0.335	0.292	0.286
Y	0.023	0.168	0.148	0.024	0.142	0.000	0.032	0.035	0.014	0.016	0.010	0.008	0.073	0.011
Ca	0.066	0.050	0.052	0.084	0.053	0.023	0.063	0.021	0.070	0.009	0.073	0.000	0.063	0.075
Zr	0.000	0.091	0.065	0.005	0.049	0.000	0.062	0.190	0.001	0.002	0.001	0.004	0.009	0.002
Hf	0.000	0.000	0.000	0.000	0.000	0.000	0.022	0.033	0.000	0.000	0.000	0.000	0.000	0.000
Fe	0.000	0.030	0.030	0.036	0.032	0.000	0.095	0.215	0.050	0.004	0.051	0.003	0.025	0.000
Total	1.111	1.150	1.154	1.179	1.146	1.101	1.202	1.201	1.241	1.119	1.239	1.110	1.266	1.173
Si	0.928	0.862	0.864	0.865	0.868	0.910	0.850	0.893	0.798	0.872	0.801	0.874	0.757	0.848
P	0.000	0.056	0.047	0.018	0.051	0.000	0.028	0.027	0.020	0.016	0.020	0.016	0.032	0.015
Total	0.928	0.918	0.911	0.883	0.919	0.910	0.878	0.920	0.818	0.888	0.821	0.890	0.789	0.863

- Not determined nd Not detected

Plate No.	Sample No.	Grain No.	Description
			Albitised granite
79	395B	8	Monazite enclosed by a rim of Fe-oxide (opaque) and included in K-feldspar. (TPPL)
80	395B	5	Clear monazite (M) showing replacement by a turbid LREE-phase (L). (TXPL)
81	411	4	Fluorite (F) with LREE-phase inclusions (L) replacing zircon (z) bearing a thorite inclusion (EPMA spot 5). (SEM)
82	411	1	Inclusions of LREE-phase showing alignment in fluorite. (SEM)
83	411	3	High magnification of LREE-phase inclusions in zircon (EPMA spots are shown). (SEM)
84	Block 411	1	Embayed zircon, overgrown by fluorite (F) and xenotime (EPMA spot 4). (RPPL)

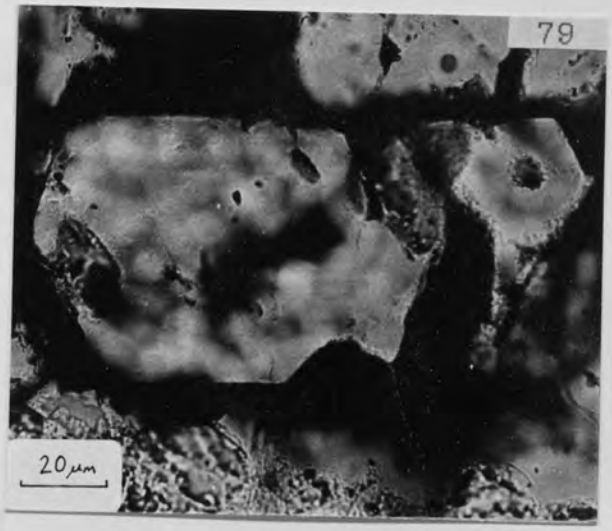
79
20μm

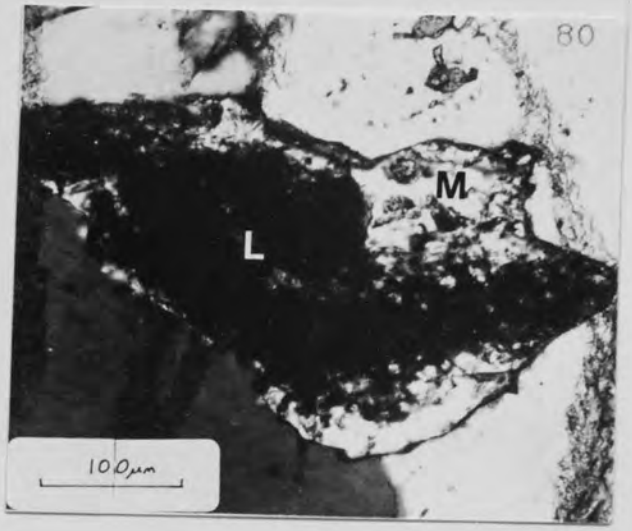
80
M
L
10.0μm

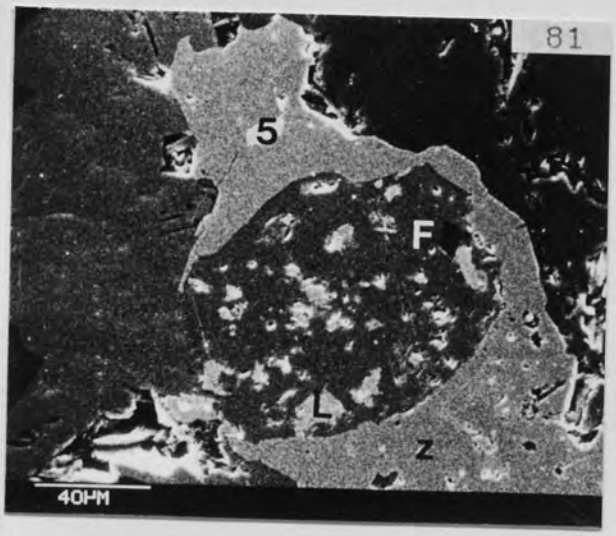
81
5
F
L
Z
40μm

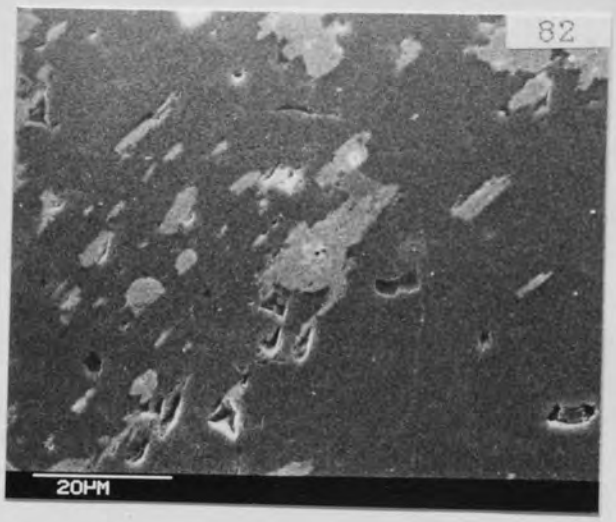
82
20μm

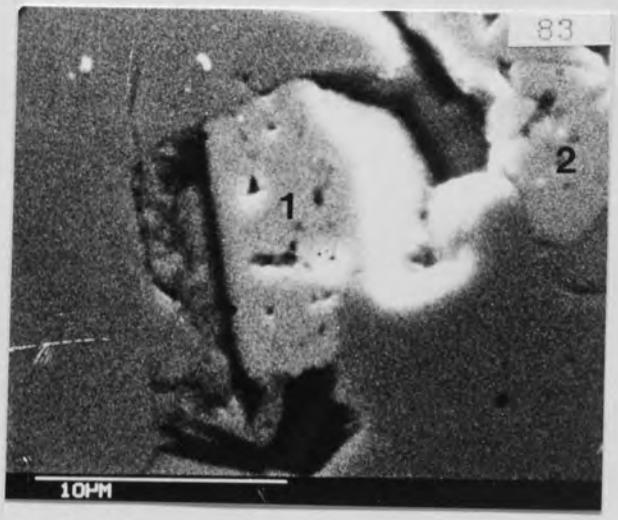
83
1
2
10μm

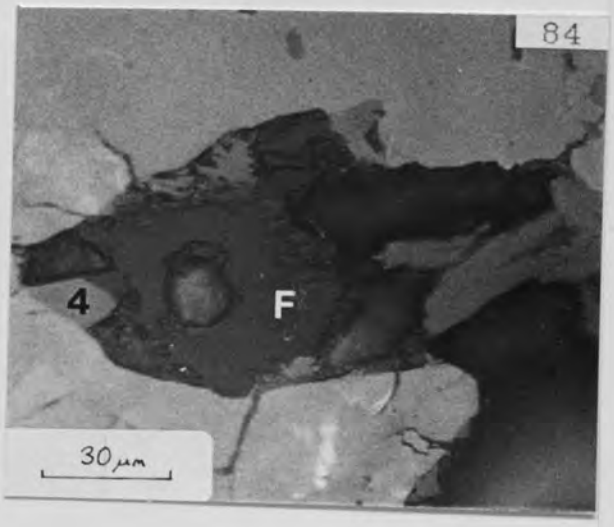
84
4
F
30μm

Table 43 Xenotime and unidentified Th-Pb-P phase

Sample No.	Grain No.	Description	Plate No.
RS6(2)	3b	Xenotime overgrowing/replacing thorite which, itself, encloses zircon. Greisenised wallrock, Ririwai lode.	100
Block 411	1	Euhedral xenotime rhomb overgrowing zircon, where it is embayed. Albitite.	84
RS10(3)	1 1a	Unidentified Th-Pb-P phase intergrown with monazite and Zr-rich thorite. Greisenised wallrock.	110

Table 43 Probe analyses of xenotime and an unidentified Th-Pb-P-phase (recalculations based on 4 oxygens)

Sample	RS6(2)		Block411	RS10(3)		
Grain	3b		1	1		1a
An.Spot	3	4	4	2	3	1
Y_2O_3	50.48	47.89	46.76	1.59	1.58	1.61
Yb_2O_3	6.10	4.40	3.19	-	-	-
Er_2O_3	5.51	4.48	4.20	-	-	-
Dy_2O_3	5.57	4.41	5.67	-	-	-
Ce_2O_3	-	-	-	1.85	1.91	1.60
La_2O_3	-	-	-	1.07	1.02	0.90
CaO	0.03	0.15	0.20	1.44	1.37	1.34
$Th O_2$	1.43	1.34	1.04	56.42	57.65	47.73
UO_2	0.22	0.44	nd	0.97	0.99	0.83
PbO	-	-	-	15.40	15.15	12.56
ZrO_2	-	-	0.36	0.06	0.04	0.06
FeO	-	-	-	0.32	0.22	13.68*
P_2O_5	21.78	29.65	27.85	13.98	14.13	12.05
SiO_2	4.27	2.39	4.07	1.12	1.15	1.32
Total	95.39	95.15	93.34	94.22	95.21	93.68
Y	1.035	0.902	0.892	0.051	0.050	0.050
Yb	0.072	0.047	0.035	-	-	-
Er	0.067	0.050	0.047	-	-	-
Dy	0.069	0.050	0.065	-	-	-
Ce	-	-	-	0.041	0.041	0.034
La	-	-	-	0.024	0.022	0.019
Ca	0.001	0.006	0.008	0.092	0.087	0.083
Th	0.013	0.011	0.008	0.768	0.777	0.628
U	0.002	0.003	0	0.013	0.013	0.011
Pb	-	-	-	0.248	0.242	0.195
Fe	-	-	-	0.016	0.011	0.661
Total	1.259	1.069	1.055	1.202	1.193	1.631
P	0.711	0.889	0.845	0.708	0.709	0.590
Si	0.165	0.085	0.146	0.067	0.068	0.076
Total	0.876	0.974	0.991	0.775	0.777	0.666

- Not determined
nd Not detected
* High Fe probably due to contamination of analysis by haematite

Table 44 Size (μm) and abundance of radioactive accessory minerals and fluorite from the Ririwai lode

Rock Type	Sample and Section No.	Zircon			Thorite		Monazite		LREE-phase		Fluorite		Other Phases		
		No.	Size Range	*	No.	Size Range	No.	Size Range	S	C+	No.	Size Range	Name(s)	No.	Size Range
M	R1/13-1		20-120		3	30-180	3	40-70		2			U-Si-phase	1	10
I	R1/13-2		10-60		1	160	1	250	1						
C C	R1/13-3		30-60		2	70-100	1	20			1	120	?Pyrochlore	1	20
R L													U-Th-Si-phase	1	25
O I	R1/13-6		20-120		1	30						<200			
N	R1/13-7		10-150	1	3	50-400	3	60-150		2		<300			
I	R1/23-1A	18	15-100	9	2	<370	2	180-250	1						
T	R1/23-1B	14	30-100		1	100							U-Th-Si-phase	1	<100
E	RS6(4)		20-100				2	10-70	3	1		120-240	Coffinite	3	30-150
G	R1/13-4		10-120	2	9	100-250	2	170			>3	100-800			
R W	R1/13-5		20-60		4	20-120	8	20-220	1		1	600			
E A	R1/23-2A	4	30-60				1	120							
I L	R1/23-2B	>30	15-120	3											
S L	RS6(2)		30-70		16	30-120	9	10-500	6		3	60-400	U-Th-Si-phase	1	10
E R													Xenotime	2	20-80
N O	RS6(3)	8	10-100		>35	20-120	2	50					Xenotime	2	20-50
I C	RS10(3)	70	10-140	26	5	40-120	3	30-100	1	1			Th-Pb-P-phase	3	40-120
S K	RS14	>8	40-120	5	5	8-100									
E	RS14(1)	>20	60-180		3	40-60									
D	RS14(2)	19	20-100	4	1	60									
G	R1/14	20	30-140	4	5	70-250									
R	R1/14-1		20-100		3	10-120	3	20-600	1	2	1	20	Xenotime	2	6
E	R1/14-2		25-120		>22	10-300	4	60-230		1					
I	R1/23-3A	35	20-160	>3			2	120-200							
S	R1/23-3B	>14	30-120				1	150							
E	R1/42-3	20	30-160		2	60-500									
N															

* No. of zircons with low reflectance, trace-element enriched patches.
\+ No. of LREE-phases of simple (S) and complex (C) compositions.

Table 45 Zircon from the Ririwai lode

Sample No.	Grain No.	An. Spot	Description	Plate No.
R1/13-4	5e		120 μm diameter zircon, partly enclosed by thorite in the greisenised wallrock.	98
		1	Low reflectance patch.	
		2	" (close to grain edge).	
		3	High reflectance area on left-side.	
		5	" "	
		6	" right-side.	
		4	" outer zone.	
	5f		90 μm diameter zircon close to the same thorite	104
		1	High reflectance core.	
		3	" edge.	
		2	Low reflectance patch close to edge.	
RS6(2)	1	4	40 μm diameter, euhedral zircon included in quartz and overgrown by minor xenotime (marked "Z" on the left side of Plate 105). Greisenised wallrock, Ririwai lode.	105
	3b	1	15 μm diameter, euhedral zircon enclosed by [illegible]	100
RS14(1)	1a	1	60-120 μm diameter, clear, subhedral to euhedral zircons clustered in quartz. Greisen, Ririwai lode.	
	9	1		
R1/14-2	1a	1	60 μm diameter, euhedral zircon ("Z" in Plate 119) belonging to a cluster of crystals in Li-mica in the greisen.	

Table 45 Probe analyses of zircon from the Ririwai lode
(recalculations based on four oxygens)

Sample	R1/13-4									RS6(2)		RS14(1)		R1/14-2
Grain	5(e)						5(f)			1	3b	1a	9	1a
An.Spot	1	2	3	4	5	6	1	2	3	4	1	1	1	1
ZrO_2	49.48	53.11	53.44	52.22	50.99	62.47	62.44	40.54	59.50	63.75	63.72	62.32	63.10	61.23
HfO_2	3.79	6.27	16.27	5.07	17.30	3.61	3.55	7.46	7.31	3.10	3.17	4.97	4.65	3.31
ThO_2	4.42	0.70	0.12	0.63	0.14	0.06	0.17	7.85	0.07	nd	0.43	0.27	0.24	0.21
UO_2	2.52	2.66	0.57	1.74	1.12	1.09	0.56	3.80	0.60	0.14	0.50	1.17	1.09	0.32
Y_2O_3	3.49	0.45	0.09	4.11	0.10	0.08	0.15	4.78	0.09	0.18	0.74	0.19	0.21	0.33
CaO	0.32	0.36	0.01	0.03	nd	nd	0.02	0.31	nd	0.08	0.15	nd	-	nd
FeO	0.73	1.65	0.19	0.45	0.09	0.08	0.17	1.02	0.06	0.39	-	0.12	-	0.26
MnO	0.58	0.87	0.01	0.01	nd	nd	nd	0.58	nd	-	-	-	-	nd
SiO_2	26.67	28.22	30.27	27.13	30.33	31.07	31.32	24.48	31.03	29.87	31.89	30.84	31.55	32.57
P_2O_5	0.41	0.14	0.06	3.35	0.08	0.13	0.10	0.95	0.11	0.24	0.25	-	-	0.10
Total	92.41	94.43	101.03	94.74	100.15	98.59	98.48	91.77	98.77	97.75	100.85	99.88	100.84	98.33
Zr	0.862	0.889	0.850	0.849	0.821	0.967	0.964	0.749	0.929	0.996	0.960	0.963	0.961	0.935
Hf	0.039	0.061	0.151	0.048	0.163	0.033	0.032	0.081	0.067	0.028	0.028	0.045	0.041	0.030
Th	0.036	0.005	0.001	0.005	0.001	0.000	0.001	0.068	0.001	0.000	0.003	0.002	0.002	0.001
U	0.020	0.020	0.004	0.013	0.008	0.008	0.004	0.032	0.004	0.001	0.003	0.008	0.008	0.002
Y	0.066	0.008	0.002	0.073	0.002	0.001	0.003	0.096	0.002	0.003	0.012	0.003	0.003	0.006
Ca	0.012	0.013	0.000	0.001	0.000	0.000	0.001	0.013	0.000	0.003	0.005	0.000	0.000	0.000
Fe	0.022	0.047	0.005	0.013	0.002	0.002	0.004	0.032	0.002	0.010	0.000	0.003	0.000	0.007
Mn	0.018	0.025	0.000	0.000	0.000	0.000	0.000	0.019	0.000	0.000	0.000	0.000	0.000	0.000
Total	1.075	1.068	1.013	1.002	0.997	1.011	1.009	1.090	1.005	1.041	1.011	1.024	1.015	0.981
Si	0.953	0.969	0.987	0.905	1.001	0.986	0.991	0.928	0.994	0.957	0.986	0.978	0.985	1.020
P	0.012	0.004	0.002	0.095	0.002	0.003	0.003	0.030	0.003	0.007	0.007	0.000	0.000	0.003
Total	0.965	0.973	0.989	1.000	1.003	0.989	0.994	0.958	0.997	0.964	0.993	0.978	0.985	1.023

- Not determined nd Not detected

Plate No.	Sample No.	Grain No.	Description
			Microclinite
92	R1/13-1	7b	Zircons included in quartz along fractures. (TPPL)
93	R1/23-1B	12	Zircon (Z) intergrown with phase showing complete solid solution from thorite (3) through U-Th phase (2) to ?coffinite (1). EPMA spots are shown. Abundant pyrite (white) occurs as overgrowths, veinlets and inclusions. (RPPL)
94	R1/13-3	7	?REE-microlite (EPMA spot 2) included in pyrite (P) and overgrowing columbite (C). The light square in the ?pyrochlore is an artefact, caused by the scanning electron beam. An unidentified U-Th-Y-Si phase (EPMA spot 5) is intergrown with the pyrite. (SEM)
95	RS6(4)	1	Interstitial, poorly crystallised coffinite (EPMA spots 1a-7) (SEM)
96	RS6(4)	3b	Coffinite intergrown with a LREE-phase. X-ray maps for U and the LREE show the distribution of the two phases. (SEM)

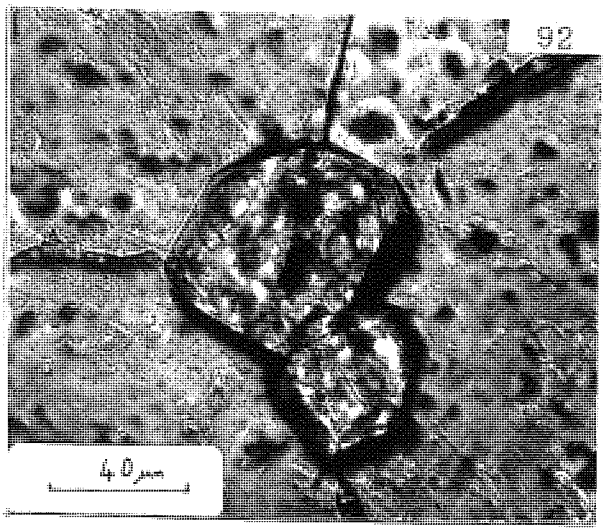
92
40μm

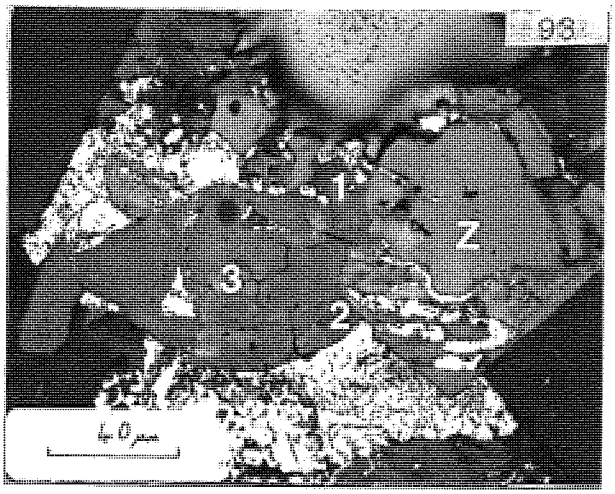
93
1
Z
3
2
40μm

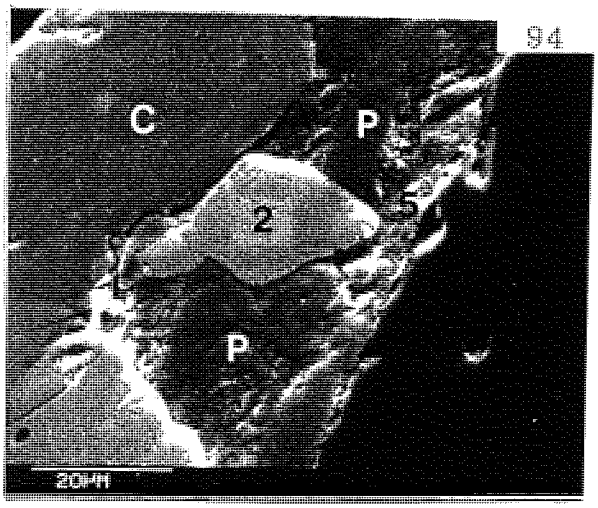
94
C
P
2
P
20μm

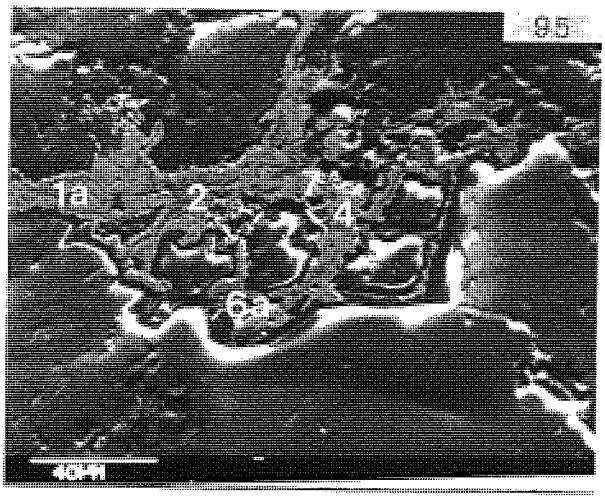
95
1a
2
4
3
6a
40μm

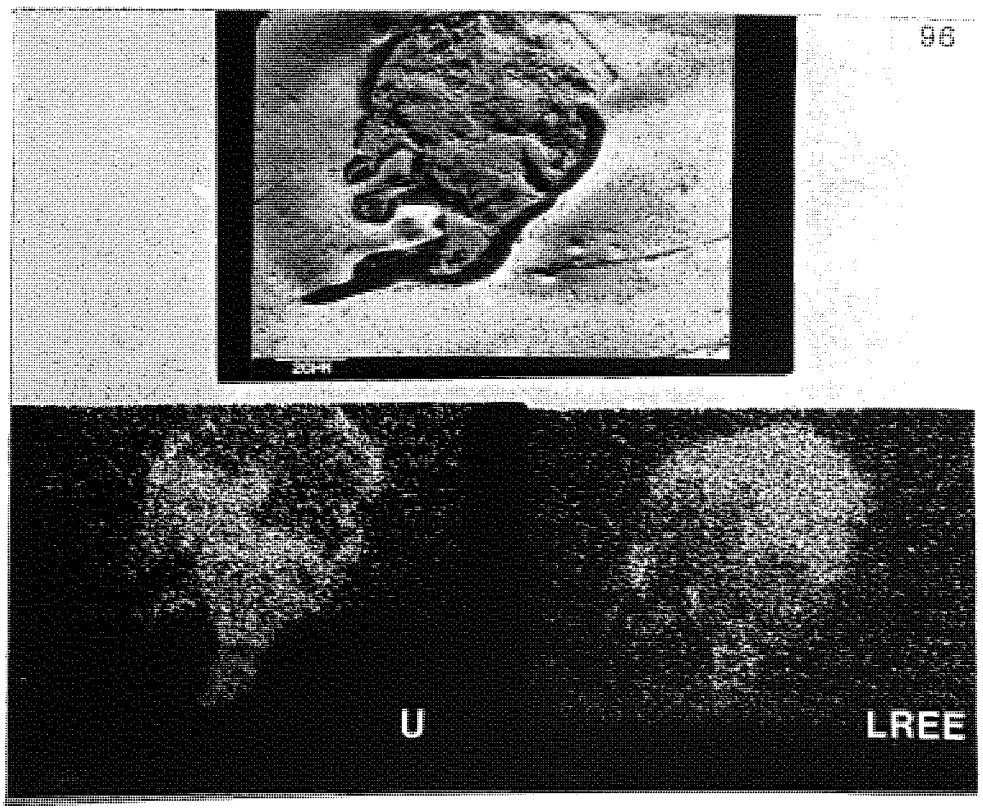
96
20μm
U
LREE

Table 46 Probe analyses of U-Si-phase and thorite from the microclinite and greisenised wallrock, Ririwai lode

(recalculations based on four oxygens)

Sample	R1/231B			RS10(3)	
Grain	12			1	
An.Spot	1	2	3	1+	1*
ThO_2	7.40	31.80	55.94	43.99	43.67
UO_2	52.04	20.14	8.73	0.81	0.69
Y_2O_3	11.08	13.87	8.49	8.22	8.53
CaO	-	-	-	0.25	0.33
ZrO_2	0.09	5.32	0.44	15.11	14.34
HfO_2	nd	0.02	nd	1.26	1.26
FeO	3.67	2.78	0.61	4.58	3.81
SiO_2	13.10	12.52	11.44	10.61	10.42
P_2O_5	1.18	2.94	1.88	4.07	4.47
Dy_2O_3	1.39	1.68	1.03	1.18	1.58
Er_2O_3	1.52	1.69	0.67	0.95	0.97
Yb_2O_3	2.83	2.63	0.91	1.77	1.50
PbO	-	-	-	2.47	-
Total	94.30	95.39	90.14	95.27	91.57
Th	0.096	0.380	0.782	0.508	0.513
U	0.663	0.236	0.119	0.009	0.008
Y	0.337	0.388	0.277	0.222	0.234
Ca	0.000	0.000	0.000	0.014	0.018
Zr	0.003	0.136	0.013	0.374	0.361
Hf	0.000	0.000	0.000	0.018	0.019
Fe	0.176	0.122	0.031	0.194	0.165
Dy	0.026	0.028	0.020	0.019	0.026
Er	0.027	0.028	0.013	0.015	0.016
Yb	0.049	0.042	0.017	0.027	0.024
Pb	0.000	0.000	0.000	0.034	0.000
Total	1.377	1.360	1.272	1.434	1.384
Si	0.750	0.658	0.702	0.538	0.538
P	0.057	0.131	0.098	0.175	0.195
Total	0.807	0.789	0.800	0.713	0.733

- Not determined nd Not detected
* Accelerating voltage = 20 kV
+ " " = 15 kV

Plate No.	Sample No.	Grain No.	Description
			Greisenised Wallrock
97	R1/13-5	14	Euhedral monazite included in Li-mica with a surrounding, pleochroic halo. (TPPL)
98	R1/13-4	5e	Zircon with low reflectance patches enriched in Th, U, Fe, Ca, Mn, Y and P (EPMA spots 1 and 2). The left half of the zircon is highly enriched in Hf (EPMA spots 3 and 5). An incomplete, outer zone contains high Y and P (EPMA spot 4). Pyrite lamellae (white) occur along zone boundaries or fractures. The zircon is partly enclosed by a 250 µm long thorite to the top and left of the photograph (see Plate 104). (RPPL)
99	RS10(3)	12	Zircon with low reflectance patches, highly enriched in Th and Fe. (RPPL)
100	RS6(2)	3b	Two euhedral zircons (1) enclosed by thorite (2) which, in turn, is replaced by xenotime (3 and 4) and overgrown by monazite (m). The xenotime partly encloses cassiterite (c). EPMA spots are shown. (SEM)
101	RS6(2)	3a	Zircon (Z) overgrown by thorite (2) and xenotime (X). An associated LREE-phase (4) is included in fluorite (f). EPMA spots are shown. (SEM)
102	RS6(2)	3b	X-ray map for Zr, Th and Y (for Plate 100).
103	RS6(2)	3a	X-ray map for Zr, Y, Th and LREE (for Plate 101).
104	R1/13-4	5	Thorite (EPMA spot 1) intergrown with zircon (z) with associated columbite (c), fluorite (F), cassiterite (s) and pyrite (p). Zircon 'e' is enlarged in Plate 98. (SEM)

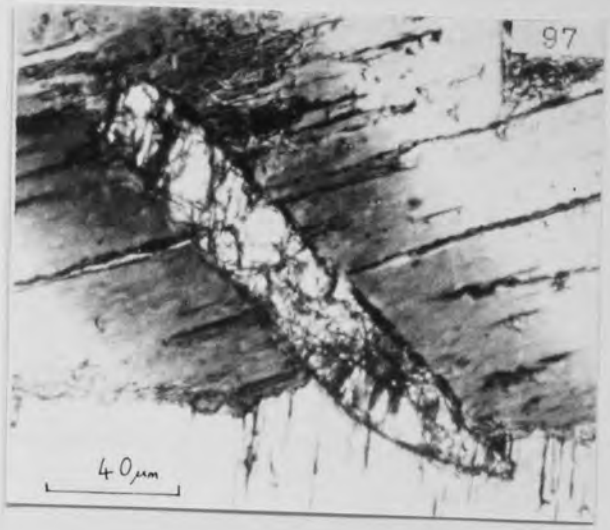
97
40µm

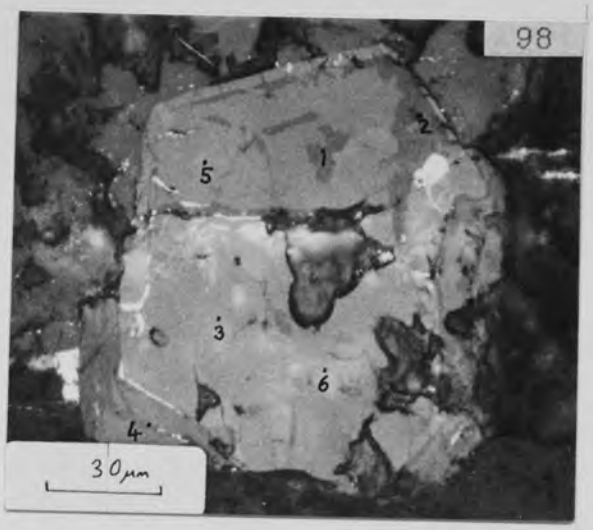
98
1
2
3
4
5
6
30µm

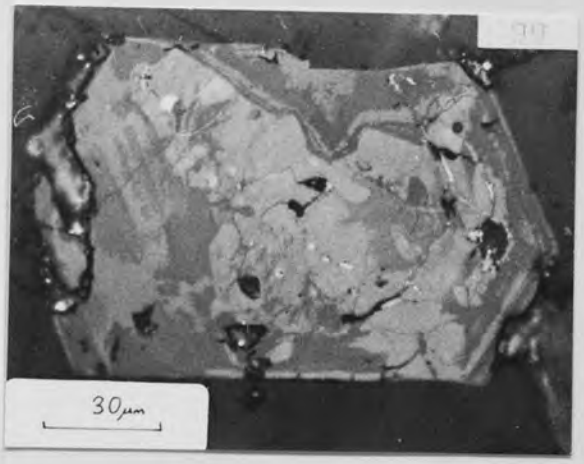
99
30µm

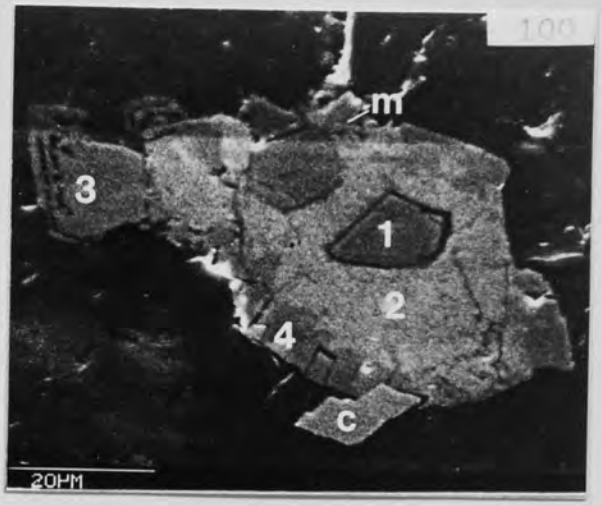
100
m
3
1
2
4
c
20µm

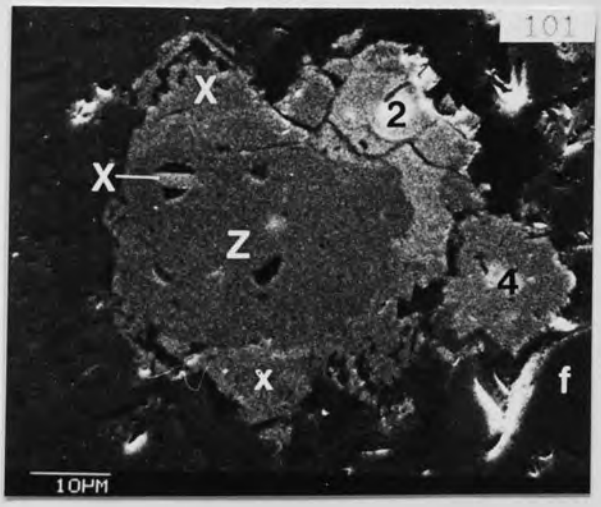
101
X
2
X
Z
4
x
f
10µm

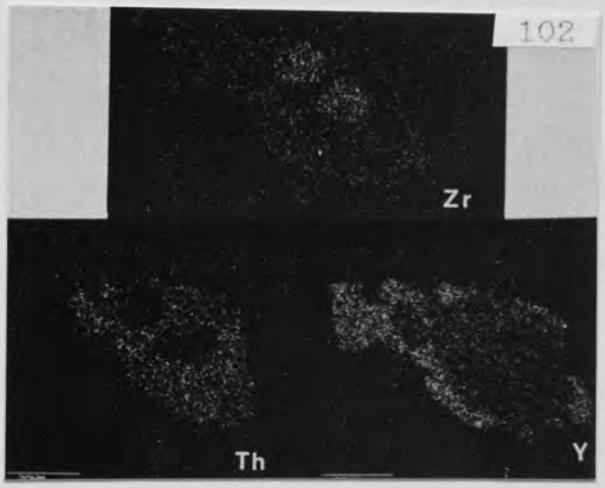
102
Zr
Th
Y

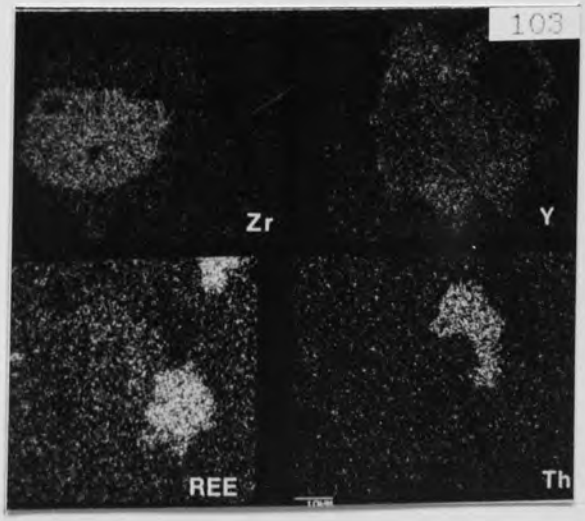
103
Zr
Y
REE
Th

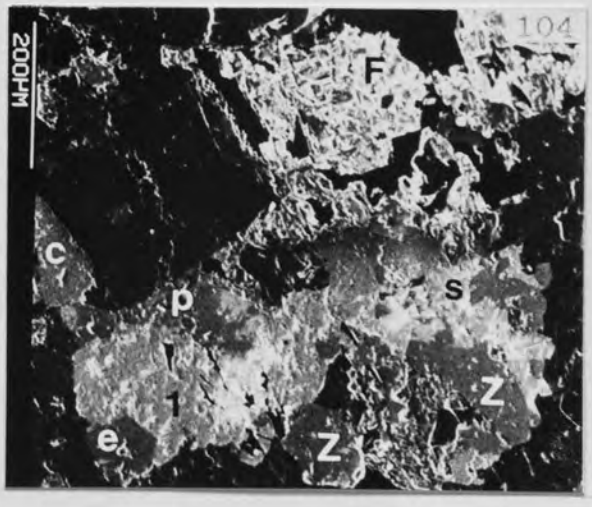
104
200µm
F
c
p
s
1
Z
Z

Plate No.	Sample No.	Grain No.	Description
			Greisenised wallrock
105	RS6(2)	1	Thorite (T) overgrowing zircon (Z), included in quartz. (SEM)
106	RS14	4	Cluster of tiny thorites (light grey) included in Li-mica. (SEM)
107	R1/13-4	2	Pale yellow thorites (t) associated with pyrite (p) and included in clear K-feldspar, along cracks. (TPPL)
108	RS6(2)	2	Thorite lozenge (EPMA spot 1) overgrown by cassiterite (C) and included in chlorite-sericite intergrowth (S). (SEM)
109	RS10(3)	2	Intergrowth of Zr-thorite (T) and altered zircon (Z). (RPPL)
110	RS10(3)	1	Intergrowth of Th-Pb-P phase (EPMA spots 2 and 3) with Zr-thorite (EPMA spot 1) and cassiterite (C), which is elongate and lies vertically in the photograph, separating the other two phases. The white speckling in the thorite and Th-Pb-P phase is due to abundant, minute inclusions of haematite. (RPPL)
111	RS6(2)	6	Cluster of U-Th-Y-Si phase grains (light grey) in chlorite-sericite intergrowth. (SEM)
112	RS10(3)	2	Monazite (m) intergrown with LREE-phases of simple (s) and complex (c) compositions (see Fig. 72 for explanatory sketches). (SEM)

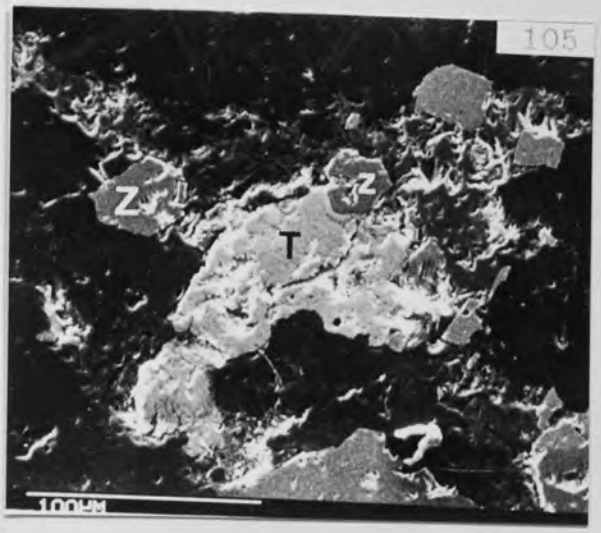
105
Z
Z
T
100µM

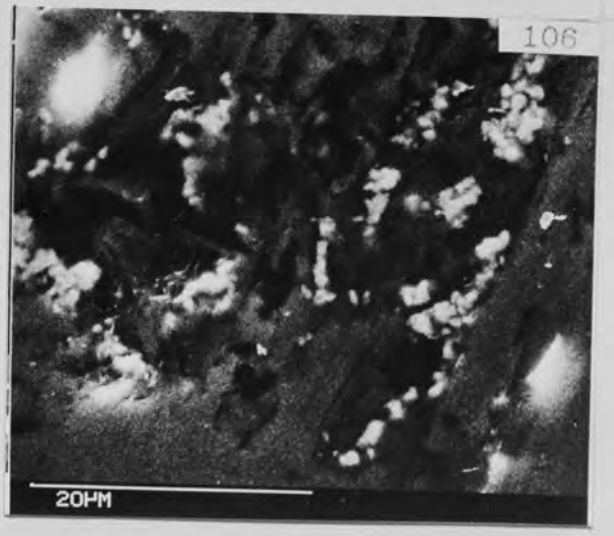
106
20µM

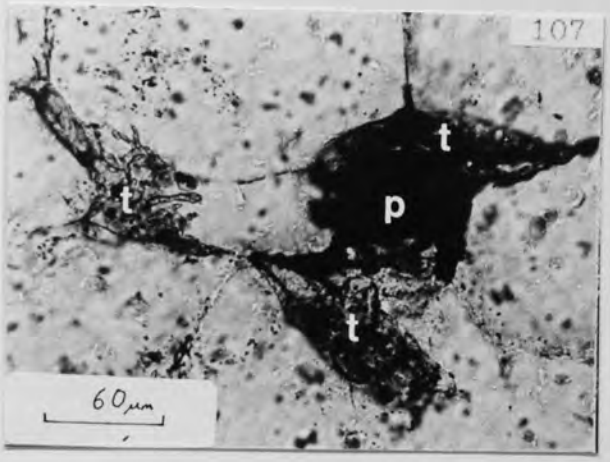
107
t
t
p
t
60µm

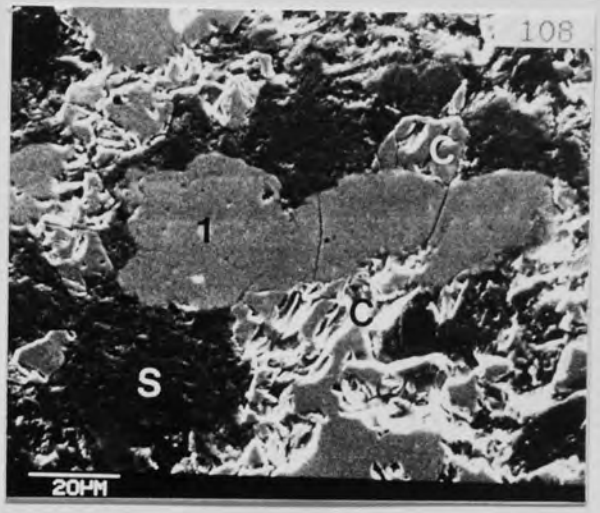
108
C
1
C
S
20µM

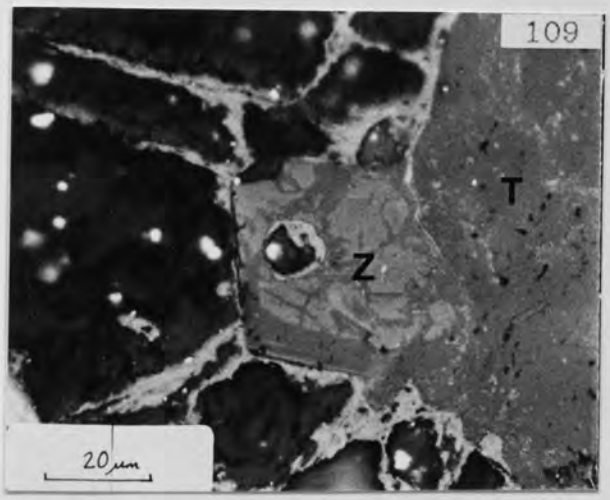
109
T
Z
20µm

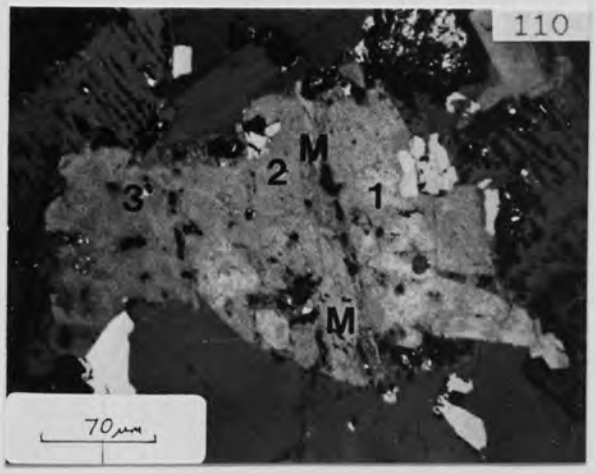
110
3
2
M
1
M
70µm

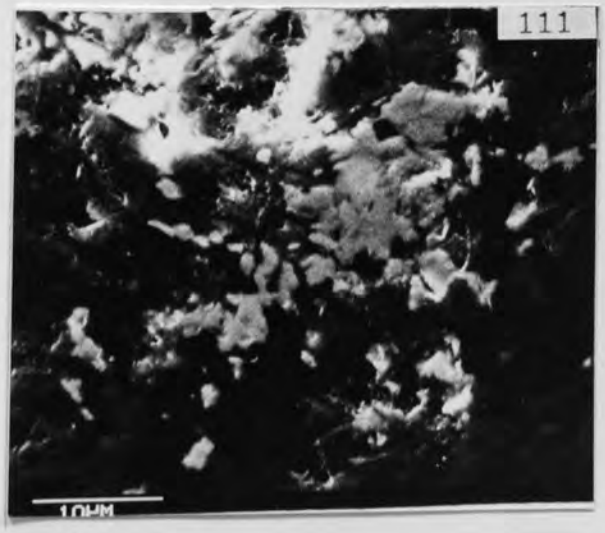
111
10µM

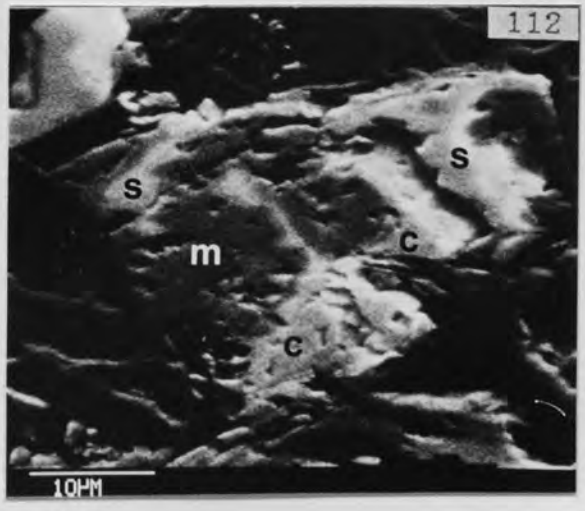
112
s
s
c
m
c
10µM

Table 47 Thorite from the greisenised wallrock, Ririwai lode

Sample No.	Grain No.	An. Spot	Description	Plate
R1/13-4	5	1	Core of a 300 µm long thorite which is intergrown with zircon, columbite, fluorite, cassiterite and pyrite.	104
RS6(2)	1	1,2	100 µm diameter thorite enclosing zircon in quartz.	105
	2	1	Thorite lozenge overgrown by cassiterite and included in chlorite-sericite intergrowth.	108
	3a	2	Thorite overgrowing zircon.	101
	3b	2	" " "	100
	7	1	40 µm long thorite lozenge included in chlorite	
	9	1	-sericite intergrowth.	
RS6(3)	1a-d		60-120 µm long, lozenge-shaped thorites clustered in chlorite-sericite intergrowth.	
RS14(1)	12	1	40 µm diameter ovoid thorite enclosed by a rim of iron-oxide and included in white mica.	

Table 47 Probe Analyses of Thorite from the Greisenised Wallrock, Ririwai Lode
(recalculations based on four oxygens)

Sample	R1/13-4	RS6(2)							RS6(3)				RS14(1)
Grain	5	1		2	3a	3b	7	9	1a	1b	1c	1d	12
An.Spot	1	1	2	1	2	2	1	1	1	1	1	1	1
ThO_2	67.96	63.57	56.72	57.65	51.12	47.43	50.09	57.49	58.79	58.79	64.01	57.27	47.75
UO_2	11.22	4.53	15.46	14.05	18.57	23.45	11.22	20.51	13.75	8.66	7.28	9.32	3.11
Y_2O_3	3.75	7.51	5.01	7.09	5.06	6.82	10.23	4.59	8.14	9.48	7.64	7.91	8.23
CaO	0.45	0.69	1.19	0.33	1.18	1.05	1.82	-	2.26	0.99	0.90	0.85	0.22
ZrO_2	nd	0.55	0.33	nd	1.04	2.38	1.10	0.07	-	-	-	-	9.28
HfO_2	-	-	-	-	-	-	-	-	-	-	-	-	0.65
FeO	1.05	0.10	0.09	0.54	-	-	nd	-	-	-	-	-	0.56
SiO_2	13.15	11.63	11.36	12.85	12.91	13.84	11.86	11.84	10.58	12.08	11.22	14.49	10.67
P_2O_5	0.94	1.96	0.92	1.15	1.19	1.23	2.20	0.78	0.90	-	-	1.15	2.95
Total	98.52	90.54	91.08	93.66	91.07	96.20	88.52	95.28	94.42	90.00	91.05	90.99	83.42
Th	0.902	0.881	0.819	0.782	0.703	0.606	0.677	0.813	0.825	0.844	0.942	0.757	0.645
U	0.146	0.061	0.218	0.186	0.250	0.293	0.148	0.284	0.189	0.122	0.105	0.120	0.041
Y	0.116	0.243	0.169	0.225	0.163	0.204	0.323	0.152	0.267	0.318	0.263	0.245	0.260
Ca	0.028	0.045	0.081	0.021	0.076	0.063	0.116	0.000	0.149	0.067	0.062	0.053	0.014
Zr	0.000	0.016	0.010	0.000	0.031	0.065	0.032	0.002	0.000	0.000	0.000	0.000	0.269
Hf	0.000	0.000	0.000	0.000	0.000	0.000	0.000	0.000	0.000	0.000	0.000	0.000	0.011
Fe	0.051	0.005	0.005	0.027	0.000	0.000	0.000	0.000	0.000	0.000	0.000	0.000	0.028
Total	1.243	1.251	1.302	1.241	1.223	1.231	1.296	1.251	1.430	1.351	1.372	1.175	1.268
Si	0.767	0.708	0.721	0.766	0.780	0.778	0.704	0.736	0.652	0.762	0.725	0.842	0.633
P	0.046	0.101	0.049	0.058	0.061	0.059	0.111	0.041	0.047	0.000	0.000	0.057	0.148
Total	0.813	0.809	0.770	0.824	0.841	0.837	0.815	0.777	0.699	0.762	0.725	0.899	0.781

- Not determined nd Not detected

Plate No.	Sample No.	Grain No.	Description
			Greisen
113	R1/14	2	"Welded clump" of zircons with low reflectance patches along outer zones. Thorite lies close to the area of this photograph. Haematite (H) surrounds the zircons. (RPPL)
114	R1/14-2		Lexan showing fission-tracks (white areas) associated with a trail of thorites across a polished thin section (negative print obtained directly from Lexan)
115	R1/14-2	2	Typical thorite with core enriched in haematite inclusions (opaque). (TPPL)
116	R1/42-3	1	Interstitial thorite containing abundant inclusions of haematite (light grey) and an overgrowth of pyrite (white, at top). EPMA spots are shown. (RPPL)
117	R1/14-1	1	Monazite aggregate (M) showing alteration to a turbid, LREE-phase (L) (TPPL)
118	R1/14-1	5	Complex Th-Y-LREE phase (R) included in Li-mica (M). (RPPL)
119	R1/14-2	1a	Complex Th-LREE phase (EPMA spot 1) overgrowing zircon (Z) (SEM)

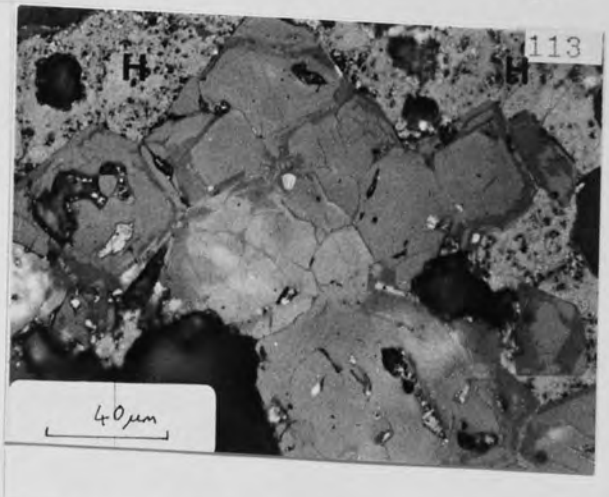
113
H
H
40µm

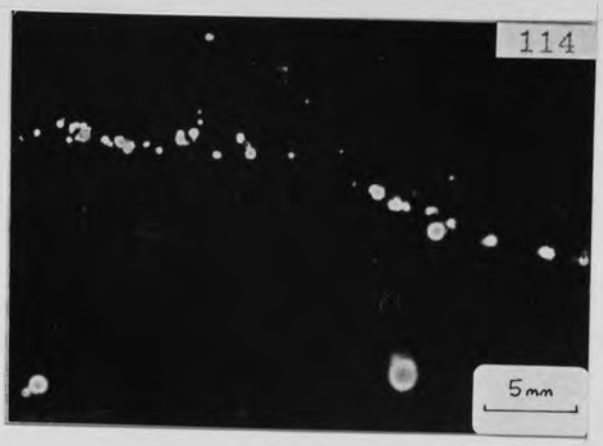
114
5mm

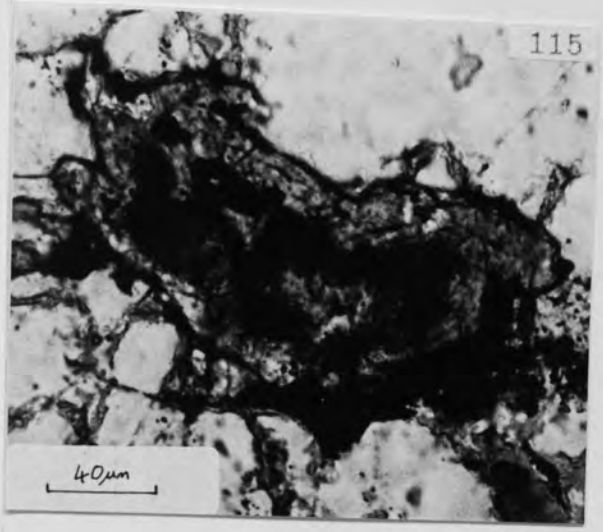
115
40µm

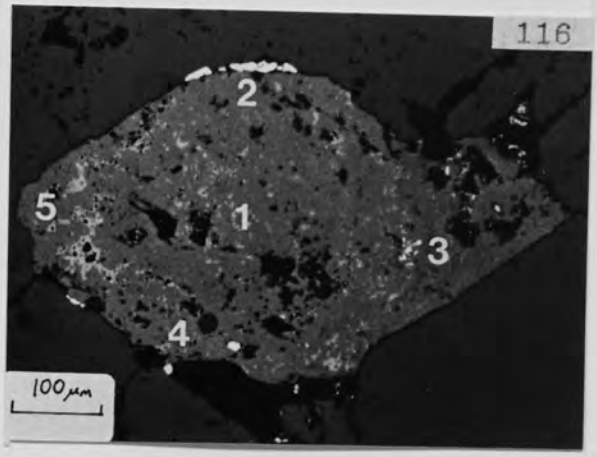
116
2
5
1
3
4
100µm

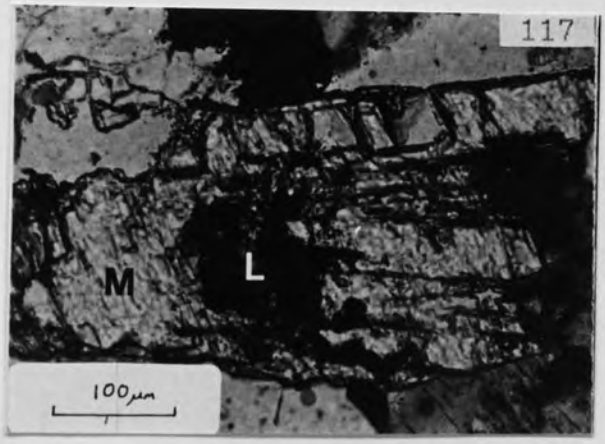
117
M
L
100µm

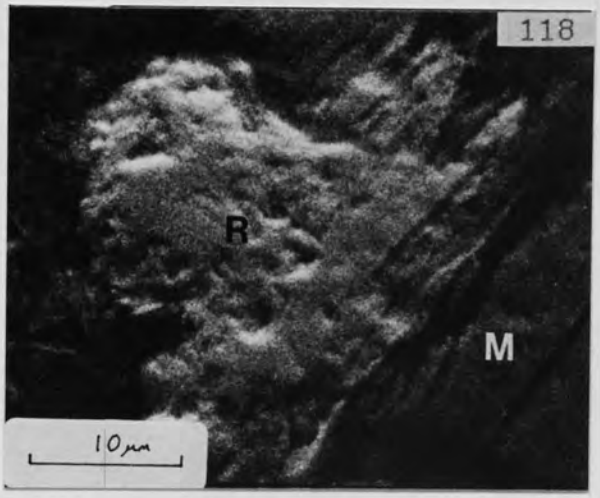
118
R
M
10µm

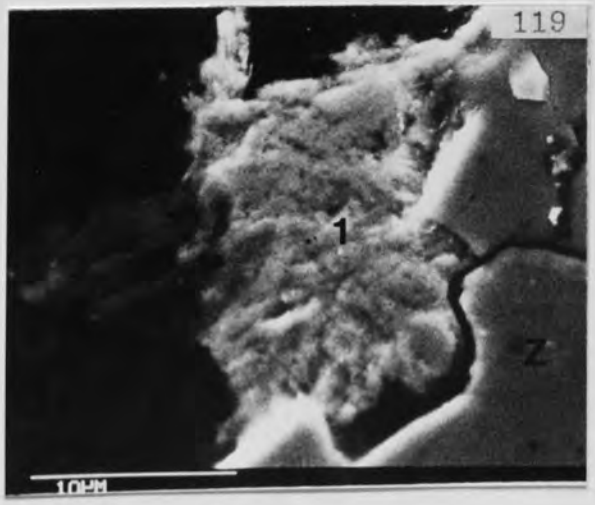
119
1
Z

Table 48 Thorite from the greisen, Ririwai lode

Sample No.	Grain No.	An. Spot	Description	Plate No.
Rl/14	2	1	200 μm diameter, haematite-rich thorite overgrowing welded clump of zircons with low reflectance patches.	113
	12	1	100 μm diameter, haematite-rich thorite.	
	11	1	70 μm " " "	
Rl/14-2	1c		300 μm diameter thorite with haematite and pyrite inclusions.	
		1	Close to grain centre.	
		3	Close to grain edge.	
	6b		90 μm long anhedral thorite included in Li-mica.	
		1	Close to grain edge.	
		2	Close to grain centre.	
	7a	1	120 μm long, lozenge-shaped thorite with orange, haematite-rich core and a rim of pyrite. Analysis spot close to centre.	
	20	1	120 μm long, anhedral clear thorite lying along fracture in quartz. Analysis spot at the centre.	
Rl/42-3	1	1-5	600 μm long, ovoid-shaped thorite in quartz. It has a thin overgrowth and inclusions of pyrite and abundant inclusions of haematite. Analysis spot 1 is in the centre and spots 2-5 close to the grain margins.	116

Table 48 Probe analyses of thorite from the greisen, Ririwai lode
(recalculations based on four oxygens)

Sample	R1/14			R1/14-2						R1/42-3				
Grain	2	12	11	1c		6b		7a	20	1				
An.Spot	1	1	1	1	3	1	2	1	1	1	2	3	4	5
ThO_2	60.28	67.05	59.55	63.11	58.71	59.05	53.52	65.52	65.42	62.93	62.47	66.23	72.75	72.22
UO_2	3.72	2.12	3.33	3.39	4.81	4.52	6.77	4.16	13.15	9.84	10.86	7.66	5.49	4.62
Y_2O_3	4.15	4.01	4.77	8.70	9.43	9.42	7.36	3.64	0.61	3.78	3.87	4.44	2.16	1.39
CaO	0.14	0.14	0.22	0.35	0.39	0.41	0.21	0.37	0.46	0.10	0.11	0.11	0.13	0.17
ZrO_2	3.57	1.18	7.54	0.62	2.92	1.47	1.62	nd	nd	nd	nd	nd	nd	nd
HfO_2	-	-	-	nd	nd	-	-	-	-	-	-	-	-	-
FeO	6.51	5.72	3.05	0.94	0.18	0.64	4.49	1.73	0.15	3.45	2.33	1.52	2.65	4.40
SiO_2	10.49	10.88	11.44	13.08	12.95	12.82	10.59	9.59	10.78	11.25	10.61	10.93	11.12	10.98
P_2O_5	2.32	2.07	2.63	2.74	2.51	2.33	1.91	1.17	0.59	0.54	0.58	1.11	0.34	0.36
Total	91.18	93.17	92.53	92.93	91.90	90.66	86.47	86.18	91.16	91.89	90.83	92.00	94.64	94.14
Th	0.814	0.912	0.764	0.810	0.753	0.775	0.761	1.027	1.000	0.914	0.934	0.962	1.058	1.050
U	0.049	0.028	0.042	0.043	0.060	0.058	0.094	0.064	0.197	0.140	0.159	0.109	0.078	0.066
Y	0.131	0.128	0.143	0.261	0.283	0.289	0.245	0.133	0.022	0.128	0.135	0.151	0.073	0.047
Ca	0.009	0.009	0.013	0.021	0.024	0.025	0.014	0.027	0.033	0.007	0.008	0.008	0.009	0.012
Zr	0.103	0.034	0.207	0.017	0.080	0.041	0.049	0.000	0.000	0.000	0.000	0.000	0.000	0.000
Hf	0.000	0.000	0.000	0.000	0.000	0.000	0.000	0.000	0.000	0.000	0.000	0.000	0.000	0.000
Fe	0.323	0.286	0.144	0.044	0.008	0.031	0.235	0.100	0.008	0.184	0.128	0.081	0.142	0.235
Total	1.429	1.397	1.313	1.196	1.208	1.219	1.398	1.351	1.260	1.373	1.364	1.311	1.360	1.410
Si	0.623	0.651	0.645	0.738	0.729	0.739	0.662	0.660	0.724	0.718	0.697	0.697	0.711	0.701
P	0.117	0.105	0.125	0.131	0.120	0.114	0.101	0.068	0.034	0.029	0.032	0.060	0.018	0.019
Total	0.740	0.756	0.770	0.869	0.849	0.853	0.763	0.728	0.758	0.747	0.729	0.757	0.729	0.720

- Not determined nd Not detected

ED spectra of zircon and Nb-Ta-Ti-oxides

Fig. No.	Sample No.	Grain No.	An. Spot	Description	Host* rock	Plate No.
29	315	14	1	Zircon. Low reflectance patch enriched in trace-elements.	BG	
30	"	7	4	" "	BG	39
31	RS10(3)	1B	1	Low-reflectance patches in zircon, close to thorite and Th-Pb-P phase.	GW	
32	305	2a	2	Pyrochlore associated with columbite.	BG	
33	"	"	1	Pb-pyrochlore intergrown with columbite.		63
34	R1/13-3	7		Microlite intergrown with pyrite, columbite and U-Si phase.	M	94
35	350	6	1	25 µm diameter pyrochlore inclusion in zircon.	BG	
36	385	6	2	Columbite.	AG	73

* For Figs. 29-67: BG = Biotite granite
AG = Albitised granite
M = Microclinite
GW = Greisenised wallrock
G = Greisen

29.

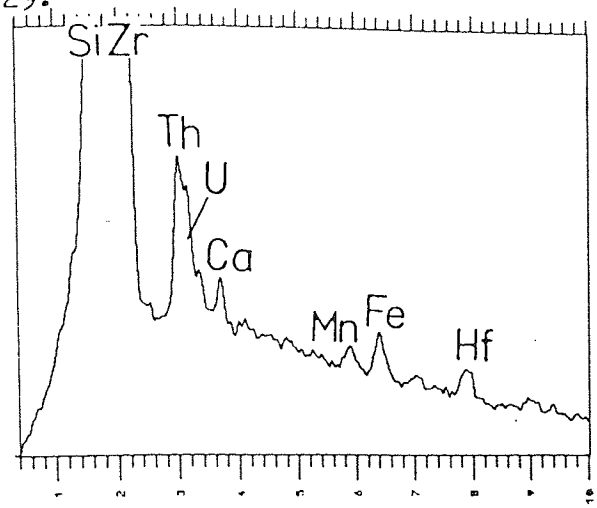

30.

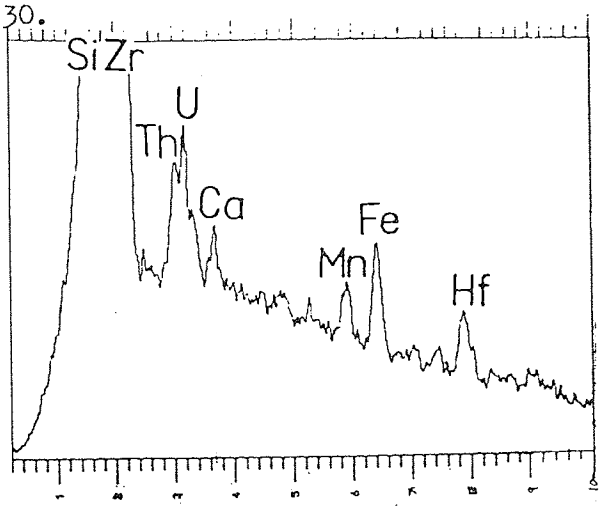

31.

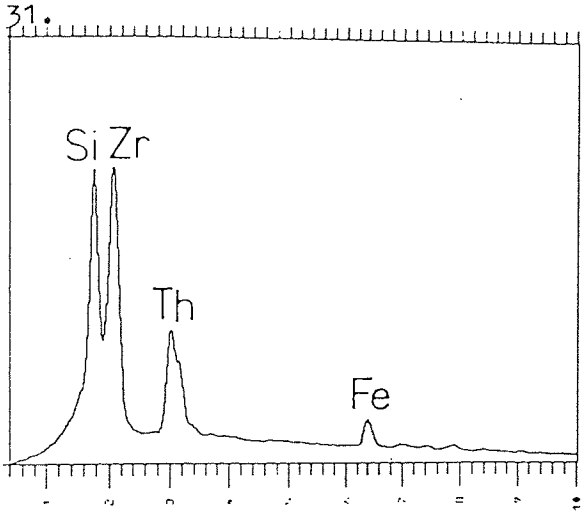

32.

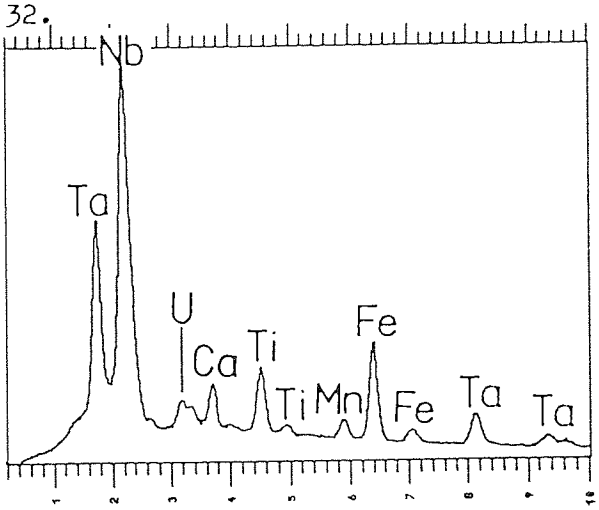

33.

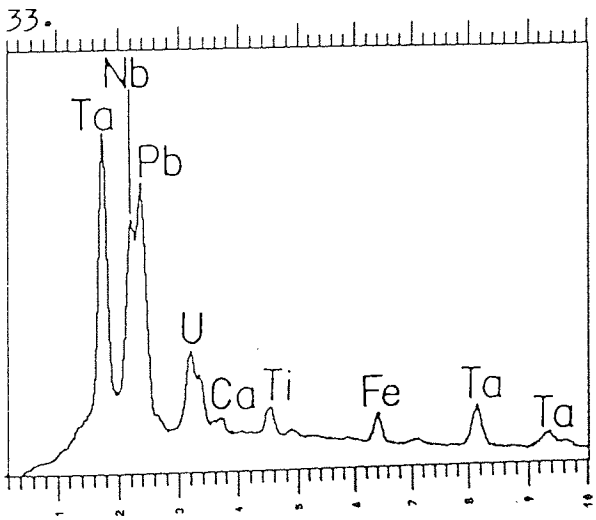

34.

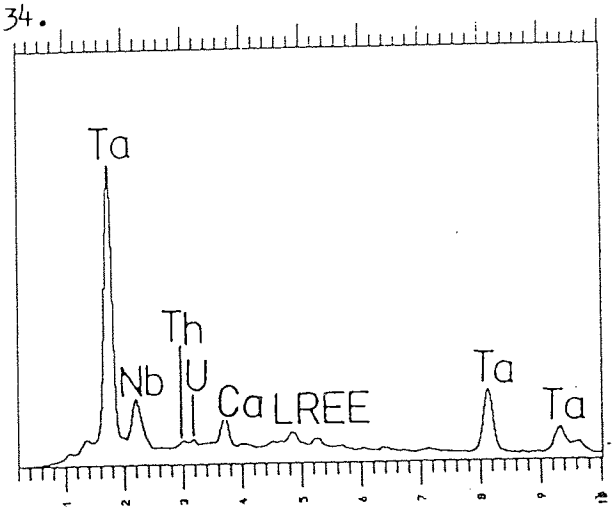

35.

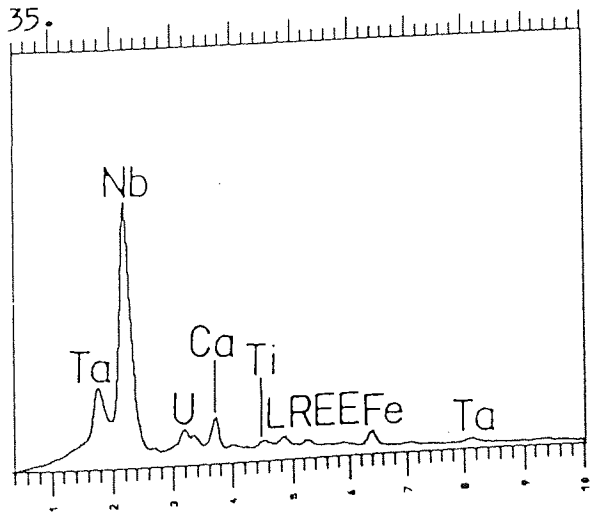

36.

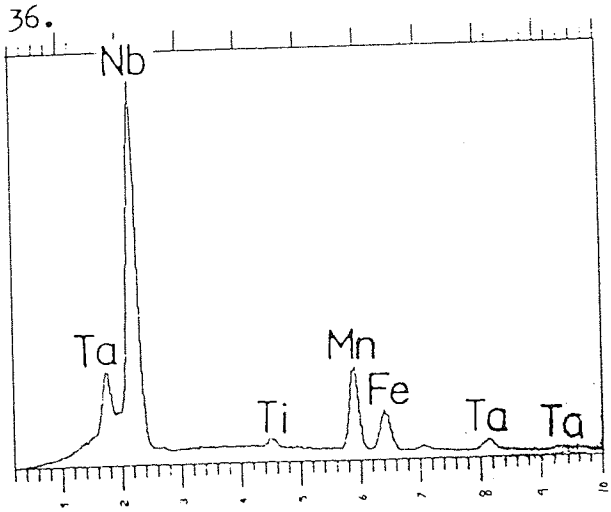

ED spectra of monazite and thorite

Fig. No.	Sample No.	Grain No.	An. Spot	Description	Host rock	Plate No.
37	R1/14-1	2	6	Monazite in quartz.	G	
38	315	6	1	Monazite, partly included in biotite.	BG	59
39	305	4	6	Thorite grains in biotite.	BG	51
40	R1/14-1	3	1	Thorite in Li-mica	G	
41	411	2	9	Uranothorite inclusion in Type 2 zircon.	AG	70
42	RS10(3)	2	25	Zr-rich thorite.	GW	109
43	R1/13-1	10	3	Lozenge-shaped thorite grain in quartz. The Si peak appears to be suppressed.	M	
44	RS10(3)	1	4	Th-Pb-P phase intergrown with thorite and monazite.	GW	110

37.

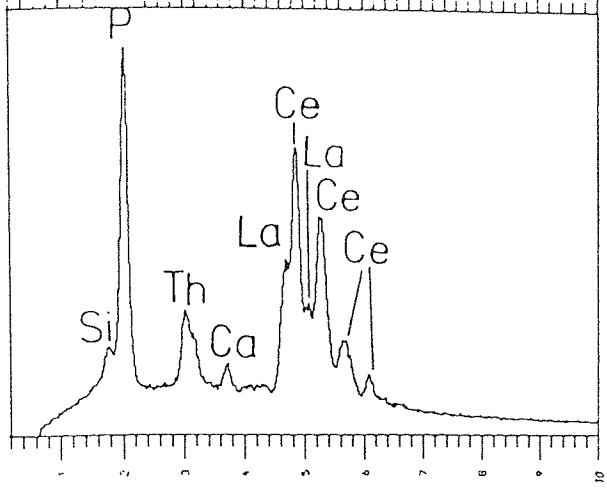

38.

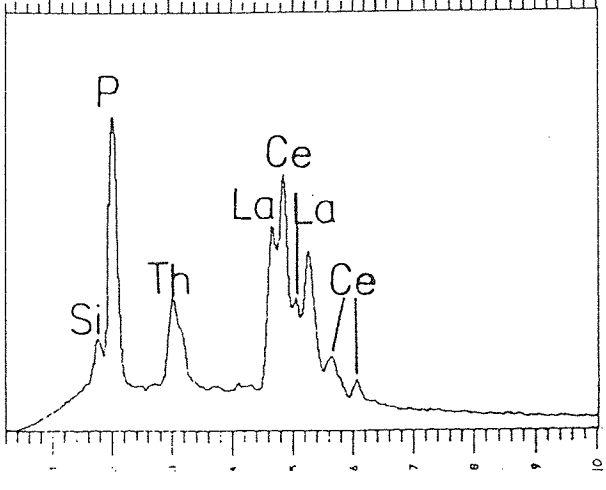

39.

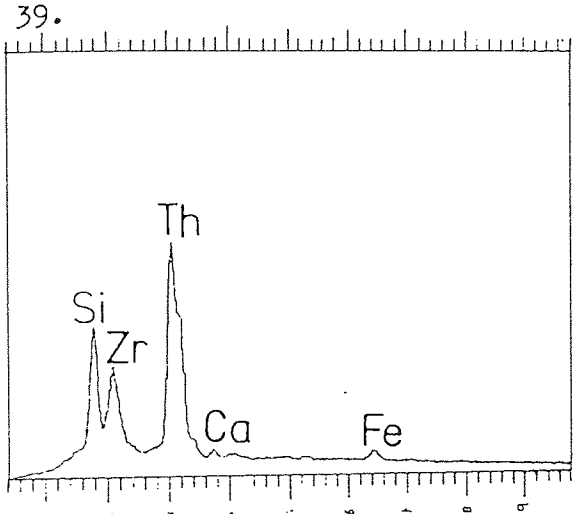

40.

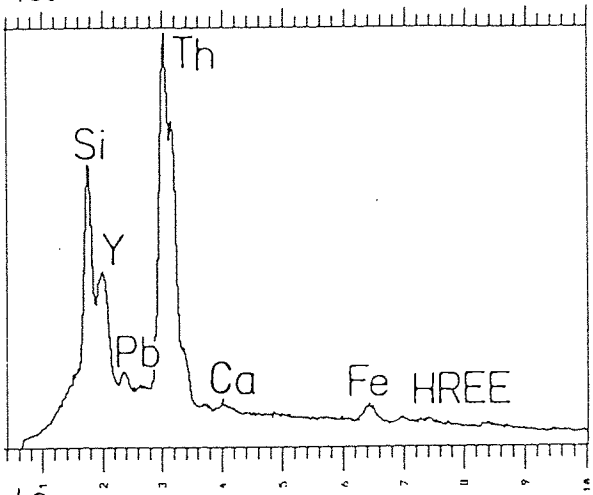

41.

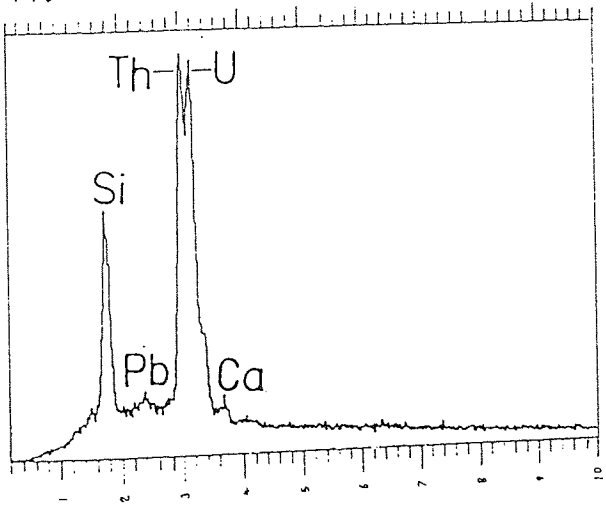

42.

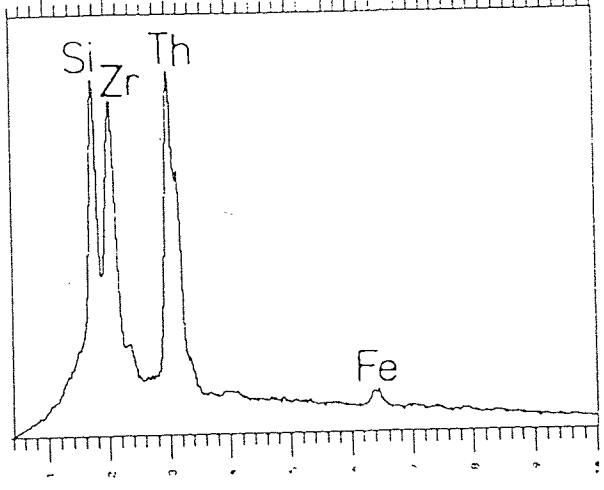

43.

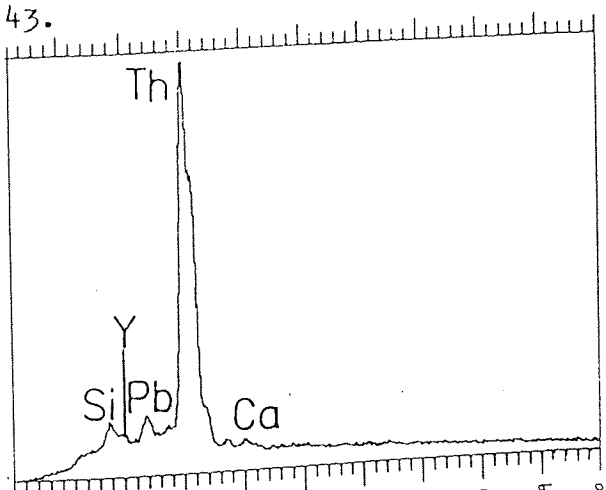

44.

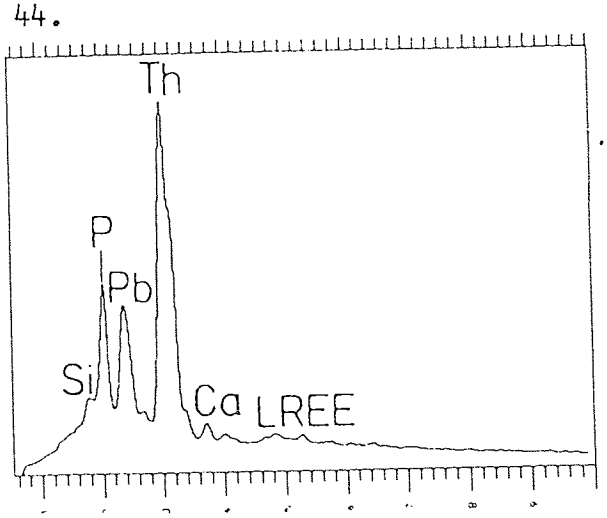

ED spectra of xenotime and U-silicates

Fig. No.	Sample No.	Grain No.	An. Spot	Description	Host Rock	Plate No.
45	RS6(3)	11	1	Xenotime overgrowth on zircon in chlorite-sericite.	GW	
46	RS6(2)	3b	7	Xenotime overgrowth on zircon	GW	100
47	"	6	1	Cluster of U-Th-Y-Si phase grains in chlorite-sericite.	GW	111
48	R1/13-3	7	5	U-Th-Y-Si phase intergrown with pyrite and ?microlite.	M	94
49	100	3	1	Coffinite.	BG	61, 62
50	RS6(4)	1	1	Coffinite.	M	95
51	R1/13-1	2	12	?Coffinite intergrown with TiO_2	M	

45.

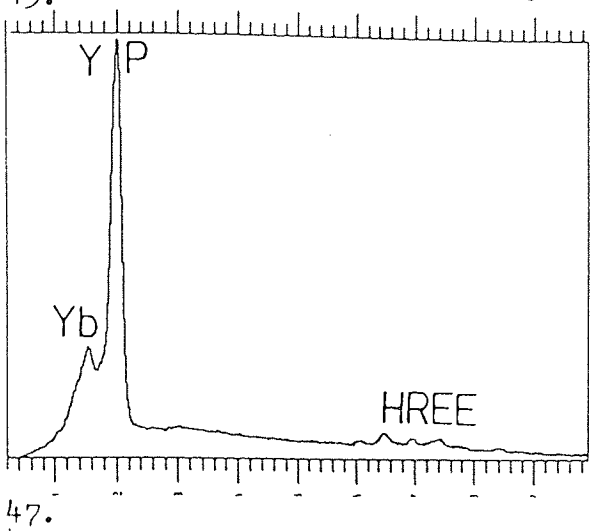

46.

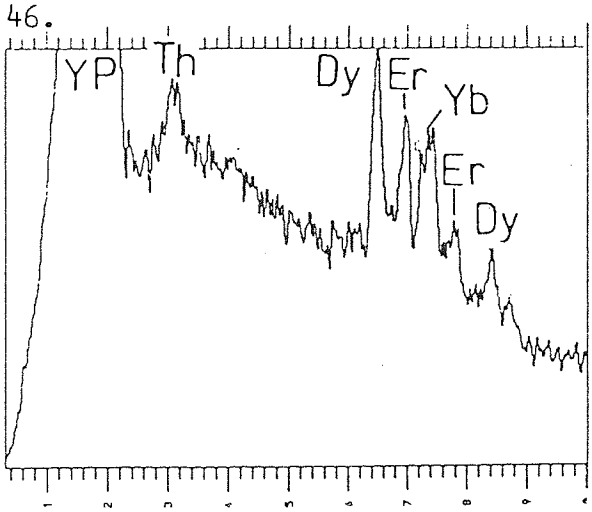

47.

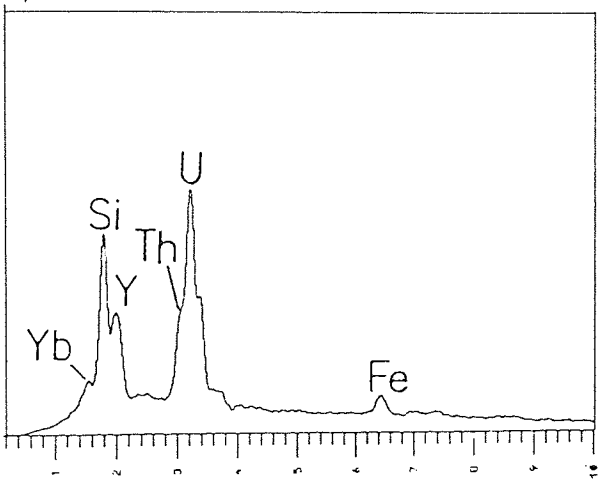

48.

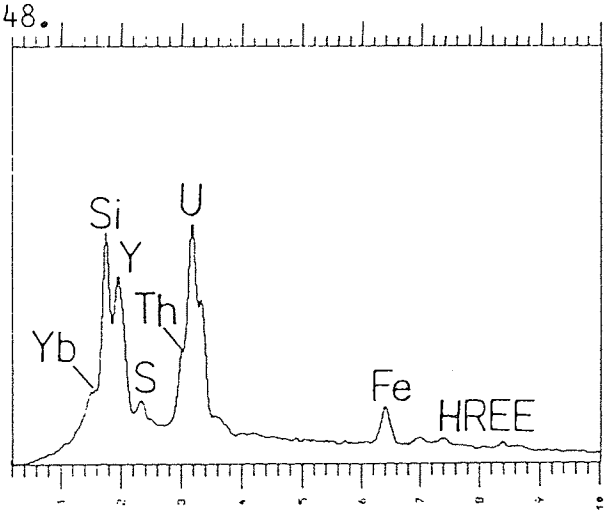

49.

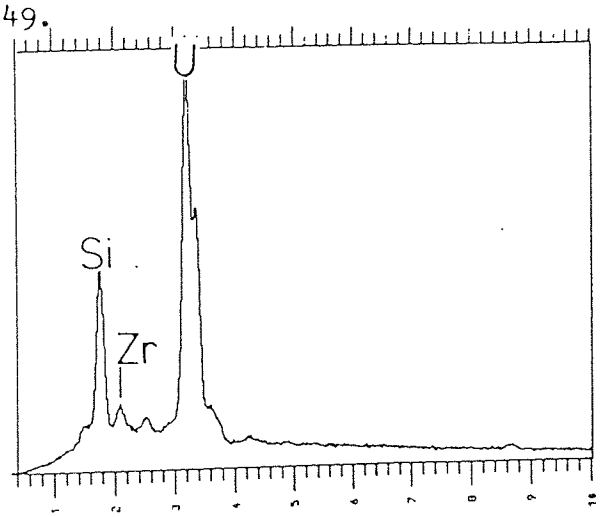

50.

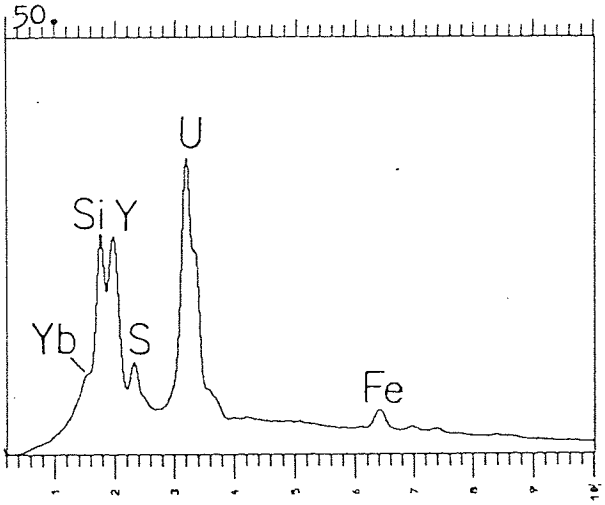

51.

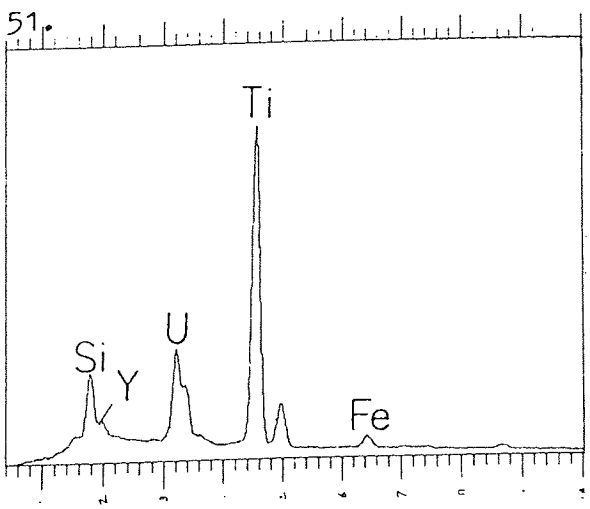

ED spectra of LREE-phase(s)

Fig. No.	Sample No.	Grain No.	An. Spot	Description	Host Rock	Plate No.
52	R1/23-1A	27	7	Complex LREE-phase overgrowing thorite.	M	
53	R1/13-7	3	2	Complex LREE-phase in fluorite.	M	
54	R1/14-1	3	10	Complex LREE-phase overgrowing thorite.	G	
55	R1/14-2	1a	2	Complex LREE-phase overgrowing zircon.	G	119
56	R1/14-1	5	6	Complex LREE-phase included in Li- mica.	G	118
57	RS6(4)	3b	2	Complex LREE-phase intergrown with coffinite.	M	96
58	R1/13-7	3	5	Complex LREE-phase in fluorite.	M	
59	RS6(4)		2	Simple LREE-phase. 15 µm across	M	

52.

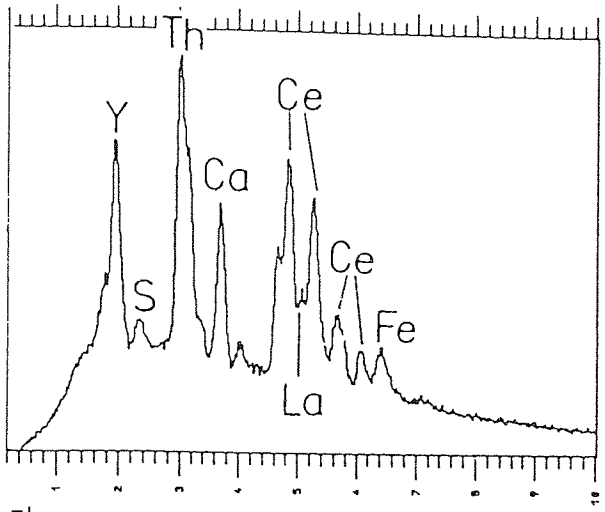

53.

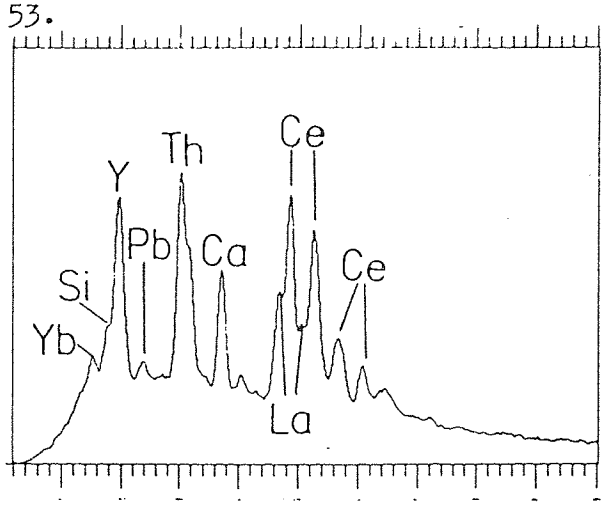

54.

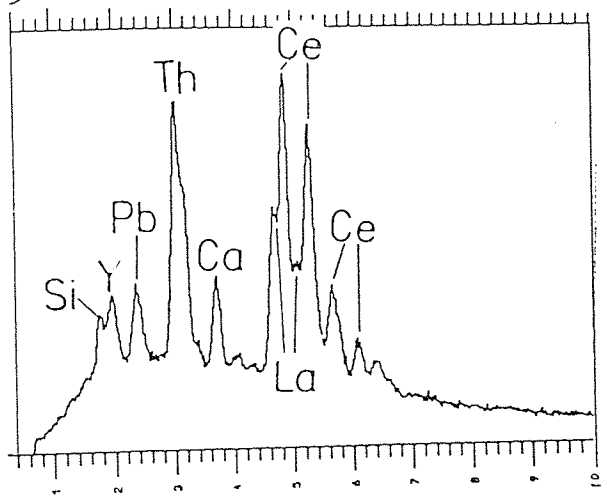

55.

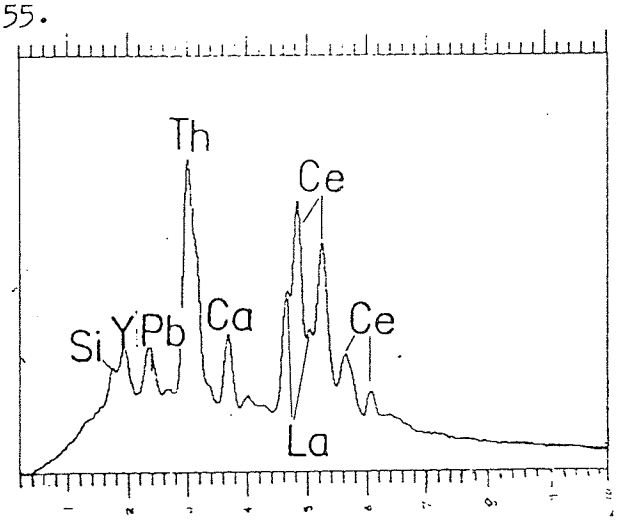

56.

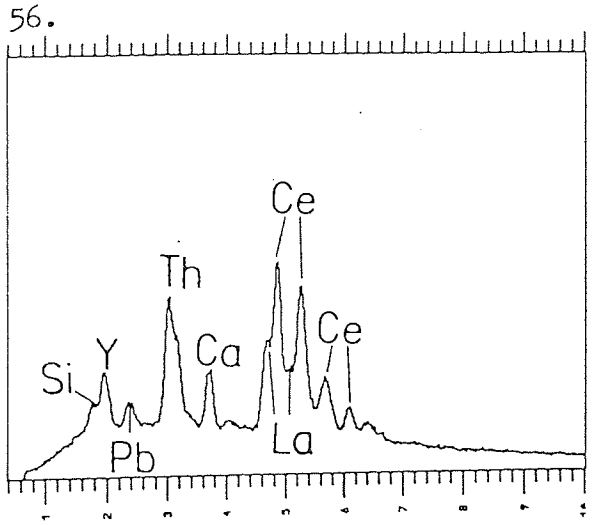

57.

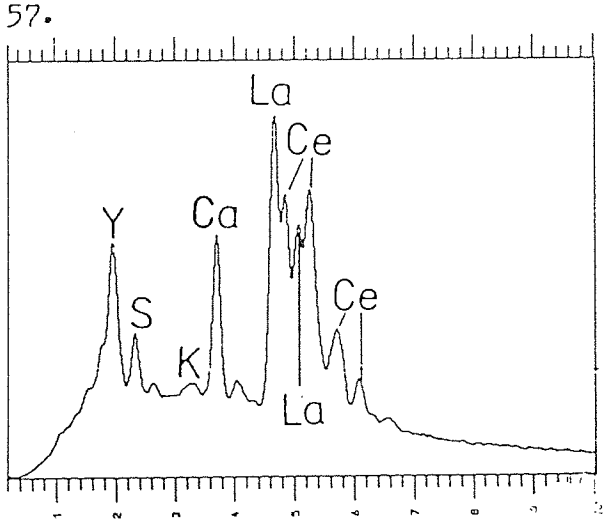

58.

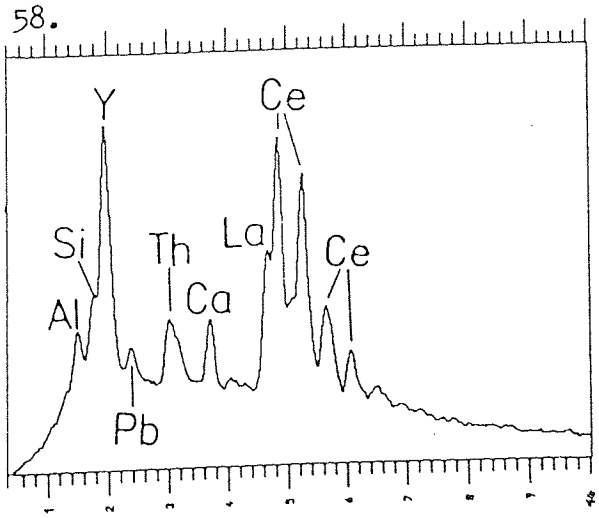

59.

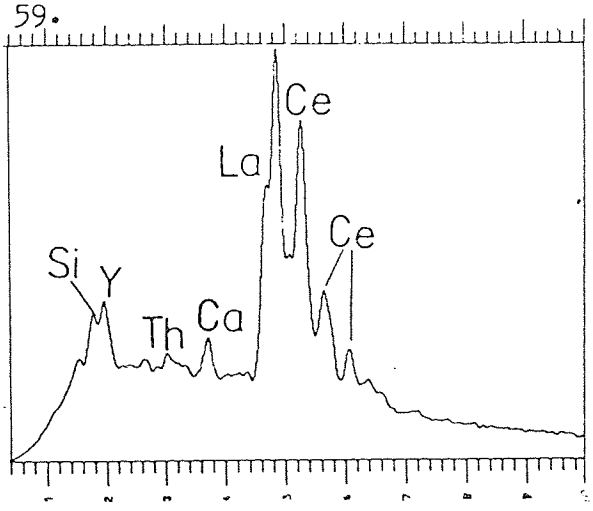

ED spectra of LREE-phase(s)

Fig. No.	Sample No.	Grain No.	An. Spot	Description	Host Rock	Plate No.
60	R1/13-6	2F	1	Complex LREE-phase, 20 µm sized inclusion in fluorite.	GW	
61	R1/13-1	1c	4	Complex LREE-phase overgrowing zircon.	M	
62	R1/13-6	2L	1	Complex LREE-phase in fluorite.	GW	
63	"	2B	2	" "	GW	
64	RS10(3)	2	6	Complex LREE-phase with minor Th and Pb, lying between simple LREE-phase and Th-Pb-LREE-phase	GW	112
65	"	"	5	Th-Pb-LREE-phase.	GW	"
66	315	6	4	Simple LREE-phase replacing monazite.	BG	59
67	411	1	1	Simple LREE-phase in fluorite.	AG	82

60.

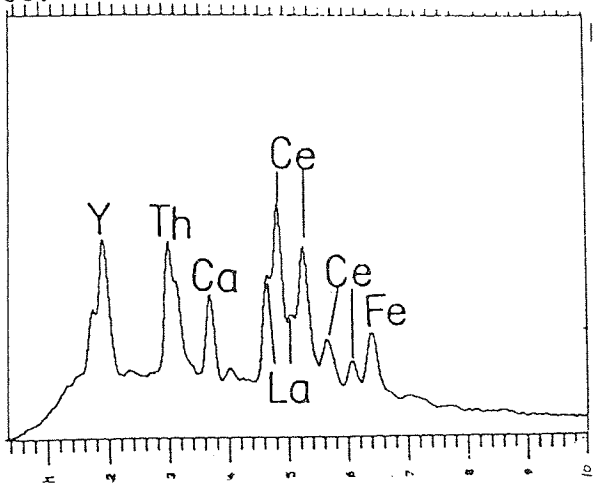

61.

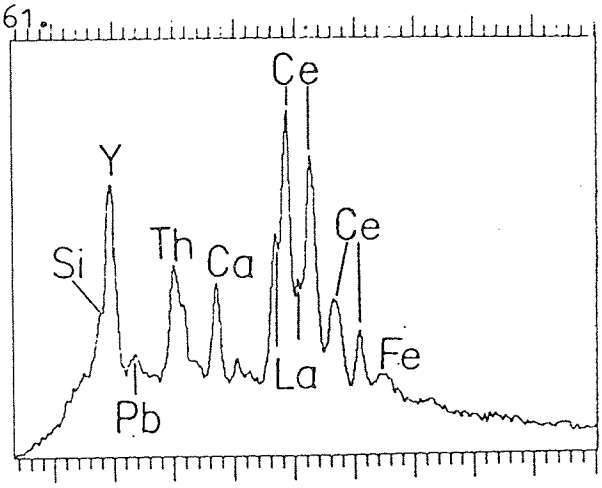

62.

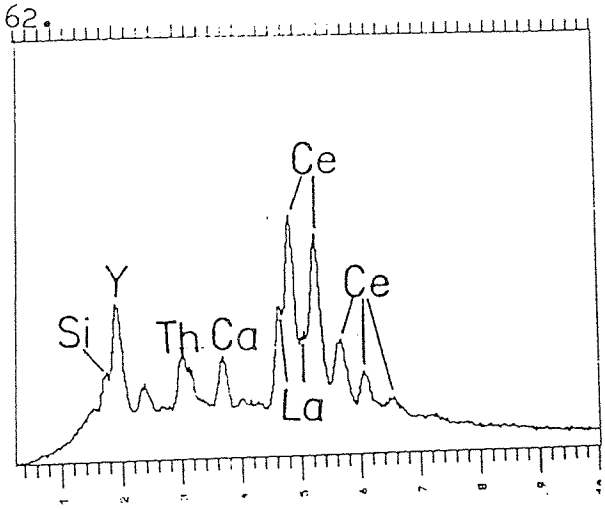

63.

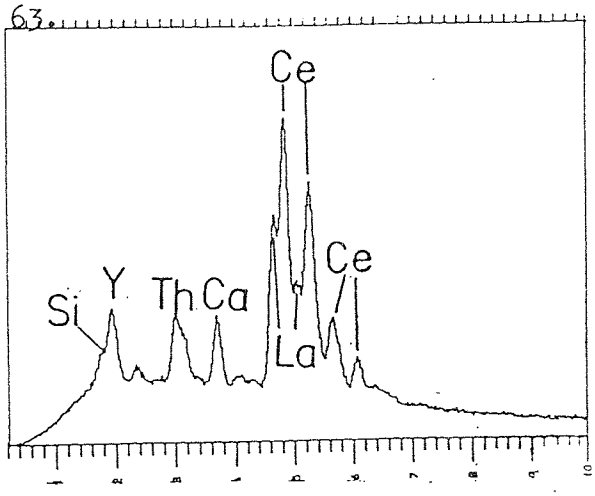

64.

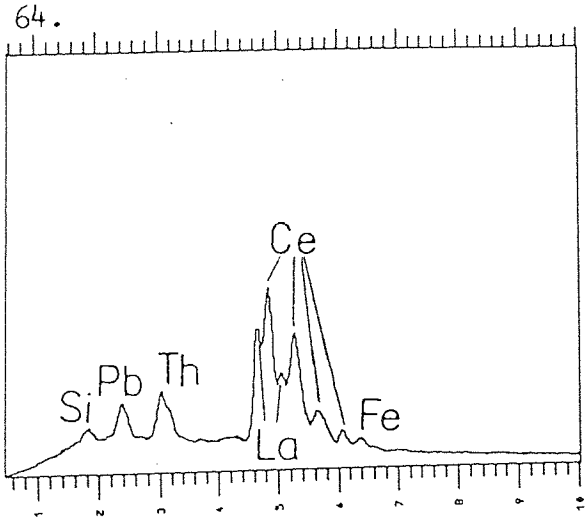

65.

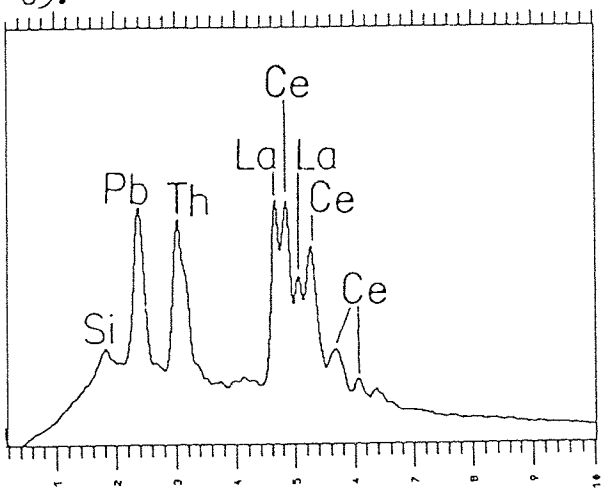

66.

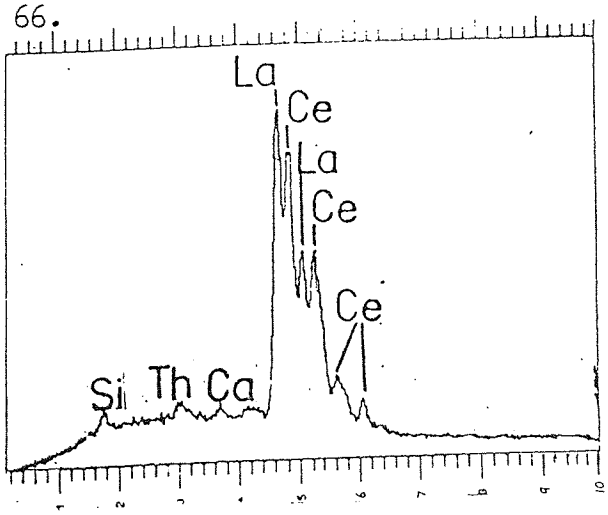

67.

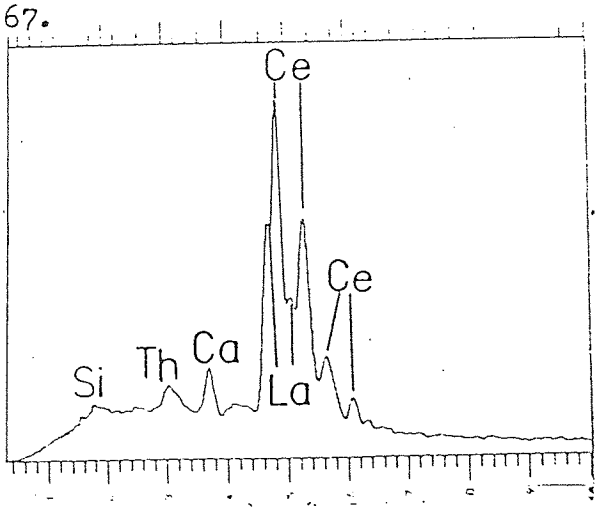

Fig.68 Wt. % Y2O3 vs wt % ZrO2 for thorite from the biotite and albitised granite

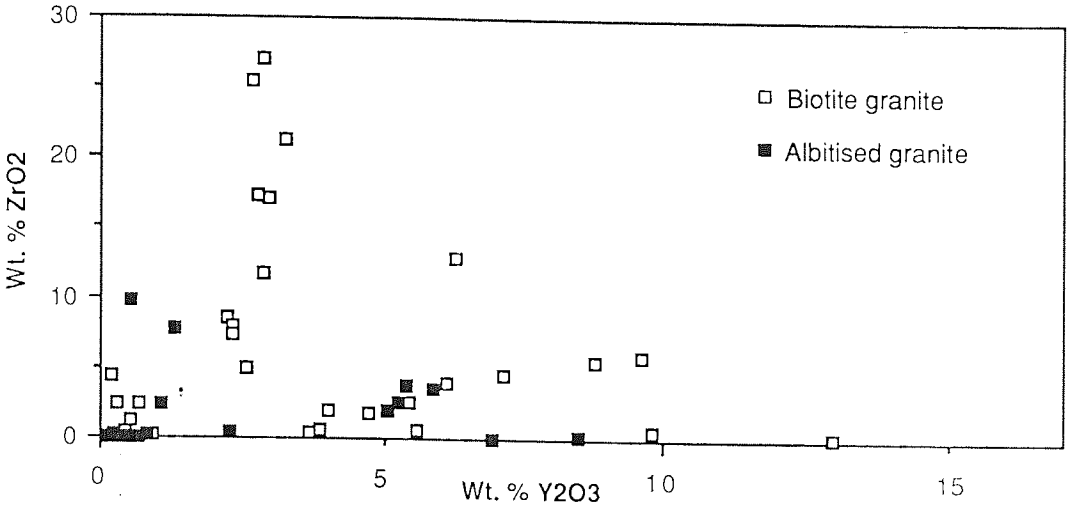

Fig.69 Wt. % Y2O3 vs wt. % ZrO2 for thorite from the greisenised granite (125) and Ririwai lode

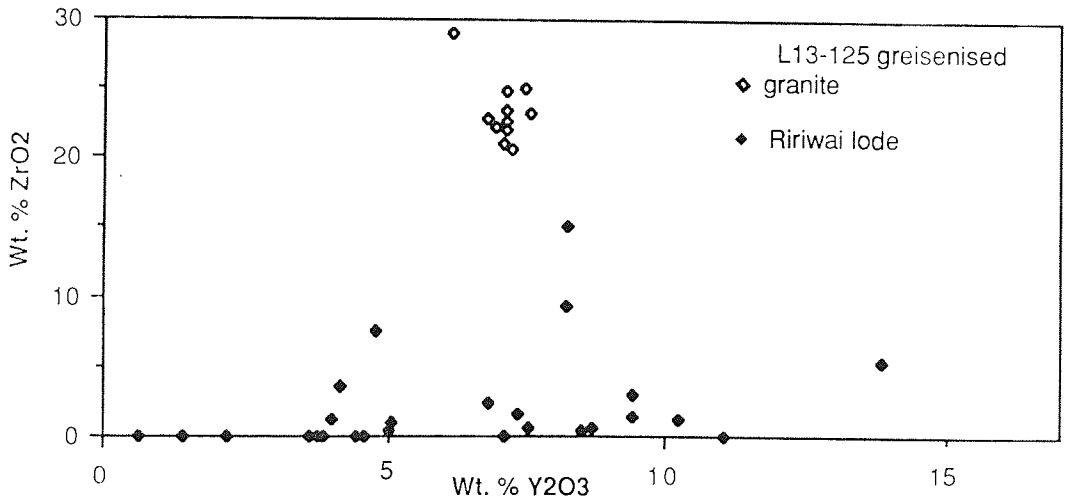

Fig.70 wt. % Y2O3 vs wt. % ZrO2 for coffinite from the biotite granite and Ririwai lode

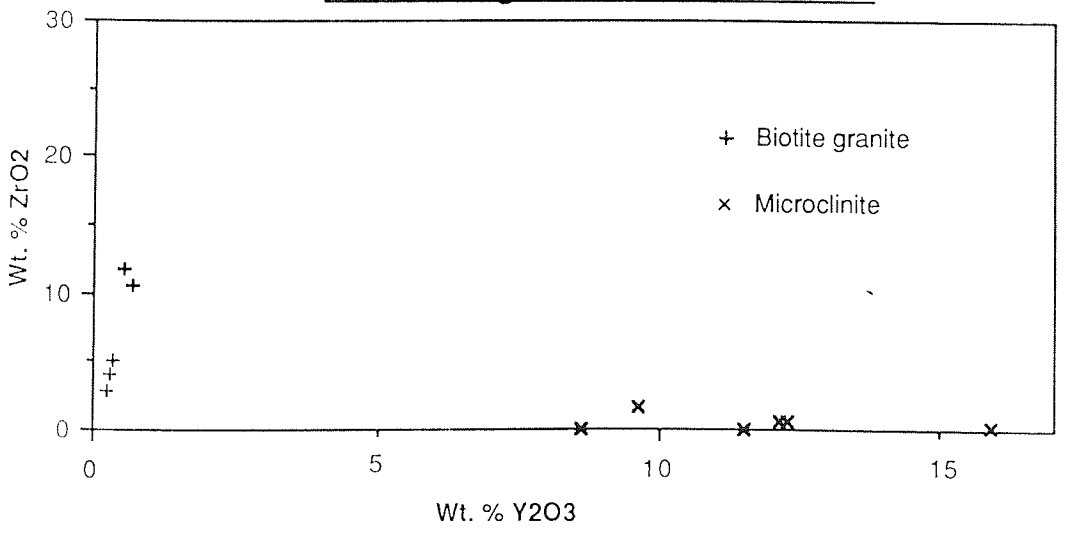

Table 49 Summary of alteration sequence and paragenesis of radioelement-bearing accessory minerals in the Ririwai biotite granite

PROCESS	Rock	Biotite Granite		Albitised Granite / Albitite		Greisenised Granite	Ririwai Lode
	Sample	N94, 100, 145-350 m	N75 & 365 m	385-411 m	416-450 m	125 m	Surface and Mine Level 1
MAGMATIC		1. Crystallisation of primary zircon in biotite, feldspar and quartz; i) Haematite-rich cores ii) Clear rims ± enriched Hf iii) Trace-element enriched overgrowths of zircon and co-precipitation of zircon with thorite inclusions	2. Crystallisation of discrete thorite grains in biotite: i) Haematite-rich cores. ii) Clear rims. 3. Crystallisation of monazite. 4. Crystallisation of pyrochlore.	(As Biotite Granite)		(As Biotite Granite)	1. Crystallisation of relatively clear, thorite-free zircon ± Hf-rich domains/rims. 2. Crystallisation of monazite.
POST MAGMATIC		1. Alteration of zircon to give low-reflectance, trace-element enriched patches (100-315 m) 2. Embayment of zircon by secondary fluorite ± LREE-phase inclusions in biotite. 3. Partial replacement of monazite by LREE-phase with fractionation of La. 4. Alteration of thorite; i) Leaching of U from rims ii) Y,P & Zr enrichment of rims iii) Hydration → thorogummite 5. Precipitation of Fe-oxide rims around thorite & zircon.	1. Alteration of primary biotite, zircon and thorite with release of Th, U, Fe, Zr, Hf. 2. Growth of a second generation of zircon. Large, haematite- and thorite-rich, interstitial grains (≡Type 2 zircon in albitised rock) 3. Clear zircon rims (≡Type 1). 4. Replacement of some zircon by thorite and growth of interstitial thorite grains. 5. Limited zircon dissolution and replacement by white mica. 6. Precipitation of Fe-oxide rims around thorite and zircon.	ALBITISATION: 1. U-rich, Type 3 zircon. 2. Chloritisation & dissolution of biotite, thorite & zircon with release of Fe,Th,U,Zr,Hf. 3. Exsolution/co-precipitation of thorite with Type 2 zircon. 4. Hf-rich, Type 1 zircon. 5. Ta-, Pb-, U-rich ?pyrochlore 6. U-rich thorite. Interstitial and overgrows/replaces zircon. 7. Dissolution of zircon and replacement by REE-rich fluorite. 8. Xenotime overgrows zircon. 9. Haematite & sulphides. 10. Dissolution of monazite.			1. Dissolution of monazite and alteration to LREE-phase.
MAGMATIC		1. Crystallisation of Zr-rich coffinite.				MICROCLINISATION	1. Chloritisation of biotite with dissolution of thorite. 2. Crystallisation of U-rich thorite, U-Th-Y-Si-phases, ?microlite and Y-coffinite. 3. Crystallisation of LREE-phases (simple & complex).
		Paragenetic Sequence and Decreasing Temperature ↓				GREISENISATION: 1. Replacement of zircon by Li-mica. 2. Crystallisation of Zr- and Y-rich thorite in Li-mica as discrete grains or overgrowing zircon. 3. Crystallisation of pyrite with thorite.	1. Crystallisation of Y-rich thorite with pyrite or Zr-, Y-rich thorite with Fe-oxide. 2. Alteration of zircon to give low-reflectance, trace-element enriched patches near thorite. 3. Y-, P-, ±Zr, ±U-enrichment of thorite rims. 4. Th-Pb-P-phase. 5. LREE-phases (simple and complex) overgrowths & incls. 6. Xenotime overgrows zircon.

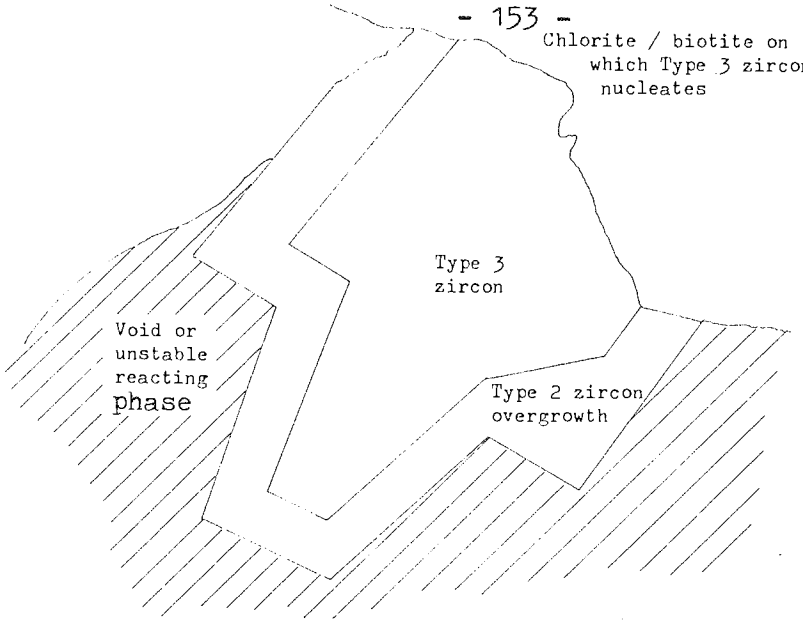

1. Type 3 zircon nucleates on biotite/chlorite and is overgrown by a zone of Type 2 zircon which grows into a void or replaces an unstable reacting mineral

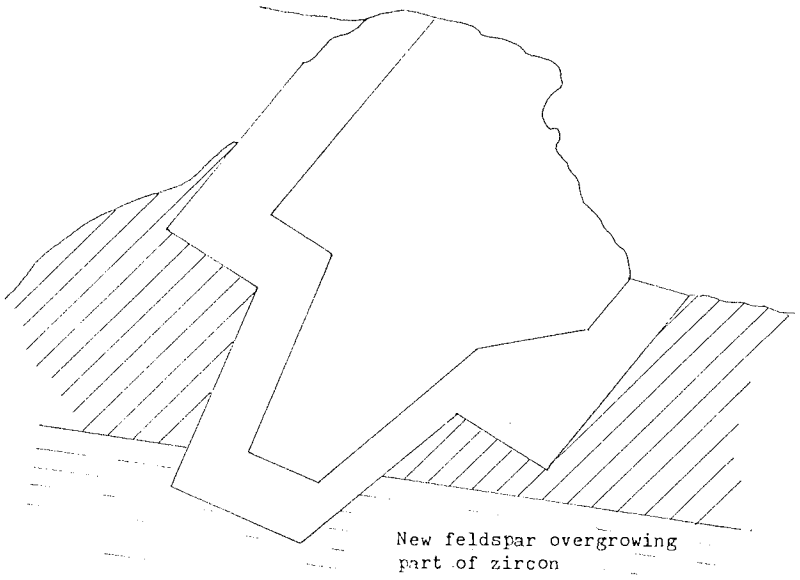

2. Feldspar overgrows part of the zircon in the void or replaces the unstable mineral, while there is a temporary cessation of zircon growth

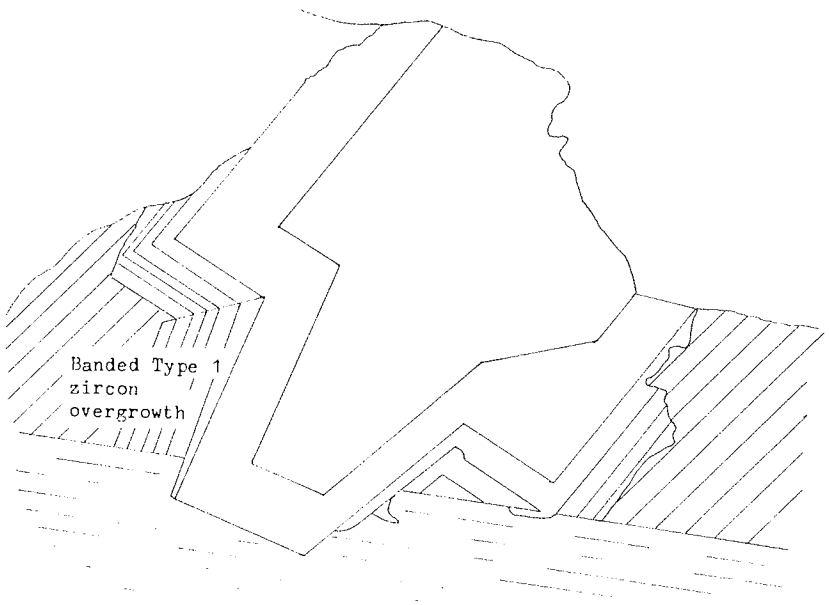

3. A further overgrowth of zircon is restricted to the void/unstable mineral and impinges on the crystal face of the feldspar. Fluctuating levels of Hf precipitation give rise to banding in the Type 1 zircon.

Fig. 71 Possible explanation of the zircon morphology in Plate 70

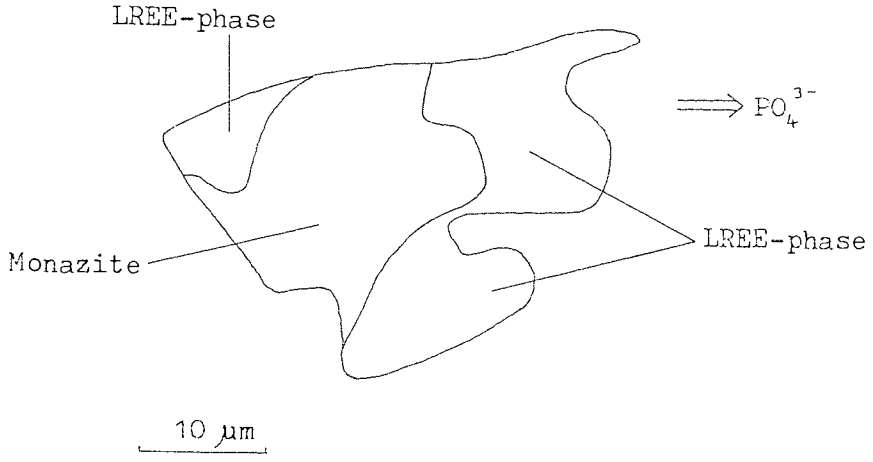

1. Monazite altered to a LREE-phase of simple composition:

$$(LREE)PO_4 \longrightarrow \text{LREE-phase} + PO_4^{3-}$$

This may have occurred before greisenisation, as a similar alteration is found in monazite from the least-altered biotite granite.

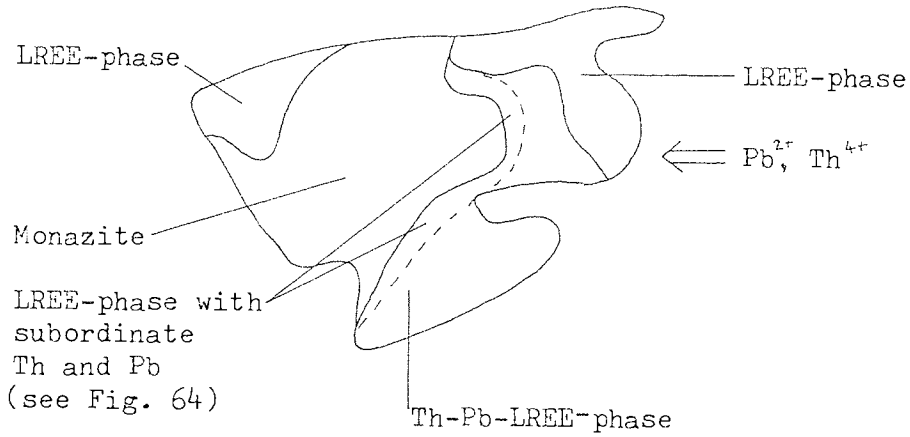

2. During greisenisation, Th^{4+} and Pb^{2+} precipitated in thorite and galena respectively and also reacted with the LREE-phase to give a complex Th-Pb-LREE phase:

$$\text{LREE-phase} + Th^{4+} + Pb^{2+} \longrightarrow \text{Pb-Th-LREE-phase}$$

Fig. 72 Possible explanation for the intergrowth of monazite, simple LREE-phase and complex Pb-Th-LREE-phase in the greisenised wallrock, Ririwai lode

(see Plate 112, Fig. 65)

Fig. 73 wt. % Y203 vs wt. % P205 for all zircons

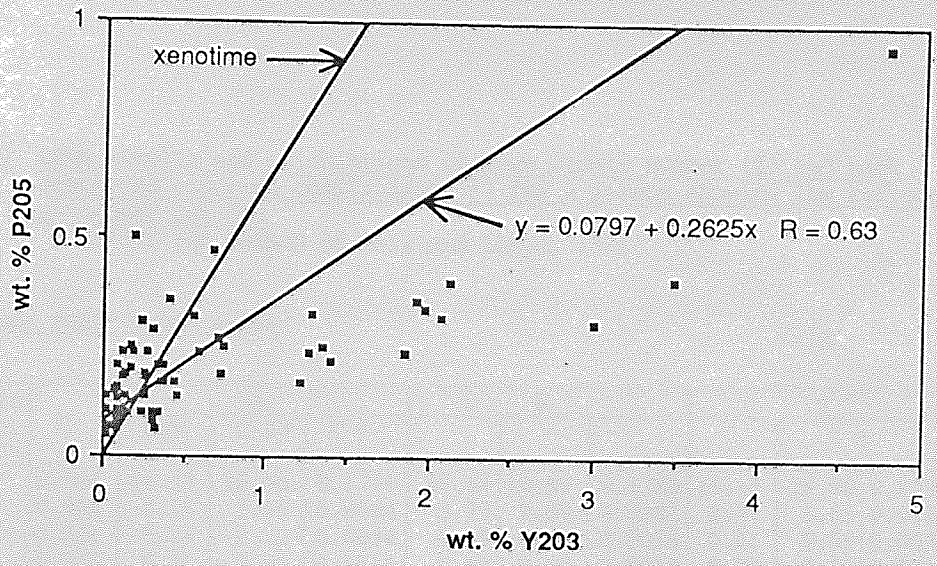

Fig. 74 wt.%ThO2 : wt.%SiO2 for all monazites

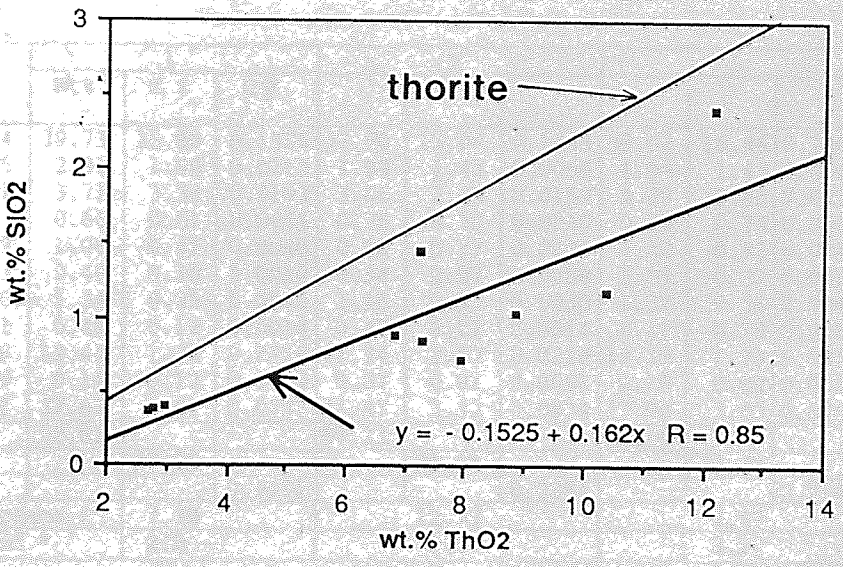

Table 50 EPMA results and calculations of mean atomic number ($\bar{Z}$) and back scattered electron coefficient ($\bar{\eta}$) for a zircon showing low reflectance secondary patches
(after the method of Hall and Lloyd, 1981)

(A) Higher reflectance areas

Analysis No. / Element	η	2			4			7			Z
		Wt%	C Z*	C η							
Zr	0.384	46.24	18.50	0.1776	46.48	18.59	0.1785	45.14	18.06	0.1733	40
Hf	0.485	2.15	1.55	0.0104	3.73	2.69	0.0181	2.31	1.66	0.0112	72
Th	0.521	0.84	0.76	0.0044	0.35	0.32	0.0018	0.61	0.55	0.0032	90
U	0.523	0.31	0.29	0.0016	0.19	0.18	0.0010	0.24	0.22	0.0013	92
Y	0.379	0.24	0.09	0.0009	0.09	0.04	0.0003	0.24	0.09	0.0009	39
Ca	0.243	0.16	0.03	0.0004	0.05	0.01	0.0001	0.68	0.14	0.0017	20
Fe	0.300	0.33	0.09	0.0010	0.29	0.08	0.0009	0.40	0.10	0.0012	26
Mn	0.291	0.09	0.02	0.0003	0	0	0	0.07	0.02	0.0002	25
Si	0.176	15.16	2.12	0.0267	15.13	2.12	0.0266	14.69	2.03	0.0255	14
P	0.189	0.04	0.01	0.0001	0.04	0.01	0.0001	0.04	0.01	0.0001	15
O	0.201	34.35	2.75	0.0690	34.48	2.76	0.0693	33.40	2.67	0.0671	8
ΣOxides		99.91			100.83			97.62			
$\bar{Z}$			26.21			26.80			25.55		
$\bar{\eta}$				0.2924			0.2967			0.2857	

* C = concentration of element

(B) Lower reflectance secondary patches (assuming water is present)

Analysis No. / Element	η	1			3			5			Z
		Wt%	C Z	Cη							
Zr	0.384	39.73	15.89	0.1526	37.70	15.08	0.1448	38.64	15.46	0.1484	40
Hf	0.485	2.31	1.66	0.0112	1.98	1.43	0.0096	1.98	1.43	0.0096	72
Th	0.521	3.71	3.34	0.0193	3.06	2.75	0.0159	4.29	3.86	0.0224	90
U	0.66	0.66	0.61	0.0035	0.76	0.70	0.0040	0.80	0.74	0.0042	92
Y	0.379	1.06	0.41	0.0040	0.96	0.37	0.0036	1.10	0.43	0.0042	39
Ca	0.243	0.49	0.10	0.0012	0.34	0.07	0.0008	1.09	0.22	0.0027	20
Fe	0.300	1.34	0.35	0.0040	1.25	0.33	0.0038	1.37	0.36	0.0041	26
Mn	0.291	0.48	0.12	0.0014	0.47	0.12	0.0014	0.41	0.10	0.0012	25
Si	0.176	12.44	1.74	0.0219	11.94	1.67	0.0210	12.32	1.73	0.0217	14
P	0.189	0.11	0.12	0.0002	0.07	0.01	0.0001	0.10	0.02	0.0002	15
O	0.201	37.67	3.01	0.0757	41.47	3.32	0.0834	37.90	3.03	0.0762	8
ΣOxides		92.61			87.23			92.10			
$\bar{Z}$			27.25			25.85			27.38		
$\bar{\eta}$				0.2951			0.2884			0.2949	
wt.% H_2O	By difference +		7.39			12.77			7.89		
	Calculated *		2.8			2.3			3.1		

+ Calculation of $\bar{Z}$ and $\bar{\eta}$ assumes wt.% H_2O = (100% - sum of oxides)
* Maximum amount of H_2O which can be incorporated in zircon by the substitution $4(OH)^- \rightleftharpoons (SiO_4)^{4-}$ (Calculation in Appendix 4)

Table 50 (continued)

(C) Lower reflectance secondary patches (assuming water is absent)

Analysis No. / Element	η	1			3			5			Z
		Wt%	C Z	C η							
Zr	0.384	38.84	15.54	0.1491	35.71	14.28	0.1371	37.65	15.06	0.1446	40
Hf	0.485	2,29	1.65	0.0111	1.95	1.40	0.0095	1.97	1.42	0.0096	72
Th	0.521	3.65	3.29	0.0190	2.93	2.64	0.0153	4.20	3.78	0.0219	90
U	0.523	0.65	0.60	0.0034	0.73	0.67	0.0038	0.78	0.72	0.0041	92
Y	0.379	1.03	0.40	0.0039	0.91	0.36	0.0034	1.06	0.41	0.0040	39
Ca	0.243	0.49	0.10	0.0012	0.32	0.06	0.0008	1.07	0.21	0.0026	20
Fe	0.300	1.33	0.35	0.0040	1.23	0.32	0.0037	1.35	0.35	0.0041	26
Mn	0.291	0.49	0.12	0.0014	0.45	0.11	0.0013	0.41	0.10	0.0012	25
Si	0.176	12.14	1.70	0.0214	11.26	1.58	0.0200	12.05	1.69	0.0212	14
P	0.189	0.11	0.02	0.0002	0.07	0.01	0.0001	0.10	0.02	0.0002	15
O	0.201	29.59	2.37	0.0595	27.17	2.17	0.0546	29.31	2.34	0.0589	8
ΣOxides		90.61			82.73			89.95			
$\bar{Z}$			26.23			23.60			26.10		
$\bar{\eta}$				0.2742			0.2496			0.2724	

(D) Comparison of % contrast (of total BSE signal) between high and low reflectance patchcs in zircon

Contrast (% of total BSE signal) $\delta = 100[\bar{\eta}(A)-\bar{\eta}(B)]/0.5[\bar{\eta}(A)+\bar{\eta}(B)]$

Analysis No.	2	3+	4	5+	7
1+	6.4	9.4*	7.9	0.7	4.1
2		15.8	1.5	7.1	2.3
3+			17.2	8.7*	13.5
4				8.5	3.8
5+					4.8

* Anomalous result
\+ Lower reflectance patch

Fig. 75 Variation of hypothetical wt. % H_2O in thorite from the Ririwai samples (calculated using method in Appendix 4)

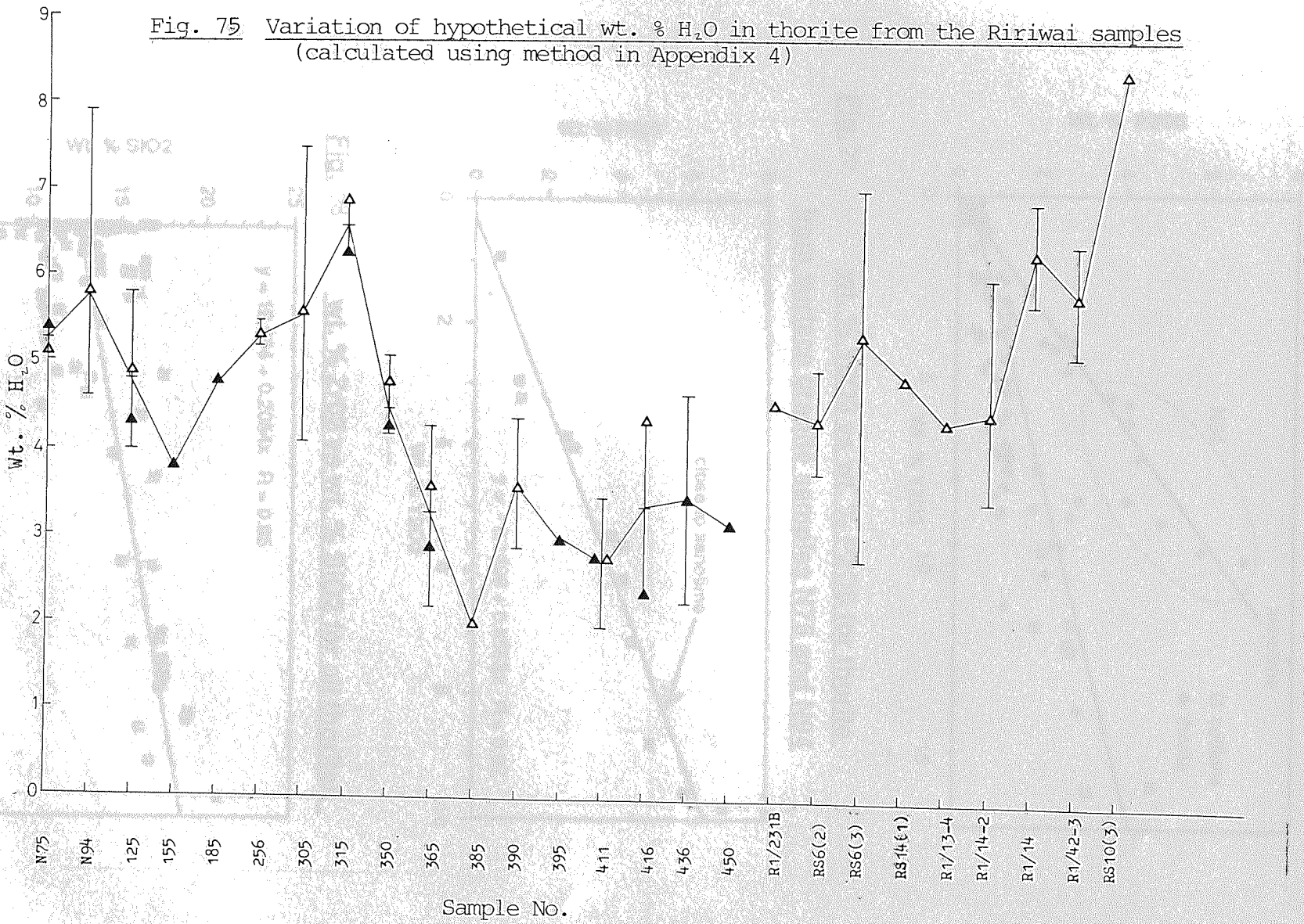

Fig. 76 wt. % Y2O3 vs wt. % P2O5 for all thorite and coffinite

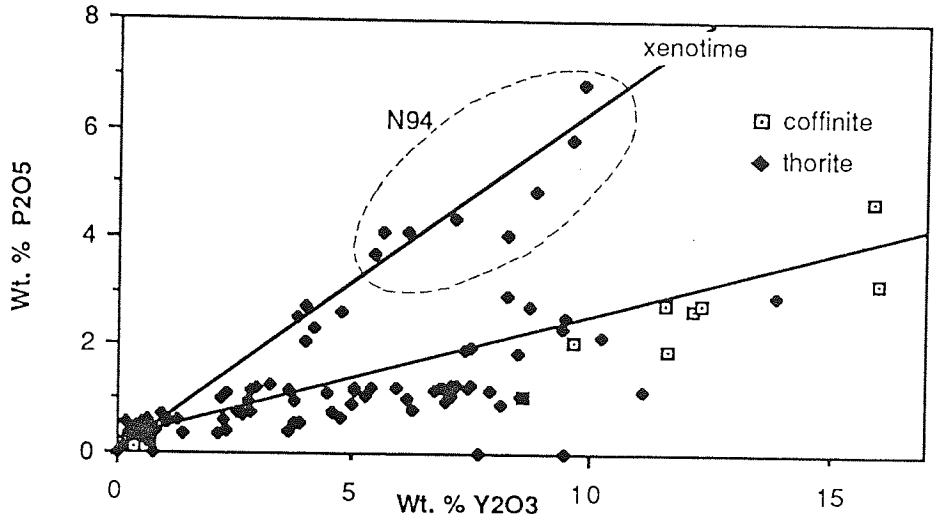

Fig. 77 wt. % Y2O3 vs wt. % P2O5 for thorite from surface granite samples N75 and N94

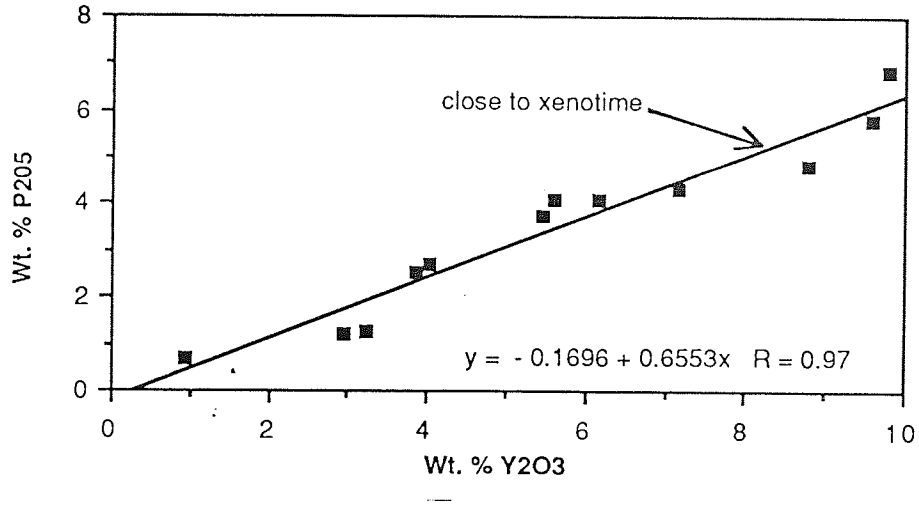

Fig. 78 wt. % ZrO2 vs wt. % SiO2 for all thorites

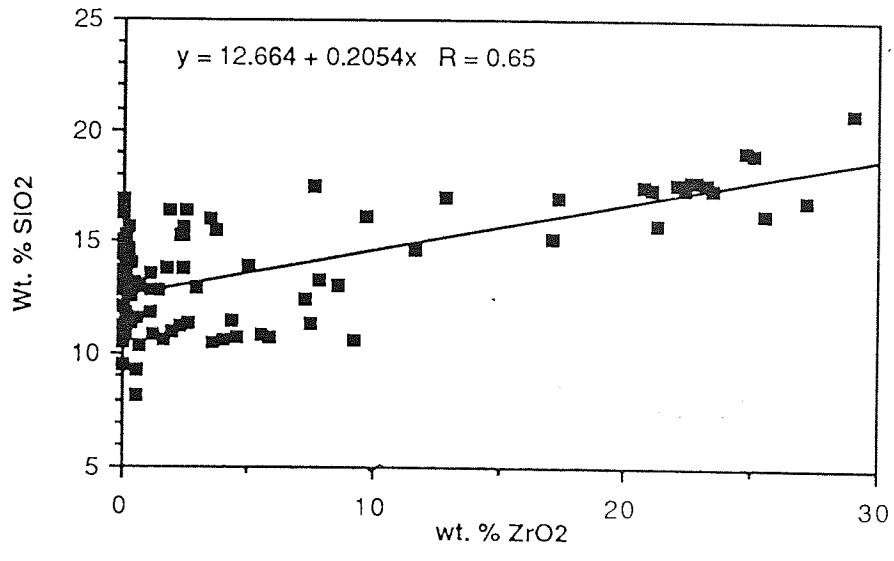

Table 51 Correlation coefficients for elements in thorite from Sample N94 (analyses in Table 31)

	ThO_2	UO_2	Y_2O_3	CaO	ZrO_2	HfO_2	FeO	SiO_2
UO_2	0.658							
Y_2O_3	-0.771	-0.632						
CaO	0.388	0.832	-0.151					
ZrO_2	-0.831	-0.897	0.600	-0.815				
HfO_2	0.025	-0.155	-0.207	-0.368	0.258			
FeO	-0.235	0.017	-0.310	-0.164	0.176	0.310		
SiO_2	-0.053	-0.422	-0.357	-0.806	0.481	0.315	0.403	
P_2O_5	-0.642	-0.517	0.975	0.004	0.441	-0.209	-0.409	-0.508

Table 52 Correlation coefficients for elements in thorite from 305 m depth (analyses in Table 33)

	ThO_2	UO_2	Y_2O_3	CaO	ZrO_2	HfO_2	FeO	SiO_2
UO_2	-0.150							
Y_2O_3	0.125	-0.913						
CaO	-0.462	0.350	-0.007					
ZrO_2	-0.304	-0.828	0.887	0.187				
HfO_2	-0.462	-0.590	0.727	0.436	0.902			
FeO	-0.082	0.889	-0.985	-0.087	-0.917	-0.755		
SiO_2	-0.294	-0.818	0.898	0.212	0.996	0.885	-0.927	
P_2O_5	0.497	-0.883	0.919	-0.238	0.663	0.438	-0.892	0.675

Table 53 Correlation coefficients for elements in thorite from 390 m depth (analyses in Table 40)

	ThO_2	UO_2	Y_2O_3	CaO	FeO	SiO_2
UO_2	0.715					
Y_2O_3	-0.966	-0.854				
CaO	0.823	0.775	-0.806			
FeO	-0.005	-0.597	0.168	-0.284		
SiO_2	-0.368	-0.209	0.377	-0.295	-0.540	
P_2O_5	-0.946	-0.893	0.997	-0.820	0.243	0.350

Table 54 Correlation coefficients for elements in thorite from Sample R1/42-3 (analyses in Table 48)

	ThO_2	UO_2	Y_2O_3	CaO	FeO	SiO_2
UO_2	-0.975					
Y_2O_3	-0.851	0.806				
CaO	0.810	-0.832	-0.903			
FeO	0.361	-0.392	-0.747	0.664		
SiO_2	0.299	-0.347	-0.241	0.009	0.371	
P_2O_5	-0.452	0.329	0.799	-0.518	-0.746	-0.236

Table 55 Hypothetical wt. % H_2O calculated for coffinite analyses in Table 37 using the formula $U(SiO_4)_{1-x}(OH)_{4x}$ (see Appendix 4)

Sample	100				
Grain	3			4	
An. Spot	1	2	3	1	2
Oxide Total	94.16	94.31	97.84	91.23	90.57
Wt. % H_2O	3.0	1.4	2.9	2.8	3.0
Sample	RS6(4)				
Grain	1				
An. Spot	1a	2	4	6a	7
Oxide Total	84.08	90.15	84.30	87.35	88.61
Wt. % H_2O	3.3	4.1	3.8	4.2	3.3

Table 56 Compositions (wt.%) of co-existing xenotime-zircon-thorite in the albitite (450 m depth)

	ZrO_2	Y_2O_3	ThO_2
Zircon host		1.02	0.56
Thorite inclusions	0.85*	5-6*	
Xenotime inclusions	nd		0.21*

* semi-quantitative analyses
nd not detected

Fig.79 Mole % Zr+Hf, Y and Th+U for zircon from the Ririwai biotite granite and its altered facies

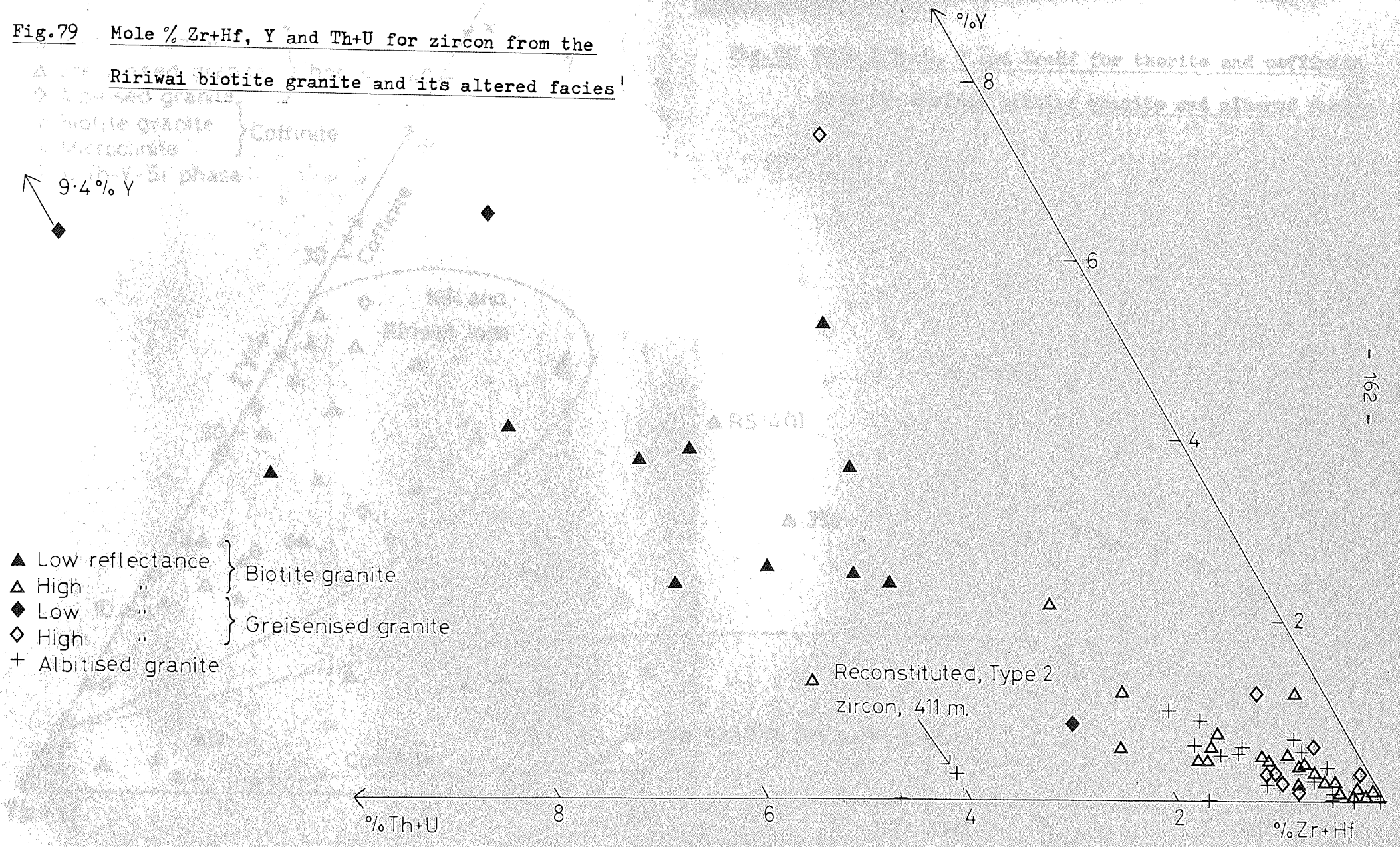

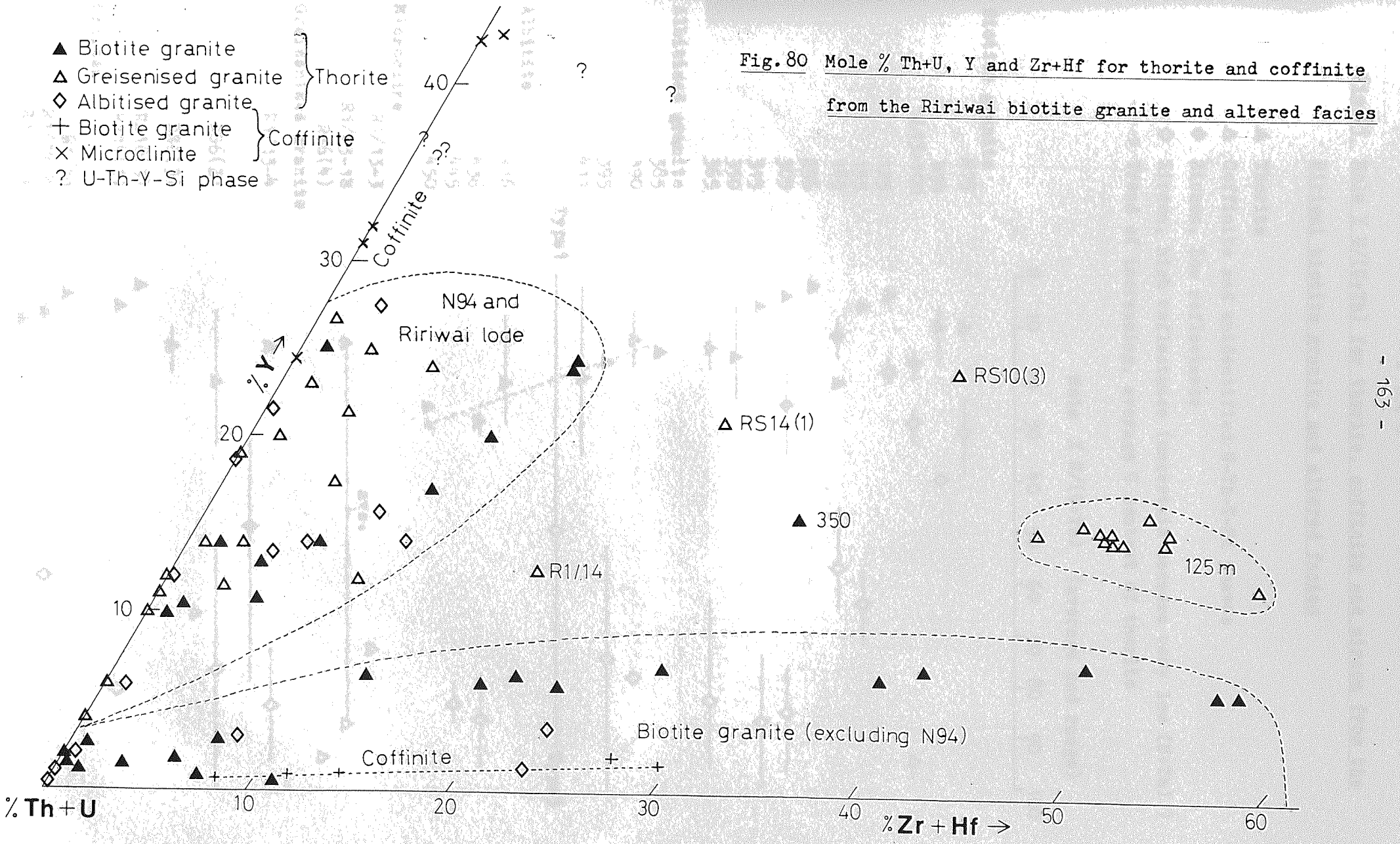

Fig. 80 Mole % Th+U, Y and Zr+Hf for thorite and coffinite from the Ririwai biotite granite and altered facies

Fig.81 Mole % U/(U+Th) for thorite, coffinite and zircon from the Ririwai biotite granite and altered facies

▲ Thorite

△ Coffinite and unidentified U-Th-Y-Si phases

◆ Zircon, low reflectance

◇ Zircon, high reflectance (uncertain because very low (U+Th))

----> Trend of increasing, average U content of thorite

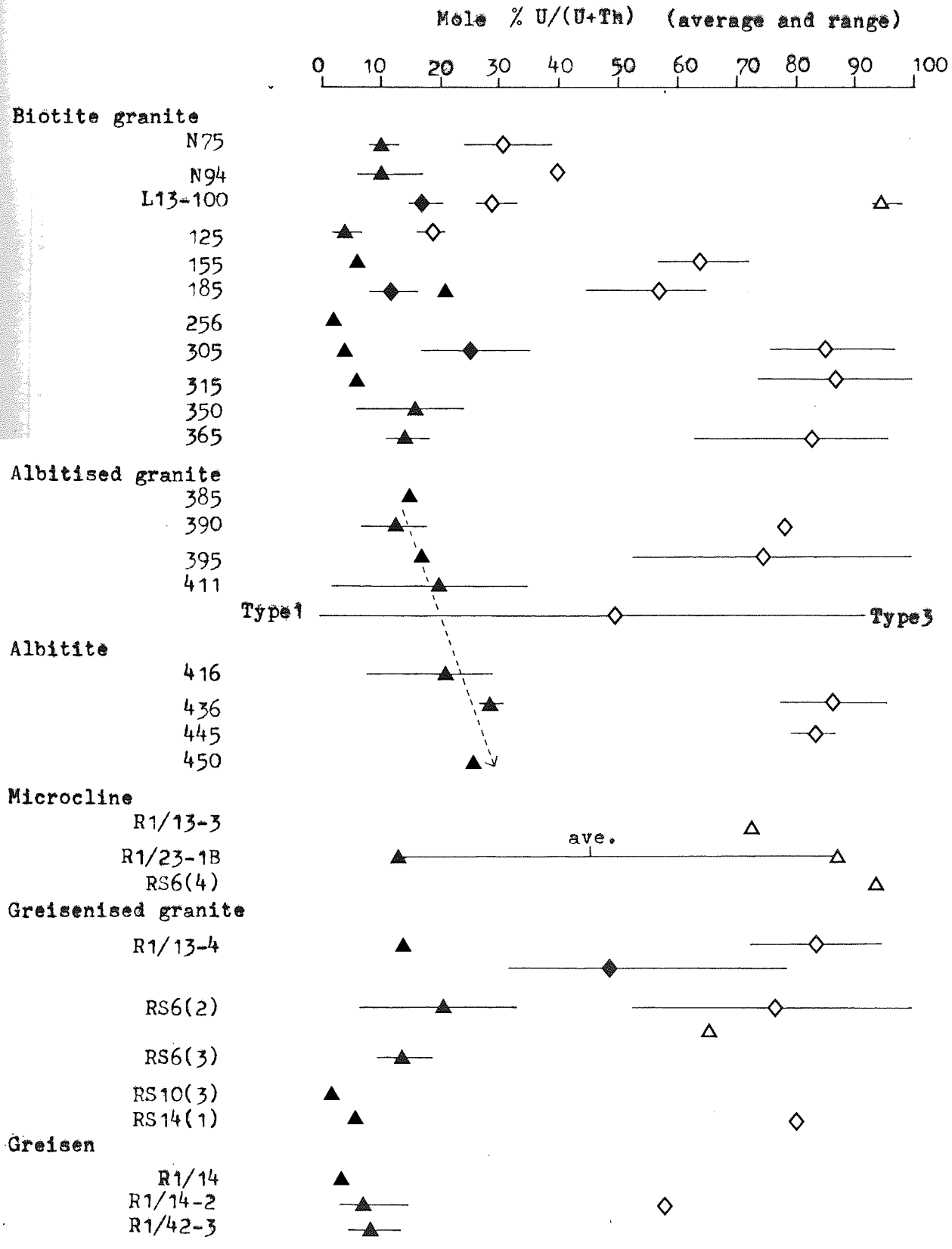

Table 57 Bulk rock analyses for U and Th of rocks from Ririwai

Sample No.	Description	U ppm	Th ppm	Th/U
N77	Biotite granite (surface)	7.5	41-62	5.5
N91	"	7.3	50-78	6.8
N92	"	8.0	62-73	7.8
*N75	"	10.0	83-111	8.3
*N94	"	-	71	-
N79	"	-	73	-
L13-10 m	Biotite granite (borehole)	30	25	0.83
L13-115 m	"	80	72	0.90
*L13-205 m	"	53	51	0.96
L13-310 m	"	58	56	0.97
*L13-411 m	"	81	73	0.90
*L13-440 m	"	66	69	1.05
R1-18	Red microclinite-quartz wallrock adjacent to lode from 30 m depth	12.8	41.7	3.25
R1-35	"	10.2	38.8	3.80
R1-40	"		(17-87)	
	(from 13 analyses)			
*R1-14	Greisen vein from 30 m depth	18.9	97.5	5.16
R1-40	"		(43-191)	
	(from 6 analyses)			

Data from Kinnaird et al. (1985b) and Mackenzie et al. (1984) in parenthesis

* Samples used in this study

Table 58 Bulk rock analyses for selected elements of surface and borehole granite samples from Ririwai (see Kinnaird et al., 1985b for full analyses)

	N75	N94	10m	26m	115m	145m	205m	256m	315m	411m	440m
Fe_2O_3	0.33	0.43	0.42	0.66	0.36	0.37	0.38	0.54	0.41	0.51	0.78
FeO	1.05	1.07	1.15	1.09	1.23	1.47	1.67	2.03	1.11	1.48	1.54
CaO	0.24	0.26	0.49	0.48	0.57	0.46	0.77	0.59	0.40	0.52	0.42
F	0.36	0.42	0.32	0.21	0.22	0.23	0.23	0.39	0.17	0.26	0.32
Li	391	278	336	250	1482	619	761	852	585	30	34
Y	696	147	127	109	134	147	144	146	129	51	56
La	234	53	-	-	-	-	-	-	-	-	-
Ce	296	149	-	-	-	-	-	-	-	-	-
Zr	399	255	233	68	413	284	343	286	602	285	309
Hf	28	14	-	-	-	-	-	-	-	-	-
Th	111	71	25	-	72	-	51	-	-	73	69

All samples are used in this study except for 10, 26 and 115m.

Table 59 A comparison of selected accessory minerals from the Taghouaji and Ririwai complexes

MINERAL	TAGHOUAJI	RIRIWAI
Zircon	1 Two main types in the amphibole and biotite granites: a Clear, anisotropic, poor in U and Th. Included in amphibole or biotite. Crystallised late from a fluid-rich, Th- and U-depleted melt. b Brown-grey, rich in inclusions (including thorite), large, corroded, high Th, U and Y, metamict. Included in feldspar and quartz. 2 Replaced by veinlets of hydrated ZrO_2 and silica.	1 Three main types in the albitised rocks. The first two are also found in certain samples of biotite granite: a Type 1 Forms clear, finely-zoned rims to Type 2. High Hf, low U and Th. Metasomatic origin. b Type 2 Rich in haematite and thorite inclusions. Anisotropic, lower U and Th than Type 3. ± high Hf. Metasomatic origin. c Type 3 Clear, metamict, high U. Forms cores in concentrically zoned grains. Metasomatic origin. All three types are typically intergrown as interstitial grains. 2 Replaced by metamict, trace-element enriched zircon and by fluorite and plagioclase.
Xeno-time	Rare. Associated with zircon in amphibole and albitic biotite granites and albitite.	As Taghouaji. In albitised and greisenised rocks.
Thorite	1 Associated with zircon as inclusions and overgrowths. Discrete, euhedral grains interstitial to or included in essential minerals. 2 Associated with iron-oxide. 3 Often compositionally impure with high but variable concentrations of Y, Zr, La and P(Table 6, Chapter 2) 4 Highest Y (11.4% Y_2O_3) from perthitic biotite granite Very low Y in greisen. 5 Highest Zr (9.55 wt% ZrO_2) from the perthitic biotite granite but also high (7-8 wt% ZrO_2) in the albitic biotite granite.	1 As Taghouaji, but anhedral. 2 As Taghouaji. 3 As Taghouaji, but with Y, Zr, P and U. 4 Highest Y (10.23 wt% Y_2O_3) generally associated with greisenised rocks but also high in a biotite granite sample. 5 Highest Zr in biotite granite and one sample of greisenised granite (27.1 wt% and 28.99 wt% ZrO_2 resp.) Albitite has very low Zr.

Table 59 (continued)

MINERAL	TAGHOUAJI	RIRIWAI
Thorite	6 Highest U (11.33wt% UO_2) in perthitic biotite granite Very low U (below detection) in the albitic biotite microgranite. 7 Wide scatter in concentrations of U, probably due to its leaching from thorite. 8 Depletion of U and Si in the core of an optically zoned zircon. 9 Positive correlation of U with Y and Zr. 10 Positive correlation between U content of thorite and the bulk U content of the host rock.	6 Highest U (28.92 wt% UO_2) in albitised granite. Complete solid solution of $USiO_4$-$ThSiO_4$ in microclinite. 7 As Taghouaji. 8 Depletion of U in the rim of a thorite. 9 Very little correlation between U and Y or Zr. 10 Not enough bulk U data to be certain of a correlation with U content in thorite, but the available data do not indicate a correlation.
LREE-phase	1 Small inclusions of Th-bearing fluocerite in fluorite ,particularly in the biotite granite. 2 Replacement of monazite by fluocerite in amphibole and biotite granites. 3 Solid solution among bastnaesite-group minerals and fluocerite, with very high Y, Th, and Si in some grains from amphibole and pyroxene granites, but not in the greisen. 4 Very low in U.	1 As Taghouaji, but bastnaesite/fluocerite? 2 As above. 3 Variable and locally very high Ca, Th, Y, Pb and Si in complex LREE-phases in greisenised and microclinised rocks only. 4 As Taghouaji.

Table 60 Summary of mineralogical and geochemical changes during subsolidus alteration of granitoids from south-east Massif Central
(modified from Table 1 in Cathelineau, 1987)

Location	Les Pierres Plantées-Margeride.	Les Bombes-Mt. Lozère Massif	St. Chely-Vareille-Margeride
Altered rock	Grandrieu peraluminous granite. Margeride monzogranite.	Bouges peraluminous granite.	St. Chely peraluminous granite.
Alteration	Quartz leaching (dominant). (Type I)	Quartz leaching and strong albitisation. (Type IIA)	Quartz leaching and albite-chlorite alteration. (Type IIB)
Accessory minerals: Stable	Monazite, zircon, apatite.	Monazite, zircon, apatite.	Apatite.
Unstable	Some monazite recrystallisation.		Monazite, zircon, sphene.
Authigenic	Anatase.	Haematite, anatase. Numerous complexes in the system ZrO_2-P_2O_5-UO_2-ThO_2-CaO-SiO_2-Y_2O_3 including; P-Y-Ca-rich uranothorite (in Table 6, Chapter 2), U-Th-REE-Y-rich zirconosilicate rims on zircon, xenotime overgrowths on thorite, apatite.	Apatite, anatase.
Geochemical changes: Depletion	Si, Fe^{2+}, (LREE).	K, Ba, Mg, Rb, Fe^{2+}.	Si, K, Mg, Fe^{2+}, Rb, LREE, U, Th.
Enrichment	Fe^{3+}, (K, Li, CO_3, Ba, Sr, F).	Na, HREE, U, Th, Y, P.	Na, Fe^{3+}.

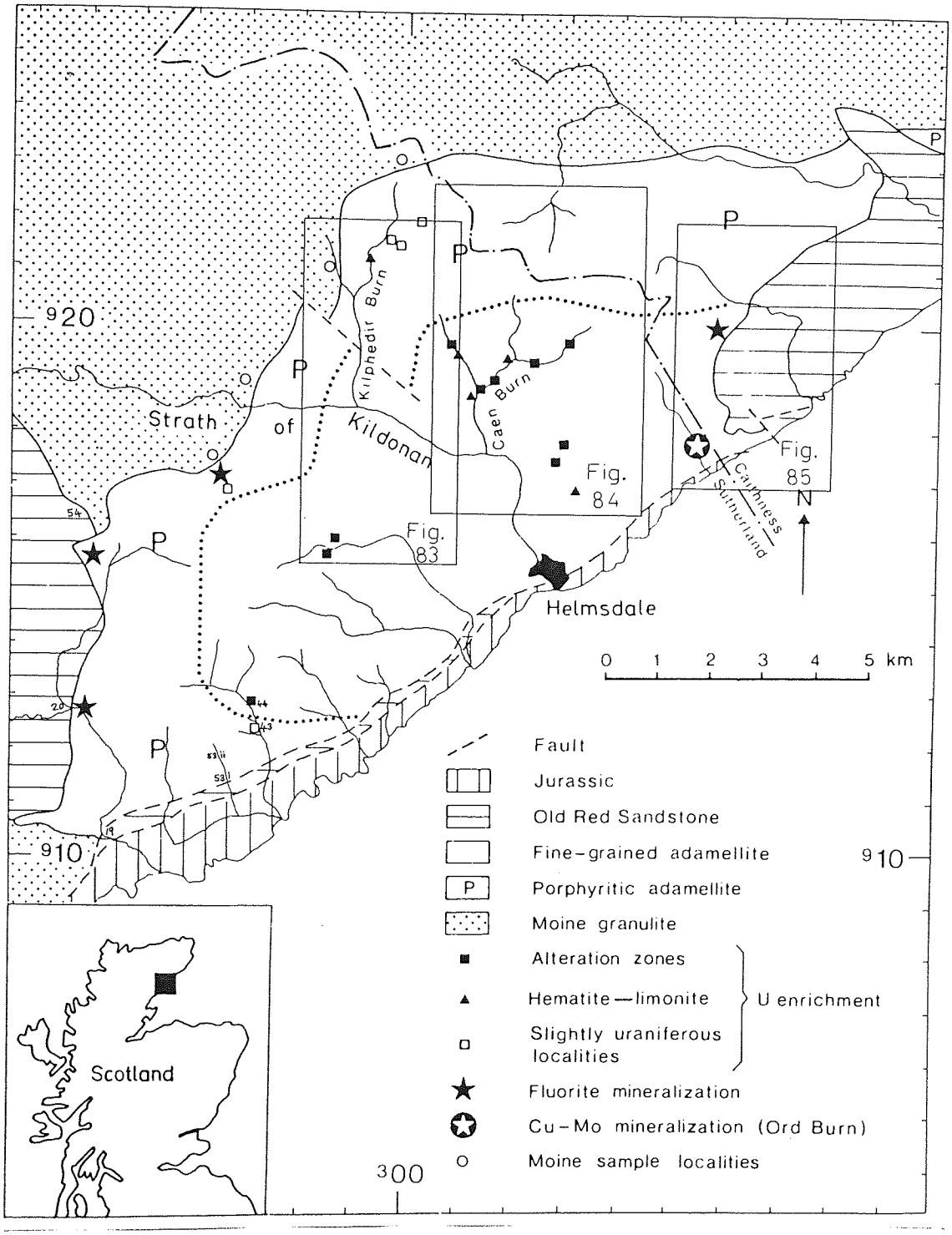

Fig. 82 Geology of the Helmsdale granite and associated mineralisation, showing sample localities and the areas covered by Figs. 83-85 (modified after Tweedie, 1979)

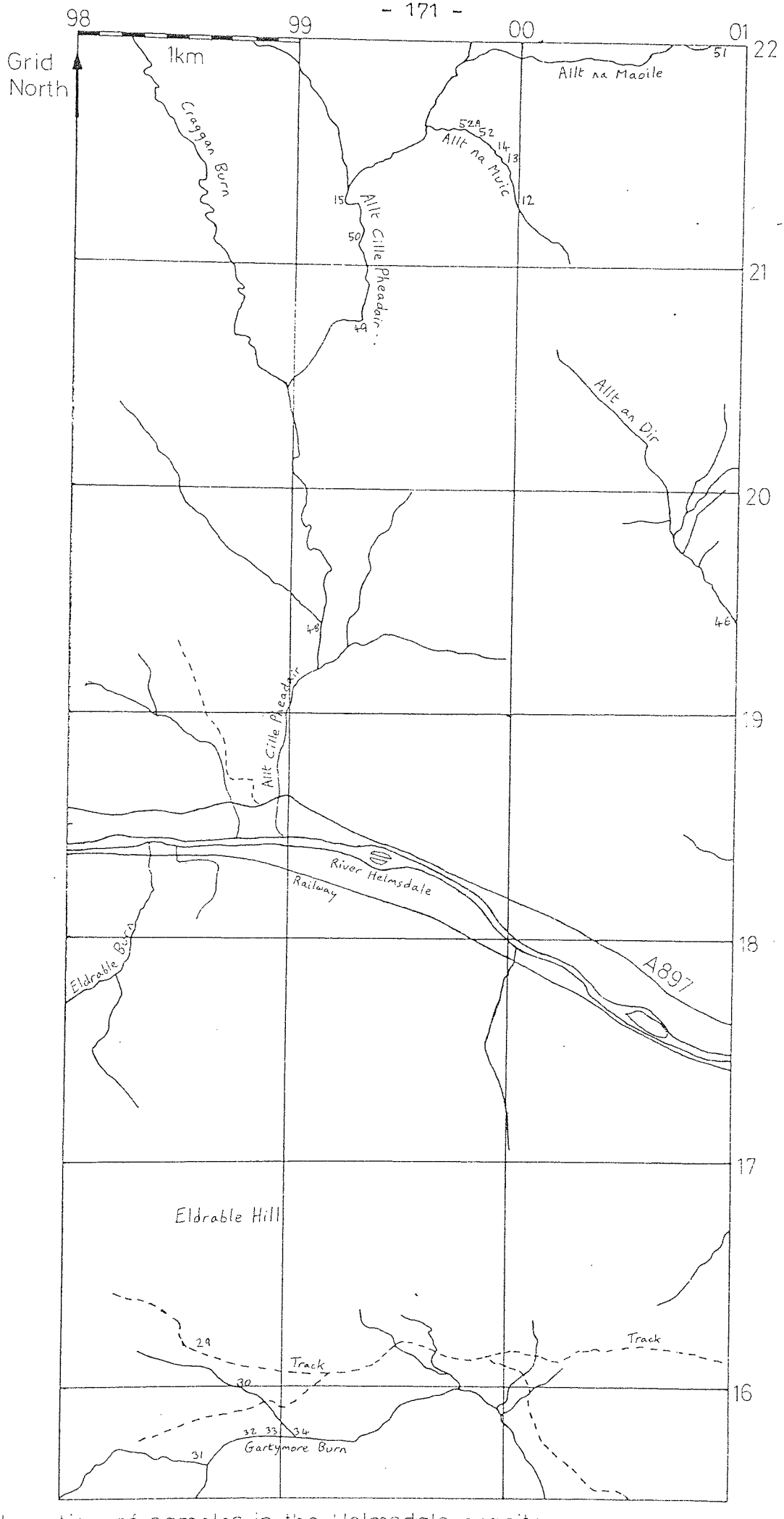

Fig. 83 Location of samples in the Helmsdale granite
(Map redrawn from OS 1:25 000 sheets NC 81/91 and NC 82/92)

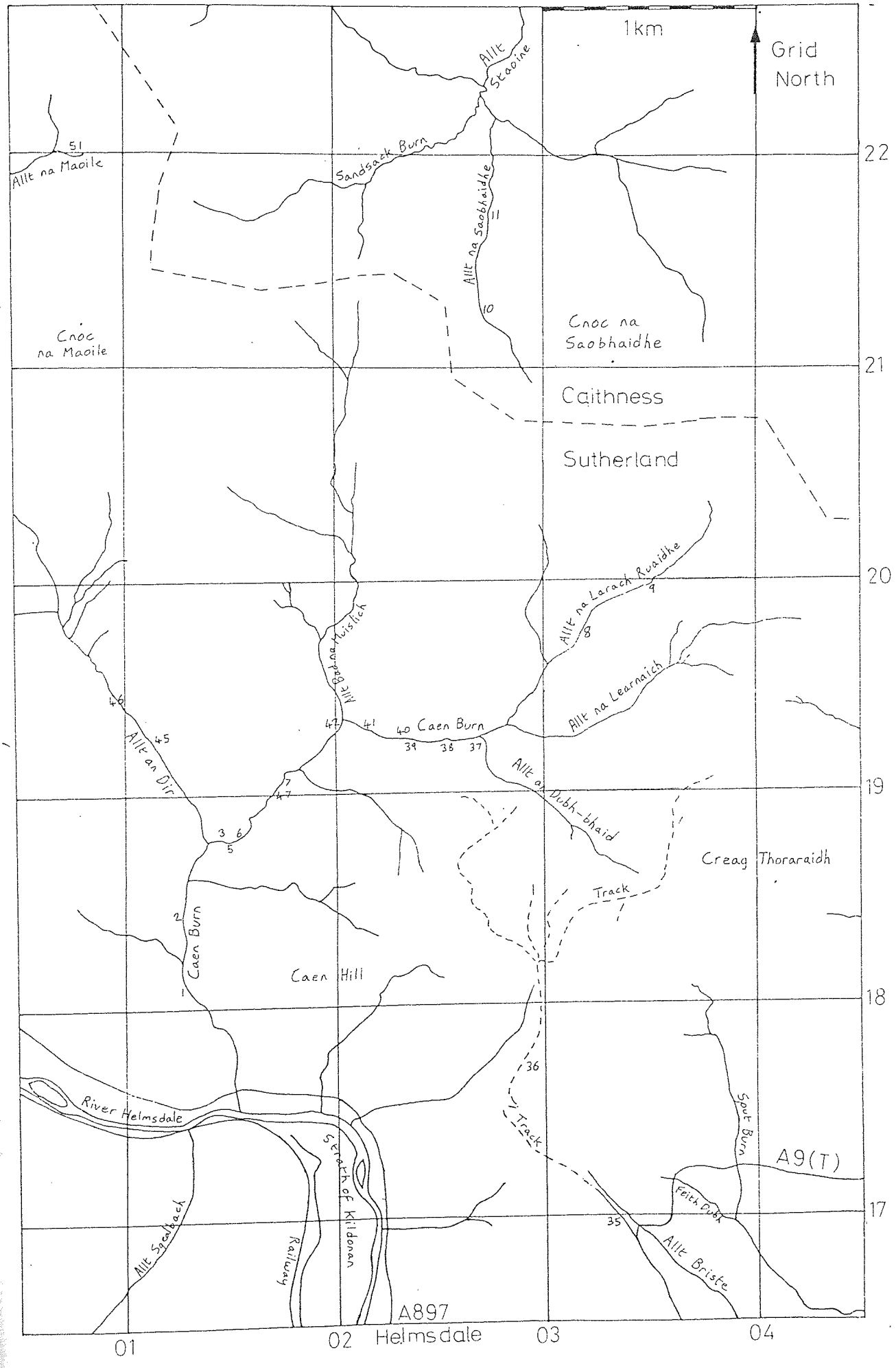

Fig.84 Location of samples in the Helmsdale granite

(Map redrawn from OS 1:25 000 sheets ND 02/12 and ND 01)

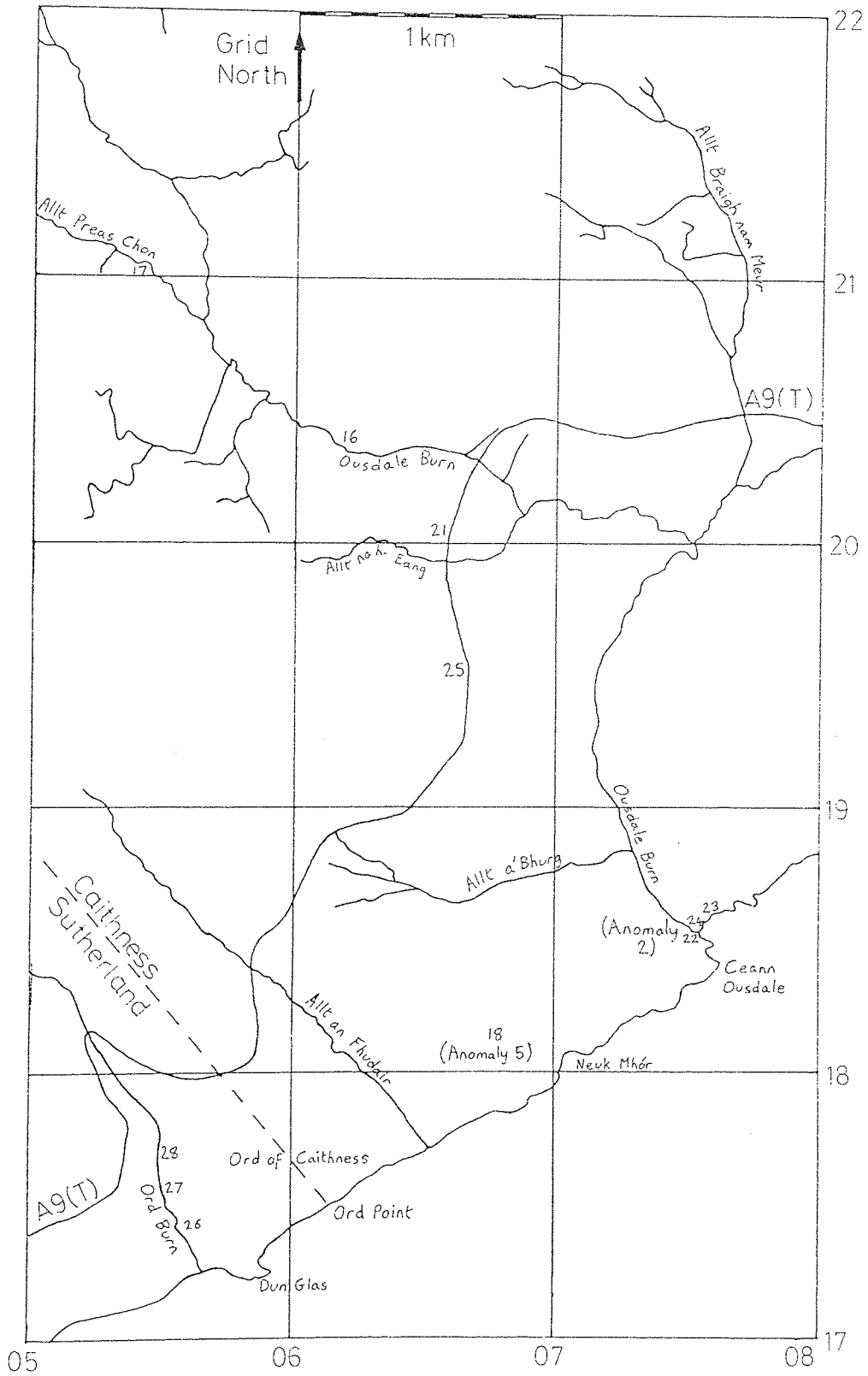

Fig. 85 Location of samples in Helmsdale granite and Ousdale arkose

(Map redrawn from OS 1:25 000 sheets ND 01 and ND 02/12)

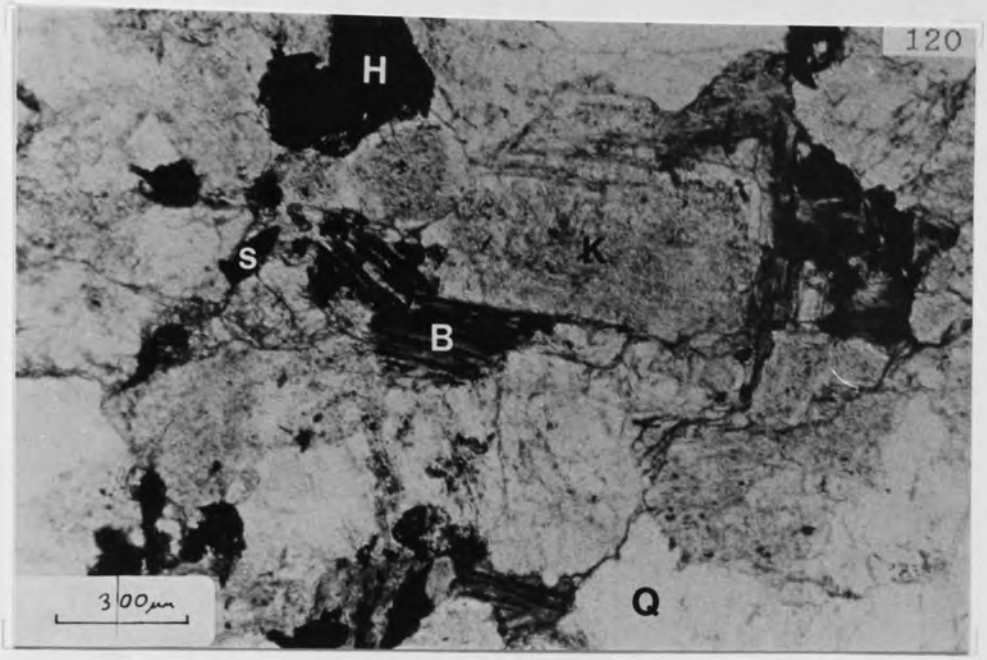

Helmsdale granite from 8 m depth in Borehole 3 (Creag Thoraraidh). K-feldspar (K), quartz (Q), altered biotite (B), haematite (H) and TiO_2 pseudomorph after sphene (S).
(TPPL)

The same area as Plate 120 .
(TXPL)

Table 61 Compilation of bulk U and Th data for the Helmsdale granite and common world granites

U ppm			Th ppm		No. of Samples	Description	Reference
Mean	Range	SD	Mean	Range			
9	1-18		21	5-37	82	Least altered	Tweedie (1979)
25	7-71		23	9-47	10	Potassic alteration zone	"
35	22-52		25	20-32	5	Haematised and limonite-stained	"
8	6-11		23	13-37	13	Cu-Mo mineralisation (Ord Burn)	"
	5.7-9.0				3	Partially altered, fine-grained	Bowie et al. (1973)
6.3	5.0-7.5				2	" porphyritic	"
3.5					1	" intermediate	"
13.6					1	Strongly altered, fine-grained	"
	10.7-18.3				4	" porphyritic	"
7.0		1.56			30	Least altered	Simpson et al. (1976)
7.54	3.6-18.1	3.61			29	"	Simpson et al. (1979)
5	2-8		21	8-33		Common world granites	Rogers and Adams (1969)

Table 62 Bulk rock U and Th data for the Helmsdale granite and Ousdale arkose

Sample Type	Sample No.(1)	Sample Description	Locality	CPS (2)	U ppm (3)	Th ppm (3)	Th/U
Least Altered	H414	Relatively fresh granite	Creag Thoraraidh, BH.4, 9m depth	-	2.8	26	9.29
	7F	1 m from alteration zone	Caen Burn	140	18	27	1.50
	35	Limonite-coated fractures	Track to Creag Thoraraidh	115	6.3	22	3.49
Reddened	13A	Very fractured and reddened	Caen Burn	180	16	39	2.44
	28A	Very reddened	Ord Burn	400	220	21	0.10
Wallrock to Alteration Zone	5B	Pinkish with green flecks	Caen Burn	200	20	25	1.25
	7D	Fractured, limonite-stained, friable	Caen Burn	300	19	29	1.53
	28C	Reddened	Ord Burn	900	14	20	1.43
	46A	Fractured and reddened	Allt an Dir	350	20	25	1.25
	53B	Pale greenish, limonite-stained	Allteenie Burn	180	12	50	4.17
	5A	Friable, green and limonite-stained	Caen Burn	140	13	26	2.00
Alteration Zone	7A	Dark-brown, soft clay zone 20 cm wide	Caen Burn	700	510	17	0.03
	28E	Yellow, sandy with clay & hydrocarbon	Ord Burn	>1000	650	8.1	0.01
	46B	Sandy	Allt an Dir	400	83	32	0.39
	53A	Limonite-stained, sandy	Allteenie Burn	230	11	44	4.00
	39B	Minor fault gauge	Caen Burn	190	62	29	0.47
Arkose	18D	Uranyl phosphate mineralisation	Anomaly 5, Ousdale	1700	1400	19	0.01
	22C	Coffinite mineralisation	Anomaly 2, Ousdale Burn	1200	310	24	0.08
	20A	Fluorite-rich	A9 Road-cutting, Ousdale	70	5.4	29	5.37
	21	Minor fluorite	Glen Loth	100	5.4	26	4.81

(1) See Figs. 82-85 and 87 for sample locations.
(2) Counts per second for exposure, using hand-held gamma scintillometer (background for granite = 70-90 cps).
(3) From instrumental neutron activation analysis. Values rounded to 2 significant figures.

Plate 122 Alteration zone of sericitised and haematised granite.
Track to Creag Thoraraidh, Location 36.

Plate 123 Alteration with U enrichment along a minor fault in the granite (bottom left to top right).
Location 39, Caen Burn.

Plate 124 Fractured and reddened, radioactive granite, giving 181 cps. Location 42, Caen Burn.

Plate 125 Reddened, porphyritic granite from Allt na Muic (Location 12)

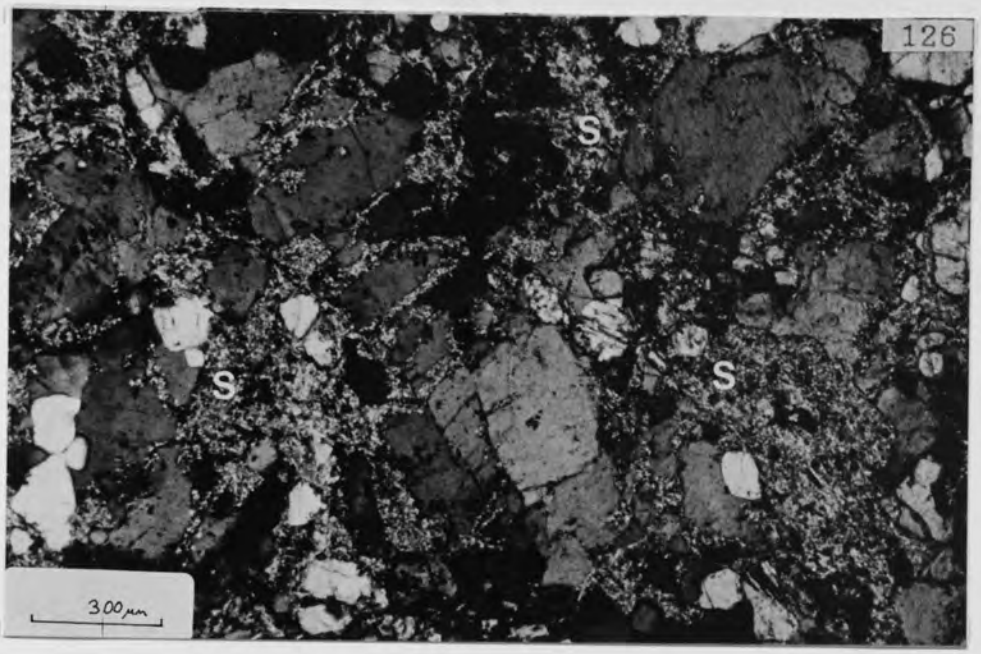

Photomicrograph of an alteration zone at Caen Burn (Location 47). Abundant sericite (S) replaces the feldspar .
(TXPL)

Plate 127 Radioactive, clay-filled alteration zone in the granite at Caen Burn (Location 7).

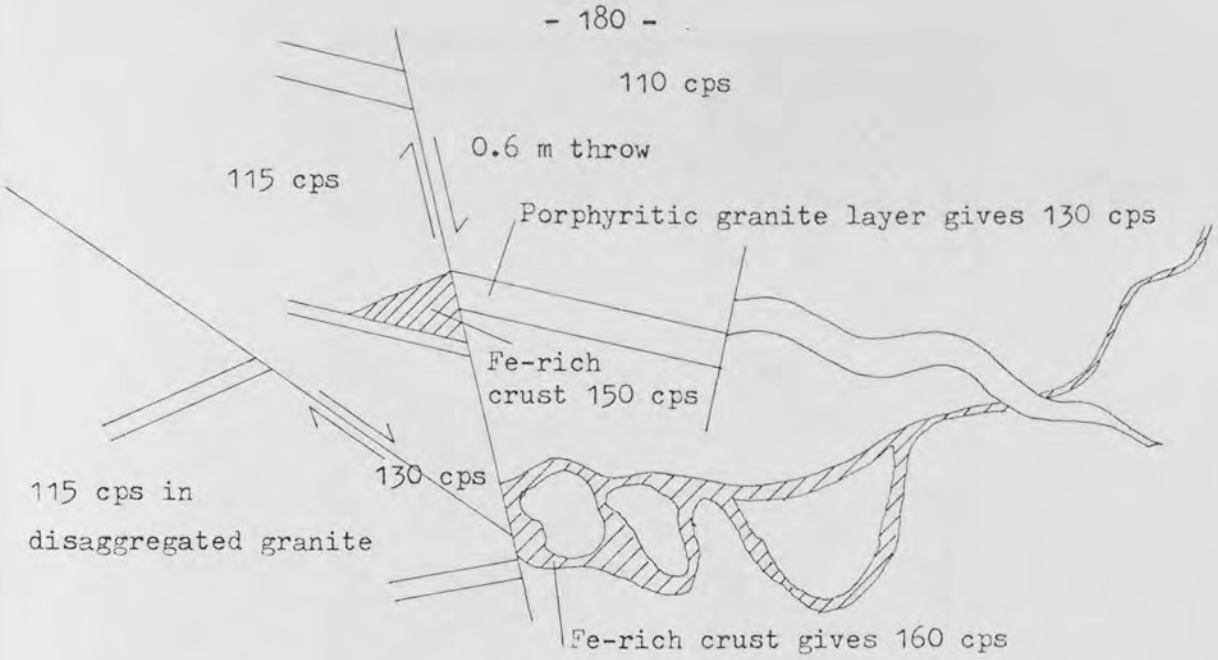

Fig. 86 Minor faulting in a 2 m high exposure of disaggregated porphyritic granite, Allt Cille Pheadair (Location 50). Higher counts are associated with Fe-oxide crusts, faults and residual granite layers.

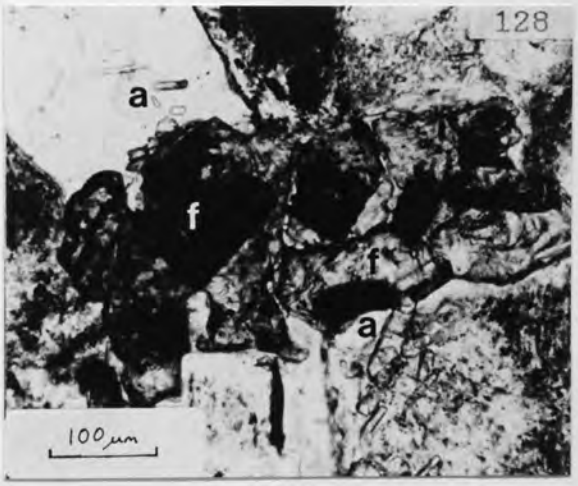

Fluorite with dark-purple cores (f). Apatite crystals (a) are included in quartz and the matrix. Arkose, BH.2,1.9m.

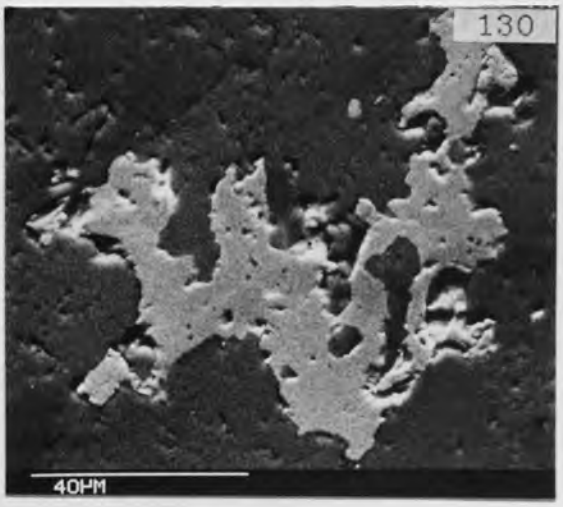

Interstitial baryte. Arkose, BH.1, 5.5 m depth. (SEM)

Interstitial calcite (c) infilling the cleavage in K-feldspar. Arkose, BH.2, 9.8 m depth. (TXPL)

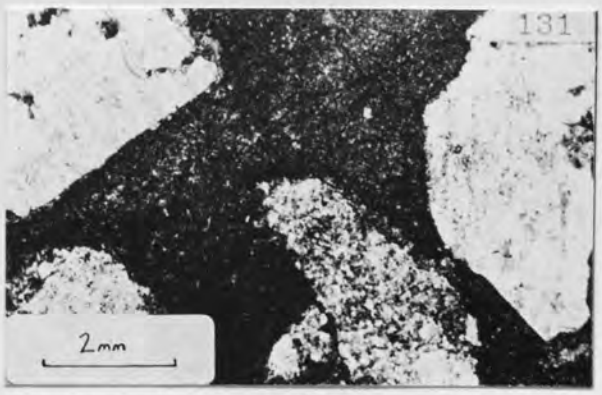

Interstitial, purple fluorite in the arkose, A9 road-cutting (Loc. 21). (TPPL)

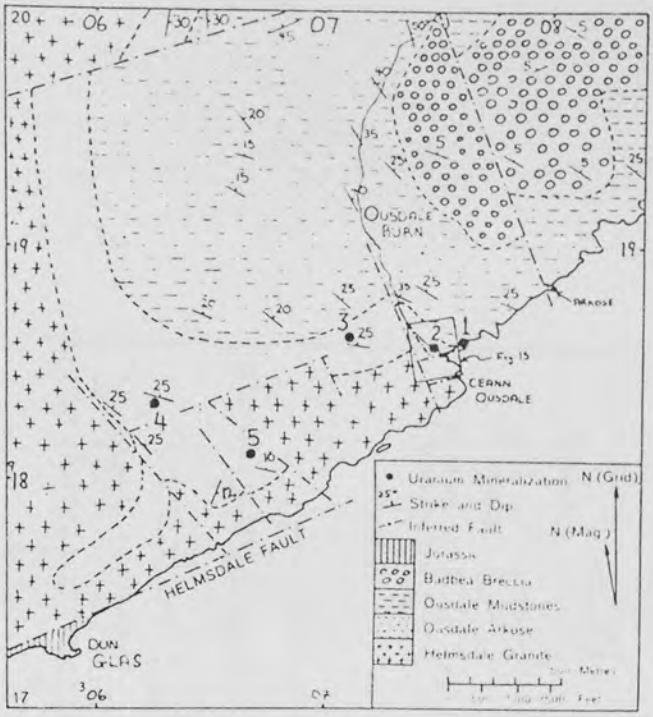

Fig. 87 General geology of Ousdale area, southern Caithness, showing principal exposures of uranium mineralization in ORS (see Figs. 82 and 85 for location) (after Gallagher et al., 1971)

Plate 132 Site of Borehole 1 (BH) in the arkose above a coastal waterfall, Ousdale Burn.
(Anomaly 2)

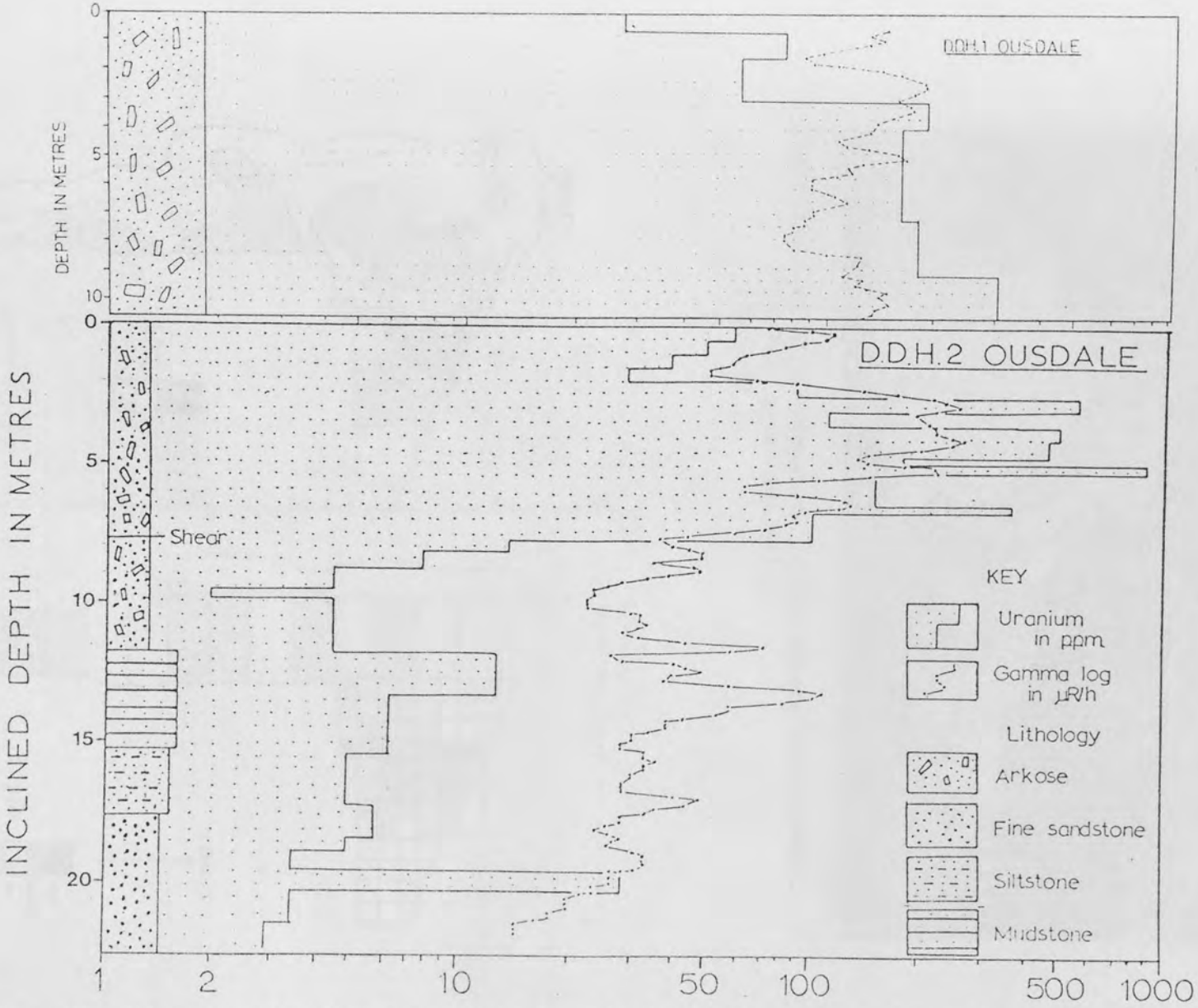

Fig. 88 Diamond drill holes 1 and 2 in Anomaly 2, Ousdale Burn (after Gallagher et al., 1971)

Plate 133 Site of excavation in the mineralised arkose, Ousdale area (see below) (Anomaly 5)

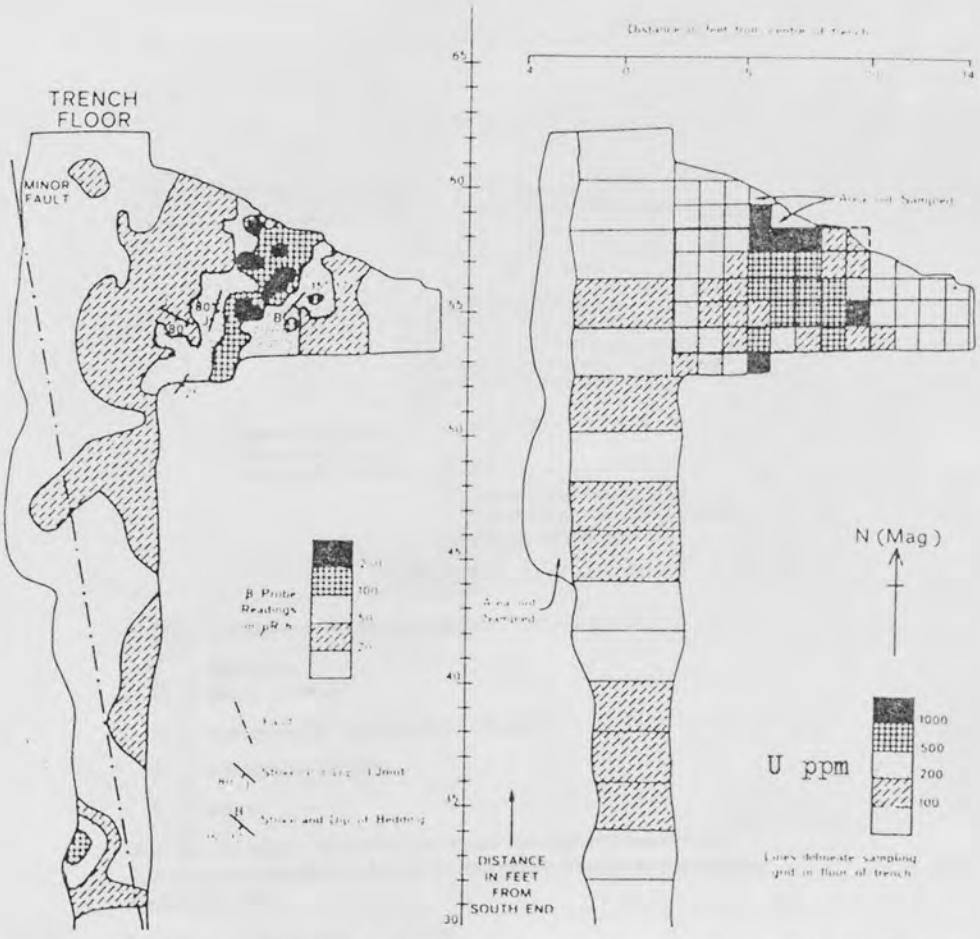

Fig. 89 Geology, radiometry and uranium content of uranium mineralization in weathered Ousdale arkose beneath trenched overburden (see Fig. 87 for location) (after Gallagher et al., 1971)

Plate 134 Joint coatings of secondary uranyl minerals in Ousdale arkose from Anomaly 5.

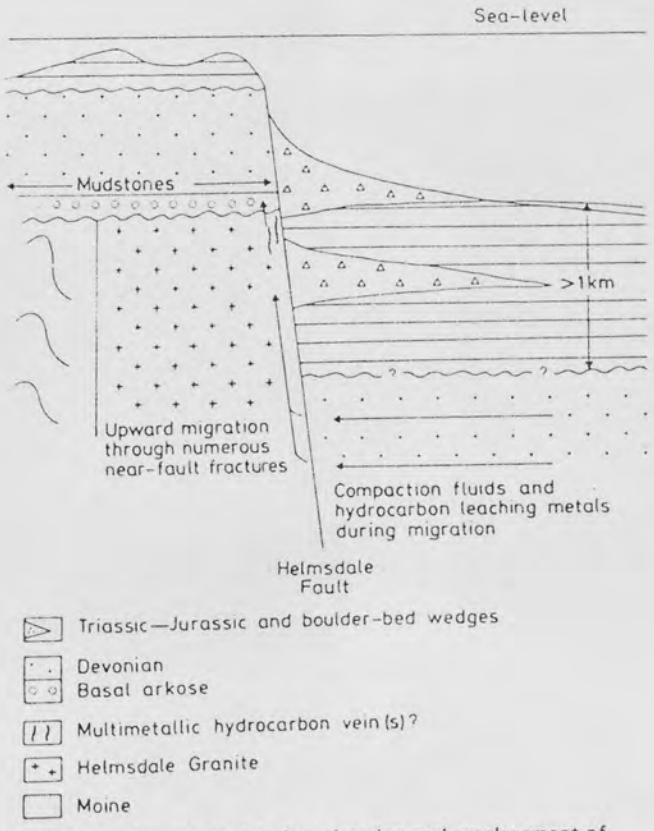

Fig. 90 Possible mechanism for migration and emplacement of metals and hydrocarbon found in Helmsdale Granite and overlying Ousdale arkose.

(after Tweedie, 1979)

Plate No.	Sample No.	Grain No.	Description
			Ousdale Arkose
135	478A		Zircon with complex zoning which is truncated by the grain boundary. BH.2, 2.4 m depth. (RPPL)
136	478A		Zircon with concentric zoning which is truncated by the grain boundary. There is a second nucleus of zoning (A). BH.2, 2.4 m depth. (RPPL)
137	480A	17	Concentrically-zoned zircon (2) with larger, outer zone /overgrowth (1). ED analysis spots are shown. BH.2, 2.9 m depth. (SEM)
138	771		Zoned zircon (centre) included in hydrocarbon, together with TiO_2 (white). BH.2, 5 m depth. (ROIL)
139	491		Zoned zircon. Surface Anomaly 5. (SEM)
140	491		X-ray map of the same zircon showing distribution of U, which appears to be unevenly concentrated in the outer zones.

Fig. No.	Sample No.	Grain No.	Description
91	802	1	Location of full analyses in zircon (see Table 63A).
92	777	1	Location of partial analyses in zircon (see Table 63B).
93	777	2	As Fig. 92.

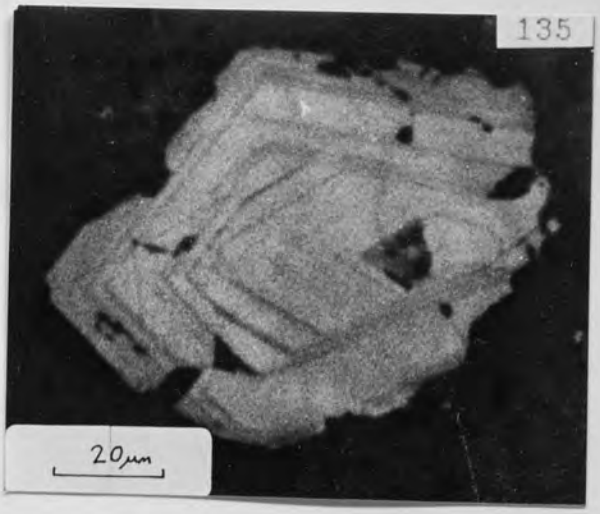

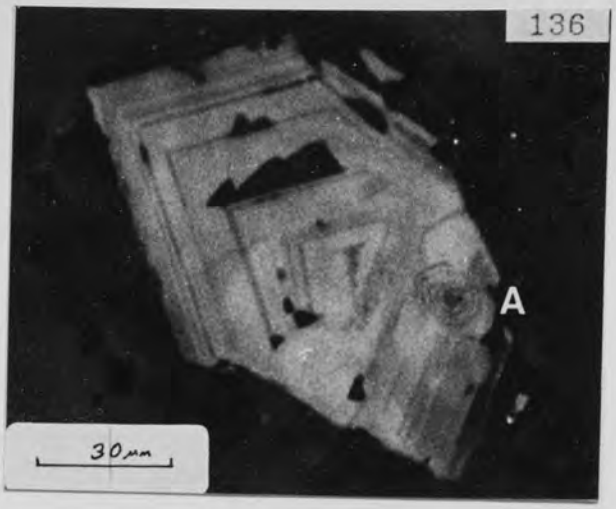

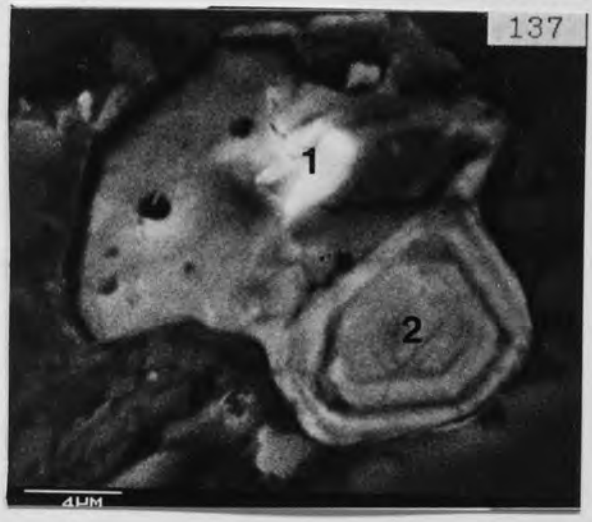

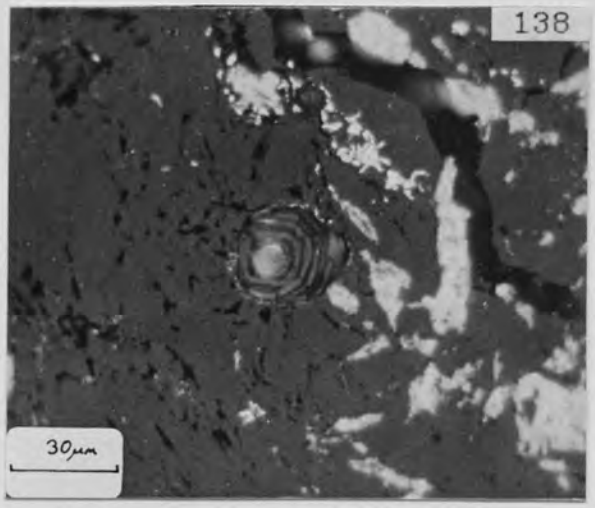

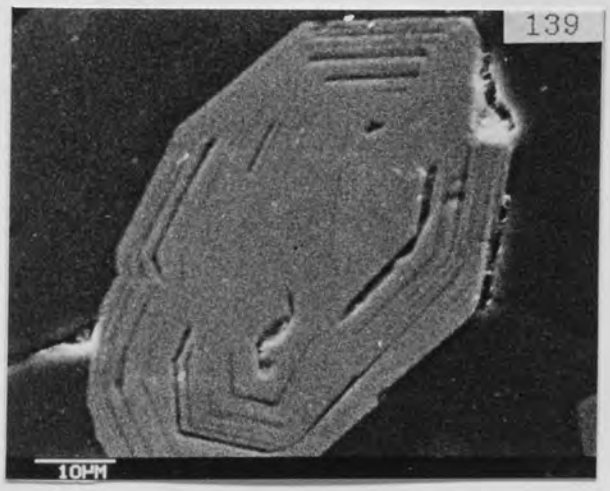

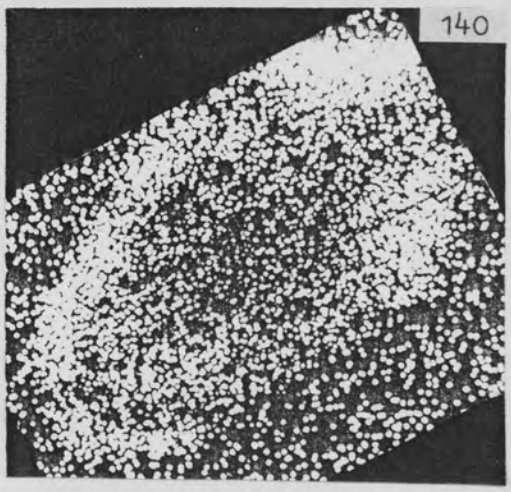

Fig. 91

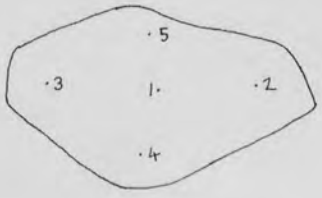

Fig. 92

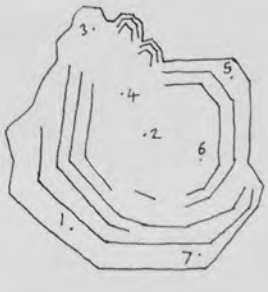

Fig. 93

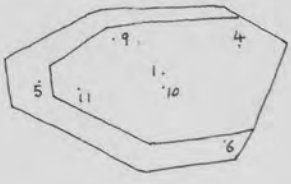

ED spectra of zircon and coffinite

Fig. No.	Sample No.	Grain No.	An. Spot	Description	Loc-ation	Plate No.
94	476A	10	11	15 µm diameter zircon included in haematite replacement of pyrite.	BH.2, 1.7 m	
95	491	1		Outer, U-enriched zone of a 70 µm long zircon.	Anom. 5	139 140
96	480A	17	1	Outer, U-enriched zone of a 20 µm diameter zircon.	BH.2 2.9 m	137
97	"	"	2	Zircon core.	"	"
98	802	10	14	Coffinite replacing TiO_2 needles.	BH.1, 5.5 m	152 153
99	802	15	6	Coffinite inclusion in TiO_2	"	
100	"	13	1	Coffinite/uraninite?	"	148
101	771	18	2	Coffinite/Cu-sulphide admixture	BH.2 5 m	

94

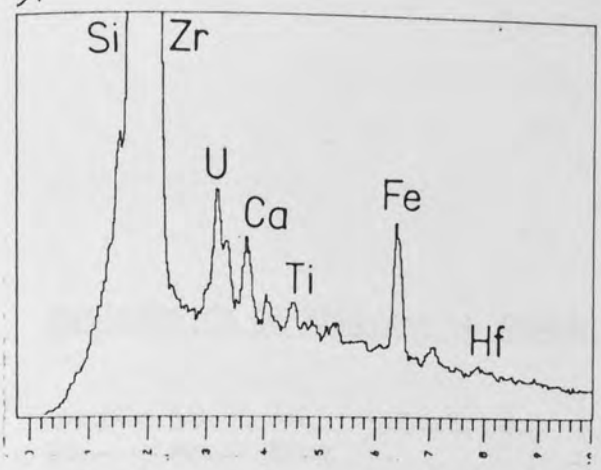

95

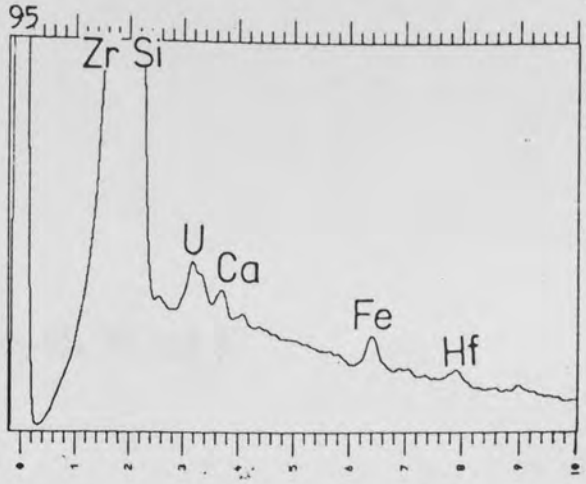

96

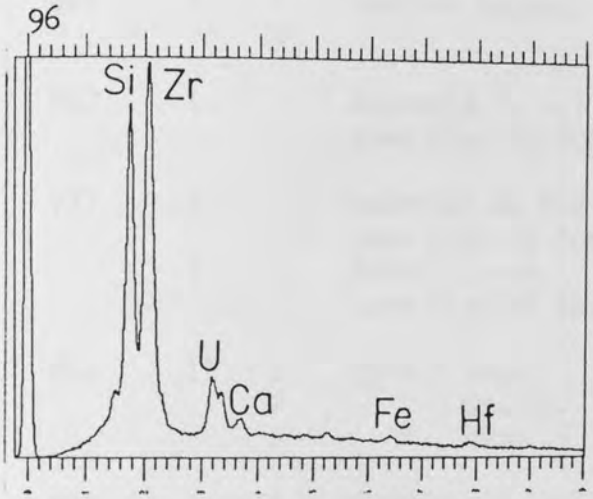

97

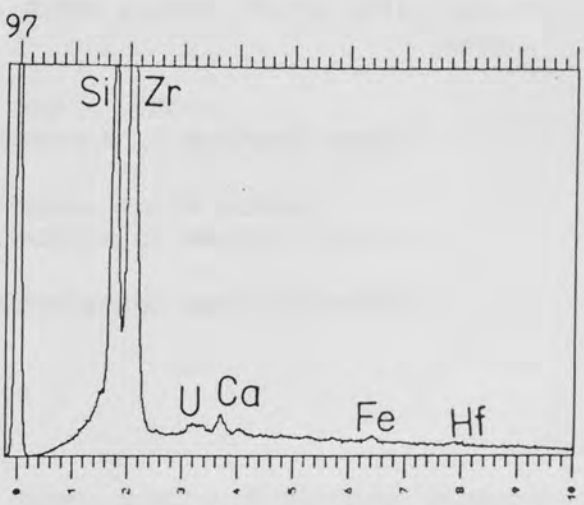

98

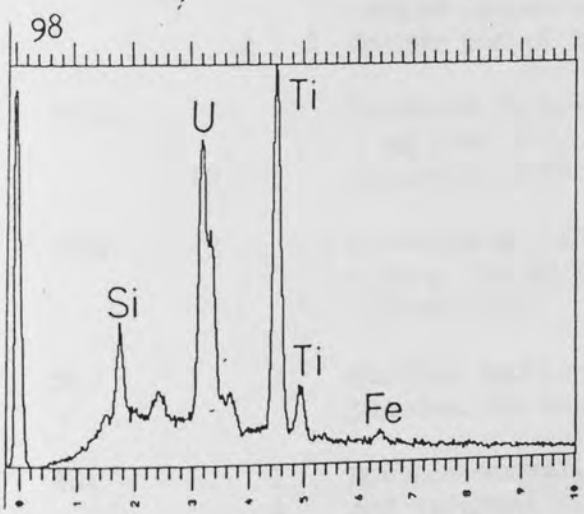

99

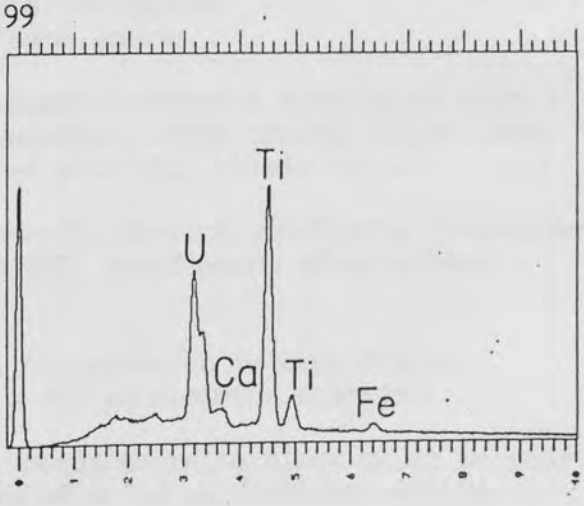

100

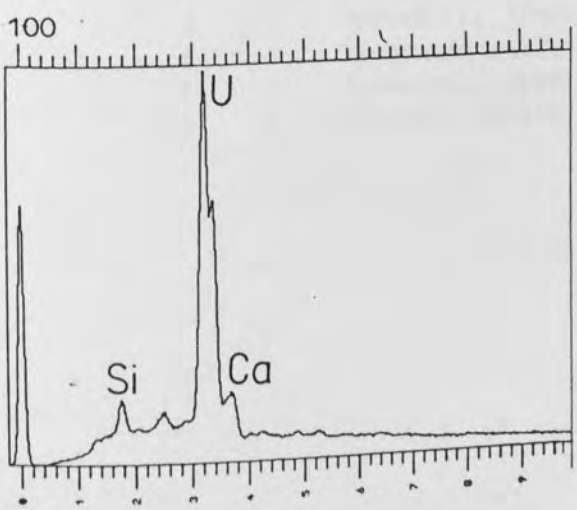

101

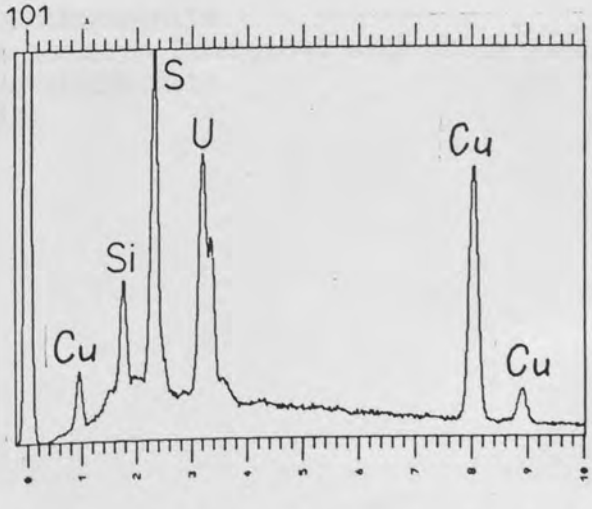

Explanation of analyses in Tables 63, 64, 66 and 67

Sample No.	Grain No.	An. Spot	Description
491	1	1	Surface Anomaly 5, zoned zircon (Plate 139), centre.
		2	" " edge.
802	1		Borehole 1, 5.5 m depth, zircon. (see Fig. 91 for location of analysis spots)
777	1		Borehole 2, 8.8 m depth, zoned zircon. (see Fig. 92 for location of analysis spots)
	2		Zoned zircon. (see Fig. 93 for location of analysis spots)
802	1	1	Sphene edge.
		2	" centre.
		3	" edge.
806	1	1	Borehole 1, 9.7 m depth, centre of elongate diamond-shaped sphene crystal in quartz.
		2 & 3	Either end of the same sphene.
471A	1		Borehole 2, 0.4 m depth. Coffinite intergrown with a 1 mm long TiO_2 pseudomorph after sphene (Plate 160).
	10		Coffinite intergrown with TiO_2 (Plate 161).
476A	20		Borehole 2, 1.9 m depth. Zr-rich ?coffinite intergrown with a 120 µm long TiO_2 pseudomorph after sphene (Plate 159).
560	1	3	Surface Anomaly 5. Orange-brown metatorbernite pseudomorph after a 400 µm diameter apatite.
491	1	2	Surface Anomaly 5. Metatorbernite along grain boundary
		4	and internal cracks of a 700 µm diameter apatite (Plate 163).
	3		Anhedral, green metatorbernite.
	4		Metatorbernite pseudomorph intergrown with white mica.
	5		Anhedral, green metatorbernite.
	1	1	Apatite (Plate 163).

Table 63A Probe analyses of zircon from borehole and surface samples of the Ousdale arkose

Sample	491		802(A)				
Grain	1		1				
An.	1	2	1	2	3	4	5
ZrO_2	63.77	62.51	65.65	63.14	63.57	65.11	66.09
HfO_2	2.46	1.39	1.43	1.56	1.75	1.83	1.89
UO_2	0.32	0.27	nd	0.08	0.19	0.06	0.11
ThO_2	0.07	0.12	0.77	nd	0.01	nd	nd
Y_2O_3	-	-	0.15	0.14	0.56	nd	0.05
SiO_2	34.73	31.70	32.95	32.34	31.80	33.00	32.89
Total	101.35	96.00	100.95	97.26	97.88	100.00	101.03

nd not detected - not determined

Recalculated to four oxygens

Zr	0.934	0.973	0.976	0.968	0.975	0.973	0.981
Hf	0.021	0.013	0.012	0.014	0.016	0.016	0.016
U	0.002	0.002	0.000	0.001	0.001	0.000	0.001
Th	0.001	0.001	0.005	0.000	0.000	0.000	0.000
Y	-	-	0.003	0.002	0.005	0.000	0.001
Total	0.958	0.989	0.996	0.985	0.997	0.989	0.999
Si	1.043	1.012	1.004	1.016	1.001	1.011	1.001

Table 63B Partial analyses of zircon

Sample	777						
Grain	1						
An.	1	2	3	4	5	6	7
HfO_2	1.57	1.64	1.67	1.52	1.96	1.86	1.39
ThO_2	0.30	0.12	0.26	0.18	0.11	0.11	1.05
Y_2O_3	0.40	-	0.62	0.20	0.20	0.27	1.07

Sample	777						
Grain	2						
An.	1	4	5	6	9	10	11
HfO_2	1.56	1.83	-	1.83	-	-	1.72
UO_2	0.10	-	0.23	0.19	0.10	0.19	-

Plate No.	Sample No.	Grain No.	Description
			Ousdale arkose
141	471		Euhedral sphene included in quartz. BH.2, 0.2 m depth. (TPPL)
142	476A	1	Pleochroic sphene included in quartz. BH.2, 1.9 m depth. (TPPL)
143	478A		Apatite, with fluid inclusions, included in K-feldspar. A small zircon (dark) lies just to the right of the apatite. BH.2, 2.4 m depth. (TPPL)
144	478A		Lexan of the area in Plate 143, showing dense fission tracks with the zircon but very few tracks with the apatite. (TPPL)
145	479A	1	Electron diffraction pattern of coffinite from BH.2., 2.5 m depth. A prominent [illegible] the right spacing to be 200 (and multiples thereoff) from coffinite. The spots are elongated in an arc shape, indicating variations of orientation from place to place within the lattice, which can be attributed to radiation damage (partial metamictisation).
146	479A	1	Electron image of the same coffinite. The spottiness is probably due to partial metamictisation of the coffinite lattice.
147	802	10	Interstitial coffinite (C) infilling feldspar cleavage. BH.2, 5.5 m depth. (SEM)
148	802	10	Interstitial coffinite. BH.2, 5.5 m depth. (SEM)

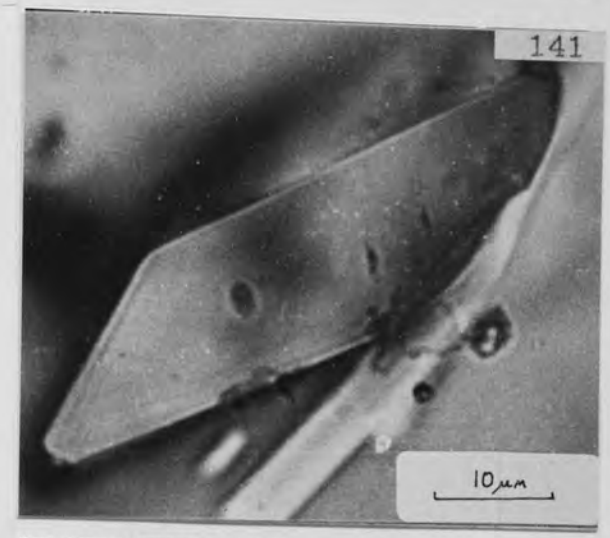
141
10μm

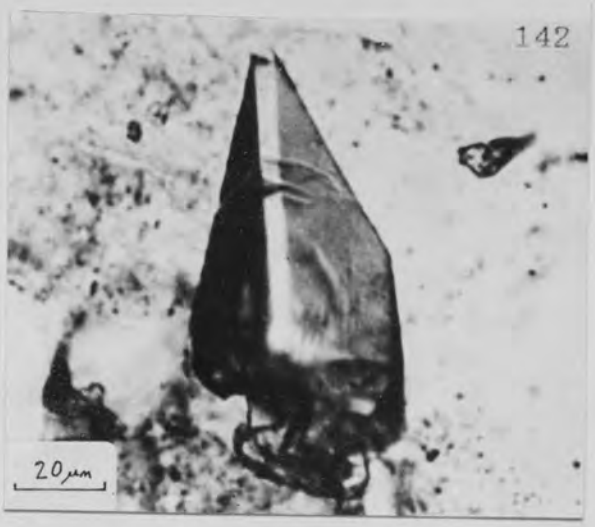
142
20μm

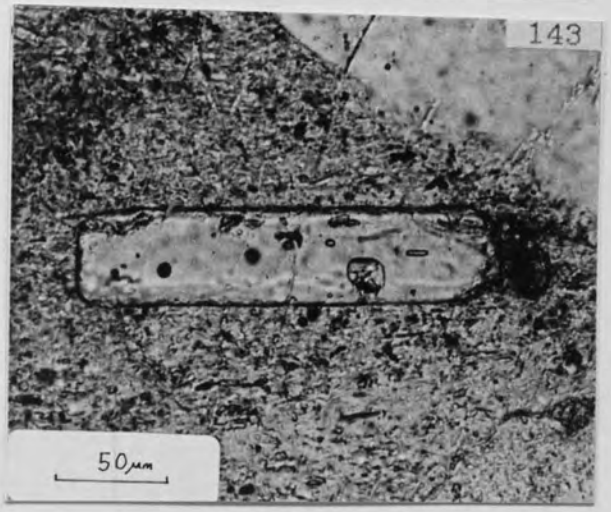
143
50μm

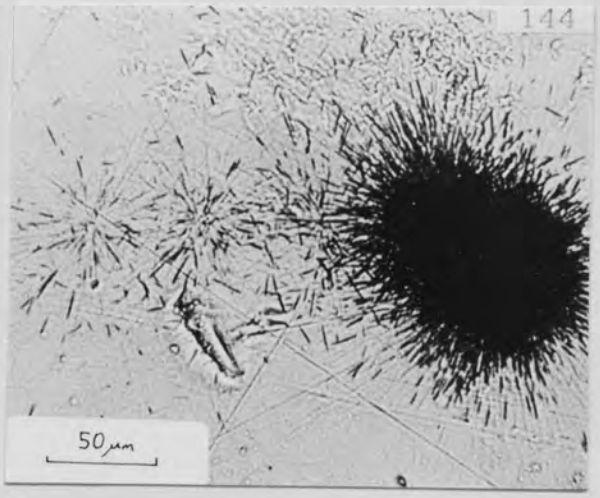
144
50μm

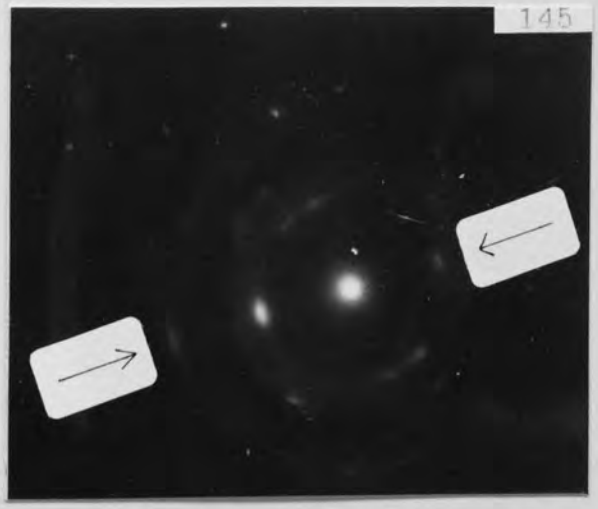
145


146
100nm

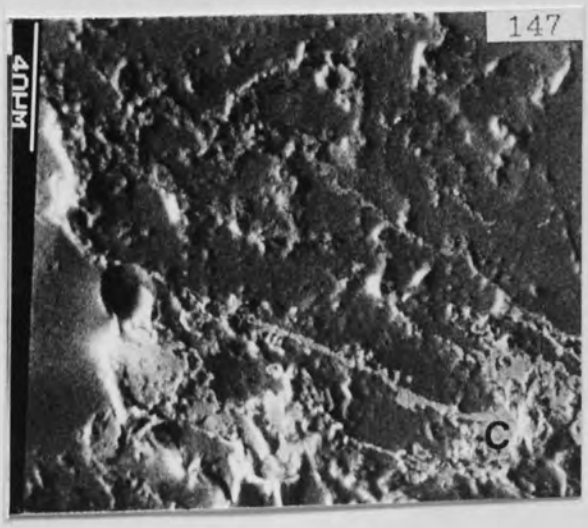
147
40μm
C

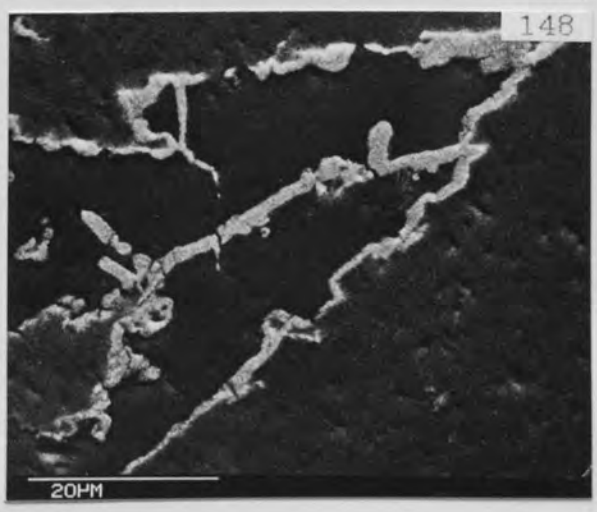
148
20μm

Table 64 Probe analyses of sphene from borehole 1 in the Ousdale arkose

Sample	802			806		
Grain	1			1		
An.	1	2	3	1	2	3
CaO	27.66	27.23	26.44	25.96	25.58	25.42
SiO_2	28.49	28.66	29.60	28.81	29.30	28.65
TiO_2	35.30	33.74	32.71	31.25	30.27	35.29
ThO_2	-	-	-	0.08	0.11	0.13
UO_2	-	-	-	0.04	0.12	0.08
Y_2O_3	-	-	-	0.36	0.37	0.42
FeO	-	-	-	7.13	6.15	5.71
Total	91.44	89.62	88.74	93.63	91.90	95.70

Recalculated to five oxygens

Ca	1.06	1.06	1.04	0.99	0.99	0.94
Ti	0.95	0.92	0.90	0.83	0.82	0.92
Th	-	-	-	nd	nd	nd
U	-	-	-	nd	nd	nd
Y	-	-	-	0.01	0.01	0.01
Fe	-	-	-	0.19	0.17	0.15
Total	2.01	1.98	1.94	2.02	1.99	2.02
Si	1.02	1.04	1.08	1.02	1.06	0.99

Table 65 XRD data of selected minerals from the Helmsdale area (d-spacings in Å)

Anatase		Rutile	Metatorbernite		Torbernite			(in hydrocarbon) Pyrite		(in hydrocarbon) Quartz		Coffinite	
E	O	E	E	O	E	O	O	E	O	E	O	E	O
	3.02		8.71	8.52	10.3	9.3	9.51	1.63	1.63	3.34	3.37	4.64	4.69
3.52	3.52	3.25	3.68	3.69	4.94	4.8	4.78	2.71	2.72	4.26	4.27	3.48	3.46
1.89	1.88	1.69	3.48	3.49	3.58	3.5		2.42	2.43	1.82	1.82	2.79	2.78
2.38	2.37	2.49	3.23	3.22	3.51	3.45	3.46	2.21		1.54	1.54	2.64	2.64
1.70		2.19	5.44	5.53	6.61		6.59	1.92	1.92	2.46	2.45	2.46	
1.67	1.66	1.62	4.93	4.90	4.48		4.38	3.13	3.13	2.28	2.24	2.18	2.18
1.48	1.48	1.36	2.93	2.95	3.67			1.45		1.38		1.99	
2.43		1.35	2.67	2.64	5.18			1.04		2.13	2.14	1.85	
2.33		0.82		2.45		3.25	3.26					1.80	1.79
				2.27		2.2	3.06					1.74	1.74
				2.14		2.02	2.84					1.56	1.55
				2.01		1.75	2.69					1.46	
				1.91		1.57	2.48					1.43	
				1.76		1.51	2.40					1.32	
												1.16	1.17

Origin of samples

Anatase: Top of Borehole 2 in Ousdale arkose.
Metatorbernite: Pseudomorphs after apatite in the Ousdale arkose, Surface Anomaly 5.
Torbernite: Green joint coatings " " .
Hydrocarbon: Peripheral band to an alteration zone in the Helmsdale granite, Ord burn (Loc. 28).
Coffinite: 5.5 m down Borehole 2 in the Ousdale arkose.

E Expected pattern for that mineral in the A.S.T.M.-P.D.F. 1977 index.
O Obtained pattern using powder camera/diffractometer (see Appendix 1, Section 7).

Plate No.	Sample No.	Grain No.	Description
			Ousdale arkose
149	771		Coffinite (lighter) replacing pyrite (p). BH.2, 5 m depth. (SEM)
150	809	1	Large intergrowth of coffinite (c) with pyrite (p). BH.1, 10.4 m depth. (RPPL)
151	809	1	The same intergrowth of coffinite (c) with pyrite (p). (TPPL)
152	802	10	Intergrowth of coffinite (light grey) with TiO_2 (dark grey). The coffinite seems to replace the TiO_2 needles. Quartz and feldspar appear black in the image. BH.1, 5.5 m depth. (BSEI)
153	802	10	Similar intergrowth to Plate 152. BH.1, 5.5 m depth. (BSEI)
154	802	10	Selective enlargement of Plate 153. (BSEI)
155	802	13	Coffinite (C) overgrowing zircon (Z). BH.1, 5.5 m depth. (BSEI)
156	771	1A	Coffinite (C) replacing and overgrowing hydrocarbon (H) BH.2, 5 m depth. (SEM)

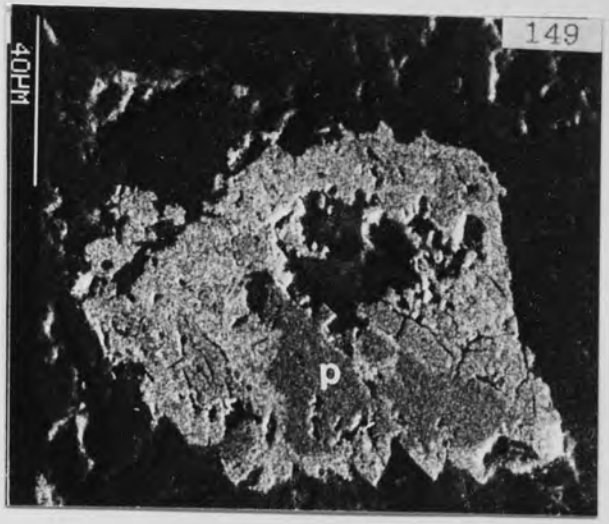
149
40HM
p

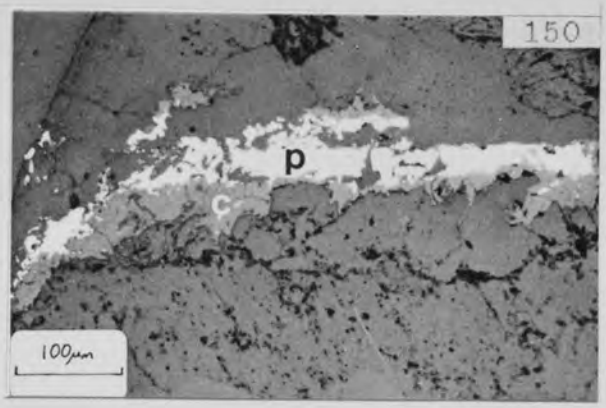
150
p
c
100µm

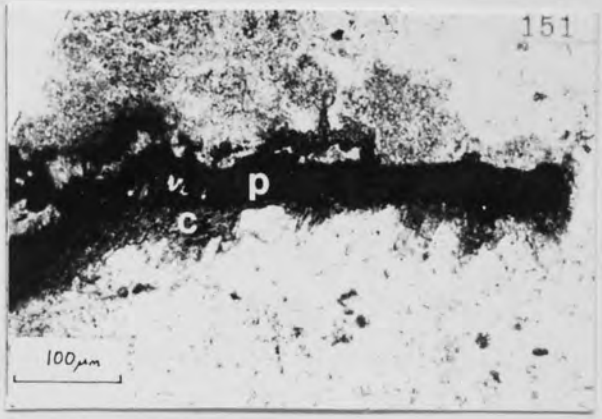
151
p
c
100µm


152
20µm


153
10µm


154
3µm

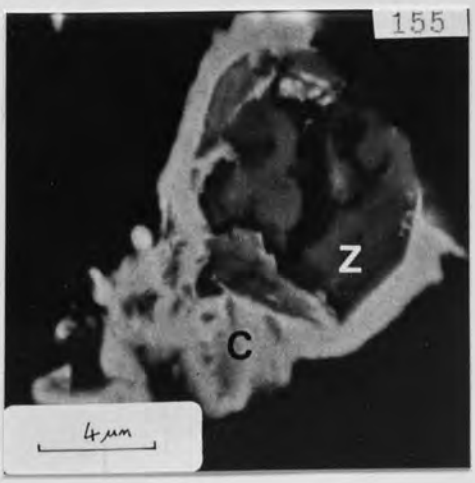
155
Z
C
4µm

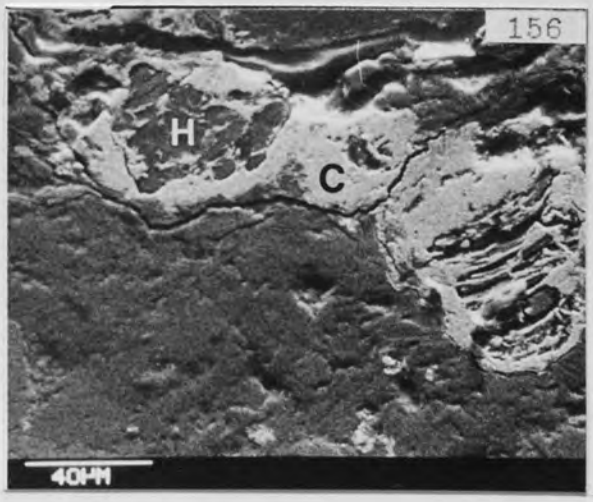
156
H
C
40HM

Plate No.	Sample No.	Grain No.	Description
			Ousdale arkose
157	802	1	U-Zr-Si phase, possibly Zr-rich coffinite. BH.1, 5.5 m depth. (SEM)
158	802	1	BSEI of the same grain, emphasising the cracks but not revealing a mixture of zircon and coffinite, which have very different back-scattered electron coefficients.
159	476A	20	U-Th-Zr-Si phase, possibly Zr-coffinite, associated with a 120 μm long TiO_2 pseudomorph after sphene. EPMA spots are shown. BH.2, 1.9 m depth. (SEM)
160	471A	1	Coffinite intergrown with part of a 1 mm long TiO_2 pseudomorph after sphene (t). EPMA spots are shown. BH.2, 0.4 m depth. (SEM)
161	471A	10	Coffinite (EPMA spots 1-3) associated with TiO_2 (T). BH.2, 0.4 m depth. (SEM)

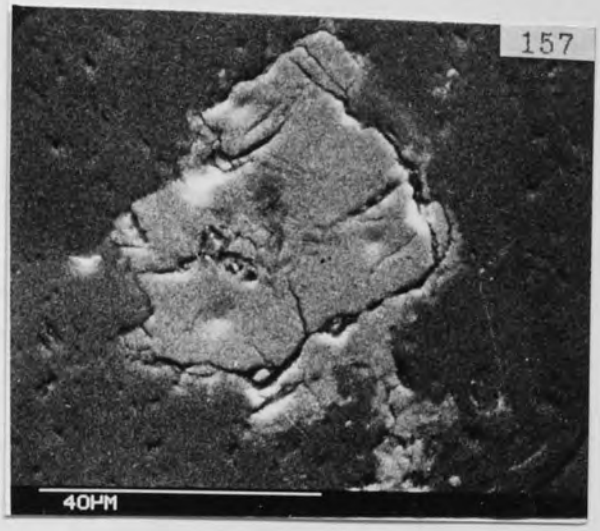
157
40µM

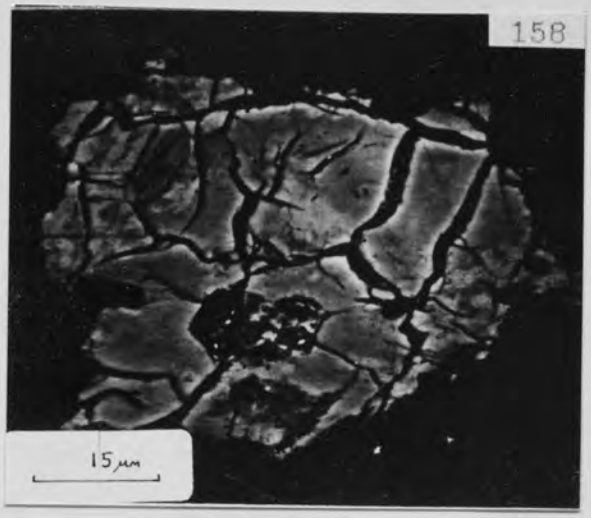
158
15µm

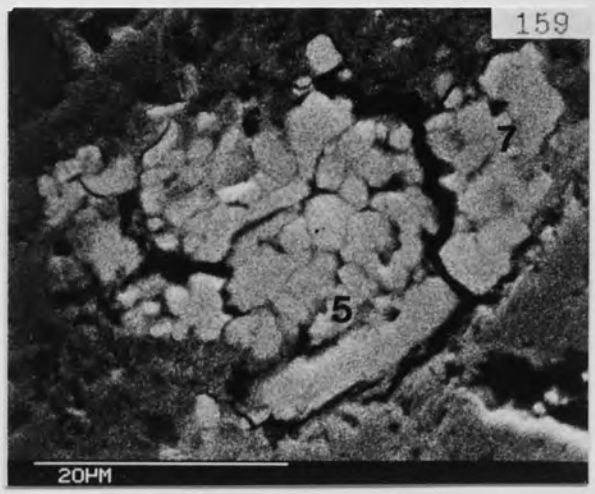
159
7
5
20µM

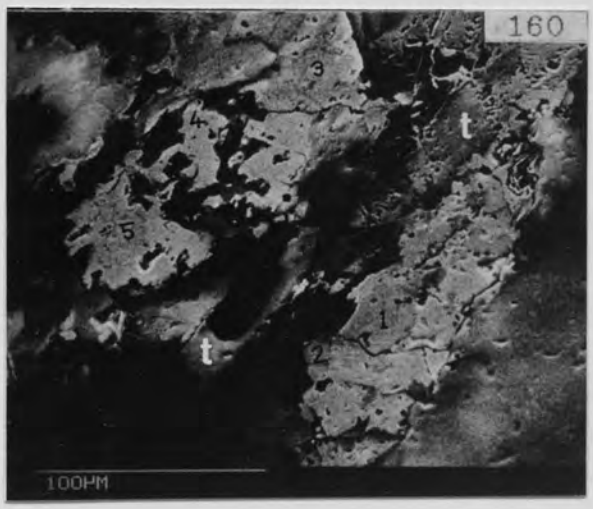
160
3
4
t
5
1
t
100µM


161
1
T
3
40µM

ED spectra of coffinite and LREE-phase(s)

Fig. No.	Sample No.	Grain No.	An. Spot	Description	Loc-ation	Plate No.
102	471A	1	1	Coffinite intergrown with TiO_2	BH.2 0.4 m	160
103	480A	20	1	Coffinite.	BH.2 2.9 m	
104	472		2	P-Th-coffinite associated with TiO_2.	BH.2 0.6 m	
105	802	1	4	Zr-coffinite.	BH.1 5.5 m	157
106	476A	20	1	Zr-coffinite, intergrown with TiO_2.	BH.2 1.7 m	159
107	771	28	6	LREE-phase.	BH.2 5 m	182
108	"	"	3	LREE-phase and ?uraninite.	"	"
109	"	"	2	" "	"	"

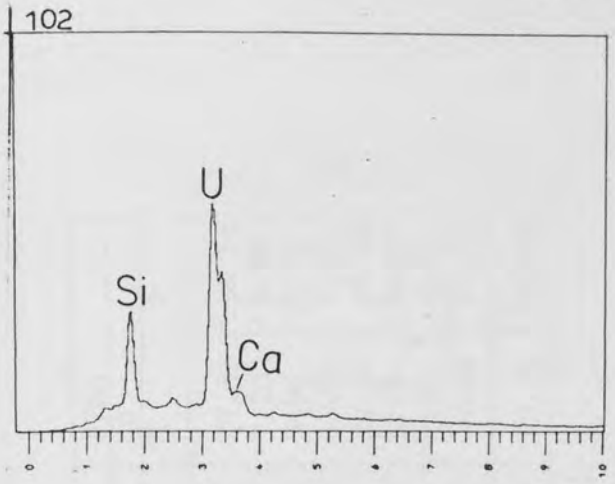
102
U
Si
Ca

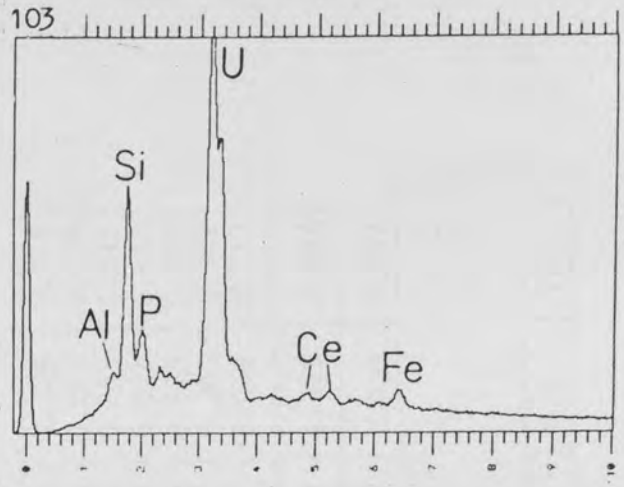
103
U
Si
Al
P
Ce
Fe

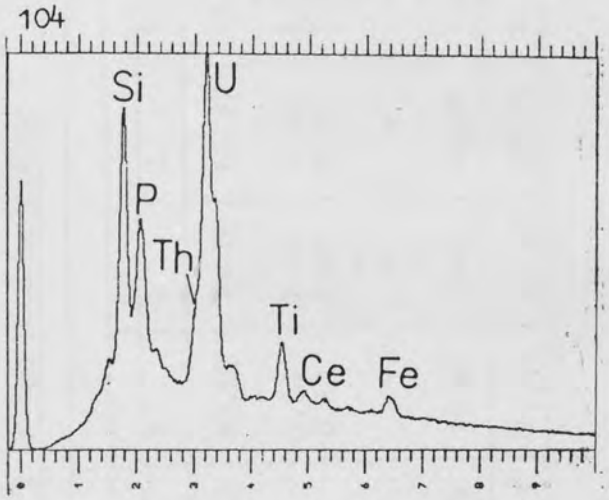
104
Si
U
P
Th
Ti
Ce
Fe

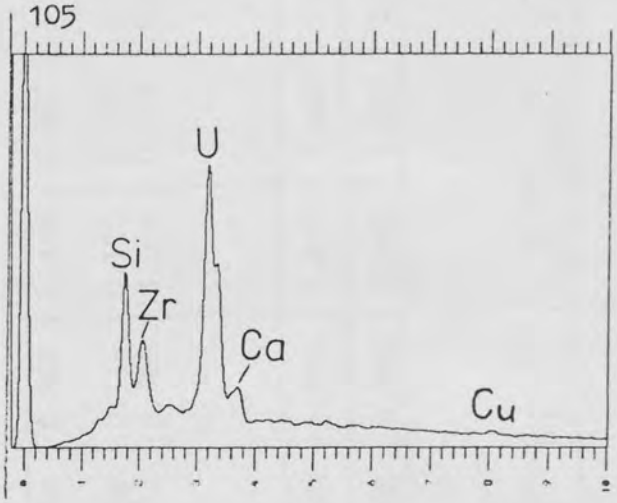
105
U
Si
Zr
Ca
Cu

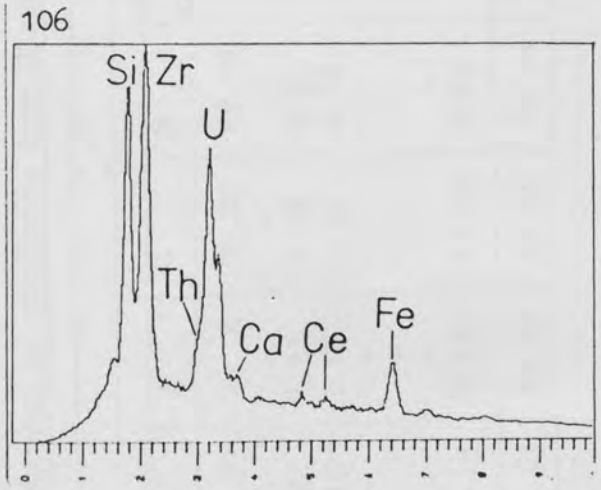
106
Si
Zr
U
Th
Ca
Ce
Fe

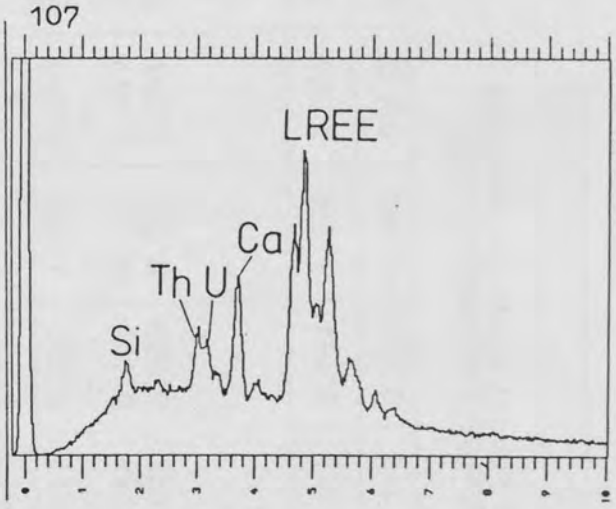
107
LREE
Ca
Th
U
Si

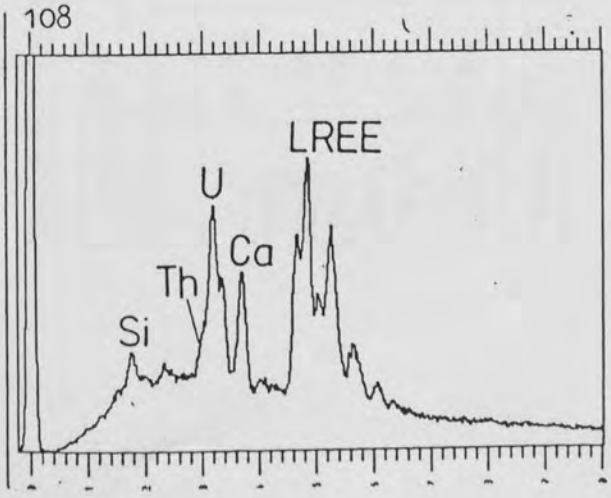
108
LREE
U
Th
Ca
Si

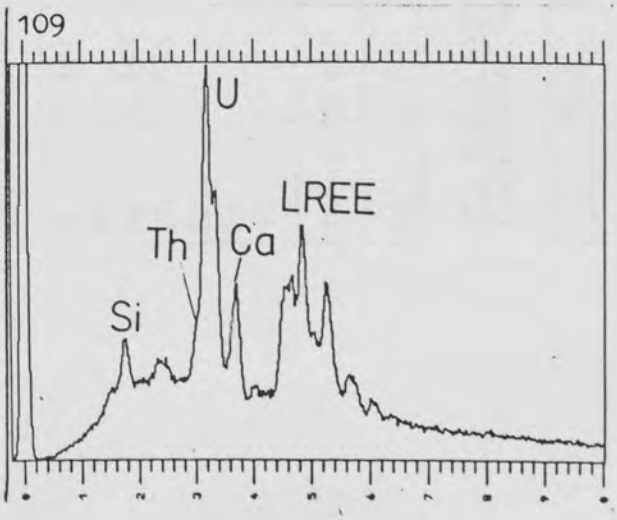
109
U
LREE
Th
Ca
Si

Table 66 Probe analyses of coffinite from Borehole 2 in the Ousdale arkose

Sample	471A										476A	
Grain	1							10			20	
An.	1	2	3	4	5	6	7	1	2	3	5	7
UO_2	66.08	70.39	77.14	73.93	68.79	70.72	62.05	79.16	66.37	77.07	27.59	26.54
ThO_2	–	–	–	–	–	–	–	–	–	–	7.20	6.93
CaO	1.59	1.87	1.51	1.78	0.21	1.58	1.54	1.97	1.93	1.67	0.96	0.79
PbO	1.56	1.15	1.87	0.19	2.23	0.20	0.40	2.89	0.79	2.20	0.78	0.76
ZrO_2	–	–	–	–	–	–	–	–	–	–	24.32	23.39
Fe_2O_3	–	–	–	–	–	–	–	–	–	–	5.08	9.89
TiO_2	–	–	–	–	–	–	–	–	–	–	0.45	0.47
SiO_2	7.94	10.26	8.13	13.76	7.95	15.19	13.81	5.41	16.66	7.92	14.22	15.91
Total	77.17	83.67	88.65	89.66	79.18	87.69	77.80	89.43	85.75	88.86	80.60	84.68

Recalculated to four oxygens

U	1.241	1.157	1.303	1.055	1.293	0.990	0.969	1.440	0.907	1.306	0.326	0.286
Th	–	–	–	–	–	–	–	–	–	–	0.087	0.076
Ca	0.144	0.148	0.123	0.122	0.019	0.106	0.116	0.173	0.127	0.136	0.055	0.041
Pb	0.035	0.023	0.038	0.003	0.051	0.003	0.008	0.064	0.013	0.045	0.011	0.010
Zr	–	–	–	–	–	–	–	–	–	–	0.629	0.553
Fe	–	–	–	–	–	–	–	–	–	–	0.203	0.361
Ti	–	–	–	–	–	–	–	–	–	–	0.018	0.017
Total	1.420	1.328	1.464	1.180	1.363	1.099	1.093	1.677	1.047	1.487	1.329	1.344
Si	0.670	0.758	0.617	0.882	0.672	0.955	0.969	0.442	1.023	0.603	0.755	0.771

Wt. % H_2O hypothetically present as (OH)
(calculated using method given in Appendix 4)

	5.3	4.6	6.7	2.8	4.9	1.4	1.1	9.1	0.2	7.0	6.5	7.1

Plate No.	Sample No.	Grain No.	Description
			Ousdale arkose
162	18L		Metatorbernite veinlet. Surface Anomaly 5. (F.O.V. = 560 μm) (TXPL)
163	491	1	Metatorbernite (light grey, hexagonal outline and veinlets; EPMA spots 2 and 4) replacing euhedral apatite (a). The dark area near the top is a hole in the section. Surface Anomaly 5. (SEM)
164	491		X-ray map for U of grain in Plate 163, showing distribution of metatorbernite.
165	491		X-ray map for P of grain in Plae 163, showing distribution of apatite and metatorbernite.
166	515		Metatorbernite (m) partially replacing apatite (a) with a zircon inclusion (z). Surface Anomaly 5. (TXPL)

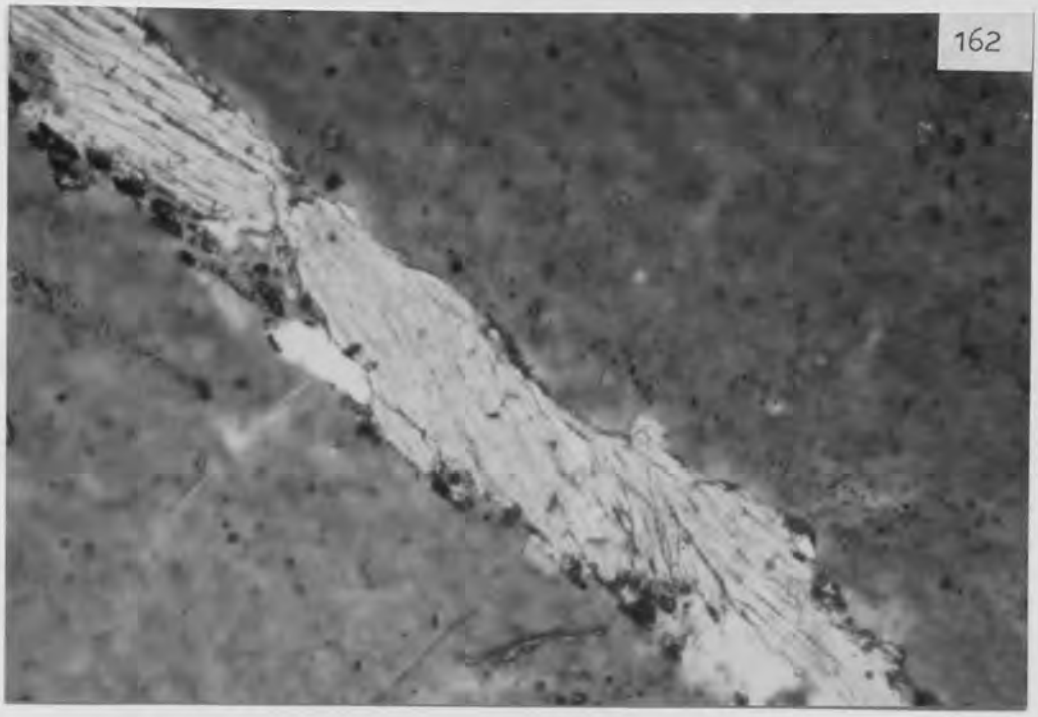
162

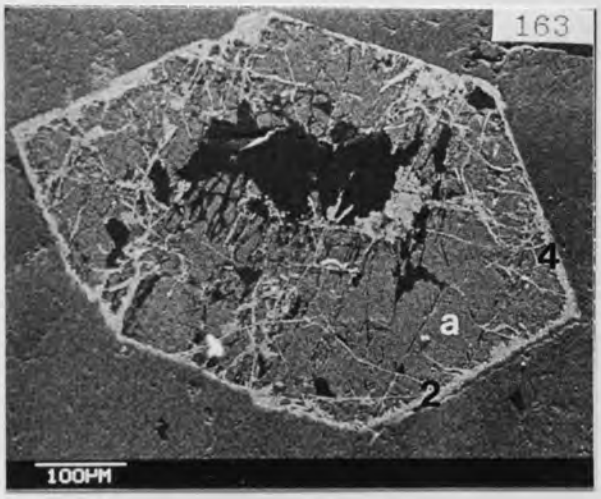
163
4
a
2
100µM

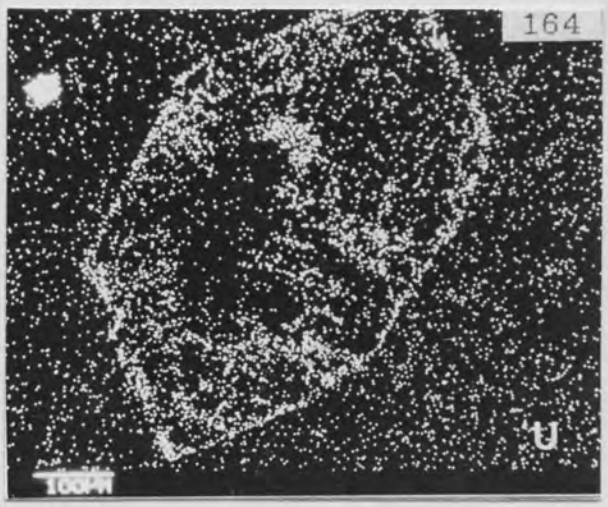
164
U
100µM

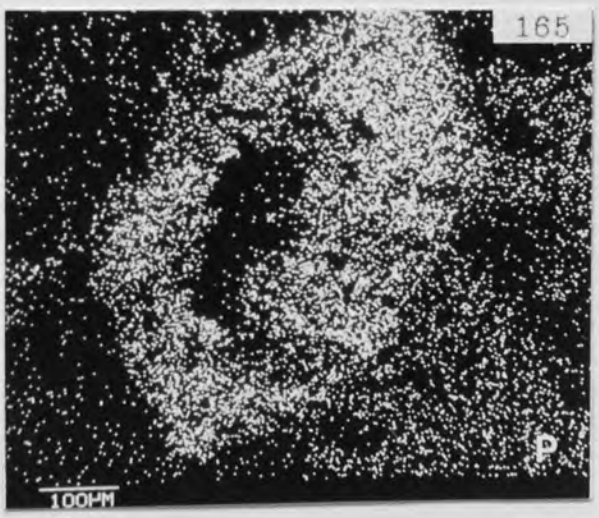
165
P
100µM

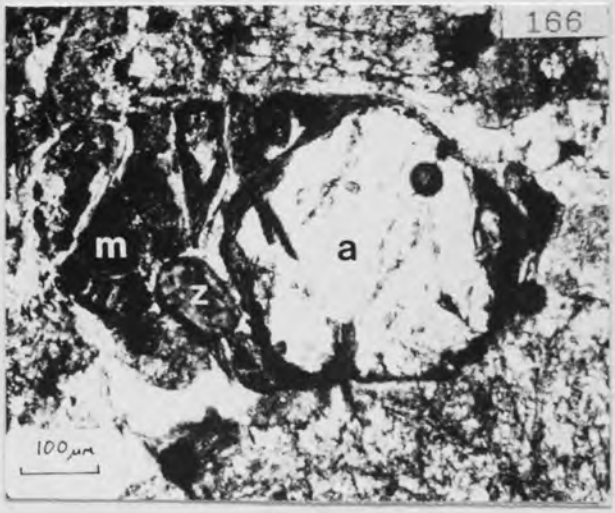
166
m
a
z
100µm

Plate No.	Sample No.	Grain No.	Description
			Ousdale arkose
167	490		Metatorbernite pseudomorph after apatite. Surface Anomaly 5 (SEM)
168	490		Metatorbernite (m) pseudomorph after a 2 mm long, tabular apatite (grain used for XRD, see Table 65). TiO_2 locally overgrows the pseudomorph (t). Surface Anomaly 5. (TPPL)
169	490		Lexan of the pseudomorph in Plate 168, showing "burned-out" fission tracks (BFT) associated with the metatorbernite and "dense fission tracks" (DFT) associated with the TiO_2. (TPPL)
170	18L		Metatorbernite (m) intergrown with white mica (W). Surface Anomaly 5. (TXPL)
171	477		Typical, subhedral anatase (Type 1 TiO_2 - see text). BH.2, 2 m depth. (RPPL)
172	473	1	Disseminated leucoxene along quartz and feldspar boundaries. BH.2, 1 m depth. (TPPL)
173	775		Trellis pattern of TiO_2, possibly representing former ilmenite lamellae in magnetite. BH.2, 8.2 m depth. (RPPL)
174	806		TiO_2 pseudomorph after sphene (opaque) with a core of calcite (clear) included in quartz. BH.1, 9.7 m depth. (TPPL)

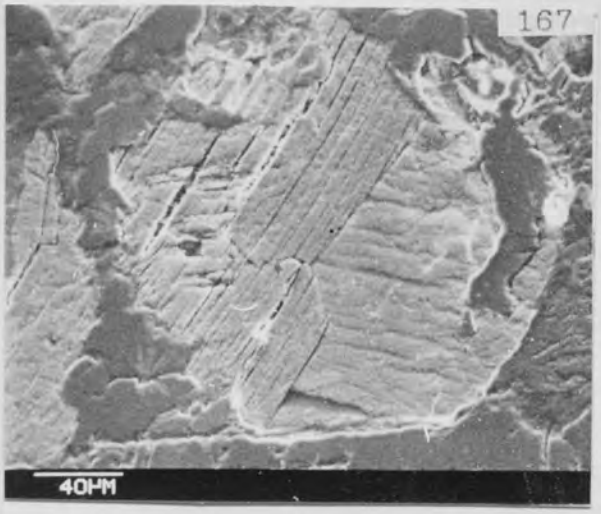
167
40μm

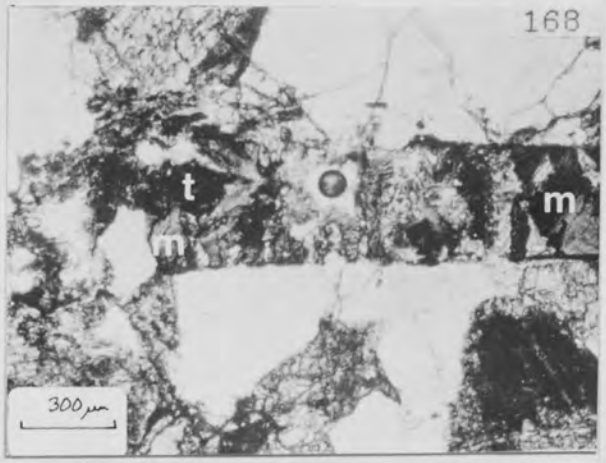
168
t
m
m
300μm


169
300μm

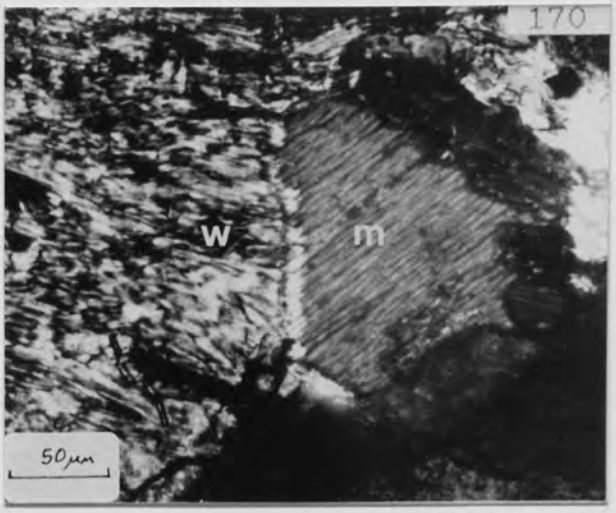
170
w
m
50μm


171
30μm

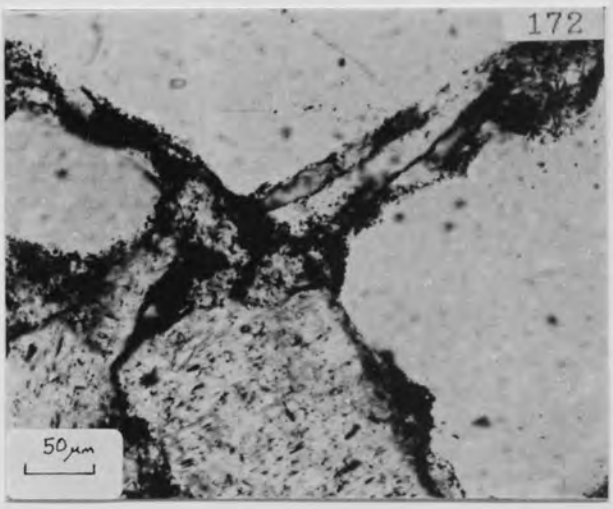
172
50μm

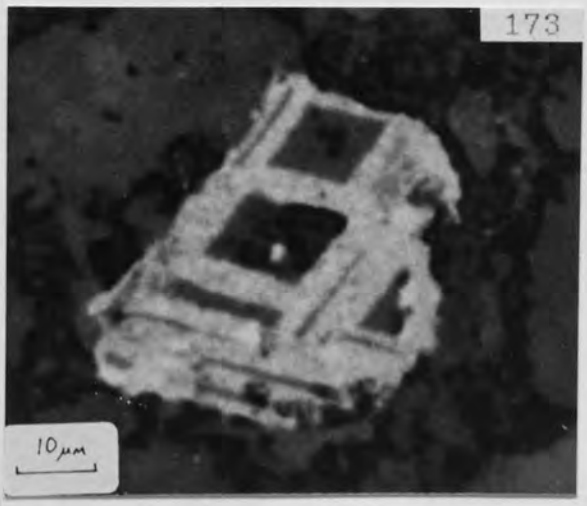
173
10μm

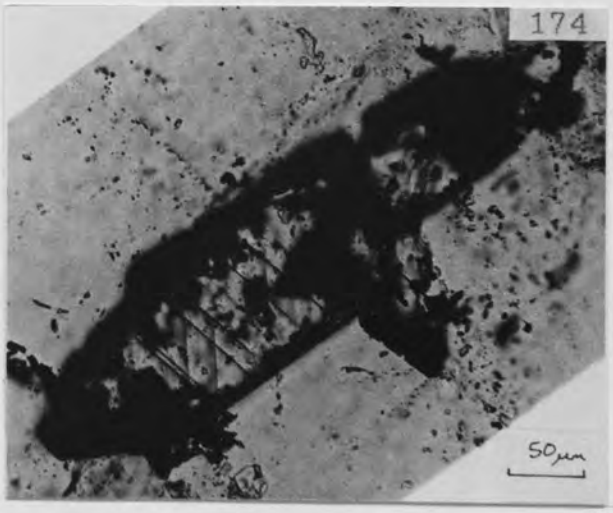
174
50μm

ED spectra of REE- and U-bearing phases

Fig. No.	Sample No.	Grain No.	An. Spot	Description	Location	Plate No.
110	771	29	1	LREE-phase and coffinite with ?uraninite.	BH.2 5 m	
111	490			Metatorbernite with limonite staining.	Anom.5	168
112	"			Fracture in K-feldspar associated with DFT.	"	
113	472		10	Pyrite altering to goethite associated with DFT.	BH.2 0.6 m	
114	476A	1	2	TiO_2 pseudomorph after sphene, associated with DFT.	BH.2 1.7 m	
115	771	1	2	Hydrocarbon associated with DFT	BH.2 5 m	177
116	"	1A	3	" " "		
117	"	19		Xenotime inclusions in hydrocarbon.	"	178

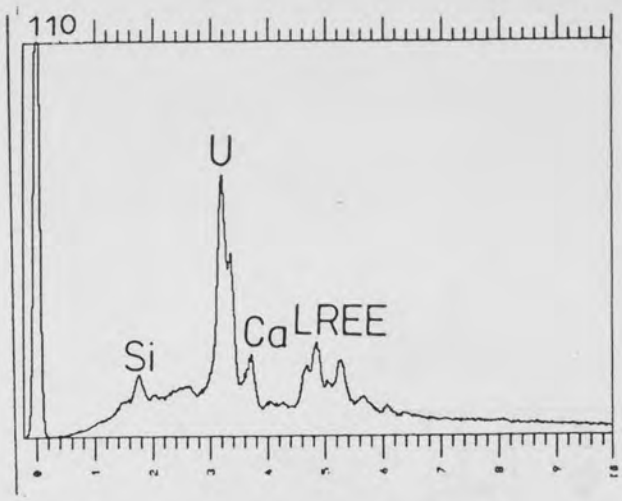
110
U
Si
Ca
LREE

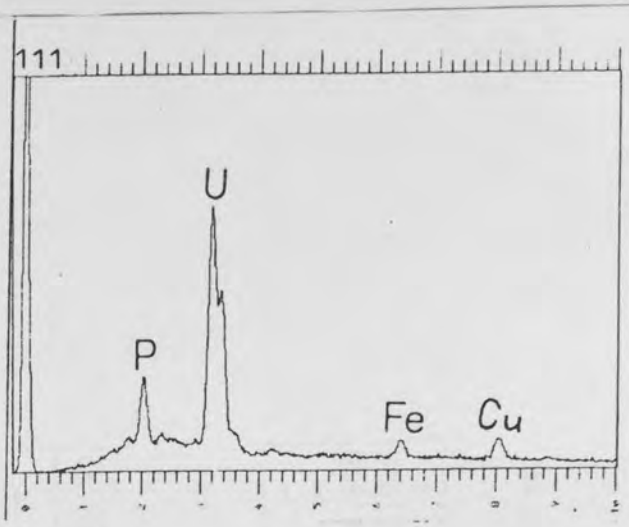
111
U
P
Fe
Cu

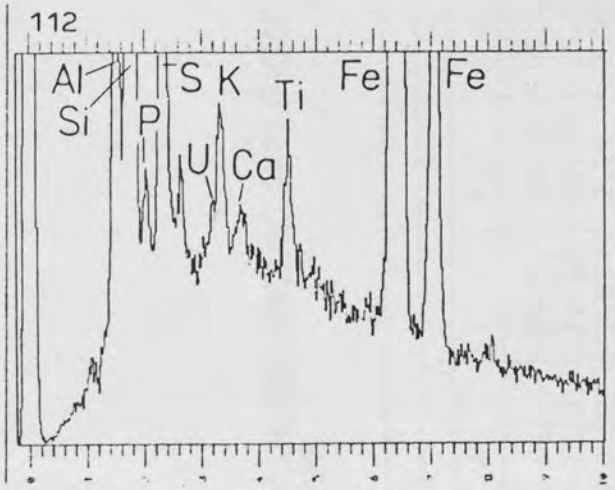
112
Al
Si
P
S
K
Ti
Fe
Fe
U
Ca

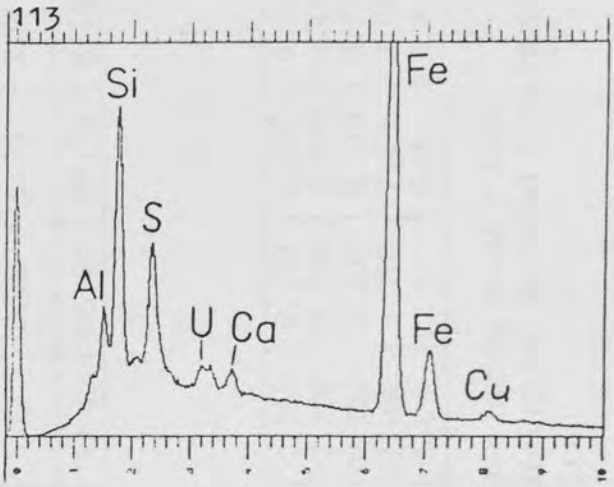
113
Si
Fe
S
Al
U
Ca
Fe
Cu

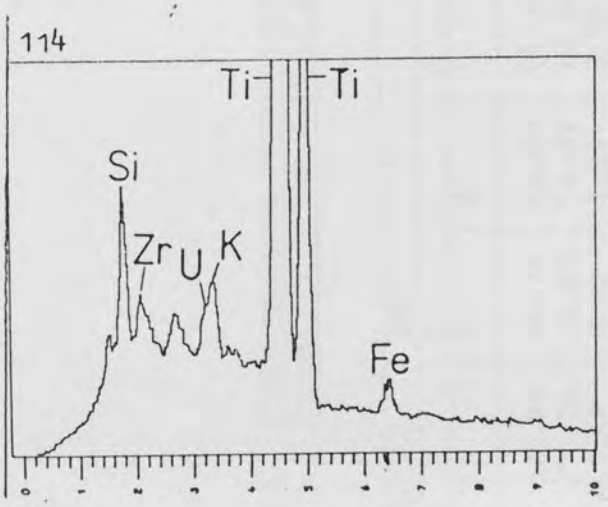
114
Ti
Ti
Si
Zr
U
K
Fe

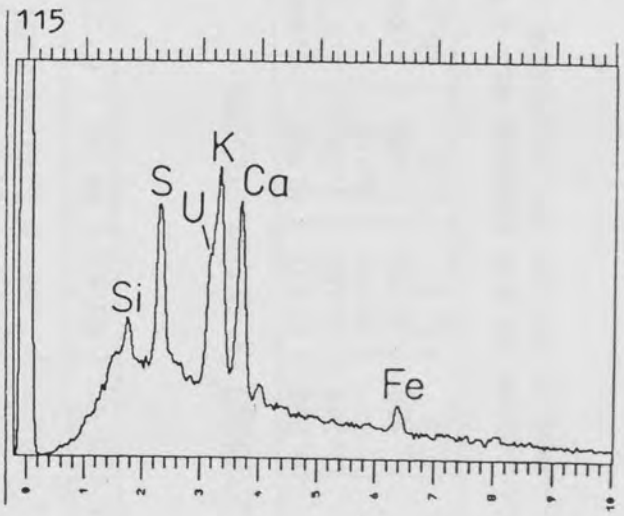
115
K
S
U
Ca
Si
Fe

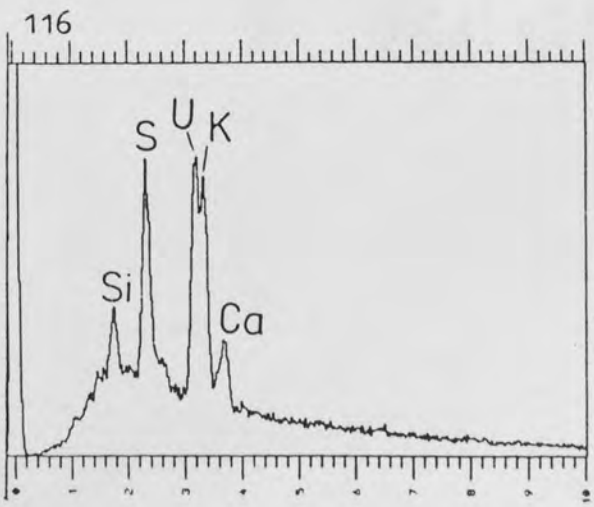
116
S
U
K
Si
Ca

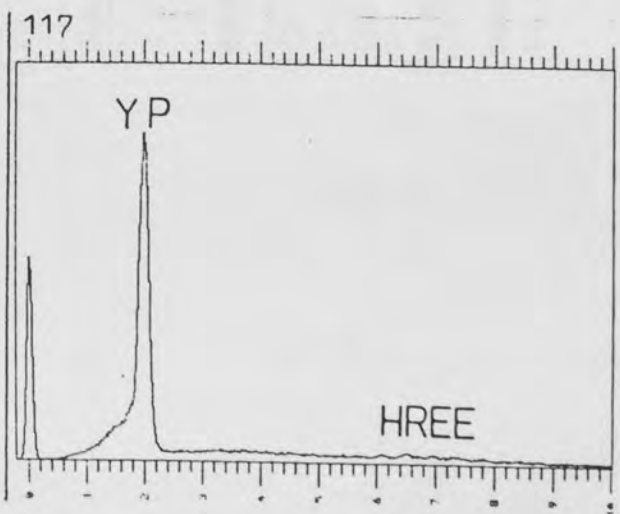
117
YP
HREE

Table 67 Probe analyses of metatorbernite and apatite* from Surface Anomaly 5 in the Ousdale arkose

Sample	560	491							
Grain	1	1		3		4		5	1*
An.	3	2	4	1	2	1	2	1	1
UO_2	76.28	66.75	69.00	64.35	68.95	69.31	74.06	66.13	-
P_2O_5	15.78	16.89	14.23	13.31	13.94	12.27	11.85	16.07	41.08
CuO	3.58	2.00	3.04	3.53	2.12	2.67	2.29	3.20	-
CaO	-	0.45	0.90	-	0.71	1.17	0.08	0.16	51.78
Fe_2O_3	nd	2.56	2.77	1.04	3.73	0.18	0.76	1.08	-
Total	95.64	88.65	89.94	82.23	89.45	85.60	89.04	86.64	92.86

Recalculated to twelve oxygens

Cu	0.386	0.227	0.359	0.448	0.255	0.332	0.282	0.371	-
U	2.284	2.108	2.263	2.272	2.308	2.396	2.538	2.130	-
Ca	-	0.072	0.151	-	0.121	0.206	0.014	0.026	4.670
P	1.905	2.150	1.881	1.894	1.880	1.710	1.636	2.086	2.930
H_2O	2.1	5.7	5.2	10.0	5.6	7.9	6.0	6.8	-

Recalculation of H_2O assumes wt. % H_2O = (oxide total - 100%)
Fe assumed to be due to iron-oxide staining and excluded from recalculation

Plate No.	Sample No.	Grain No.	Description
			Ousdale arkose
175	473	7	TiO_2 pseudomorph after sphene with a small zircon inclusion (z). BH.2, 1 m depth. (ROIL)
176	480A		Pyrite-marcasite intergrowths (P) overgrowing hydrocarbon (H). BH.2, 2.9 m depth. (RPPL)
177	771		Irregular strands of TiO_2 (light grey) in hydrocarbon. BH.2, 5 m depth. (ROIL)
178	771	19	Inclusion of xenotime (X) in hydrocarbon (H). BH.2, 5 m depth. (SEM)
179	771	4	Xenotime (X) overgrowing zircon (Z). BH.2, 5 m depth. (SEM)
180	480A	15	LREE-phase (L) overgrown by pyrite (P). BH.2, 2.9 m depth. (SEM)
181	771	31	LREE-phase (L) intergrown with slightly lighter coffinite (U). BH.2, 5 m depth. (SEM)
182	771	28	LREE-phase (6) intergrown with slightly brighter ?uraninite (2 and 3). ED analysis spots are shown. BH.2, 5 m depth. (SEM)


175
Z
40 µm

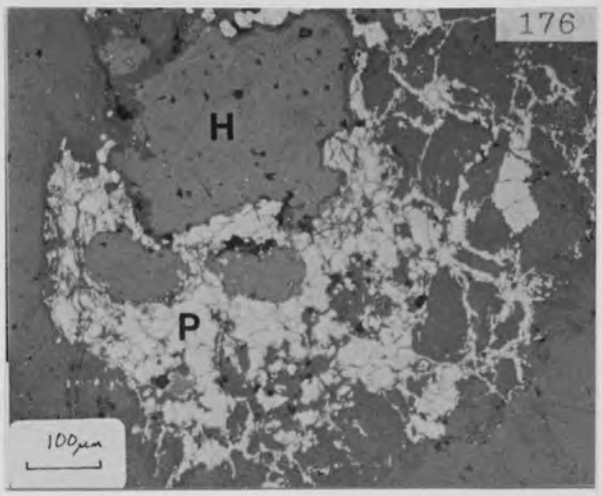
176
H
P
100 µm

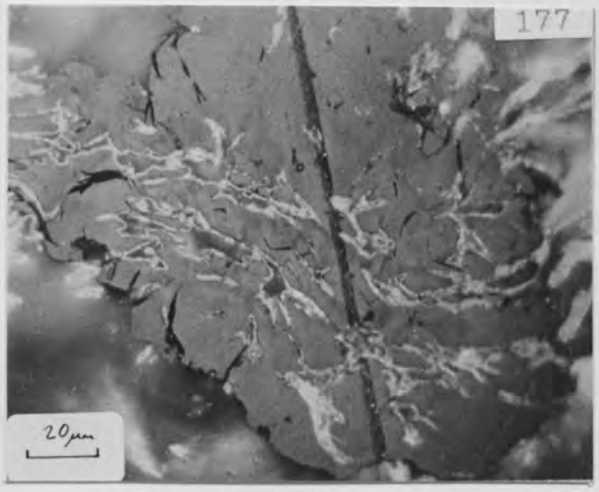
177
20 µm

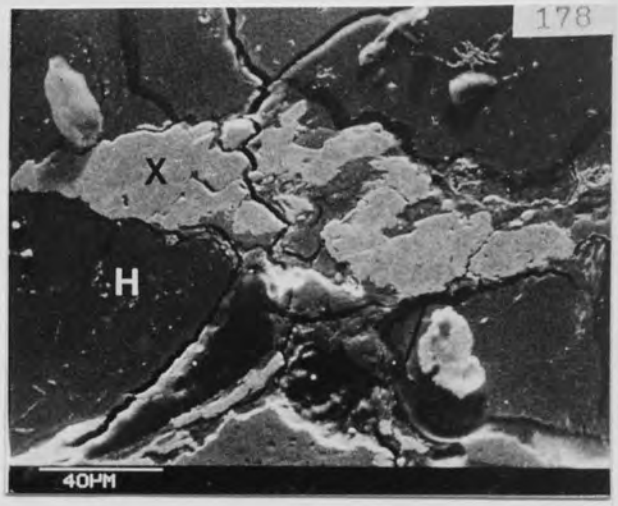
178
X
H
40µM

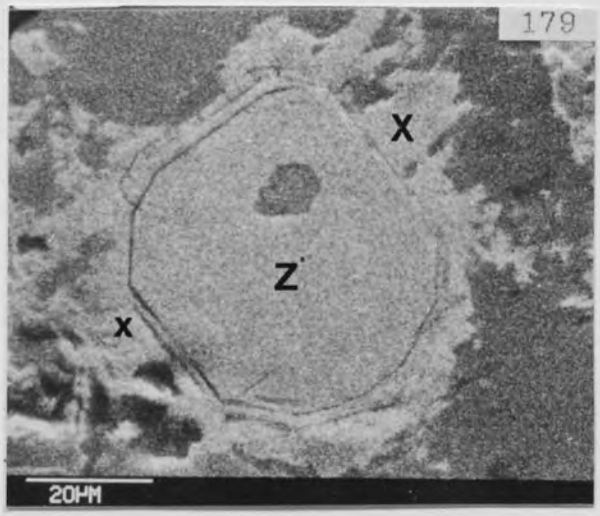
179
X
Z
X
20µM

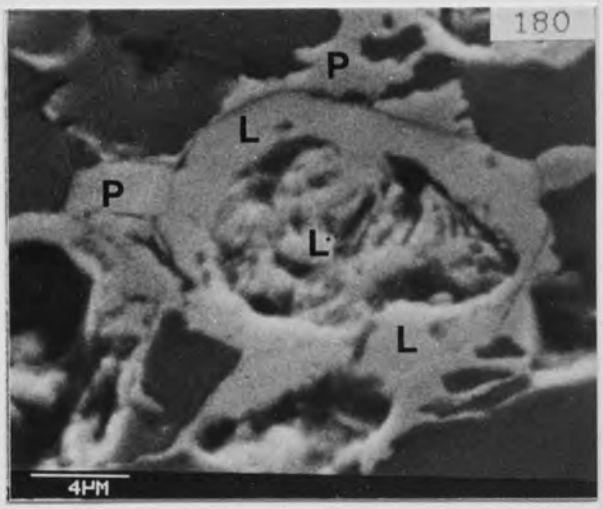
180
P
L
P
L
L
4µM

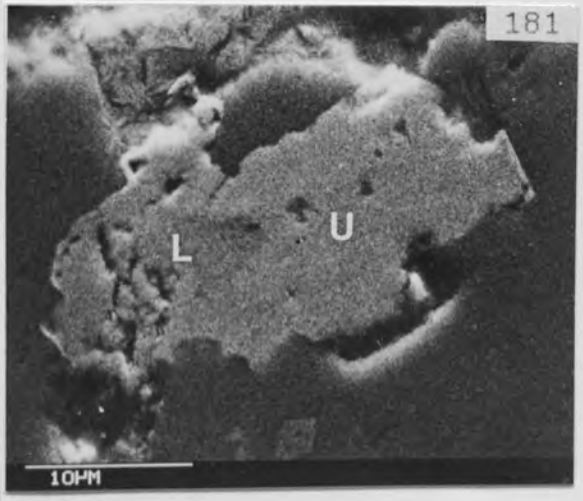
181
L
U
10µM

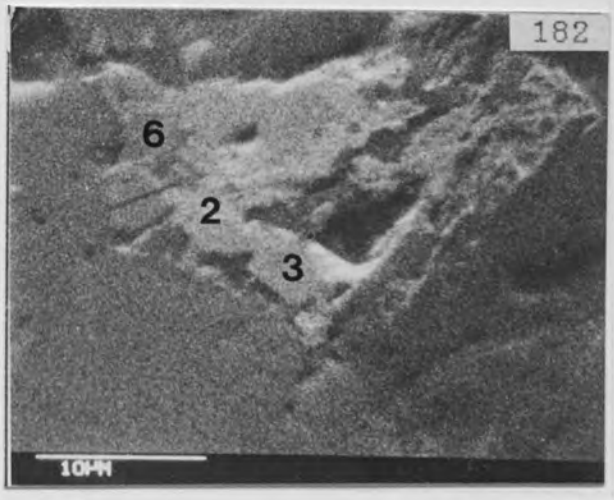
182
6
2
3
10µM

ED spectra of REE- and U-bearing phases

Fig. No.	Sample No.	Grain No.	An. Spot	Description	Location	Plate No.
118	771	4	1	Xenotime overgrowing zircon.	BH.2 5 m	179
119	"	31	5	LREE-phase	"	181
120	"	"	6	LREE-phase and coffinite admixture.	"	"
121	802	20		Ca-LREE-phase.	BH.1 5.5 m	
122	490			TiO_2 and Fe-oxide staining	Anom.5	
123	28F		1	Hydrocarbon from alteration zone in Helmsdale granite.	Ord Burn	

118

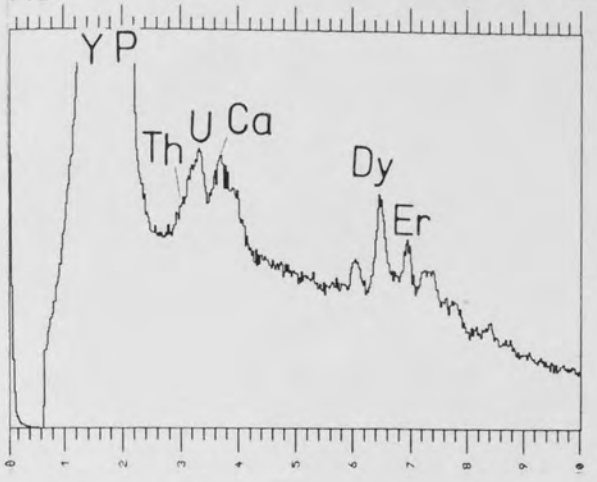

119

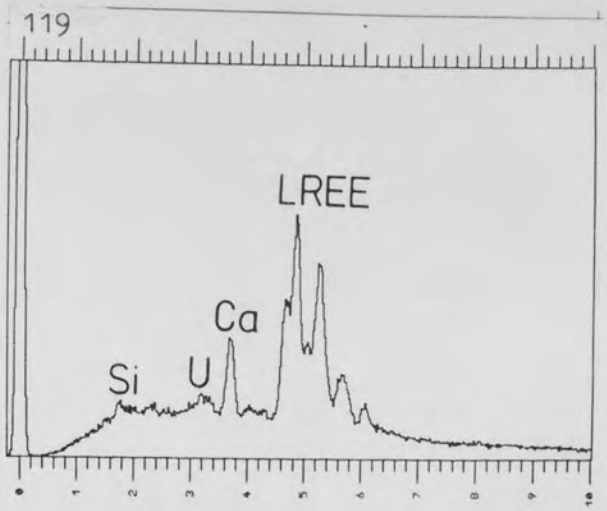

120

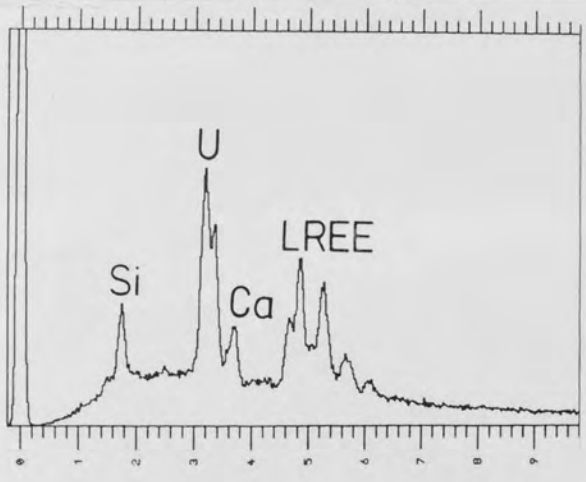

121

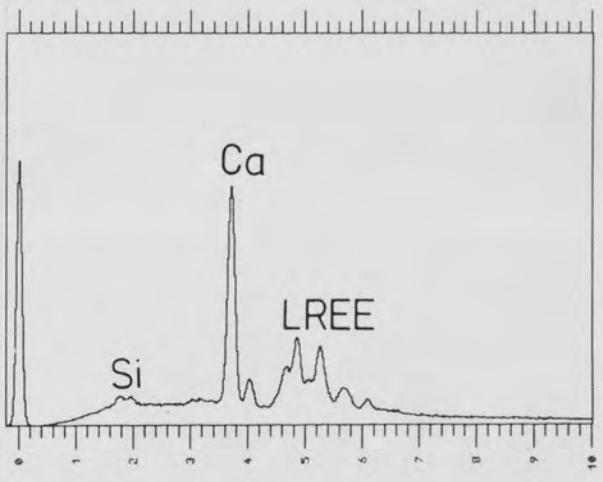

122

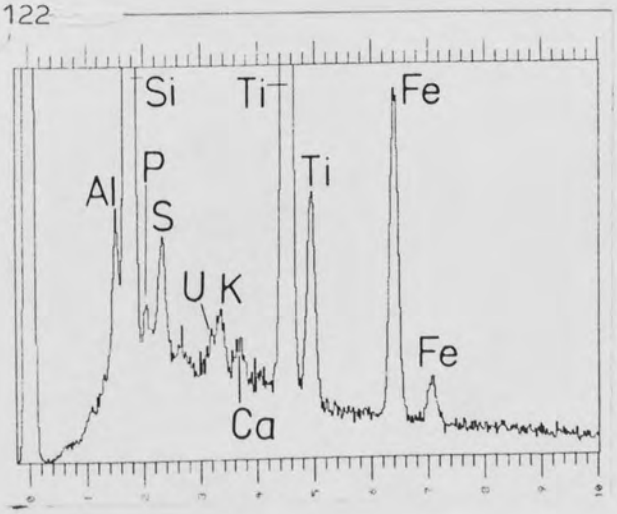

123

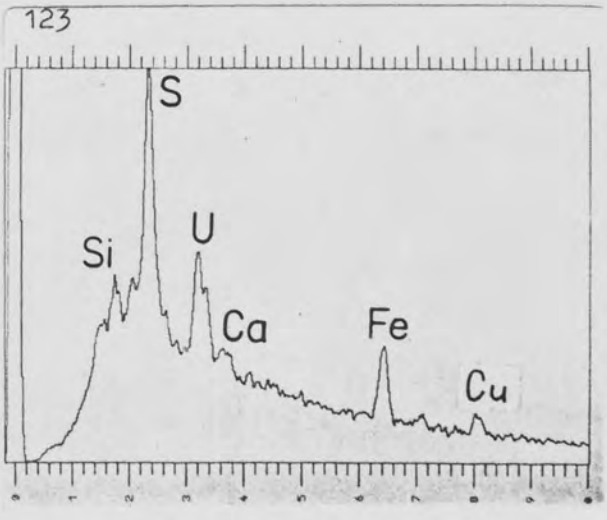

Plate No.	Sample No.	Grain No.	Description
			Ousdale arkose
183	562		Low magnification of mineralised arkose with large quartz clasts (white). Surface Anomaly 3. (TPPL)
184	562		Lexan of the same sample, showing fission-tracks (dark areas) along quartz clast boundaries and in the arkose matrix. (TPPL)
185	22C		Lexan superimposed on section of arkose, mineralised with coffinite. The Lexan is slightly offset (to the right) to reveal fission tracks (dark patches) associated with hair-line fractures in quartz (f). (Surface Anomaly 2, site of Borehole 1). (TPPL)
186	804	1	Lexan superimposed on section of arkose, mineralised with coffinite. The Lexan is slightly offset (to the bottom) to reveal fission tracks (dark patches) associated with veinlets of calcite (C) and quartz (Q) which cut K-feldspar. BH.1, 7.7 m depth. (TPPL)
187	774		Lexan showing fission tracks (white areas) associated with anastomising marcasite veins. The fission tracks originate from the matrix between marcasite crystals. BH.2, 7.8 m depth. (negative print obtained directly from Lexan)
			Helmsdale granite
188	42	3	Sphene included in quartz. Caen Burn. (TPPL)
189	42	3	Lexan of the same sphene, showing point sources of fission tracks at either end of the crystal. (TPPL)
190	39B	1	Euhedral martite (right) with superimposed Lexan (slightly unfocussed) off-set to the left. Fission tracks are concentrated around the martite grain boundary. Caen Burn. (TPPL)

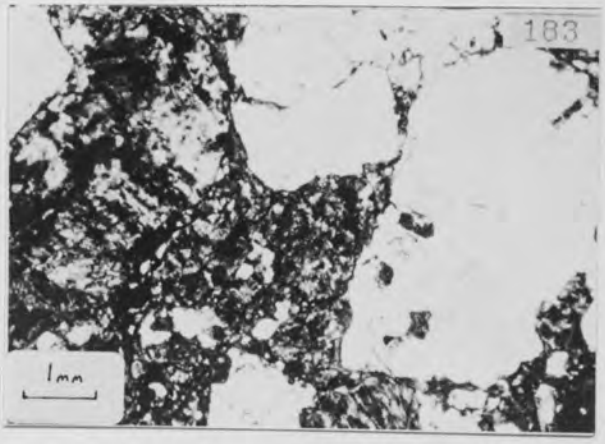
183
1mm

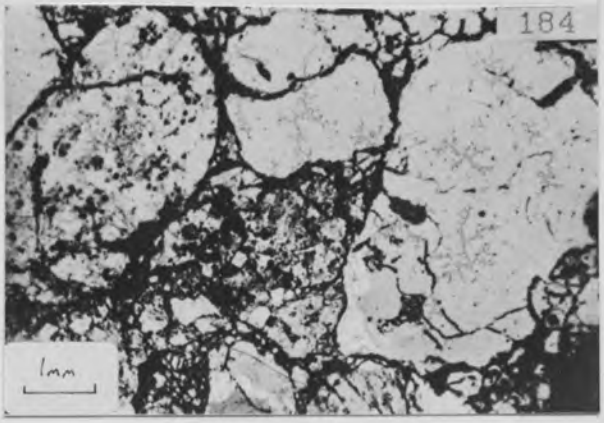
184
1mm

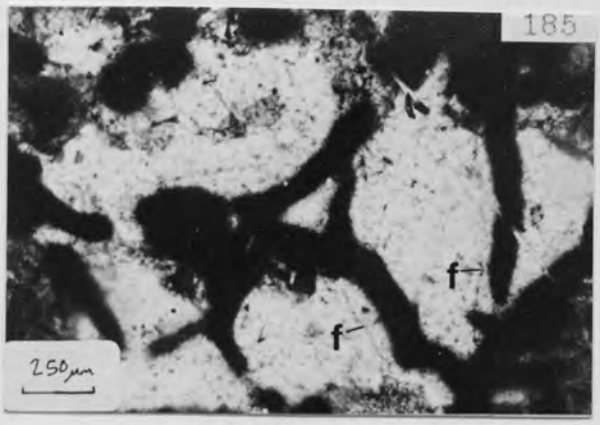
185
f
f
250µm

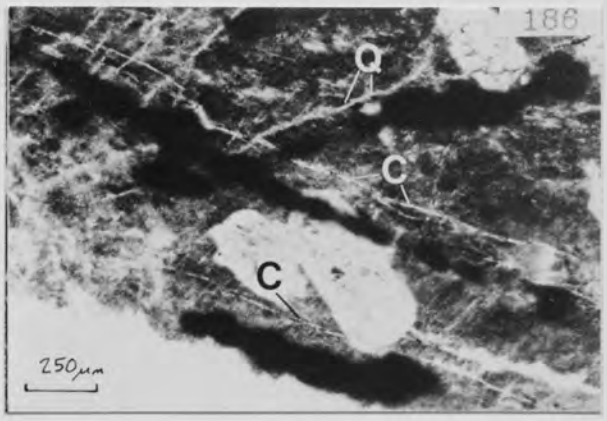
186
α
C
C
250µm

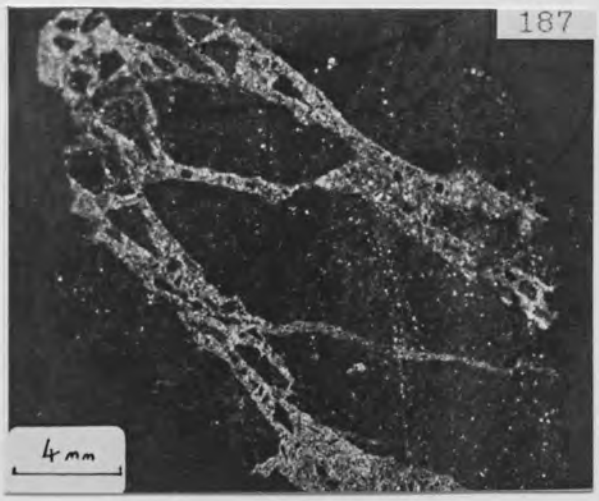
187
4mm

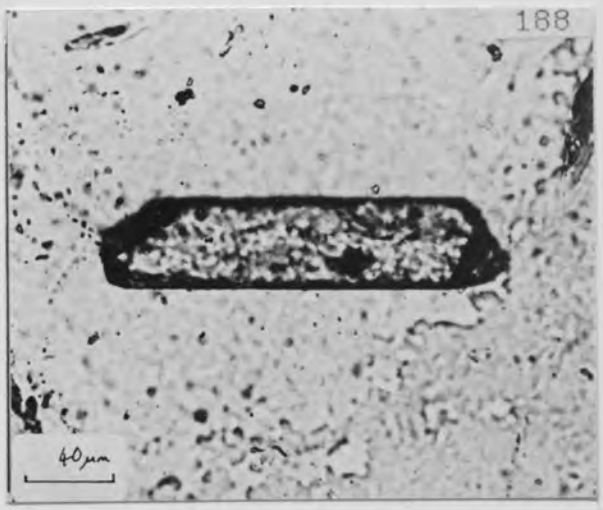
188
40µm

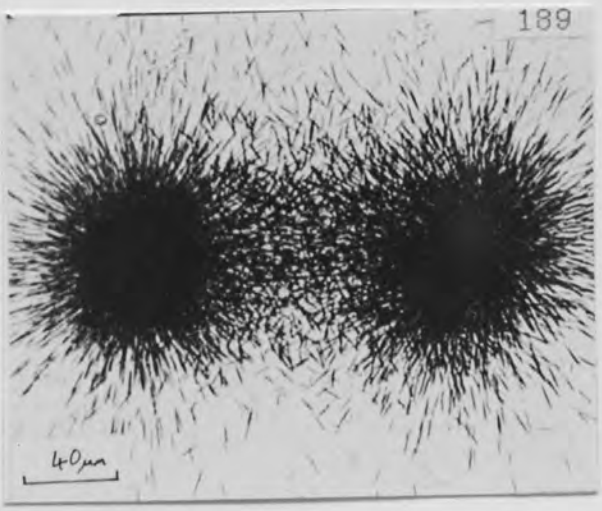
189
40µm

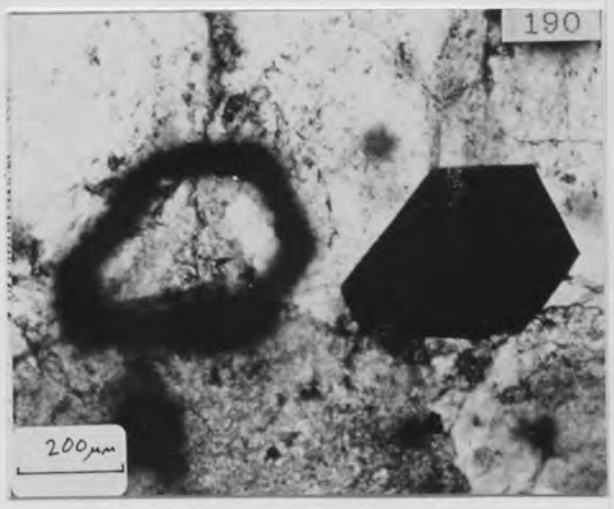
190
200µm

Plate No.	Sample No.	Grain No.	Description
			Helmsdale granite
191	28G		Part of a 2 mm diameter pyrite crystal (top) included in a quartz vein. Haematite occurs along the grain boundary and internal cracks. Ord Burn. (RPPL)
192	28G		Lexan of the area in Plate 191, showing fission tracks (dark) associated with the haematite-filled cracks and grain boundary but not with the pyrite itself. (TPPL)
193	H37B	2	TiO_2 and haematite pseudomorph after sphene (S) partly enclosed by biotite (B). The biotite cleavage is deformed in the region of the pseudomorph. Borehole 3, Creag Thoraraidh, 8 m depth. (RPPL)
194	53C	1	TiO_2 pseudomorph after sphene, with fine-grained leucoxene around the periphery (l) and well-crystallised anatase in the core (a). Bleached, [illegible] granite from an alteration zone. Lothmore valley. (RPPL)
195	53C	1	Lexan of the area in Plate 194, showing fission tracks (dark) associated with the peripheral leucoxene (l) but not with the central anatase crystals (a). (TPPL)
196	47C		Sericite-clay patches (S) in an alteration zone, with quartz (Q), a TiO_2 pseudomorph after sphene (T) and haematite (H). Caen Burn. (TXPL)
197	47C		Lexan of the area in Plate 196, showing high track densities (dark) associated with TiO_2 pseudomorph (T) and haematite (H) but evenly dispersed, very low track densities associated with sericite (S). No tracks are associated with quartz (Q). (TPPL)


191
400µm


192
400µm

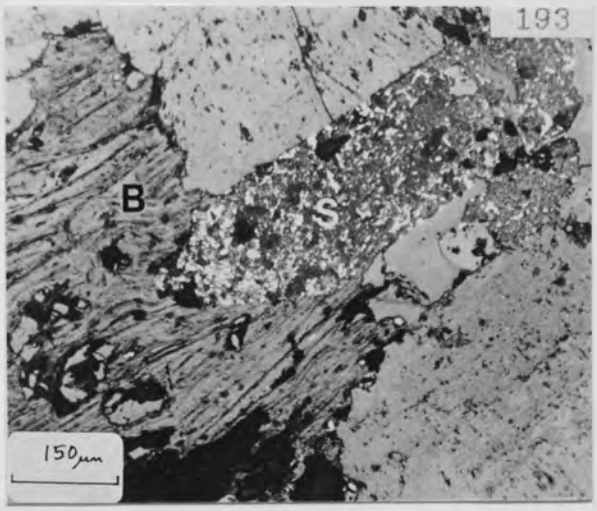
193
B
S
150µm

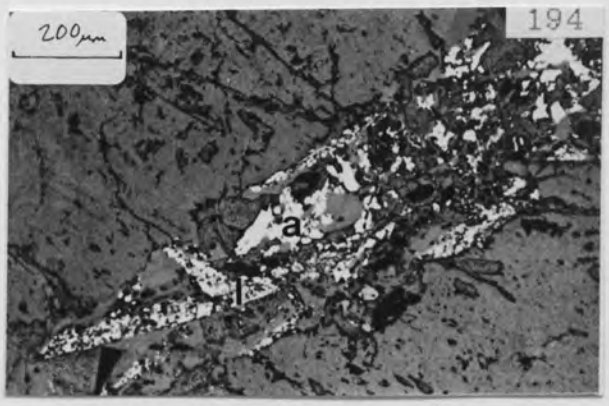
194
200µm
a
I

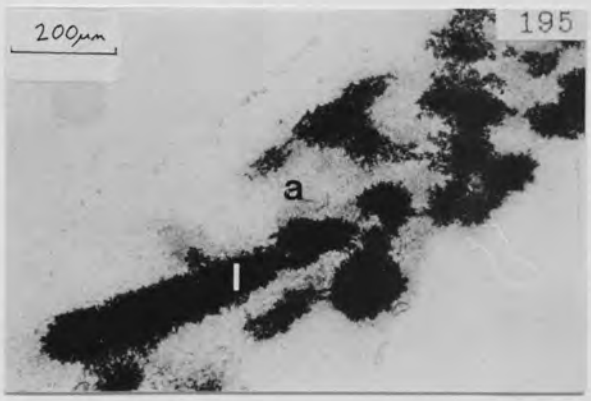
195
200µm
a
I

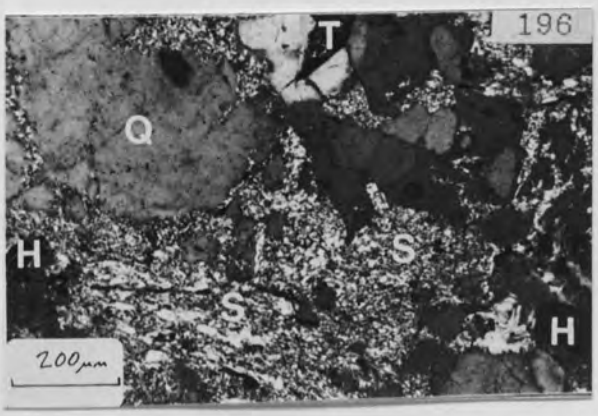
196
T
Q
H
S
S
H
200µm

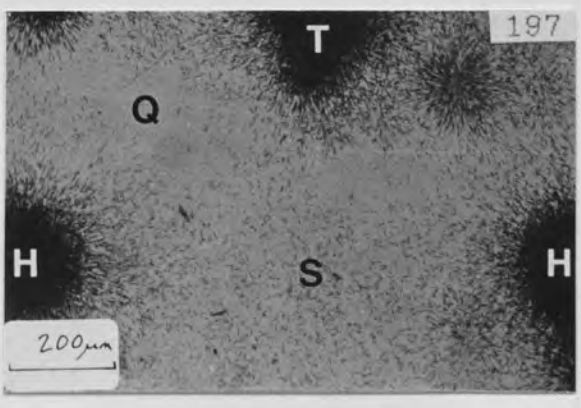
197
T
Q
H
S
H
200µm

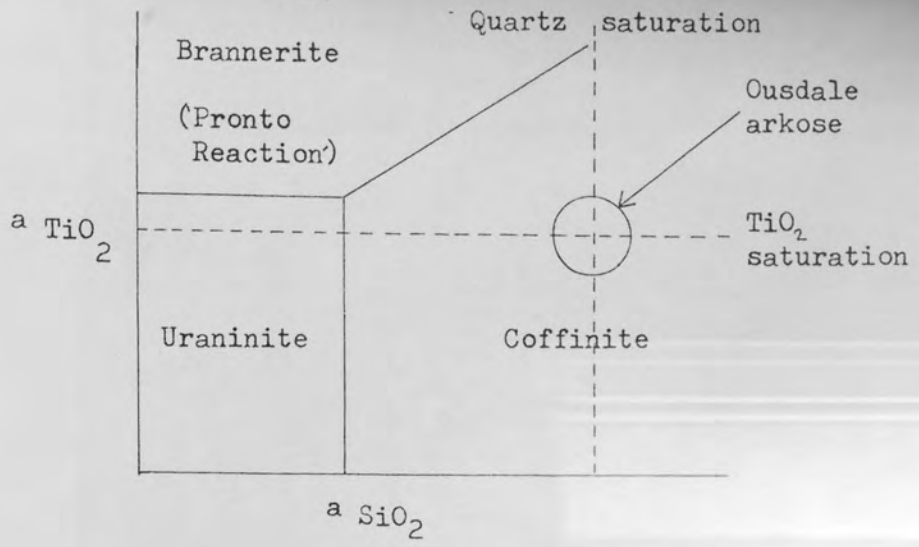

a) Low Temperatures (<360°C)

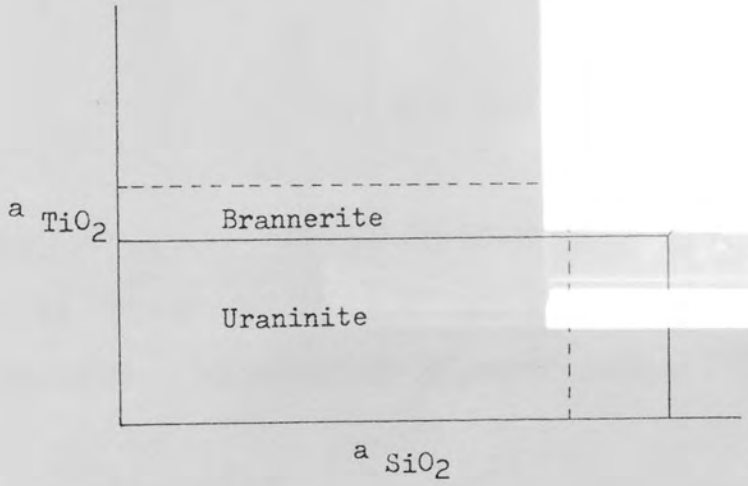

b) Intermediate Temperatures

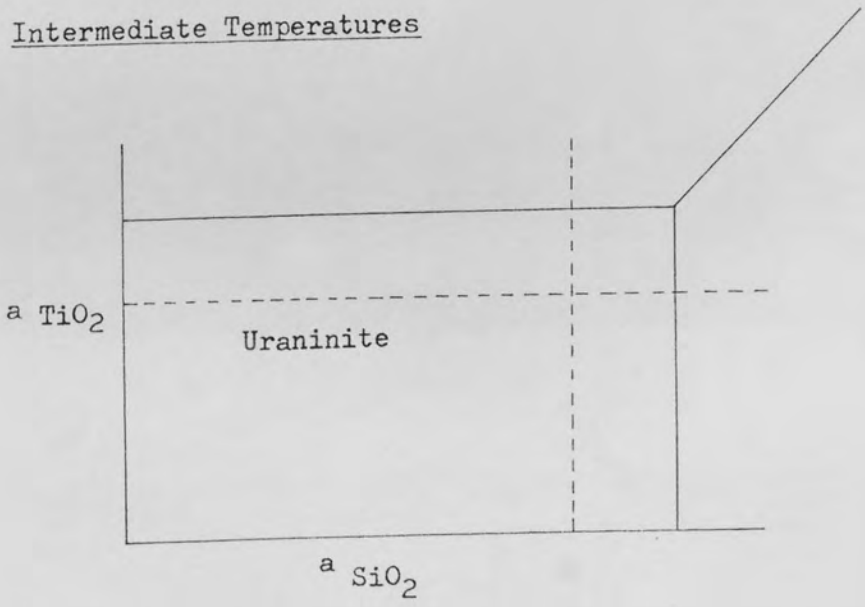

c) High Temperatures

Fig. 124 Proposed stability relations in the system UO_2-TiO_2-SiO_2 at various temperatures and constant pressure (schematic)

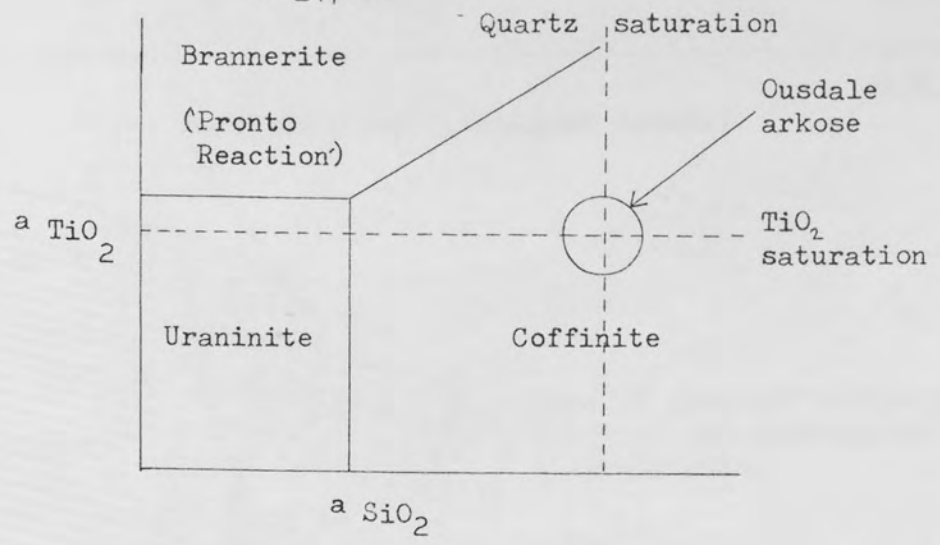

a) Low Temperatures (<360°C)

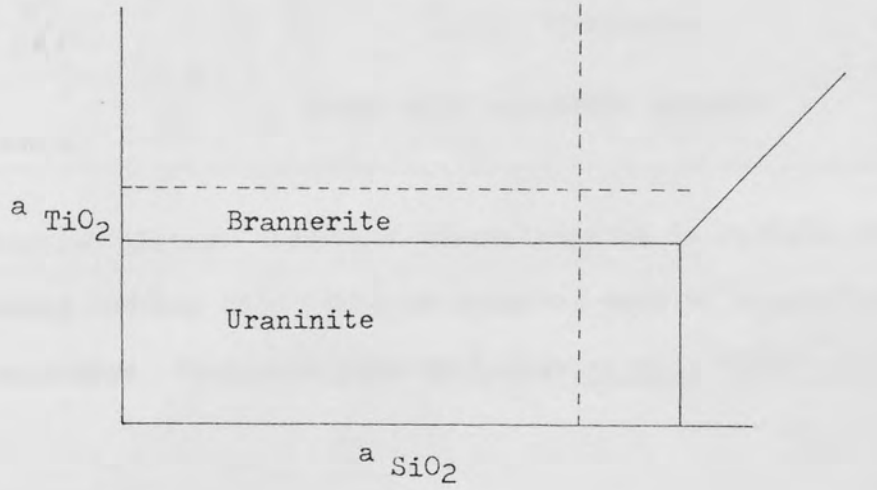

b) Intermediate Temperatures

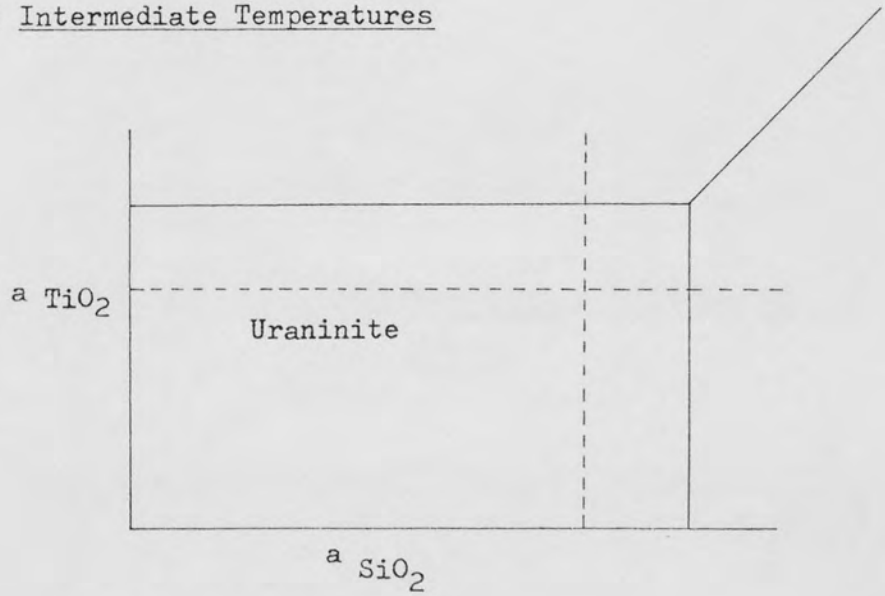

c) High Temperatures

Fig. 124 Proposed stability relations in the system UO_2-TiO_2-SiO_2 at various temperatures and constant pressure (schematic)

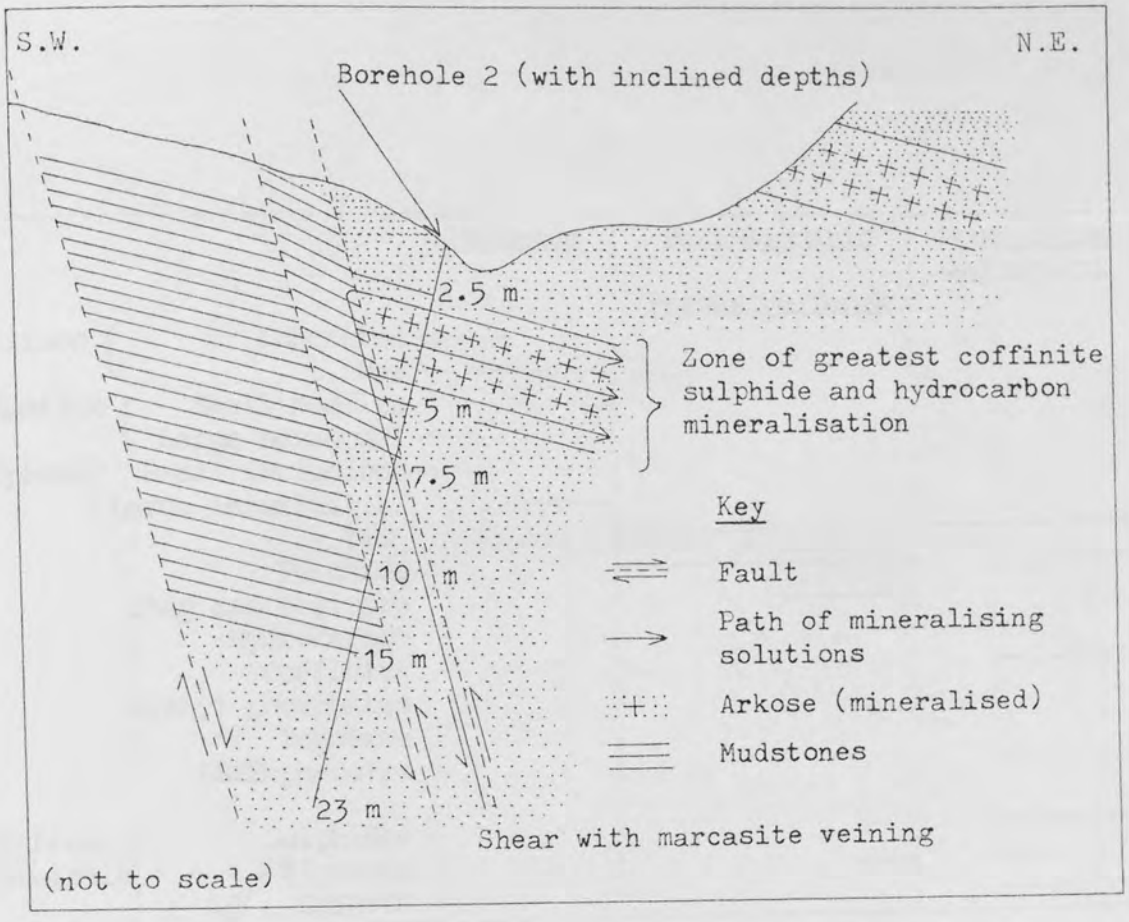

Fig. 125 Section through coffinite mineralisation in Ousdale arkose, lower Ousdale Burn, showing proposed path of mineralising solutions (modified from Gallagher et al., 1971)

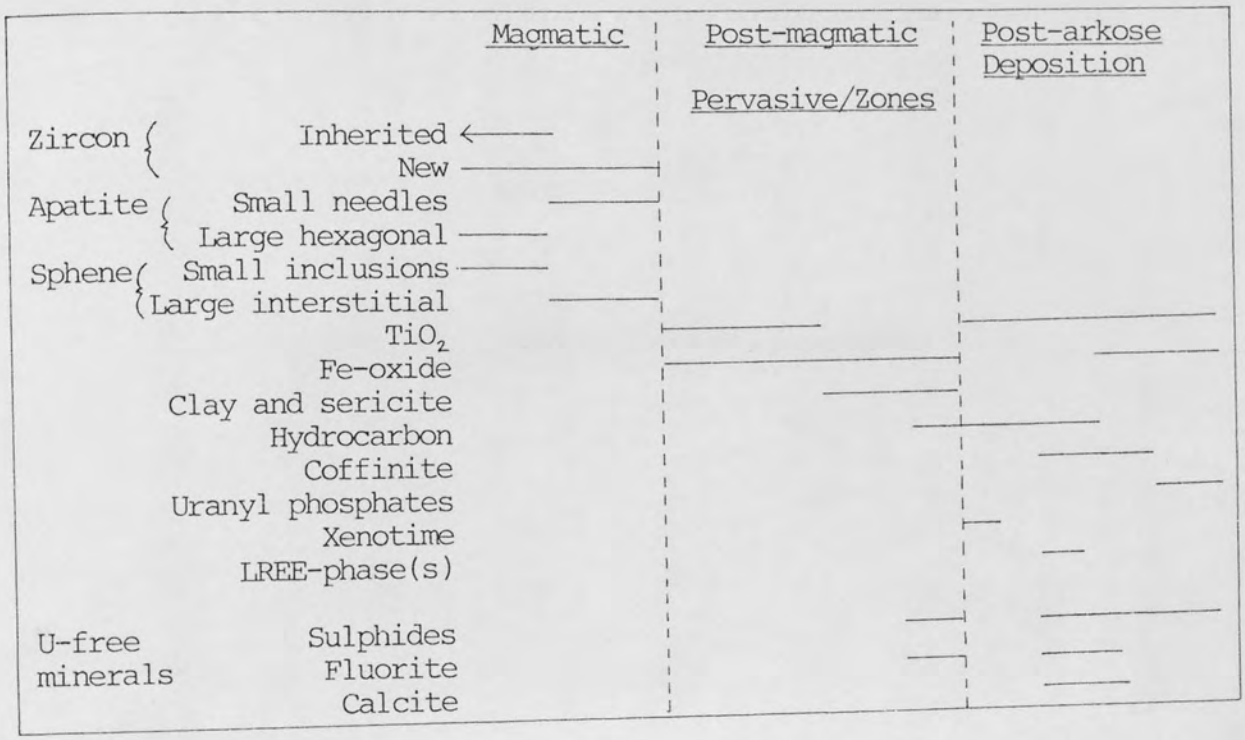

Fig.126 Paragenesis of uranium sites and other accessories in the Helmsdale granite and Ousdale arkose

Table 68 Comparison of the Ousdale U deposit, Scotland and the Olympic Dam Cu-U-Au deposit, Australia

Feature	Olympic Dam (Roberts and Hudson, 1983)	Ousdale
1. Geological Setting	Middle Proterozoic basement sediments and volcanics in an arched graben, overlying an alkali granite.	Lower Devonian sediments overlying a Caledonian adamellite, cut by a Lower Devonian, reactivated, transcurrent fault (Helmsdale fault).
2. Host rock to the mineralisation	Predominantly matrix-poor granite breccias to matrix-rich polymict breccias, deposited in an arid, subaerial environment along active fault-scarps.	Poorly sorted, coarse-grained arkose derived from the the underlying granite and deposited subaerially during activation of the Helmsdale fault.
3. Alteration	Haematisation of the underlying granite. Pervasive haematisation, chloritisation and sericitisation.	Haematisation, sericitisation and clay alteration of the granite; prior to mineralisation of the arkose?
4. U minerals	Fine-grained uraninite associated with lesser coffinite (intergrown with sulphides). Restricted brannerite (with TiO_2).	Coffinite (intergrown with sulphides, hydrocarbon, TiO_2). Secondary uranyl phosphates.
5. Other ore minerals	Chalcopyrite, pyrite, chalcocite, bornite. Native gold, silver and copper. Bastnaesite and florencite.	Chalcopyrite, pyrite, marcasite and covellite. Hydrocarbon with associated trace xenotime. Traces of unidentified LREE-phases.
6. Gangue minerals	Fluorite, haematite, quartz, sericite, TiO_2. Lesser chlorite, siderite, baryte.	Fluorite, calcite, baryte, haematite, TiO_2.
7. Genesis	Synsedimentary (related to volcanism?) / syndiagenetic. Younger epigenetic with structural control.	Epigenetic, fault-controlled.

Fig. 127 Cartoon showing the effect of metasomatism on the U- and Th-bearing accessories of the Ririwai biotite granite

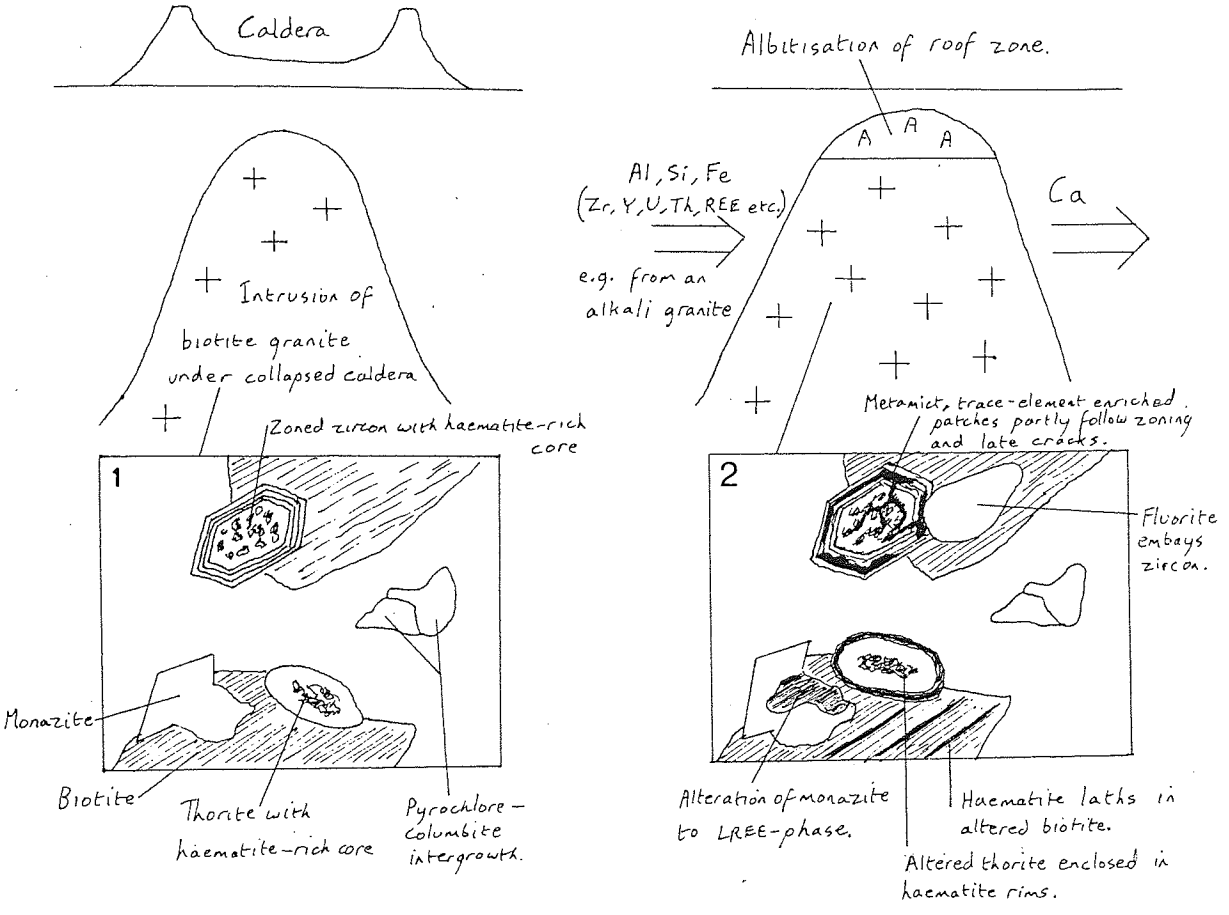

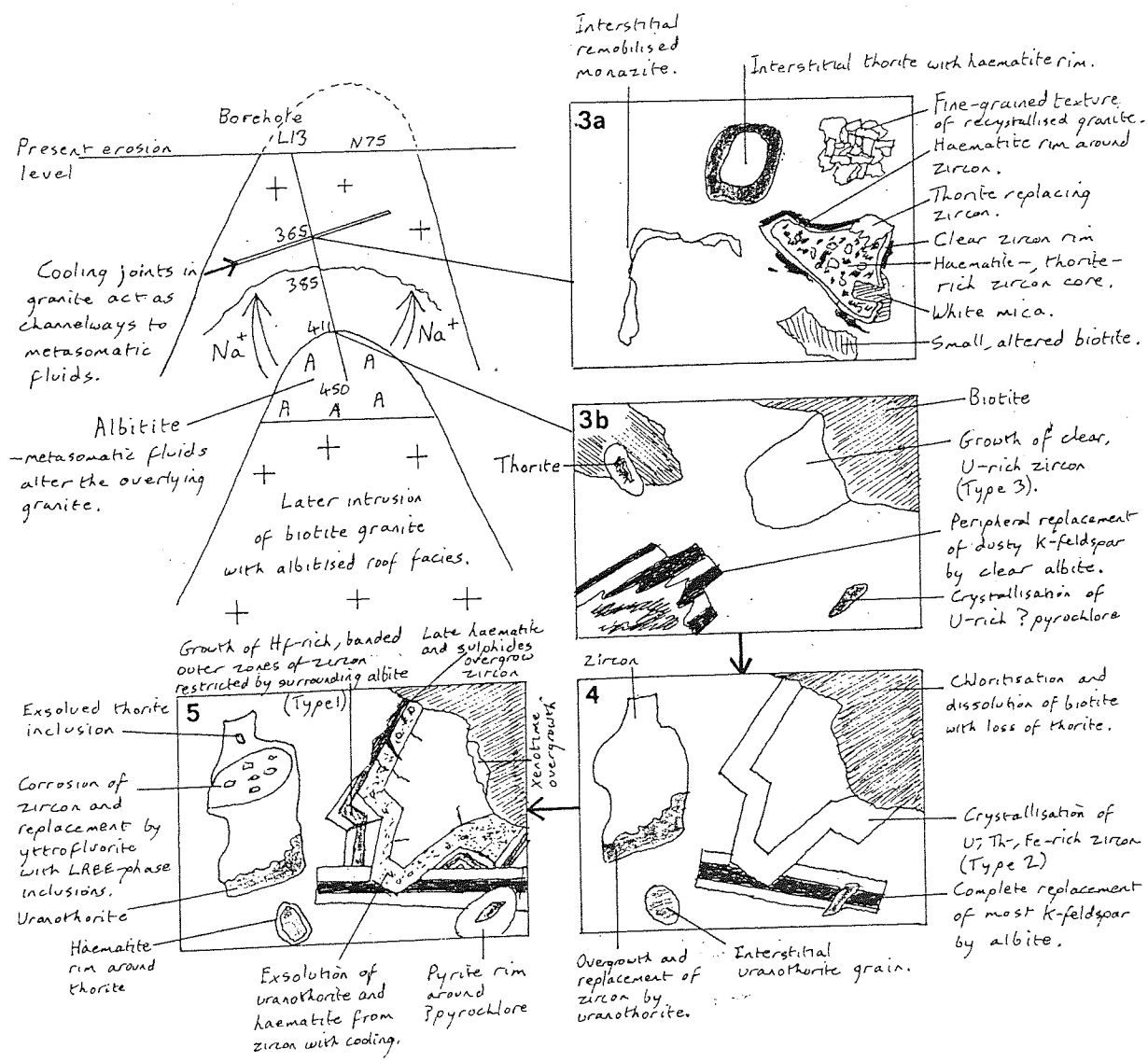

Fig. 127 (continued)

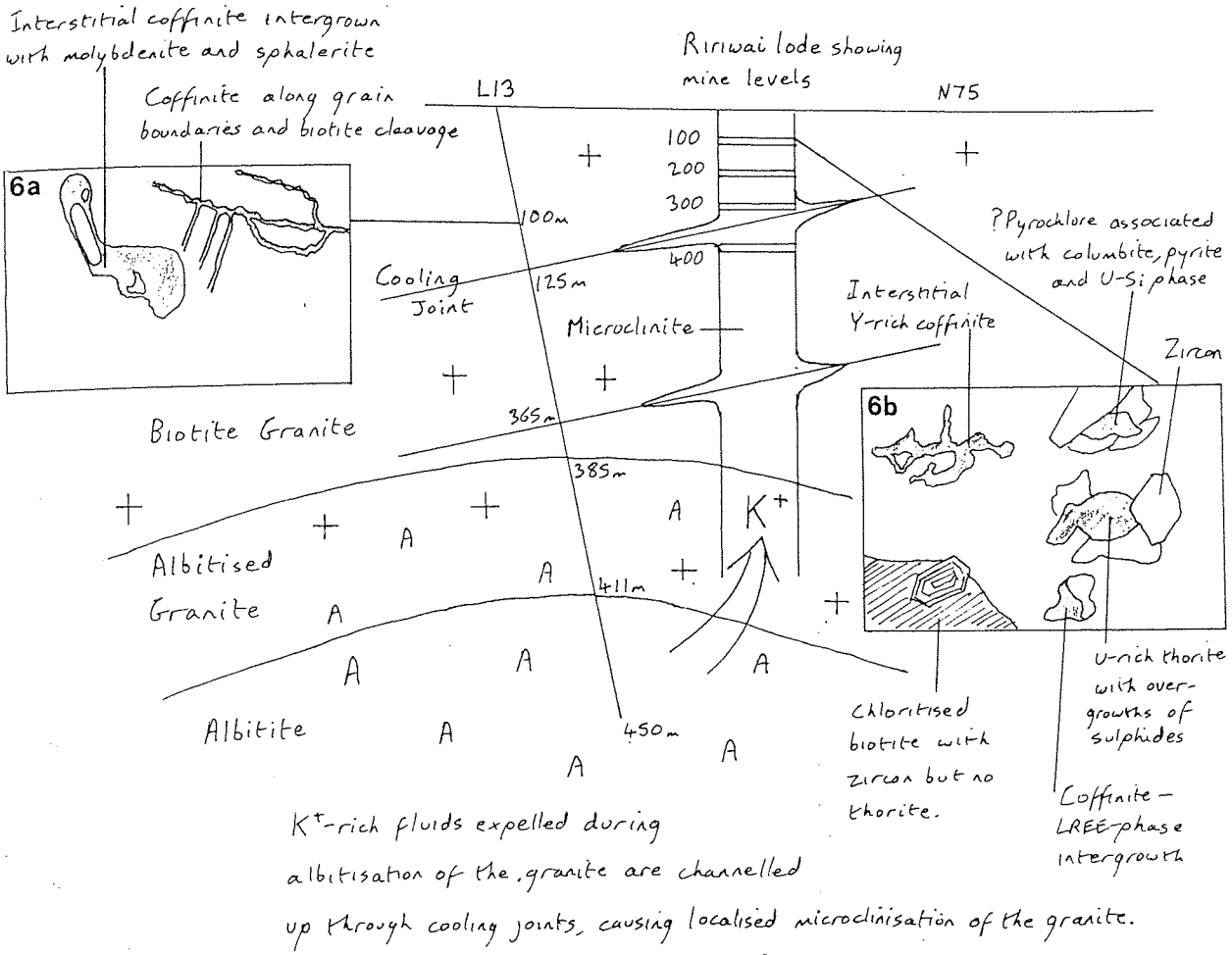

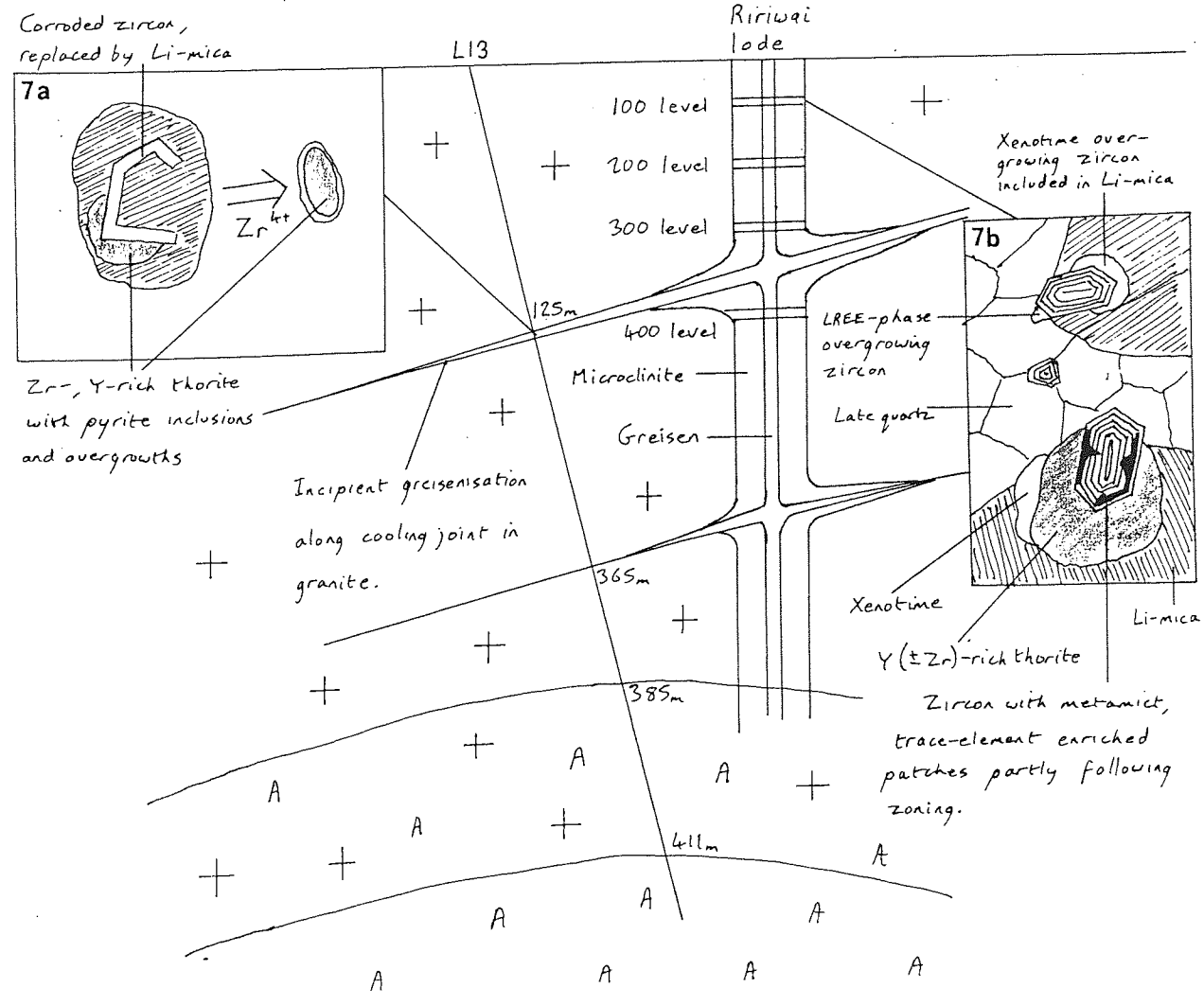

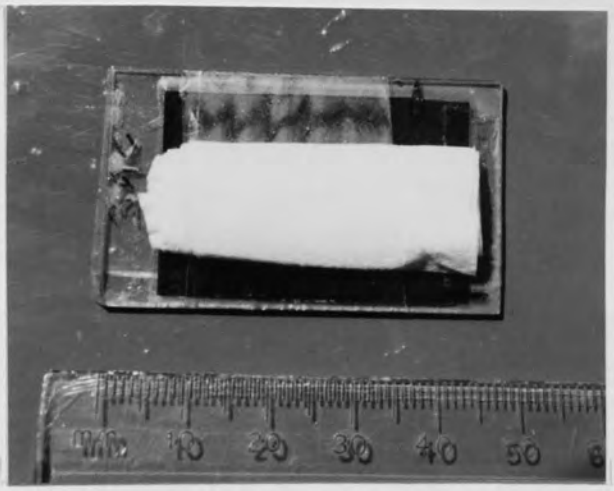

Plate 198 Cellulose nitrate alpha particle detector (dark red) tightly bound to a polished section. The white tissue wad keeps the detector firmly pressed against the section.

Plate 199 Circular Lexan fission track detectors atta ched to square polished sections. 40 sections are stacked inside the aluminium container, such that Lexan overlays are in direct contact, back to back for each pair of sections.

Table 69 EPMA detection limits* (wt. %) for various elements and minerals

Element (line)	Zircon	Thorite	Coffinite	Monazite	REE-phase	Xenotime	Pyrochlore	Th-Pb-P -phase	Meta-torbernite
Si	0.01-0.02	0.01-0.02	0.01	0.01	0.01	0.01-0.02	0.01-0.02	0.01	
P	0.01-0.02	0.01-0.02	0.01-0.02	0.01-0.02	0.01	0.02-0.03	0.01	0.02	0.01
Ca	0.01-0.04	0.01-0.02	0.01-0.02	0.01-0.02	0.01-0.02	0.01-0.02	0.01-0.02	0.02	0.01
Ti							0.02-0.03		
Mn	0.04-0.07						0.09		
Fe	0.04-0.07	0.06-0.11	0.05-0.10		0.07		0.06-0.09	0.10	0.07
Cu									0.06-0.07
Y	0.03-0.07	0.04-0.05	0.04	0.04	0.03-0.04	0.04-0.07	0.04	0.04	
Zr	0.04-0.07	0.02-0.07	0.05		0.04-0.05		0.05	0.05	
Nb							0.04-0.06		
La				0.06-0.08	0.06-0.08		0.06-0.08	0.08	
Ce			0.06	0.06-0.09	0.06-0.09		0.06-0.08	0.09	
Pr				0.24-0.40	0.39-0.42				
Nd ($L\alpha$)				0.10					
Nd ($L\beta$)				0.29-0.48	0.26-0.50				
Sm				0.33	0.33-0.37				
Dy		0.13-0.23				0.18			
Er		0.14-0.25				0.21		0.23	
Yb		0.14-0.25				0.22		0.25	
Hf	0.06-0.21	0.14-0.30	0.14					0.26	
Ta							0.14-0.26		
Pb		0.08	0.07		0.07		0.08	0.07	
Th	0.05-0.07	0.06-0.09	0.07-0.08	0.06-0.08	0.01-0.08	0.06-0.09	0.07	0.08	
U ($M\alpha$)	0.01-0.08	0.03-0.15	0.07-0.08	0.07-0.10	0.07-0.08	0.02-0.10	0.07-0.08	0.08	0.07
U ($M\beta$)		0.09	0.10						

* Detection limit at 99% confidence limit = $\frac{3\sqrt{B}}{I}$. CONC

where: B = background counts
I = peak counts
CONC = apparent wt. % of element (before ZAF correction)

Plate 200 Cambridge Microscan V electron microprobe.

The various control units labelled are for:

A Vacuum pump

B Counters

C Spectrometer Bragg angles

D Electron-optics

E Sample manipulation

F Power supply

There are two spectrometers (1 and 2).

Table 70 Conditions and standards used during EPMA for different elements

Z	Element	Line	Crystal	Bragg angle 2θ	Counter	Standard	Element Conc. (wt.%)
11	Na	K_α	RAP	54°15′	F	Jadeite	11.34
13	Al	"	"	37°14′	"	Corundum	52.91
14	Si	"	PET	109°09′	"	Zircon	15.20
15	P	"	"	89°31′	"	Apatite	18.11
16	S	"	"	75°49′	"	Pyrite	53.45
19	K	"	"	50°40′	"	Orthoclase	12.40
20	Ca	"	"	45°11′	"	Apatite	37.44
22	Ti	"	"	36°39′	"	Metal	100
23	Mn	"	LiF	62°56′	S	Mn_3O_4	72.03
26	Fe	"	"	57°29′	"	Magnetite	72.36
29	Cu	"	"	45°00	"	Metal	100
33	As	"	PET	33°58′	F	Semi-metal	100
39	Y	$L_{\alpha 1}$	"	95°03′	"	Metal	100
40	Zr	"	"	87°56′	"	Zircon	49.49
41	Nb	"	"	81°47′	"	Metal	100
57	La	"	"	35°50′	"	LaB_6	68.17
58	Ce	"	"	34°04′	"	$CeAl_2$	72.20
59	Pr	$L_{\beta 1}$	LiF	68°15′	"	PrF_3	71.15
60	Nd	"	"	65°07′	S	NdF_3	88.36
62	Sm	"	"	59°30′	"	SmF_3	72.41
64	Gd	$L_{\alpha 1}$	"	61°06′	"	GdF_3	73.35
66	Dy	"	"	56°36′	"	DyF_3	73.97
68	Er	"	"	52°37′	"	ErF_3	74.59
70	Yb	"	"	49°04′	"	YbF_3	75.14
72	Hf	"	"	45°53′	"	Metal	100
73	Ta	"	"	44°24′	"	Metal	100
82	Pb	M_α	PET	33°56′	F	Galena	86.62
90	Th	"	"	56°27′	"	Metal	100
92	U	"	"	53°07′	F/S	Metal, UO_2	100, 87.98
92	U	M_β	"	50°16′	F	or Glass	4.05

Counter: F = gas flow; S = sealed.

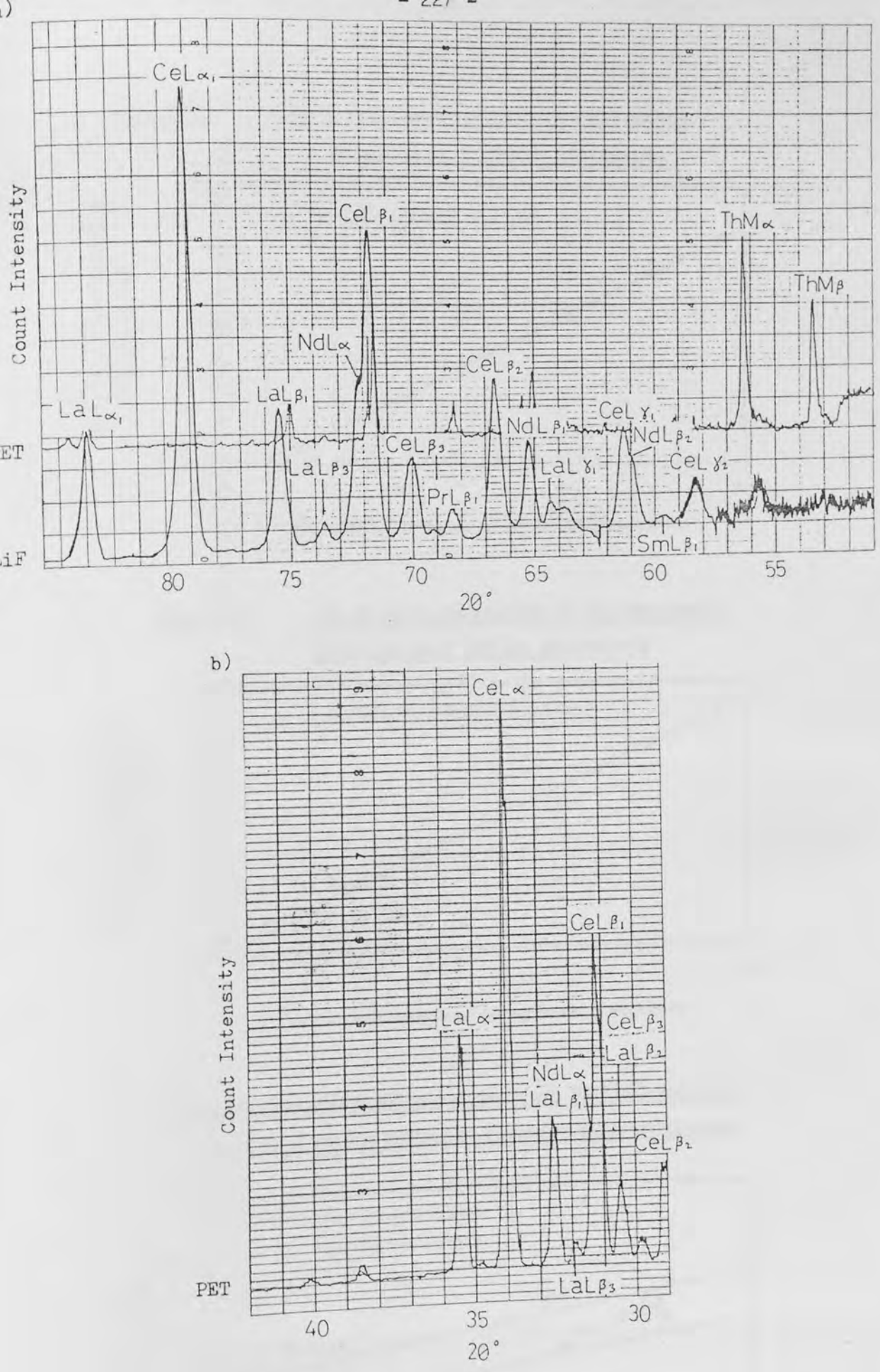

Fig. 128 Wavelength dispersive spectra for monazite using a) PET (top) and LiF b) PET analysing crystals

Fig. 129A Wt. % ZrO_2 measured in zircon using Zr metal and zircon standards

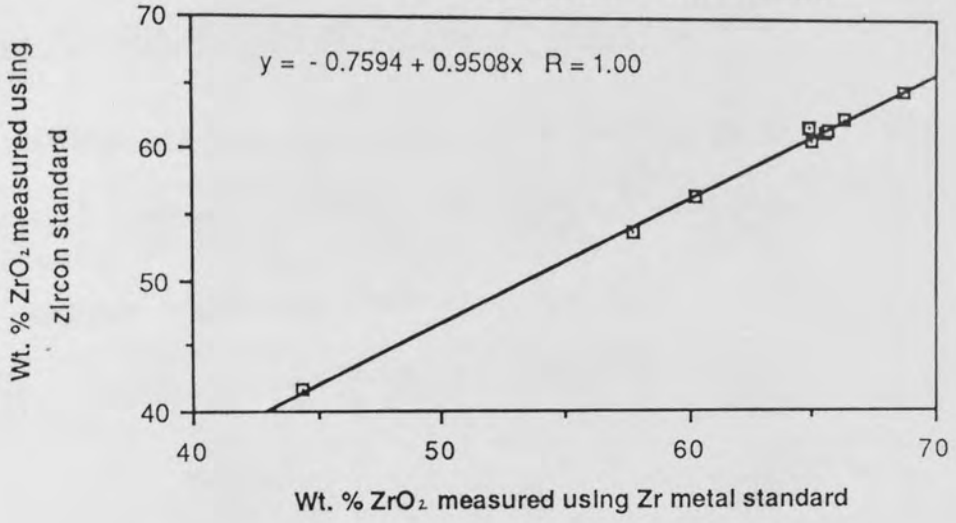

Fig. 129B Wt. % ZrO_2 measured in thorite using Zr metal and zircon standards

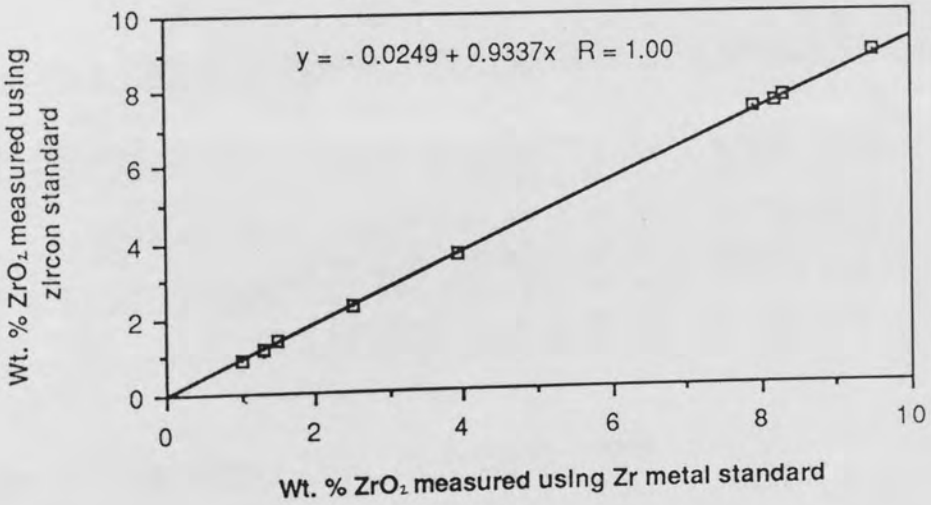

Fig. 130 The effect of increasing wt. % ThO_2 content on UM_α/UM_β for different counter flow mixtures

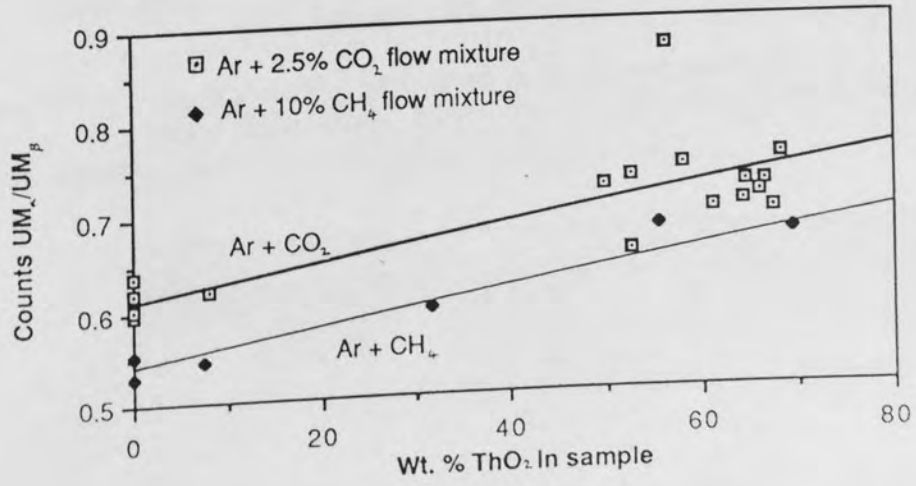

Table 71 Composition of U glass standard UG2

By neutron-activation analysis (after Smellie et al., 1978):

U_3O_8	CaO	Al_2O_3	SiO_2	Total
4.78	25.05	30.08	40.08	99.99

By electron microprobe (this study):

U_3O_8	CaO	Al_2O_3	SiO_2	Total
5.63	24.33	28.81	39.31	98.07

Table 72 Checking different standards for U by electron microprobe (15 kV accelerating voltage)

Coffinite (Grain 1, Sample 471A, Borehole 2 in the Ousdale arkose)

Line used	Mα			Mβ		
Standard used	Metal	Oxide	Glass	Metal	Oxide	Glass
Wt. % U (before ZAF)	45.52*	48.45	70.31	46.73*	50.32	69.23
	45.17+	48.25	65.66	44.55+	48.55	70.19
Wt. % U (after ZAF)	61.14*	58.70	62.49	62.35*	60.41	61.78
	60.75+	58.51	59.34	60.14+	58.79	62.43

Uraninite (a sample from the Zambian Copperbelt)

Line used	Mα			Mβ		
Standard used	Metal	Oxide	Glass	Metal	Oxide	Glass
% U (before ZAF)	72.32*	77.58	100.68	70.82*	78.80	100.44
	70.59+	76.36	104.80	69.62+	76.70	107.72
% U (after ZAF)	84.02*	81.73	80.25	82.96*	82.51	80.14
	82.46+	80.60	81.96	81.77+	80.82	83.34

* Metal standard freshly polished and carbon coated.
\+ Metal standard tarnished, after being left in a dessicator in air for one month.

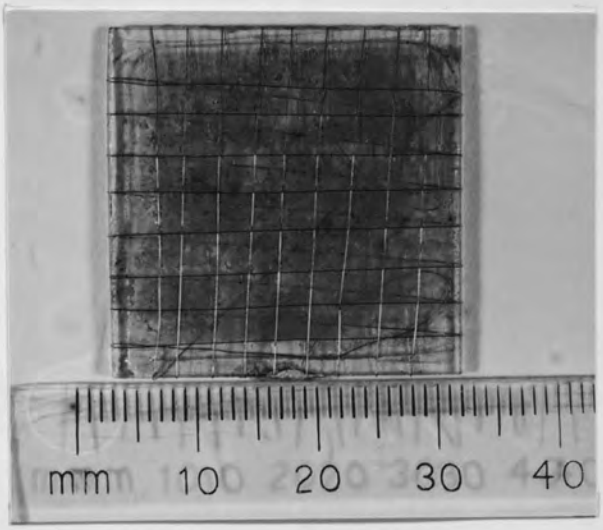

Plate 201 Wire-grid wound around a polished thin-section in order to facilitate grain location under the SEM.

Plate 202 Cambridge S150 scanning electron microscope (SEM) with Link energy dispersive spectrometer (on left).

Table 73 Comparison of INAA results for U using the long and short irradiation methods

Sample No.	Long	Short	$\frac{\lvert(\text{Long}-\text{Short})100\rvert}{\text{Long}}$
5A	13.4	15.4	14.9
5B	19.7	19.6	0.5
7A	510	488	4.3
7D	19.0	21.1	11.1
7F	18.4	20.9	13.6
13A	16.0	15.7	1.8
18D	1398	1422	1.7
20A	5.4	5.9	9.3
21	5.4	7.1	31.5
22C	309	308	0.3
28A	216	218	0.9
28C	13.8	15.1	9.4
28E	646	612	5.3
35	6.3	7.1	12.7
39B	62.1	63.1	1.6
46A	19.7	21.9	11.2
46B	83.2	91.0	9.4
53A	10.6	12.0	13.2
53B	12.1	14.0	15.7
H414	2.8	3.4	21.4
SY-2	291	265	8.9
SY-2	299	280	6.4